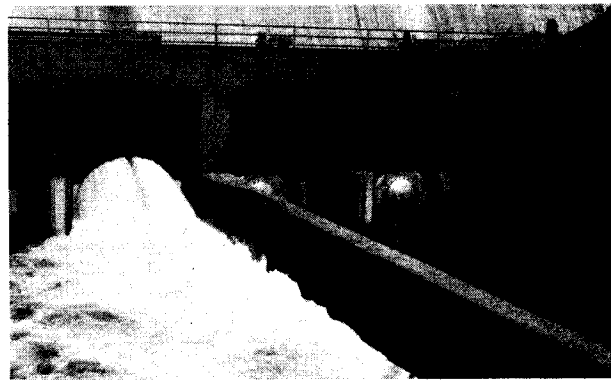
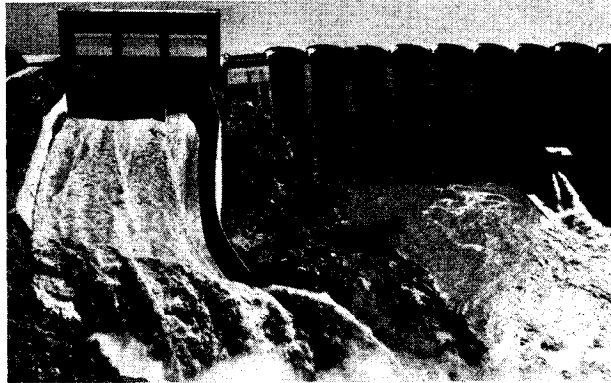


A WATER RESOURCES TECHNICAL PUBLICATION
ENGINEERING MONOGRAPH NO. 41



AIR-WATER FLOW IN HYDRAULIC STRUCTURES

**UNITED STATES DEPARTMENT
OF THE INTERIOR
WATER AND POWER RESOURCES SERVICE**

TECHNICAL REPORT STANDARD TITLE PAGE

1. REPORT NO. Engineering Monograph No. 41	2. GOVERNMENT ACCESSION NO.	3. RECIPIENT'S CATALOG NO.	
4. TITLE AND SUBTITLE Air-Water Flow in Hydraulic Structures		5. REPORT DATE December 1980	
		6. PERFORMING ORGANIZATION CODE	
7. AUTHOR(S) Henry T. Falvey		8. PERFORMING ORGANIZATION REPORT NO. Engineering Monograph No. 41	
9. PERFORMING ORGANIZATION NAME AND ADDRESS Water and Power Resources Service Engineering and Research Center PO Box 25007 Denver, Colorado 80225		10. WORK UNIT NO.	
		11. CONTRACT OR GRANT NO.	
12. SPONSORING AGENCY NAME AND ADDRESS Same		13. TYPE OF REPORT AND PERIOD COVERED	
		14. SPONSORING AGENCY CODE	
15. SUPPLEMENTARY NOTES			
16. ABSTRACT <p>The purpose of this report is to summarize the work that has been completed on air-entrainment and air-demand in both open- and closed-conduit flows. The intent was to produce a concise reference source from which design manuals, monographs, and charts for specific applications could be prepared. Areas that need additional research have been identified. The report was prepared from available reference material. In several areas, data from several references have been combined to produce generalized curves. Includes 64 figs., 74 ref., 3 app., and 155 pp.</p>			
17. KEY WORDS AND DOCUMENT ANALYSIS a. DESCRIPTORS-- / *air demand/ *air entrainment/ *open channels/ *closed conduits/ *design criteria/ *air-water interfaces/ *shaft spillway/ air bubbles/ aeration/ vents/ vacuum breakers/ relief valves/ jet aerodynamics b. IDENTIFIERS-- c. COSATI Field/Group 1300 COWRR: 1407			
18. DISTRIBUTION STATEMENT Available from the National Technical Information Service, Operations Division, Springfield, Virginia 22161.		19. SECURITY CLASS (THIS REPORT) UNCLASSIFIED	21. NO. OF PAGES 155
		20. SECURITY CLASS (THIS PAGE) UNCLASSIFIED	22. PRICE

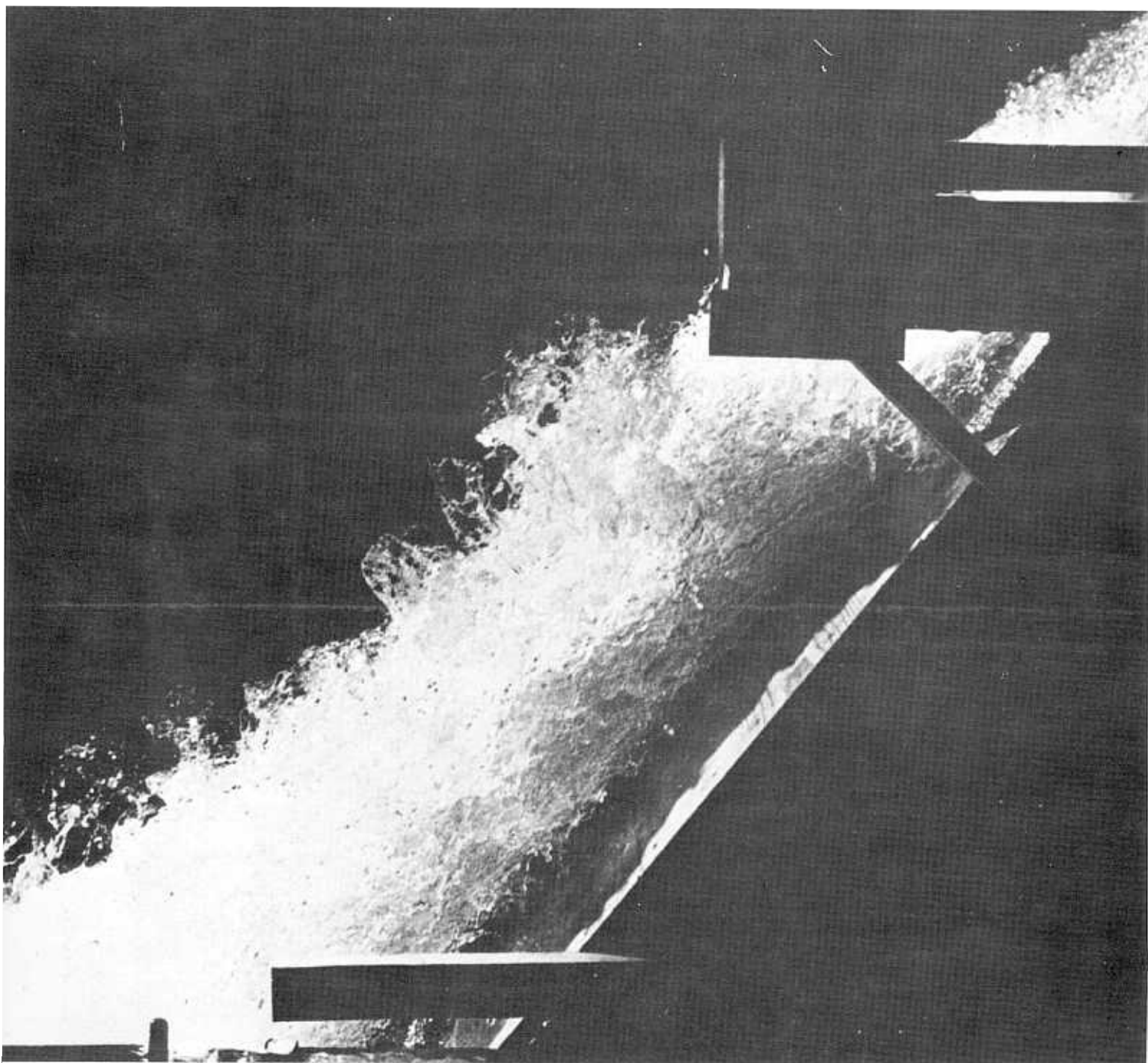
A WATER RESOURCES TECHNICAL PUBLICATION
Engineering Monograph No. 41

AIR-WATER FLOW IN HYDRAULIC STRUCTURES

By Henry T. Falvey
Engineering and Research Center
Denver, Colorado 80225

United States Department of the Interior
Water and Power Resources Service





FRONTISPIECE.—*High velocity jet from a slide gate. P801-D-79275*

As the Nation's principal conservation agency, the Department of the Interior has the responsibility for most of our nationally owned public lands and natural resources, protecting our fish and wildlife, preserving the environmental and cultural values of our national parks and historical places, and providing for the enjoyment of life through outdoor recreation. The Department assesses our energy and mineral interests of all our people. The Department also has a major responsibility for American Indian reservation communities and for people who live in Island Territories under U.S. administration.

ENGINEERING MONOGRAPHS are published in limited editions for the technical staff of the Water and Power Resources Service and interested technical circles in Government and private agencies. Their purpose is to record developments, innovations, and progress in the engineering and scientific techniques and practices which are used in the planning, design, construction, and operation of water and power structures and equipment.

First Printing 1980



U.S. GOVERNMENT PRINTING OFFICE
DENVER, COLORADO

For Sale by the Superintendent of Documents, U.S. Government Printing Office,
Washington, D.C. 20402, or the Water and Power Resources Service, Attention 922,
P.O. Box 25007, Denver, Colorado 80225.

Preface

The material assembled in this report is the result of studies extending over many years by a large number of engineers. Ellis Pickett at the U.S. Army Engineer Waterways Experiment Station in Vicksburg, Mississippi, supplied a reference list dealing with air-water problems. Personnel of the Water and Power Resources Service E&R Center, Water Conveyance Branch made their files and drawing on air design criteria in pipelines available for publication in this report. Prior to publication, the report was reviewed by Ellis Pickett and Ted Albrecht with the U.S. Army Engineers; and by engineers in the Dams, Mechanical, and Water Conveyance Branches, E&R Center, Water and Power Resources Service. The many constructive comments by these individuals and the assistance of Richard Walters who provided continuity and technical editing is greatly appreciated.

Letter Symbols and Quantities

Symbol	Quantity	Symbol	Quantity
A	Cross sectional area of water prism	d	Flow depth
A_a	Cross sectional area of airflow passage	d_b	Bulked flow depth
A_c	Cross sectional area of air core in a vertical shaft	d_e	Deflector height
A_d	Cross sectional area of conduit	d_n	Nappe thickness
A_o	Orifice area	d_o	Orifice diameter
A_p	Cross sectional area of penstock	d_t	Total depth of underlying and air free zones
A_v	Cross sectional area of vent	d_{95}	Bubble diameter for which 95 percent of the air, by volume, is contained in bubbles of this diameter or smaller
a	Ratio of bubble terminal velocity in turbulent flow to terminal velocity in still water	E	Relative width of the frequency spectrum
a_0	Mean air distribution function	exp	Napierian logarithm equal to 2.71828, approximately
a_1	Mean air distribution constant	f	Darcy-Weisbach friction factor
B	Width of rectangular chute	G	Gate opening
b	Width of flow channel	G_g	Mass velocity of gas
b_n	Nappe width	G_l	Mass velocity of liquid
b_s	Empirical coefficient accounting for sand grain roughness	g	Gravitational constant (acceleration)
C	Air concentration	H	Hydraulic radius of prototype air vent
C_a	Actual air concentration	H_f	Fall height of a water jet
C_b	Drag coefficient on a bubble	H_m	Head across orifice
C_d	Discharge coefficient based on 100 percent gate opening	H_n	Net head across turbine
C_f	Local loss coefficient	H_o	Distance from channel invert to energy grade line
C_l	Air concentration at $d_t/2$	H_t	Total potential and kinetic energy
C_m	Air concentration measured by a pitot tube sampler	h	Mean wave height
C_o	Orifice discharge coefficient	h_a	Height of airflow passage
C_s	Drag coefficient on a sphere	h_f	Distance from inlet to the water level in the vertical shaft
C_t	Air concentration at the bottom of the mixing zone	h_l	Head loss per unit length
\bar{C}	Mean air concentration	h_m	Head across manometer
c	Waterhammer wave celerity	h_w	Allowable head rise in penstock
D	Conduit diameter	K_e	Entrance loss
D_b	Smaller dimension of a rectangular conduit	K_s	Singular (form) loss
D_d	Diameter of water drop	k	Von Karman universal constant equal to 0.4
D_e	Equivalent bubble diameter	k_r	Coefficient of roughness
D_s	Larger dimension of a rectangular conduit	k_s	Sand grain roughness

LETTER SYMBOLS and QUANTITIES—Continued

Symbol	Quantity	Symbol	Quantity
L	Length of conduit or vent	r_s	Relative roughness of conduit (rugosity to diameter ratio)
L_c	Distance to start of self-aeration	S	Submergence depth
L_r	Prototype to model scale ratio	S_o	Pipe slope
L_s	Distance between stiffener rings	S_f	Slope of energy grade line
M	Unit mass	s	Root-mean-square value of wave height distribution
M_o	Maximum difference in elevation between a wave crest and the mean water level	s_w	Root-mean-square value of water surface distribution
m	Air concentration distribution coefficient	T	Top width of flow passage
N	Safety factor	t	Pipe wall thickness
n	Manning's roughness coefficient	U	Free stream velocity
n_v	Velocity distribution power-law coefficient	U_d	Velocity of water drop relative to air velocity
P	Energy dissipated	U_j	Water jet velocity
P_g	Normal distribution function	u	Local air velocity
P_h	Probability that the wave height is equal to given height	V	Mean flow velocity
P_w	Probability that the water surface is equal to or greater than the given elevation	V_f	Terminal velocity of bubbles in turbulent flow
p	Pressure intensity	V_i	Nappe velocity at impact
p_a	Allowable internal pressure	V_m	Minimum velocity required to entrain air
p_{atm}	Atmospheric pressure	V_o	Maximum water surface velocity
p_c	Collapse pressure	V_s	Terminal velocity of bubbles in slug flow
p_{in}	Internal pressure	V_t	Terminal velocity of bubbles in still water
p_n	Nappe perimeter	W	Wetted perimeter
Q	Discharge	x	Distance from start of boundary layer growth
Q_a	Volume flowrate of air	y	Distance normal to channel bottom (flow depth)
Q_c	Critical discharge	y_a	Distance from water surface
Q_r	Discharge from reservoir	y_c	Conjugate depth
Q_w	Volume flowrate of water	y_e	Effective depth
q	Unit discharge	y_k	Critical depth
q_a	Insufflation rate of air per unit surface area	y'	Normal distance to the bottom of the mixing zone
R	Bubble radius	z	Elevation
R_b	Equivalent bubble radius		
R_c	Radius of curvature of the bubble cap		
R_j	Thickness of annular jet		
r	Water jet radius		

LETTER SYMBOLS and QUANTITIES—Continued

Symbol	Quantity	Symbol	Quantity
α alpha	Angle chute invert makes with horizontal	E	Eötvös number $= \frac{\gamma D^2}{\sigma}$
β beta	Ratio of volumetric airflow rate to waterflow rate	E_u	Euler number $= \frac{\Delta p}{\rho V^2}$
γ gamma	Specific force of water	F	Froude number $= \frac{V}{(gD)^{1/2}}$
δ delta	Boundary layer thickness	P	Prandtl velocity ratio $= \frac{V}{(\tau_o/\rho)^{1/2}}$
ϵ epsilon	Mass transfer coefficient of bubbles	P_o	Poiseuille number $= \frac{h_a^2 (dp/dx)}{2\mu V}$
ξ zeta	Air concentration distribution constant	R	Reynolds number $= \frac{VD}{\nu}$
η eta	Normalized wave height	R_x	Distance Reynolds number $= \frac{Vx}{\nu}$
θ theta	Void fraction	W	Weber number $= \frac{V}{(\sigma/\rho D)^{1/2}}$
κ kappa	Gas constant		
λ lambda	Density ratio		
μ mu	Dynamic viscosity		
μ_a	Dynamic viscosity of air		
μ_w	Dynamic viscosity of water		
ν nu	Kinematic viscosity		
ν_f	Water viscosity		
π pi	Ratio of the circumference of any circle to its radius, 3.14159...		
ρ rho	Density		
ρ_a	Air density		
ρ_w	Water density		
ρ_g	Gas density		
ρ_l	Liquid density		
ρ_m	Density of manometer fluid		
σ sigma	Interfacial surface tension		
τ_o tau	Wall shear stress		
τ_j	Shear stress at water jet		
v_{atm} upsilon	Specific volume of air at atmospheric pressure		
v_*	Shear velocity		
ψ psi	Multicomponent flow parameter		
ω omega	Volume of gas bubble		
ω_a	Volume of air		
ω_w	Volume of water		
∞	Infinity		

Contents

	<i>Page</i>
Preface	v
Letter Symbols and Quantities	vi
Introduction	1
Purpose and Applications	3
Summary and Conclusions	5
Open Channel Flow	7
Introduction	7
Bubble Dynamics	8
Terminal Velocity of a Single Bubble in Still Water	8
Bubble Size in Shear Flows	10
Terminal Velocity of Bubbles in Turbulent Flow	12
Vertical and Longitudinal Flow Structure	14
Design Parameters	16
Location of Beginning of Aeration	16
Location of Fully Aerated Flow	19
Air Concentration Profiles	19
Definition of concentration	19
Air distribution in the mixing zone	21
Air distribution in the underlying zone	22
Mean air concentration	24
Water Surface Location	28
Effect of Air Entrainment Flow on Stilling Basin	
Performance	36
Closed Conduit Flow	37
Classification of Flow	37
Flow in Partially Filled Conduits	41
Model Predictions	41
Air vent not designed	42
Air vent designed	44
Analytic Estimates	44
Flow Having a Hydraulic Jump That Fills the Conduit	48
Flows From Control Devices	51
Flows From Valves	52
Flows From Gates	54
Falling Water Surface	54
Air Vent Design Criteria for Closed Conduits	57
Purpose	57
Location	57
Maximum Airflow Rate	57
Structural Considerations	57
Physiological Effects	57
Safety of Personnel	59

CONTENTS—Continued

	<i>Page</i>
Freeze Protection	59
Cavitation Damage	59
Water Column Separation	59
Air Vent Design Criteria for Pipelines	60
Introduction	60
Gravity Systems	61
Vertical alinement criteria	61
Horizontal alinement criteria	62
Vent location	62
Pumping Systems	65
Vent Structure Design Considerations	65
Evacuation of air during filling	65
Removal of air during operation	66
Prevent pipe collapse during draining	69
Flows in Vertical Shafts	77
Classification of Airflows	77
Region I Airflow Rates	79
Region II Airflow Rates	80
Reverse Airflow in a Vertical Shaft	80
Submergence	80
Free Falling Water Jets	81
Jet Characteristics	81
Airflow Around the Jet	82
Air Entraining Characteristics as a Falling Jet Enters a Pool	83
Bibliography	87
Appendix	93
I Probability Depth Probe	95
II Mean Air Concentration, Free Surface Flow, Computer Program	97
III Air Demand, Falling Water Surface, Computer Program ...	113
Introduction	113
Junction Energy Equations	113
Turbine Characteristics	115
Geometry	118

CONTENTS—Continued

FIGURES

<i>Number</i>		<i>Page</i>
1	Forms of air-entrainment on a spillway	9
2	Large gas bubble in a liquid	10
3	Terminal velocity of air bubbles in filtered or distilled water as a function of bubble size, Haberman and Morton [26] ..	11
4	Terminal velocity of bubbles in turbulent flow	13
5	Structure of open channel flow, Killen and Anderson [42]	14
6	Air entraining flow regimes in open channel flow	15
7	Experimentally determined local loss coefficient C_f , Bormann [11]	18
8	Location of inception of air entrainment	20
9	Cumulative Gaussian probability and measured air concentration distributions in the mixing zone	22
10	Actual air concentration distribution in mixing zone	23
11	Air concentration distributions of channel flow on steep slopes Straub and Anderson [66]	24
12	Interfacial tension	26
13	Air entrainment coefficient	29
14	Air entrainment in open channel flow	30
15	Examples of air entrainment in chutes	31
16	Definitions of aerated flow depth	32
17	Relation of aerated to nonaerated flow depth	34
18	Probability density distribution for different values of the width of the energy spectrum	35
19	Probability description of water surface in a chute	36
20	Flow patterns in horizontal pipes, Baker [7]	38
21	Flow pattern sketches, Alves [1]	39
22	Effect of conduit diameter on terminal velocity of a bubble, Collins [16]	40
23	Influence of air pressure in conduit on airflow rate, Sikora [65] .	41
24	Model tests on a spillway, Sikora [65]	43
25	Discharge coefficients for orifice at end of pipe	45
26	Airflow above water surface	47
27	Air entrainment with hydraulic jump closing conduit	49
28	Forces on a stationary bubble	50
29	Bubble motion in closed conduits flowing full	51
30	Slug flow in inclined pipes, Runge, and Wallis [61]	52
31	Valve and gate data, Kohler [44]	53
32	Airflow rate for two 1375-mm fixed-cone (Howell-Bunger) valves	55
33	Falling water surface	56
34	Comparison of field data with computer prediction	58
35	Air vent, Shadow Mountain Dam, Colorado-Big Thompson Project, Colorado	60

CONTENTS—Continued

FIGURES—Continued

<i>Number</i>		<i>Page</i>
36	Pipeline configurations	61
37	Plan and profile of a gravity pipeline	62
38	Vent structure	63
39	Typical irrigation system air valve installation	64
40	Vent location at changes in pipe slope	65
41	Air binding in a pipeline	66
42	Large-orifice air valve	67
43	Performance curves for large-orifice air release valves	68
44	Typical small-orifice air release valve	69
45	Performance curves for small-orifice air release valves	71
46	Typical frost protection installation	72
47	Collapsing pressure of a steel pipe with stiffener rings	73
48	Performance curves for large-orifice vacuum relief valves	74
49	Specific volume and barometric pressure of air as a function of elevation	75
50	Required air relief orifice diameter to prevent collapse of steel pipelines	76
51	Observed air blowback in morning glory spillway at Owyhee Dam, Oregon	77
52	Typical types of vertical shaft inlet structures	78
53	Vertical shaft spillway discharge characteristics	78
54	Breakup of a water jet from a hollow-jet valve	84
55	Water drop breakup	85
56	Velocity distribution for flow over a flat plate, Bormann [11] ...	86

APPENDIX

I-1	Electronics schematic	96
I-2	Probe schematic	96
I-3	Controls in utility box	96
III-1	Definition sketch at penstock intake	114
III-2	Typical turbine characteristics of runner specific speed 230	116
III-3	Turbine loss coefficient	117
III-4	Air volume in penstock	118
III-5	Water surface area	118

Introduction

In many engineering projects a strong interaction develops between the water flowing through a structure and the air which is adjacent to the moving water. Sometimes the interaction produces beneficial effects. However, more often than not, the effects are not beneficial and the remedial action required to reduce the effects can be costly.

Cases in which air-water interaction develop include:

- Open channels with fast flowing water that require depths adequate to contain the air which is entrained within the water
- Morning-glory spillways that must have a capacity to convey the design flood and its entrained air
- Vertical shafts that entrain large quantities of air at small water discharges
- Measuring weirs that need adequate ventilation to prevent false readings and to eliminate surging
- Outlet gates that require adequate aeration to prevent the development of low pressures—which can lead to cavitation damage
- Emergency gates at penstock entrances that require ventilation to prevent excessive negative internal pressures during draining or emergency gate closures

- Sag pipes (inverted siphons)¹ that can be damaged due to blowback of entrained air
- Long pipelines that require air release and vacuum relief valves

From these cases it is noted that air-water flows can be generalized into three basic flow types:

1. Air-water flows in open channels,
2. Air-water flows in closed conduits, and
3. Free-fall water flows.

The first type usually is called *air-entraining* flow because air is entrained into the water mass. The second basic flow type generally is referred to as *air-demand*. The term *air-demand* is both misleading and technically incorrect, since an air vent does not demand air any more than an open valve demands water. However, since the term has been in common use for over 20 years, efforts to improve the nomenclature seem rather futile. The third type is referred also to as *air-entraining flow*.

¹"siphon, inverted—A pipe line crossing over a depression or under a highway, railroad, canal, etc. The term is common but inappropriate, as no siphonic action is involved. The suggested term, *sag pipe*, is very expressive and appropriate." *Nomenclature for Hydraulics*, Comm. on Hyd. Str., Hyd. Div., ASCE, 1962.

Purpose and Application

The purpose of this report is to summarize the work that has been done on *air-entrainment* and *air-demand* regarding the most recent theories and to suggest ways in which the results can be applied to design. The intent was to produce a concise reference of material from which design manuals, nomographs, and charts for specific applications could be prepared.

Although many generalizations of the data can be made, some types of flow conditions that are encountered in practice can be treated only by individual studies with physical models. These cases are identified when they occur.

Additional studies are needed in many areas. Some of the most critical areas requiring further research include the following:

- Effects of turbulence and air concentration on bubble dynamics
- Fluid dynamics in the developing aeration regime of free-surface flow
- Effects of hydraulic and conduit properties on probabilistic description of water surface in free-surface, high-velocity flow
- Effect of pressure gradients on air flow in partially-filled, closed conduits
- Bubble motion in closed-conduit flows for conduit slopes exceeding 45-degrees
- Effects of ambient pressure levels on cavitation characteristics of gates and valves discharging into a closed conduit
- Interaction between the air and a free jet

Summary and Conclusions

Methods have been developed to predict the mean air concentration and the concentration distribution with open channel flow. A new description of the free water surface in high velocity flow is proposed which more accurately represents actual conditions in high velocity flow. The effect of air entrainment on the performance of a stilling basin can be estimated using a bulked flow concept. A computer program (app. II) is presented with which the mean air concentration in steep chutes and spillways can be estimated.

With exception of a falling-water surface and decreasing flow in pipelines, closed conduit flows require model studies. When properly conducted and analyzed, model studies will yield accurate data for estimating air-flow

rates. Experimental methods are discussed. A computer program (app. III) is presented which can be used to predict the airflow rate with a falling-water surface. Design charts are presented for sizing air relief valves and vacuum valves on pipelines.

The airflow rate in vertical shafts was found to be extremely dependent upon the flow conditions at the shaft inlet. Equations are included for estimating the airflow rate having various inlet conditions.

Factors influencing the airflow rate around free falling jets are discussed. This area is identified as one needing additional research. Equations are presented from which the air entraining characteristics of a jet entering a pool can be estimated.

Open Channel Flow

INTRODUCTION

In observing flow in a chute or on an overflow spillway, one normally observes a region of clear water where the water enters the chute or spillway. Then—at some distance downstream—the water suddenly takes on a milky appearance. Lane [46] suggested that the “white water” begins when the turbulent boundary layer from the floor intersects the water surface. The validity of this assumption has been verified by many researchers. The cases in which the boundary layer creates the air entrainment are referred normally to as *self-aerated* flows. However, this is not the only way in which air entrainment can begin on chutes and spillways. The American Society of Civil Engineers Task Committee on Air Entrainment in Open Channels [5]² has summarized tests in which air entrainment is generated by the boundary layer on the side walls of chutes. They also reported tests in which air entrainment was observed downstream of piers on overflow spillways. This latter case is the result of the flow rolling over on itself as it expands after passing through the opening between the

piers. Levi [49] reported on longitudinal vortices on spillway faces. These vortices can entrain air if they intersect the water surface. All of these forms of air entrainment are apparent in figure 1.

Air entrainment implies a process by which air enters into a body of water. Normally, the appearance of “white water” is considered to be synonymous with entrainment. This is not always true. For instance, if the water surface is rough enough and moving at a sufficiently high velocity, the surface will appear to be white even though the water volume contains no air. The whiteness of the water is caused by the large number of reflections coming from different angles off the rapidly moving highly irregular surface (refer to frontispiece). For high water velocities, one’s eye does not respond rapidly enough to observe each individual reflection. Instead, these individual reflections blur into a fuzzy mass which appears white. High speed photography of “white water” demonstrates this effect very well. This leads one to the obvious conclusion that a flow could conceivably appear frothy but actually does not entrain any air! With air in the water, reflections also come from the surface of the bubbles. These reflections produce the same impression

²Numbers in brackets refer to the bibliography.

of "white water" as the water surface reflections.

Experiments have shown that flow in channels with mild slopes do not entrain air even though the boundary layer intersects the water surface. Thus, some degree of turbulence must be exceeded for the entrainment process to begin.

The turbulence causes the water surface to become irregular enough to trap bubbles of air. These bubbles of air are then diffused downward into the body of water if the vertical water velocities induced by the turbulence in the flow are larger than the terminal velocities of the bubbles. The *terminal velocity* V_t of a bubble is defined as the rate of rise of a bubble in a liquid in which the effects of turbulence, walls, other bubbles, and acceleration are negligible. The interaction of the terminal velocities of bubbles and the turbulence are considered in the following section.

BUBBLE DYNAMICS

Terminal Velocity of a Single Bubble in Still Water.

In still water, surface tension is the predominant effect on the shape of very small bubbles. Therefore, small bubbles tend to be perfect spheres. The motion of these bubbles through a fluid can be described by a balance between the buoyant forces and the viscous forces. However, as the bubbles become larger, surface tension effects become small with respect to shear forces. The shape of these larger bubbles can be approximated by a spherical cap having an included angle of about 100 degrees and an unstable relatively flat base (fig. 2). Because different effects predominate at different bubble diameters, one can expect the correlation between the bubble size and its terminal velocity to vary as the bubble diameter varies. Haberman and Morton [26] have experimentally

determined the terminal velocity as a function of the bubble size (fig. 3).

Assuming the bubble to be a rigid sphere, the terminal velocity V_t of small bubbles can be written as

$$V_t = \frac{2}{9} \left\{ \frac{R^2 g [1 - (\rho_g / \rho_w)]}{\nu_f} \right\} \quad (1)$$

where

g = gravitational constant (acceleration), 9.81 m/s²

R = bubble radius, mm

ν_f = water kinematic viscosity,
1.5 × 10⁻⁶ m²/s at 10 °C

ρ_w = water density, 1000 kg/m³ at
10 °C

ρ_g = air density, 1.29 kg/m³ at 10 °C

This also is known as Stokes' solution.³ Substituting the respective values for air, water, and gravity into equation 1 gives the terminal velocity of a small air bubble in meters per second as

$$V_t = 1.45 R^2 \quad (2)$$

Theoretically, this relation is valid only for bubble radii R smaller than 0.068 mm.

For bubble radii between 0.068 and 0.40 mm, the empirical relation

$$V_t = 0.625 R^2 \quad (3)$$

fits the data.

With bubble radii between 0.40 and 10 mm, the terminal velocity is about equal to 0.25 m/s. As the bubble diameter increases from 0.4 to

³G.G. Stokes was the first investigator to analytically determine the drag on a slowly moving sphere in a viscous fluid falling as a result of its mass relative to the fluid mass.

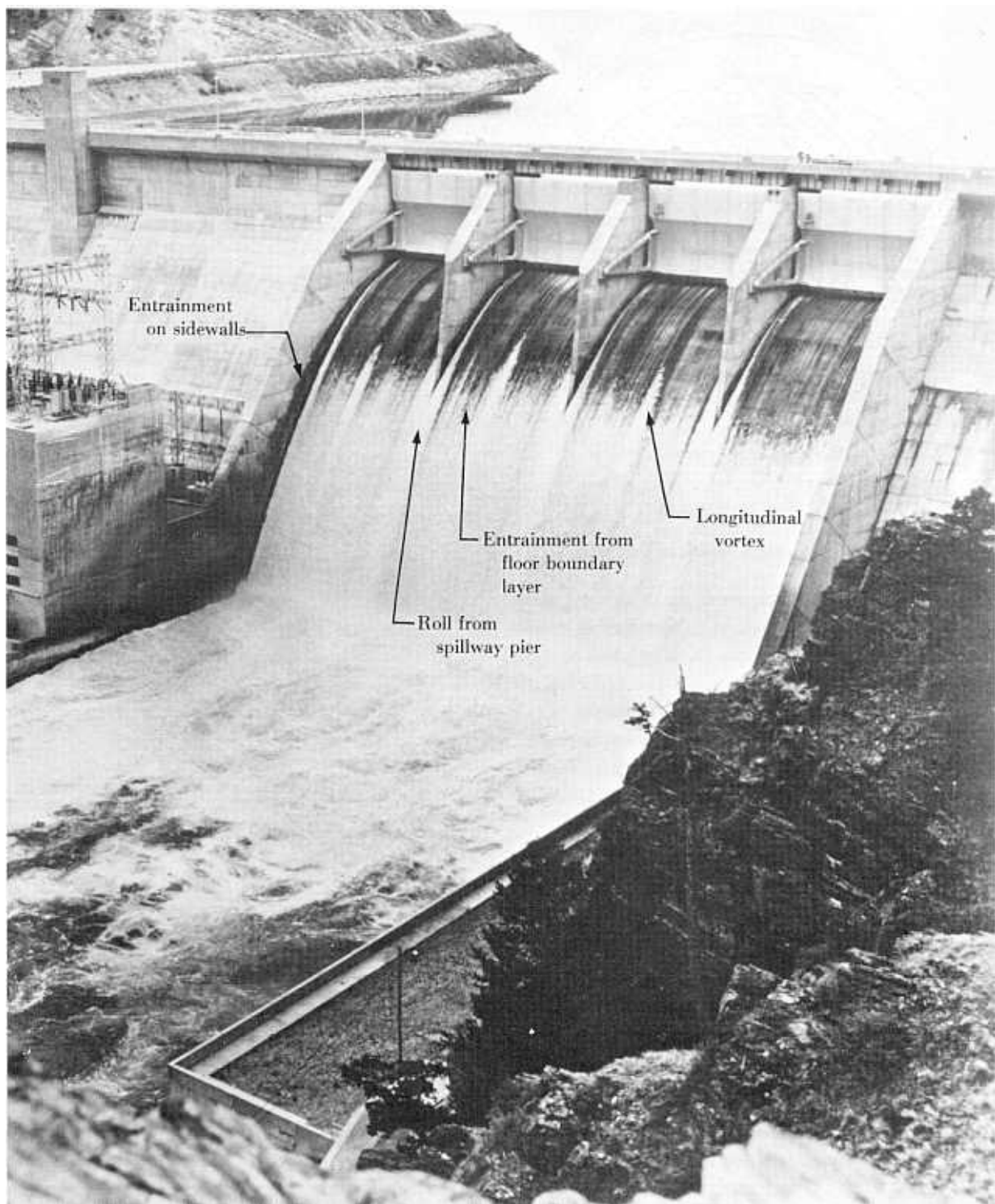


FIGURE 1.—Forms of air entrainment on a spillway—Canyon Ferry Dam, Montana. P801-D-79276

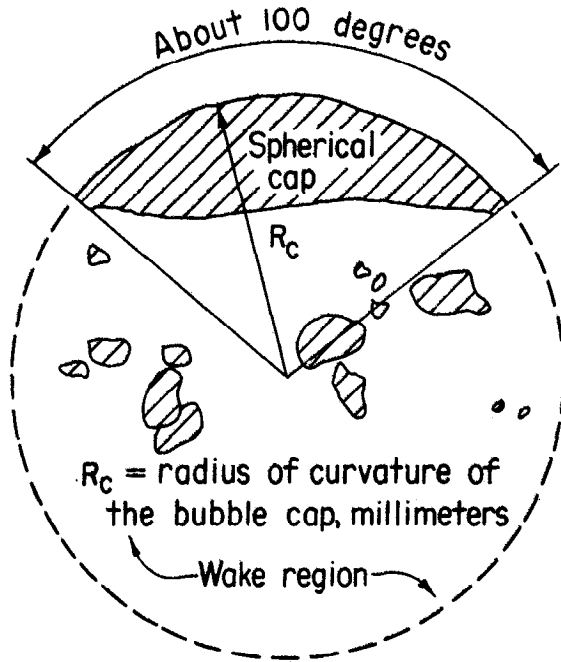


FIGURE 2.—Large gas bubble in a liquid.

10 mm, its form changes from a sphere to a spherical segment. When the diameter is about 2 mm, an instability in the bubble path can be observed. This instability gives the bubbles an irregular or spiral trajectory. Comolet [17] argues that in this region both buoyant and surface tension forces are significant with respect to inertial forces, and proposes the equation

$$V_t = \left(1.04 g R_b + \frac{1.07 \sigma}{\rho_w R_b} \right)^{1/2}, \text{ m/s} \quad (4)$$

where

R_b = the radius of a sphere whose volume equals the volume of the gas bubble, mm

$$= \left(\frac{3\omega}{4\pi} \right)^{1/3}$$

g = gravitational constant = 9.81 m/s²

σ = interfacial surface tension

σ = 0.0728 N/m for air-water

ρ_w = water density = 988 kg/m³

ω = volume of gas bubble, mm³

Using the above values for various constants gives

$$V_t = [0.01 R_b + (0.079/R_b)]^{1/2} \quad (5)$$

For bubbles larger than 10 mm, the terminal velocity is only a function of the ratio between the buoyant and inertial forces. Davies and Taylor [18] show the terminal velocity is

$$V_t = \frac{2}{3} (g R_c)^{1/2} \quad (6)$$

where R_c is the radius of curvature of the bubble cap.

Using this relation and the spherical segment geometry of figure 2, the terminal velocity in terms of an equivalent radius can be shown to be equal to

$$V_t = (g R_b)^{1/2} \quad (7)$$

or

$$V_t = 0.10 R_b^{1/2} \quad (8)$$

for R_b in millimeters and V_t in meters per second.

This equation approaches Comolet's relation (eq. 4) asymptotically when the bubble radius becomes large.

Bubble Size in Shear Flows

The mean bubble size in flowing water or in mechanically agitated systems is determined primarily by the shearing stresses within the fluid. This effect can be visualized by examining the two extreme conditions. Assume that very small bubbles are introduced into a turbulent flow. As the bubbles rise, they tend to form into a mass or agglomerate because of entrainment in each other's wake. As the individual bubbles touch they coalesce to form a

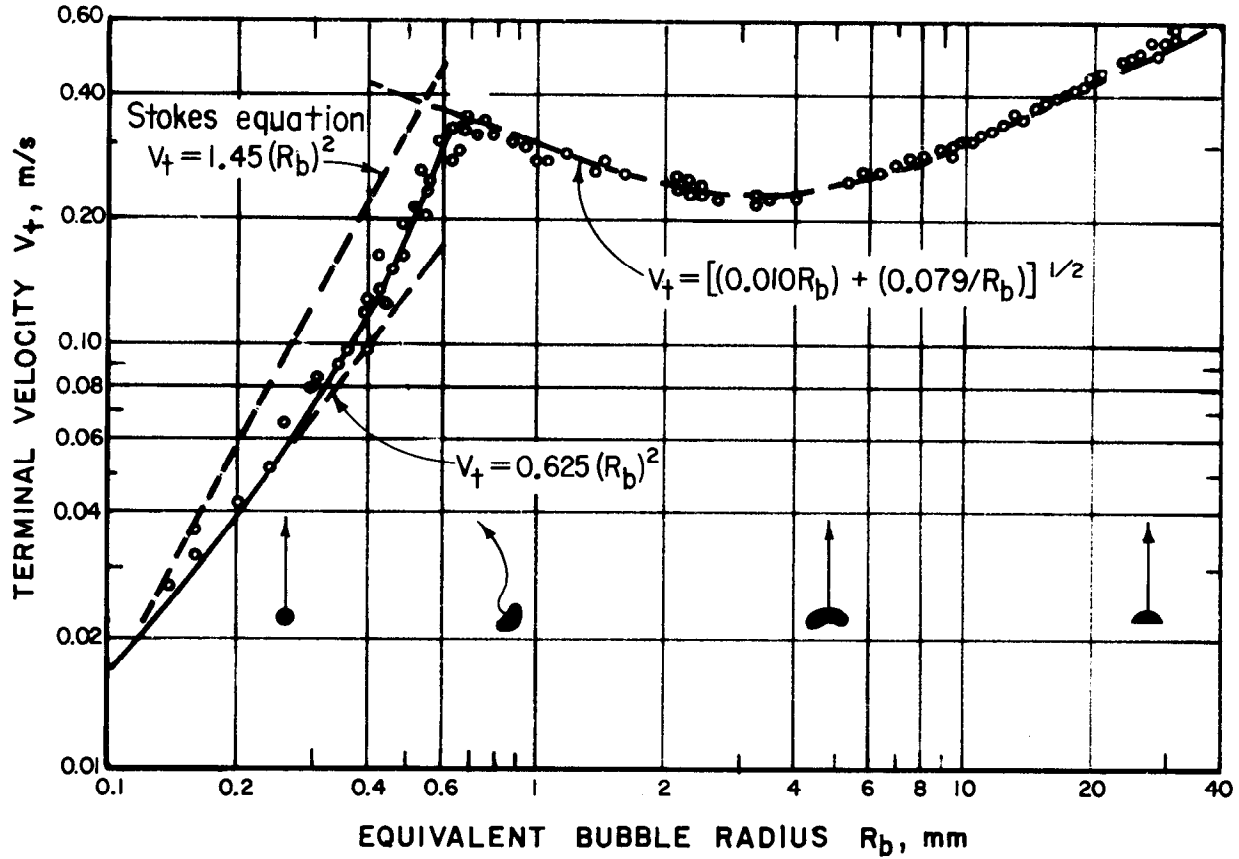


FIGURE 3.—Terminal velocity of air bubbles in filtered or distilled water as a function of bubble size, Haberman and Morton [26].

larger bubble. This process continues until larger and larger bubbles are formed.

At the other extreme, assume that a very large bubble is introduced into a turbulent flow. The turbulence of the flow field introduces shear stresses which tends to tear or fracture the bubble into smaller and smaller bubbles.

Due to the simultaneous action of agglomeration and fracture, it can be inferred that some critical bubble size is reached which represents a balance between surface tension forces and fluid stresses. This relation is expressed through a suitably defined Weber number W . The only equation available for estimating the

critical bubble size was developed by Hinze [35]. The equation is

$$d_{95} = 0.725 \left[\left(\frac{\sigma}{\rho_w} \right)^3 \left(\frac{M}{P} \right)^2 \right]^{1/5} \quad (9)$$

where

d_{95} = bubble diameter for which 95 per cent of the air, by volume, is contained in bubbles of this diameter or smaller

P/M = rate of energy dissipation per unit mass

ρ_w = fluid density

σ = interfacial surface tension

The rate of energy dissipation per unit mass for flow in pipes can be estimated in the following manner; Rouse [59] showed that the rate of energy dissipation in a length of conduit L is given by

$$P = Q \gamma h_l \quad (10)$$

where

Q = discharge

h_l = head loss through a length of conduit L

γ = specific force of fluid

The unit mass is given by

$$M = q_w AL = \frac{q_f Q L}{V} \quad (11)$$

where

A = cross sectional area of conduit

V = mean flow velocity

Therefore, for flow in conduits, the rate of energy dissipation per unit mass is given by

$$\frac{P}{M} = \frac{gh_l V}{L} = g S_f V \quad (12)$$

where S_f = slope of energy grade line = h_l/L

Substitution of the rate of energy dissipation per unit mass of equation 12, into 9 gives

$$d_{95} = 0.725 \left[\left(\frac{\sigma}{q_w} \right)^3 \left(\frac{1}{g S_f V} \right)^2 \right]^{1/5} \quad (13)$$

In dimensionless terms equation 13 can be written as

$$\frac{d_{95}}{D} = 0.658 \left[\left(\frac{\sigma}{\gamma D^2} \right)^3 \left(\frac{D^5 g}{Q^2} \right) \left(\frac{1}{S_f} \right)^2 \right]^{1/5} \quad (14)$$

where D = conduit diameter

The first dimensionless ratio $\gamma D^2/\sigma$ is known as the Bond, Eotvös or Laplace number. The second ratio $D^5 g/Q^2$ is another form of the Froude number $V/(gD)^{1/2}$. Additional information concerning the mean concentration distribution of the bubbles and the direction of their motion in nonhorizontal flows can be found in this chapter (Design Parameters—*Air distribution in the mixing zone*) and in the following chapter (Flow in Partially Filled Conduits—Analytic Estimates).

Terminal Velocity of Bubbles in Turbulent Flow

Even though a bubble diameter can be determined for turbulent flow from equation 14, the terminal velocity of these bubbles cannot be determined simply from figure 3. The figure can be used only to estimate the terminal velocity of single bubbles in still water. Both turbulence and the presence of other bubbles modify the terminal velocity shown on figure 3.

As with sediment particles, turbulence tends to keep the air bubbles in suspension. Thus, the effect of turbulence is to reduce the terminal velocity of the bubbles. If V_t is the terminal velocity of bubbles in still water, then V_f is the terminal velocity in a turbulent flow. Their relation can be expressed as

$$V_f = a V_t \quad (15)$$

where a is an empirically determined variable.

Haindl [28] determined the relation between the variable a and a form of the Froude number F applicable to annular jumps. By making appropriate assumptions, the Froude numbers were converted to equivalent quantities of the dimensionless discharge parameter. The relation between the variable a and the dimensionless discharge parameter is given on figure 4.

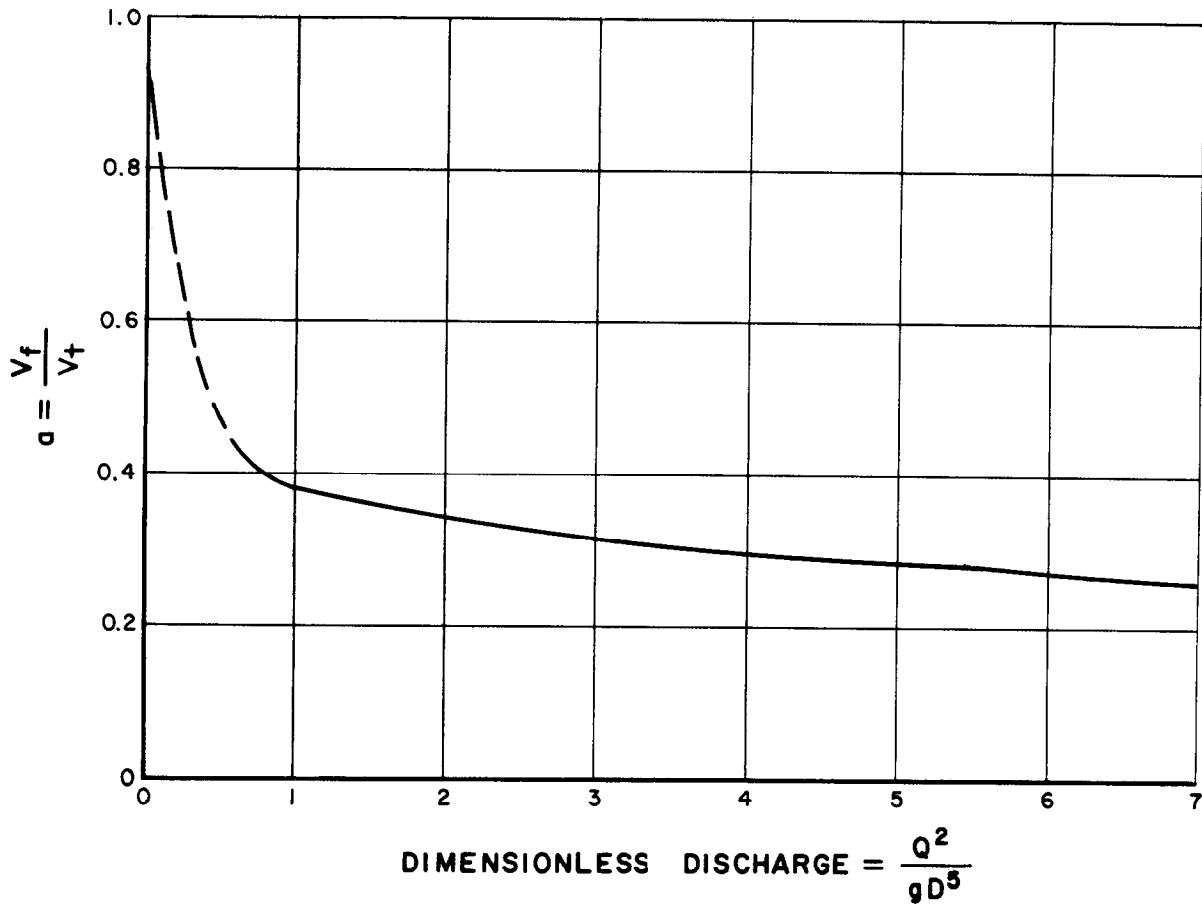


FIGURE 4.—Terminal velocity of bubbles in turbulent flow.

The effect of turbulence on the bubbles can be visualized by considering the buoyant and the turbulent diffusion forces acting on the bubbles. The bubbles tend to move upward because of buoyancy. Whereas turbulence tends to move bubbles from areas of high concentration into areas of low concentration. The balance between mass flow rates caused by these two forces is given—normal to the channel bed by

$$CV_f = \epsilon \frac{dC}{dy} \quad (16)$$

where

C = local air concentration

V_f = terminal velocity of bubbles in turbulent flow

y = vertical direction

ϵ = mass transfer coefficient of bubbles

If a functional relation could be obtained for V_f and ϵ , then the air concentration as a function of depth could be determined.

References could not be found that indicate the magnitude of the effect of air concentration on the terminal velocity of a bubble. Further

research into the effects of turbulence and air concentration on air bubble dynamics definitely is needed.

VERTICAL AND LONGITUDINAL FLOW STRUCTURE

The vertical structure of the flow in open channels with highly turbulent flows can be divided into four zones, Killen [41] and Killen and Anderson ([42], fig. 5). These are:

1. An upper zone of flying drops of water,
2. A mixing zone where the water surface is continuous,
3. An underlying zone where air bubbles are diffused within the water body, and
4. An air free zone.

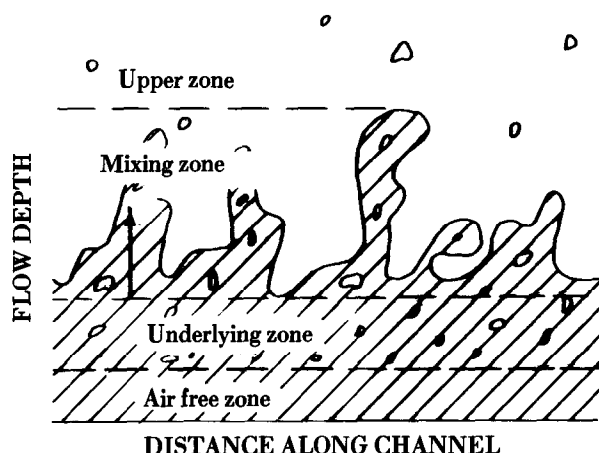


FIGURE 5.—Structure of open channel flow, Killen and Anderson [42].

The *upper zone* consists of water particles that have been ejected from the mixing zone. These particles can rise a considerable distance above the mean water surface. Normally, this region is neglected in engineering considerations since its mass is small.

The *mixing zone* consists of a region of surface waves having random amplitudes and frequencies. A knowledge of the characteristics in

the mixing zone is extremely important since all air ingested into the main body of the water or released from the flow must pass through this zone. Also, the maximum wave heights that occur in the mixing zone determine the height of the open channel sidewalls if overtopping is to be prevented.

The *underlying zone* is a region into which the waves do not penetrate. The air concentration at any depth in this zone is determined by the number of air bubbles and their size. The primary factor influencing the air concentration distribution is the turbulence intensity distribution throughout the flow. Using turbulent boundary layer theories, it has been possible to develop correlations for the air concentration distribution in this zone. However, the problem has not been solved completely since the air bubbles tend to inhibit the turbulence. The interrelations between air concentrations, bubble size distribution, and turbulence intensities have not been determined yet.

An *air-free zone* exists only in that section of the channel where aeration is still developing. In most practical applications, the boundary between the air free zone and the underlying zone cannot be determined accurately. At the interface, the air concentration has a very small value and the rate of change in concentration with depth is small. Halbron et al., [31] noted extremely fine bubbles which could not be detected near the bottom of their channel by the air concentration measuring apparatus; this indicates that the location of the interface may in fact be a function of the sensitivity of the measuring instrument.

In addition to defining the flow structure in a vertical plane, it also is possible to identify flow regimes in a longitudinal direction for flow in a wide channel. Here, a wide channel is defined as one in which the channel width is greater than five times the flow depth. Borman [11] identifies three distinct regions in self-aerating flows in wide channels. They are:

1. A regime of no air entrainment where the turbulent boundary layer has not reached the water surface,
2. A regime of developing air entrainment in which the air concentration profiles are not constant with distance, and

3. A regime of fully developed air entrainment in which the air concentration profiles are constant with distance.

Keller, Lai, and Wood [39] divide Bormann's middle regime into two sections. The first is a region where the aeration is developing, but the air has not reached the bottom of the chute. The second is a region where the air has reached the bottom of the chute, but the air concentration profile continues to vary with distance (fig. 6).

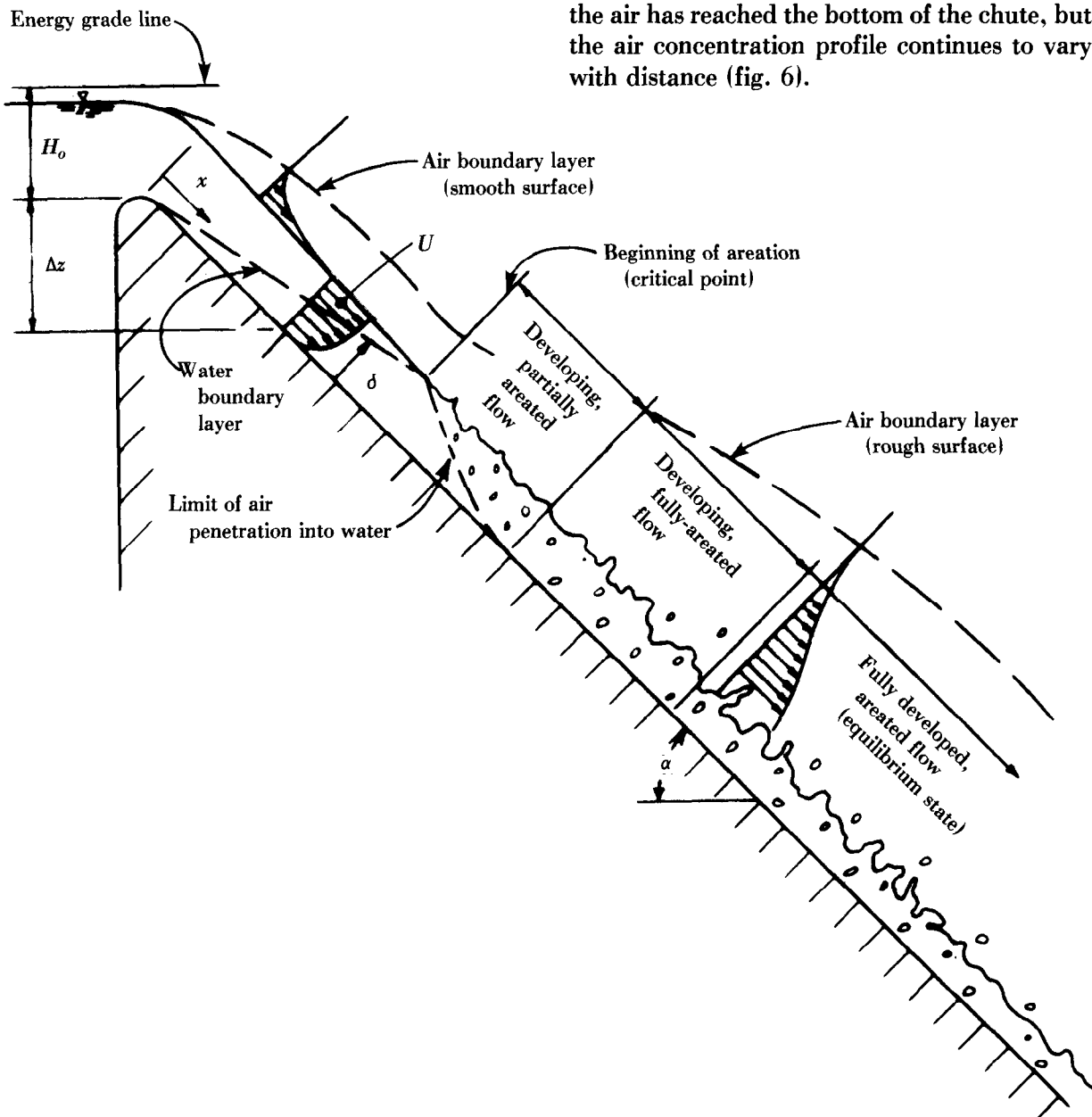


FIGURE 6.—Air entraining flow regimes in open channel flow.

DESIGN PARAMETERS

From an engineering viewpoint, the significant parameters in the design of a conveyance structure are:

- Distance to the beginning of aeration
- Distance to fully develop aerated flow
- Mean air concentration in the flow
- Flow depth of the aerated flow
- Water and air velocities in the aerated flow

The results of investigations concerning these parameters are presented in the following sections.

Location of Beginning of Aeration

The point at which "white water" begins in a wide channel generally is accepted to be the location where the turbulence effects generated at the channel floor first reach the water surface. Many different investigators have proposed equations for the location of this so-called "critical point." Many of the early predictions were rather poor. However, as the understanding of boundary layer growth over smooth and rough surfaces has improved, predictions of the "critical point" location also have improved. Although some questions concerning the theory still exist, present methods yield results that are sufficiently accurate for engineering purposes.

Typical examples of early correlations for the boundary layer thickness δ are those by Annemuller [4] who gave

$$\frac{\delta}{x} = 0.01 \quad (17)$$

where x = distance from start of boundary layer growth,

Hickox [34] who gave

$$L_c = 14.7 q^{0.53} \quad (18)$$

where

L_c = distance to start of self-aeration

q = unit discharge, cubic feet per second per foot of width,

and Beta et. al., [10] who recommended values of

$$\frac{\delta}{x} \text{ between } 0.016 \text{ and } 0.01.$$

Schlichting [63] applied the results of measurements made in a pipe directly to a flat plate and found that the boundary layer thickness was given by

$$\frac{\delta}{x} = 0.37 \left(\frac{Ux}{\nu_f} \right)^{-0.2} \quad (19)$$

where

x = distance measured from the chute entrance

U = free stream velocity

δ = distance from the boundary at which the velocity equals 99 percent of U

ν_f = kinematic viscosity of water

The free stream velocity is

$$U = [2g(\Delta z + H_o - d \cos \alpha)]^{1/2} \quad (20)$$

where

d = water depth of computational point

g = gravitational constant (acceleration)

H_o = total head on crest

Δz = difference in elevation from crest to computational point

α = angle channel makes with horizontal

Equation 19 is also the expression used by Rouse [59] for flow over smooth surface. In

analyzing the results of Bauer [8], Halbronn [30] showed that the value of the coefficient for open channel flow should be equal to 0.16 instead of 0.37.

Equation 19 neglects two important considerations:

1. The surface can be hydraulically rough, and
2. Intermittent turbulence is present at a distance of up to 1.2δ from the channel floor.

A hydraulically rough surface is one in which

$$\frac{u_* k_s}{\nu_f} \geq 70 \quad (21)$$

where

k_s = equivalent sand grain roughness

ρ_w = water density

τ_o = wall shear stress

u_* = shear velocity = $(\tau_o/\rho_w)^{1/2}$

If the surface is rough, then the effect of the roughness height must be included in the computations.

The second consideration means that "white water" generally will occur before the boundary layer, as previously defined, actually reaches the water surface. Bormann [11] circumvented this difficulty by redefining the boundary layer thickness. Keller and Rastogi [40] recognized the same problem. Their point of incipient air entrainment also occurs at a location which lies somewhat above the previously defined boundary layer thickness. Thus, these methods account for the intermittent turbulence that occurs outside the conventionally defined boundary layer thickness.

Bormann [11] used a rather novel method of determining the "critical point." Bormann's method involves the simultaneous solution of equations relating local loss coefficient C_f , boundary layer thickness δ , and the distance Reynolds number R_x . In Bormann's scheme the local loss coefficient can be viewed as a

parametric term through which the other parameters are related. The appealing aspect of this approach is that it can be compared with the presently available equations for flow over smooth and rough boundaries.

The correlations relating the boundary layer thickness δ and the local loss coefficient C_f are

$$\frac{1}{C_f^{1/2}} = 3.85 \log \left(\frac{\delta U}{\nu} C_f \right)^{1/2} + 3.67 \quad (22)$$

for hydraulically smooth surfaces, and

$$\frac{1}{C_f^{1/2}} = 3.85 \log \left(\frac{\delta}{k_s} \right) + 6.45 \quad (23)$$

for hydraulically rough surfaces.

The correlation between distance Reynolds number and the local loss coefficient was determined empirically from

$$C_f = \frac{b_s}{(\log R_x)^{2.38}} \quad (24)$$

where R_x = distance Reynolds number = $\frac{Ux}{\nu}$

The b_s value (fig. 7) can be approximated by

$$b_s = 0.32 + 8.15 k_s^{0.47} \quad (25)$$

where

b_s = empirical coefficient accounting for sand grain roughness

k_s = equivalent sand grain roughness, mm

Alternatively, the value of b_s can be approximated by

$$b_s = 0.66 k_s^{0.23} \quad (26)$$

For this approximation, the sand grain roughness must be equal to or greater than 0.01 mm; any smaller values represent a smooth surface.

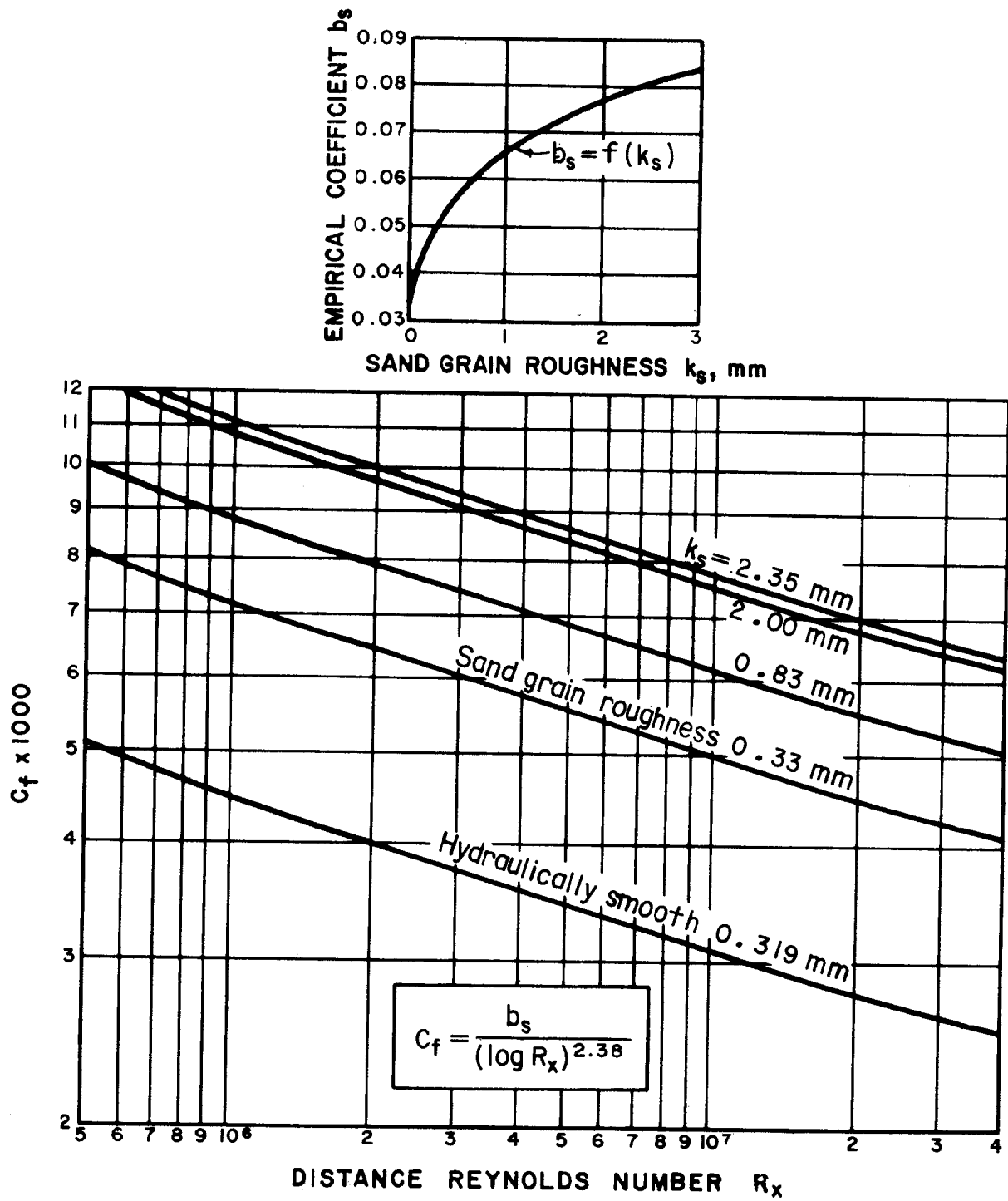


FIGURE 7.—Experimentally determined local loss coefficient C_f , Bormann [11].

To solve these equations it is necessary to use the following trial and error procedure.

- a. Determine the energy grade line elevation H_o where y_k equals the critical depth from

$$H_o = 1.5 (y_k)^{1/2} = 1.5 \left(\frac{q^2}{g} \right)^{1/3} \quad (27)$$

- b. Estimate the water depth d at a given distance x from the entrance
- c. Calculate the freestream velocity U from

$$U = [2g(H_o x + \sin \alpha - d \cos \alpha)]^{1/2} \quad (29)$$

- d. Determine the local loss coefficient C_f as a function of the boundary layer thickness δ using equations 22 or 23 as appropriate. In these equations the flow depth assumed in b. is used for the boundary layer thickness.
- e. Calculate the local loss coefficient as a function of distance Reynolds number from equation 24 where the distance Reynolds number is defined as

$$R_x = \frac{Ux}{\nu} = \frac{U^3}{2g \nu \sin \alpha} \quad (30)$$

- f. Repeat steps b. through e. with revised values of depth until the same values are obtained for the local loss coefficients in equations 22 or 23 and 24.

As an example, this procedure was applied to a surface having a sand grain roughness k_s , which corresponds to a float finish concrete surface. This finish is equivalent to a Manning's roughness coefficient of 0.013. The results are presented in a set of design curves shown on figure 8. Similar curves can be prepared for other values of Manning's coefficients.

Finally, the latest development in calculating the distance to the point of air entrainment is by Keller and Rastogi [40]. Their method involves

integrating the equations of motion using a finite element scheme. The calculated velocity profiles agree very well with the experimentally determined values. However, their studies have not been put into a form that is useful for designers.

Location of Fully Aerated Flow

The location at which the flow becomes fully aerated has not been studied. Straub and Lamb [67] show that a constant air concentration distribution can be achieved, but the distance required for its development is not specified. Bormann [11] measured the location of the air-water interface, but not the concentration profile. For Bormann's results one can imply that the length of the developing aeration regime is of the same order as the length of the developing boundary layer regime.

Keller, Lai, and Wood [39] indicate that the length of the developing aeration region can be defined in terms of the air concentration. In their definition, the length of the developing region is at least as long as the distance from the "critical point" to a location where a 5-percent air concentration has reached middepth of the total flow depth. The data by Straub and Lamb [67] show that this criterion is inadequate.

The length of the developing aeration regime cannot be determined analytically. This is one area in which additional research could be pursued gainfully.

Air Concentration Profiles

Definition of concentration.—The conventional definition of concentration is the quantity—usually measured by volume—of a material A either dissolved or suspended in another material B. Thus, if material A is air and material B is water, air concentration would be the volume of air in a given volume of water.

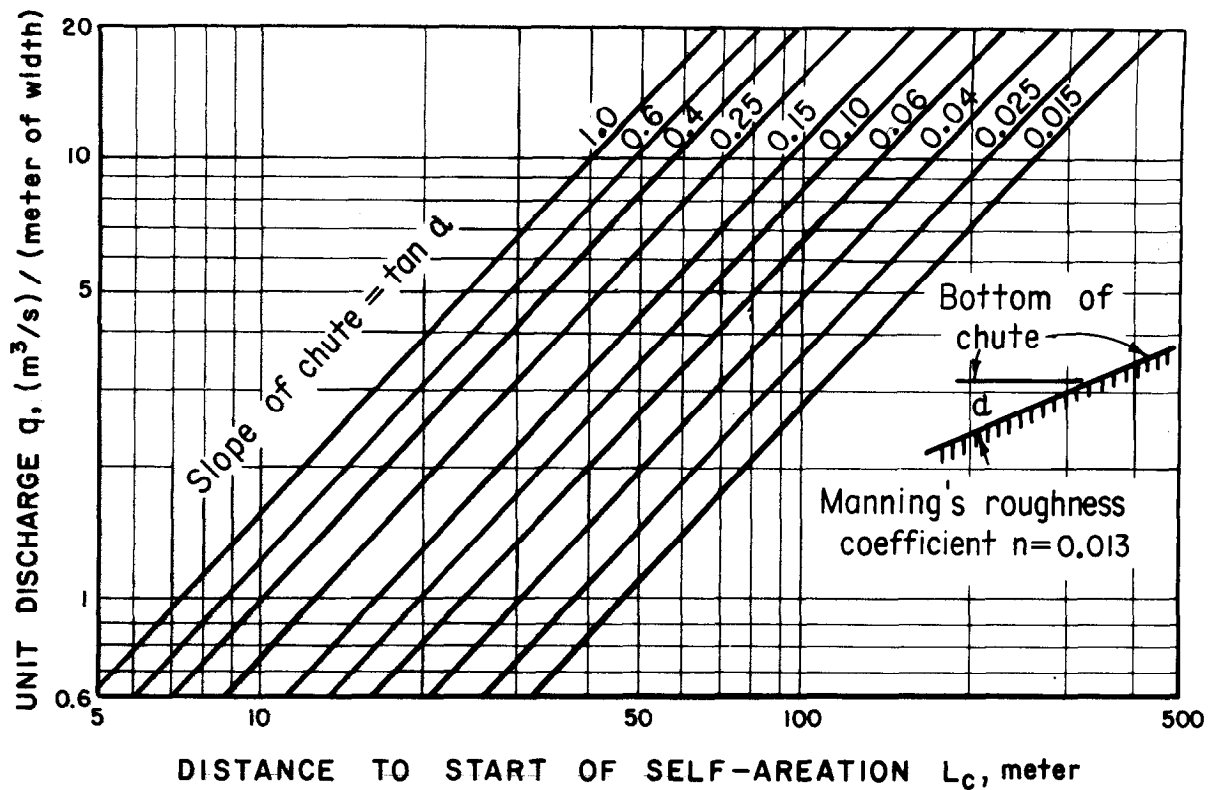


FIGURE 8.—Location of inception of air entrainment.

However, when the amount of suspended material becomes large, the reference volume is the sum of the volume of material B and the volume of material A. In this case the average air concentration \bar{C} is given by

$$\bar{C} = \frac{\omega_a}{\omega_a + \omega_w} \quad (31)$$

where

ω_a = volume of air
 ω_w = volume of water

This latter definition of concentration is used throughout this report.

The concentration also can be expressed in terms of volumetric flow rates as

$$\bar{C} = \frac{Q_a}{Q_a + Q_w} = \frac{\beta}{\beta + 1} \quad (32)$$

where

Q = discharge
 $\beta = Q_a / Q_w$

The early method of measuring the concentration of air-water flows used a pitot-tube-type sampler developed by Viparelli [72]. This type of device gives accurate results in the *underlying zone* (fig. 4). However, in the *mixing zone*, the sampler records not only air in water, but also the air between the waves. Therefore, the measurements indicate air concentrations that are too large in the mixing zone. It should be noted that in some cases the total air discharge and not air concentration is desired. For instance, in closed conduit flow, the total air discharge is required for proper vent sizing. In this case, the pitot tube sampler would yield the desired air flow quantities in all four air flow zones.

Killen and Anderson [42] showed that the air concentration—as indicated by a pitot tube sampler—is related to the actual air concentration in the water by

$$C_a = \frac{C_m - 1 + P_w}{P_w} \quad (33)$$

where

C_a = actual air concentration in percent of volume

C_m = air concentration measured by a pitot tube sampler

P_w = probability that the water surface is equal to or greater than the given elevation (refer to the following sec.—*Air distribution in the mixing zone*)

The water surface probability in equation 33 can be measured with electrical probes described by Killen [41]. He also reported on an electrical device that measures the actual air concentration directly.

Almost all references to air concentration in the bibliography include values for the amount of air between the waves. Therefore, values for the amount of air in flowing water generally are excessive. Unless noted otherwise, the term “air concentration” refers only to the amount of air actually entrained in water.

Air distribution in the mixing zone.—Many investigators have observed that measured air concentration distribution obeys one law in the *mixing zone* and another in the *underlying zone*. Apparently, these two laws were discovered by Anderson [2] who examined the results of a large number of experiments.

Investigators reasoned that in the *mixing zone* the air concentration should follow a

Gaussian law of normal probability, since this is also the law for the wave height distribution. They found the relation is given by

$$\frac{dC_m}{dy} = \frac{2(1-C_t)}{h\pi^{1/2}} \exp \left[-\left(\frac{y'}{h} \right)^2 \right] \quad (34)$$

where

C_m = air concentration (including the air between the waves) at any elevation in percent of total volume

C_t = air concentration at the bottom of the mixing zone

h = mean wave height = $2^{1/2}s$

s = standard deviation of the wave height distribution

y = distance normal to the channel bottom

y' = distance normal to the bottom of the mixing zone, figure 5

The integral form of the equation is

$$\frac{1-C_m}{1-C_t} = \frac{2}{\pi^{1/2}} \int_{y'}^{\infty} \exp \left[-\left(\frac{y'}{h} \right)^2 \right] d\left(\frac{y'}{h} \right) \quad (35)$$

This equation is almost identical to the cumulative Gaussian or normal distribution function

$$P_g = \frac{1}{(2\pi)^{1/2}} \int_{-\infty}^{\eta} \exp \left(-\frac{\eta^2}{2} \right) d\eta \quad (36)$$

where $\eta = y'/s$

The air distribution equation, equation 35, includes a factor of 2 because the relation applies to positive values of y' ; whereas equation 36 applies to both positive and negative values

of y' . By reversing the limits of integration in equation 36, it can be shown that

$$\frac{1}{(2\pi)^{1/2}} \int_{\eta}^{\infty} \exp\left(-\frac{\eta^2}{2}\right) d\eta = 1 - P_g \quad (37)$$

Combining equation 35 with equation 37 gives

$$\frac{1 - C_m}{1 - C_t} = 2(1 - P_g) \quad (38)$$

Values of the normal distribution function P_g can be found in statistics texts. A graphical representation of the normal distribution function and the air concentration distribution is given in figure 9.

The actual air concentration in the waves is a function of the wave height probability and the air concentration at the bottom of the mixing zone. The relation is given by

$$C_a = \frac{P_w - 2(1 - C_t)(1 - P_g)}{P_w} \quad (39)$$

For the wave height distribution given in this chapter (Design Parameters—Water Surface Location), a family of curves can be derived for the actual air concentration distribution in the *mixing zone* (fig.10). The maximum upper limit of these curves is discussed in the following subsection *Mean air concentration*.

These distributions are valid for both the developing and the fully developed aerated flow regimes. They can be used for the determination of the air concentration at any elevation if the standard deviation of wave height distribution and the air concentration at the bottom of the mixing zone are known. Unfortunately, these parameters can neither be predicted in the developing aerated flow regime nor in the fully developed aerated flow regime. Therefore, the equations only can be used to fit experimental data. Additional research is needed in this area.

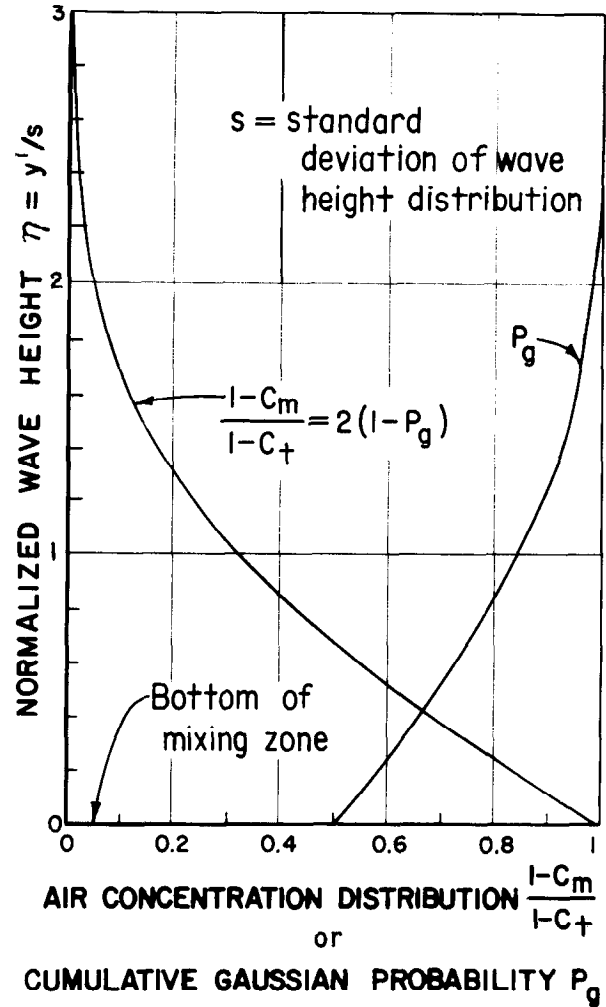


FIGURE 9.—Cumulative Gaussian probability and measured air concentration distributions in the mixing zone.

Air distribution in the underlying zone.—The *underlying zone* consists of a region into which waves do not penetrate. Straub and Anderson [66] were successful in deriving an equation that describes air distribution in this zone (also refer to Streeter [68]).

They defined the bubble mass transfer coefficient ε as

$$\varepsilon = \xi k (\tau_o / Q_l)^{1/2} \left(\frac{d_t - y}{d_t} \right) y \quad (40)$$

where

d_t = total depth of underlying and air free zones

k = Von Karman universal constant equal to 0.4

ξ = air concentration distribution constant

ρ_l = liquid density

τ_o = wall shear stress

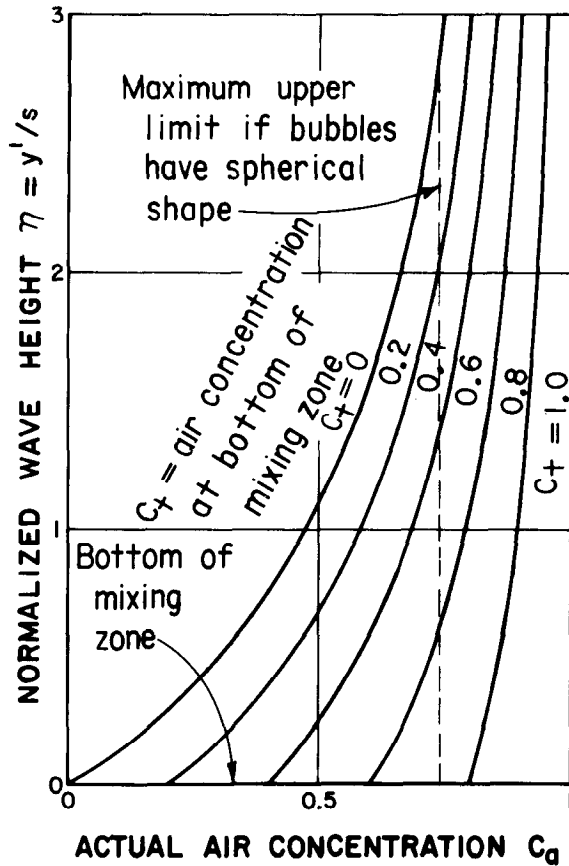


FIGURE 10.—Actual air concentration distribution in the mixing zone.

This relation makes ϵ equal to zero at both the channel floor and at the interface between the *mixing zone* and the *underlying zone*. Actually, the expression is not valid at the interface since air is transported across the boundary. However, by substituting equation

40 for the mass transfer coefficient ϵ into equation 16—and assuming the terminal velocity of bubbles is constant—upon integration one obtains

$$C = C_1 \left(\frac{y}{d_t - y} \right)^m \quad (41)$$

where

$$m = \frac{V_f}{\xi k (\tau_o / \rho_l)^{1/2}} = \frac{V_f}{\xi k u_*}$$

C = local air concentration

C_1 = air concentration at $d_t/2$

u_* = shear velocity = $(\tau_o / \rho_l)^{1/2}$

This equation fits the data well for fully developed aerated flows by properly selecting C_1 , d_t , and m (fig. 11). The measured air concentration distribution in the *mixing zone* given by equation 38 also will give good results. The satisfactory fit of the data with these two equations implies that turbulent diffusion and buoyancy are the two most important factors affecting the determination of the air concentration distribution in the fully developed aerated flow zone.

In the developing aerated flow regime, equation 41 is not valid. In the developing aeration regime two conditions must be considered. The first condition is where air is being insufflated into the flow. For this case, the governing equation is

$$q_a = \epsilon \frac{dC}{dy} - CV_f \quad (42)$$

where q_a = insufflation rate of air per unit surface area

The other condition is that of excess air being present in the water. In this condition, air is released from the flow until an equilibrium state is reached. Equation 42 also is valid for this condition except the sign q_a will be negative which indicates that air is leaving the water.

$C_1 = \text{AIR CONCENTRATION AT } d_+/2$

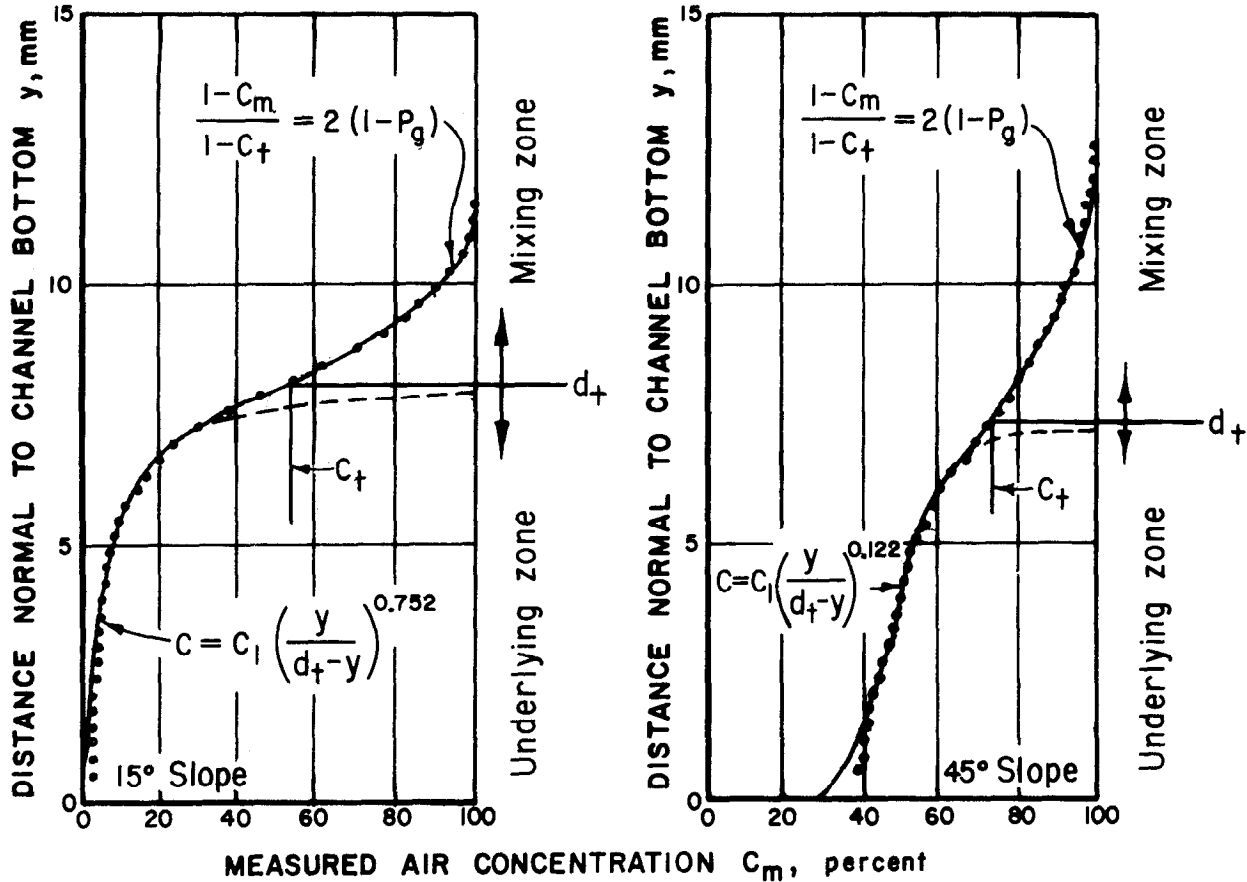


FIGURE 11.—Air concentration distributions of channel flow on steep slopes, Straub and Anderson [66].

Killen [41] measured air concentration distributions for the first condition of air insufflation. However, no one has developed equations for the observed distribution. This is another area needing additional research.

Mean air concentration.—The mean air concentration for the entire flow stream is defined by

$$\bar{C} = \frac{1}{d_m} \int_0^{d_m} C_a dy \quad (43)$$

The depth d_m represents some upper bound for the water surface. Straub and Anderson [66]

define the depth as representing that point where the measured air concentration is 0.99. A more reasonable reference depth would be the depth which is exceeded by only 1 percent of the waves.

The air concentration C_a in equation 43 is the actual air concentration and does not include air moving between the waves (in this chap., Design Parameters—*Definition of concentration*). However, all the published data were measured with a pitot-tube-type sampler and, thus, include the interwave air motions in the *mixing zone*. The mean air concentration \bar{C} based on the actual air concentration C_a distribution can be estimated by the following

reasoning. The upper limit of the air concentration can be approximated by assuming the bubbles to be spherical. If they retain a spherical shape, Gardner [23] showed that the air concentration for the bubbles packed in their most dense configuration is about 75 percent. The upper limit for the Straub and Anderson data [66] is about 84 percent. Thus their data are roughly 12 percent too high.

Since the air concentration is obtained from an integration of the local air concentration distribution, buoyancy and turbulent diffusion must be the most significant parameters which influence the mean concentration for any flow. The buoyant forces are governed primarily by the bubble size. With respect to turbulence, Hinze [35] indicates that bubbles tend to be broken up by both viscous shear forces and turbulent shear forces. This tendency to be broken up is resisted by interfacial tensile forces. For high enough degrees of turbulence, the viscous shear forces are insignificant with respect to the turbulent shear forces. With solid boundaries the significant parameter defining the turbulent shear forces is the wall shear stress, τ_o .

The following presents the development of an empirical equation to predict the mean air concentration in the fully developed aerated flow zone. The development is based upon the classical methods of dimensional analysis.

Assuming that buoyancy and turbulent diffusion are significant, it is possible to express the volume flow of air Q_a as a function of:

- Gravity
- Turbulent shear stress
- Interfacial forces
- Fluid properties of both air and water
- Characteristic flow dimensions

The expression is

$$Q_a = f(V, b, d, g, \mu_a, \mu_w, Q_a, Q_w, \sigma, \tau_o) \quad (44)$$

where

Q_a = volume flow of air, m^3/s

V = water velocity, m/s

b = width of flow channel, m

d = water depth, m

g = gravitational constant (acceleration) = 9.81 m/s^2

μ = dynamic viscosity, $\text{N} \cdot \text{s}/\text{m}^2$

ρ = density, kg/m^3

σ = interfacial surface tension, N/m

τ_o = wall shear stress, Pa

$f(\)$ = denotes "a function of"

Subscripts a and w refer to air and water, respectively.

Using V , d , and ρ_w as the repeating variables results in the following dimensionless parameters.

$$\begin{aligned} & \frac{Q_a}{V^2} \\ & = f \left(\frac{\tau_o}{V^2 \rho_w}, \frac{\sigma}{V^2 d \rho_w}, \frac{Q_a}{Q_w}, \frac{\mu_a}{\mu_w}, \frac{\mu_w}{V d \rho_w}, \frac{b}{d}, \frac{g d}{V^2} \right) \end{aligned} \quad (45)$$

By examining the magnitude of these dimensionless terms and transforming some of them, it is possible to develop parameters that should be used for correlating the available model and prototype data. For instance, the dependent parameter can be written as

$$\frac{Q_a}{V d^2} = \frac{Q_a}{V d b} \left(\frac{b}{d} \right) = \frac{Q_a}{Q_w} \left(\frac{b}{d} \right) \quad (46)$$

Since

$$\beta = \frac{Q_a}{Q_w} \quad \text{and} \quad \bar{C} = \frac{\beta}{\beta + 1}$$

by definition, the mean concentration is also a function of the same dimensionless terms given above.

The first independent parameters in the parenthesis of equation 47 can be written as

$$\frac{1}{P^2} = \frac{\tau_o}{V^2 \rho_w}$$

where P = Prandtl velocity ratio = $\frac{V}{(\tau_o / \rho_w)^{1/2}}$

The Prandtl velocity ratio represents the ratio of the inertial force to the wall shear force.

For the condition of uniform flow on a wide, steep chute, the wall shear stress τ_o is given by

$$\tau_o = \gamma d \sin \alpha \quad (47)$$

where

d = flow depth

α = angle chute invert makes with horizontal

γ = specific force of fluid

substituting this into the Prandtl velocity ratio P gives

$$\frac{\tau_o}{V^2 \rho_w} = \frac{\gamma d \sin \alpha}{V^2 \rho_w} = \frac{g d \sin \alpha}{V^2} = \frac{\sin \alpha}{F^2} \quad (48)$$

where F = Froude number = $\frac{V}{(gd)^{1/2}}$

Thus for uniform flow on wide, steep chutes, the parameters $\sin \alpha / F^2$ represents the ratio of turbulent shear forces to the inertial forces.

The tensile force parameter, $\sigma / (V^2 d \rho_w)$, is simply the reciprocal of the Weber number squared

$$\frac{\sigma}{V^2 d \rho_w} = \frac{1}{W^2} \quad (49)$$

where W = Weber number = $\frac{V}{(\sigma / \rho_w d)^{1/2}}$

The Weber number represents the ratio of the inertial forces to the interfacial tensile forces. The surface tension is only a function of temperature (fig. 12)

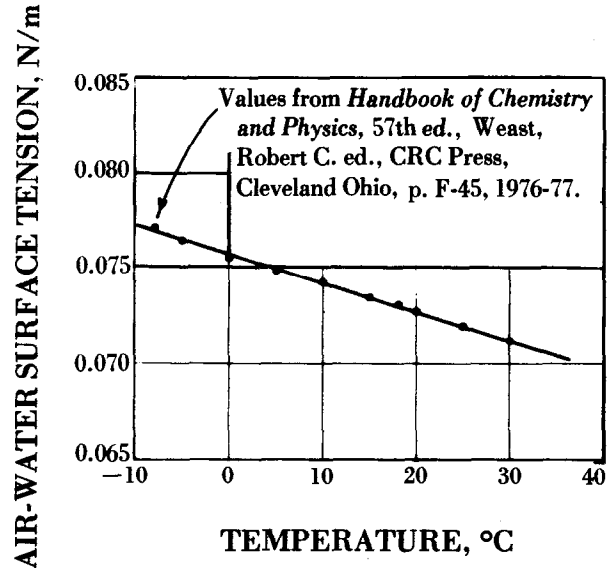


FIGURE 12.—Interfacial surface tension.

The bubble size is determined by the ratio of turbulent shear forces to the interfacial tensile forces. In terms of the previously developed parameters, the ratio is

$$\frac{g d \sin \alpha}{V^2} \left(\frac{V^2 d \rho_w}{\sigma} \right) \quad (50)$$

Reducing this ratio to the first power of V and generalizing results in

$$\frac{(\sin \alpha)^{1/2} W}{F} \quad (51)$$

The ratio of viscous forces to inertial forces can be written as

$$\frac{\mu_w}{V d \rho_w} = \frac{\nu}{V d} = \frac{1}{R} \quad (52)$$

where R = Reynolds number

The use of channel width b and flow depth d in the list of variables implies the use of a rectangular cross section. More generality can be obtained by the use of the hydraulic radius as the significant length parameter. The hydraulic radius is defined by

$$H = A/W \quad (53)$$

where

A = cross sectional area of water prism
 W = wetted perimeter

With the exception of the Froude number, the hydraulic radius seems to be the most appropriate characteristic length to correlate air entrainment for any cross sectional shape.

The effective depth is the characteristic length to be used with the Froude number. The effective depth y_e is defined as

$$y_e = A/B$$

where

A = cross sectional area of water prism
 B = top width of water prism

By using the above transformations, the mean air concentration can be written as

$$\bar{C} = f \left(\frac{(\sin \alpha)^{1/2} W}{F}, W, \frac{Q_a}{Q_{iw}}, \frac{\mu_a}{\mu_w}, R, F \right) \quad (54)$$

Equation 54 represents a seven-dimensional surface. Determining relations between all the variables is practically impossible. However, the problem can be made simpler by neglecting those independent variables which have either a small range of values or a negligible effect on the mean air concentration. For example, the tensile force varies less than 10 percent over the

temperature range normally existing in the field and laboratory (fig. 12). Therefore, the tensile force parameters, W , of equation 49 can be neglected.

Neglecting the tensile force parameter does not mean that the ratio of the turbulent shear to interfacial tensile force parameter also can be neglected. This latter ratio, which governs the bubble diameter, must be retained.

For flows that are turbulent enough to entrain air naturally, the dynamic pressure forces determine the size of the largest air bubbles. These dynamic forces are a result of changes in velocity over distances that are about the same scale as the diameter of the bubble. For typical flows on spillways and in steep chutes the dynamic forces predominate over the viscous forces. Therefore, the dimensionless terms involving viscosity are not significant with respect to the magnitude of the other terms.

Finally, the dimensionless density ratio varies almost linearly from 0.0012 at 4 °C to 0.0011 at 30 °C. Therefore, this term also can be considered as unimportant for the temperature range that is typical in hydraulic structures.

The reduced form of equation 54 is

$$\bar{C} = f \left(\frac{(\sin \alpha)^{1/2} W}{F}, F \right) \quad (55)$$

This equation represents a three-dimensional surface which can be defined from experimental and field investigations. The Straub and Anderson [66] data from model studies and data from prototype studies of Michels and Lovely [54] as well as Thorsky et. al., [70] were used to determine the functional relations between the mean air concentration \bar{C} , Froude number F , and turbulent-interfacial tension force ratio.

The variation of the mean concentration as a function of Froude number was determined

from the model data. For this correlation the turbulent-interfacial tension force ratio was approximately constant. With mean air concentrations less than 0.6, the correlation had the form

$$\bar{C} = a_0 + a_1 F \quad (56)$$

where a_0 is a function of the turbulent to interfacial tension force ratio.

The values of a_1 for turbulent to interfacial tension force ratios of 0.166, 0.114, and 0.085 are 0.0469, 0.0486, and 0.0556, respectively. Although the value of a_1 apparently increases as the turbulent to interfacial tension force ratio decreases, the data are insufficient to support the conclusion. Therefore, a_1 was taken to be equal to the mean of the values or 0.050.

The function a_0 was determined from both the model data and tests on prototype chutes and spillways. The prototype values correspond with the initiation of air entrainment. The values of a_0 were determined from the equation

$$a_0 = \bar{C} - 0.05F \quad (57)$$

The curve

$$a_0 = - \frac{(\sin \alpha)^{1/2} W}{63F} \quad (58)$$

approximately fits the data (fig. 13).

Therefore, the mean air concentration correlation is given by

$$\bar{C} = 0.05F - \frac{(\sin \alpha)^{1/2} W}{63F} \quad (59)$$

for

$$0 \leq \bar{C} \leq 0.6$$

If \bar{C} is greater than 0.6, the air concentration values must be taken from the empirical curves on figure 14.

With the exception of the spillway data, the Froude and Weber numbers were calculated using the relation for normal depth without aeration. The model tests correspond with fully developed aerated flow.

In the absence of any better information, these curves also can be used to estimate the mean air concentration in developing flow. For this case, the Froude and Weber numbers are calculated from the depth and velocity values that result from the gradually varied flow computations without considering aeration of the flow.

The use of these curves are illustrated by an example.

• Example

Given a rectangular chute 15 meters wide, calculate the development of the air entrainment along the length of the chute. The discharge is 20 m³/s. The channel is built on a 1:3 slope and has a Manning's n value of 0.0100.

The computer program HFWS (app. II) was used to compute the water surface profile and the mean air concentrations profile (fig. 15). The program can be used with either drawdown or backwater curves for rectangular, trapezoidal, circular, and transitional cross sections.

Water Surface Location

One of the first concepts that developed in self-entraining flows was bulking. With this concept, the air was considered to be evenly distributed throughout the flow. As a result, the depth of the mixture was increased by a predictable amount (fig. 16). The relation is given by

$$\frac{d_b}{d} = \frac{1}{1 - \bar{C}} \quad (60)$$

where

d = flow depth (without aeration)

d_b = bulked flow depth

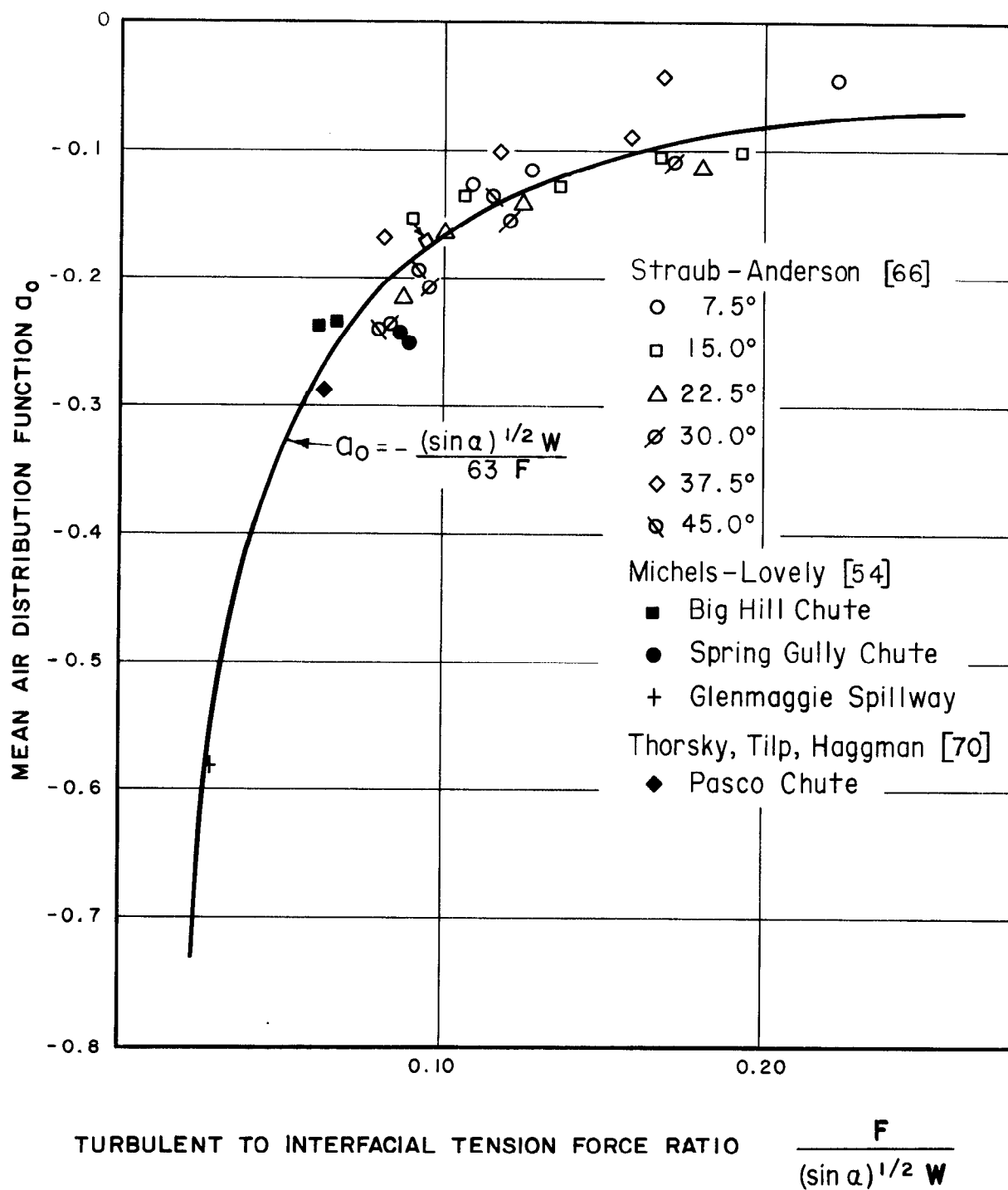


FIGURE 13.—Air entrainment coefficient.

AIR-WATER FLOW IN HYDRAULIC STRUCTURES

- g = gravitational constant
 V = mean flow velocity
 W = weber number = $V/(\sigma/\rho y_e)^{1/2}$
 y_e = effective depth
 α = angle chute invert makes with horizontal
 ρ = density of water
 σ = interfacial surface tension

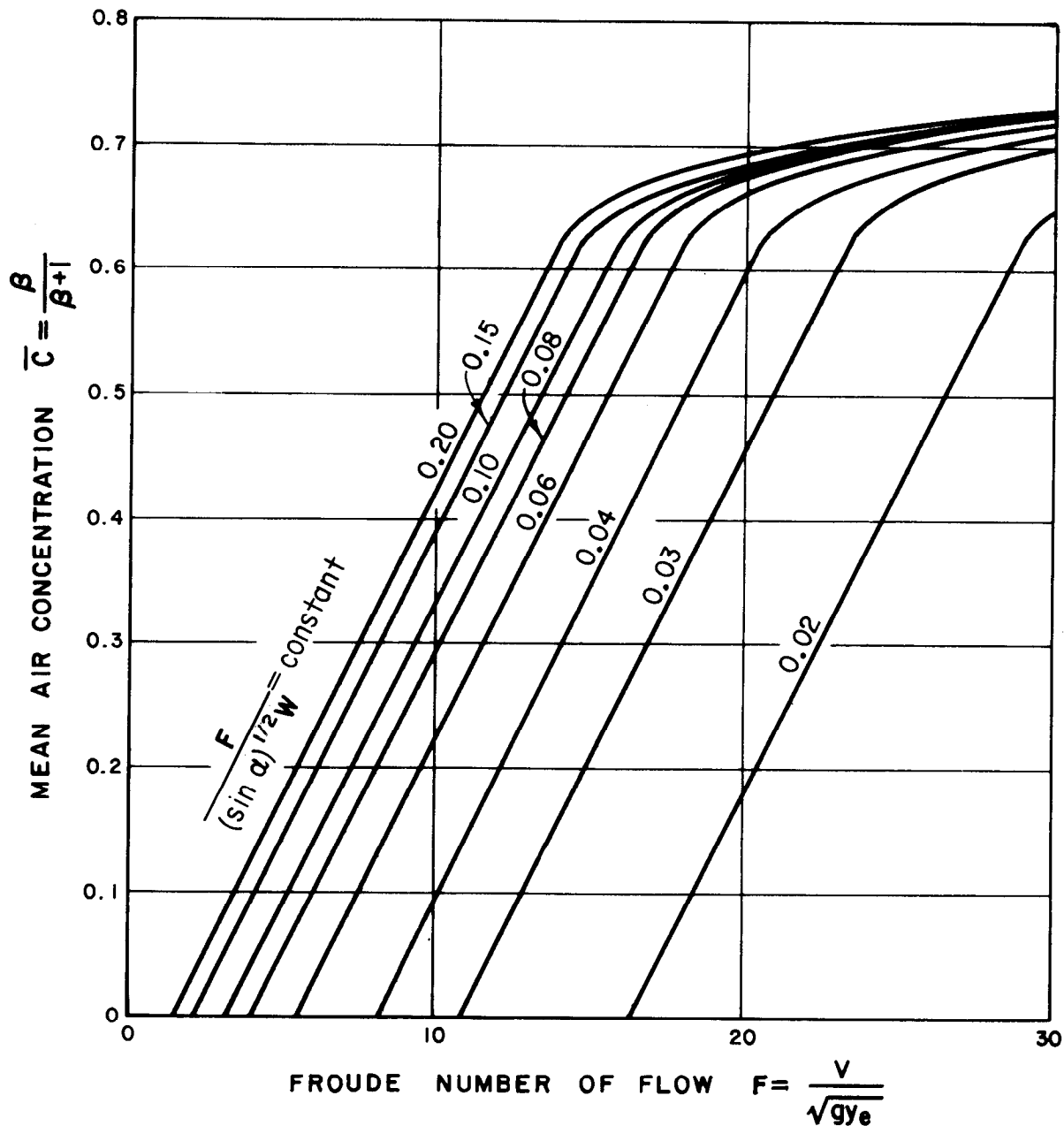


FIGURE 14.—Air entrainment in open channel flow.

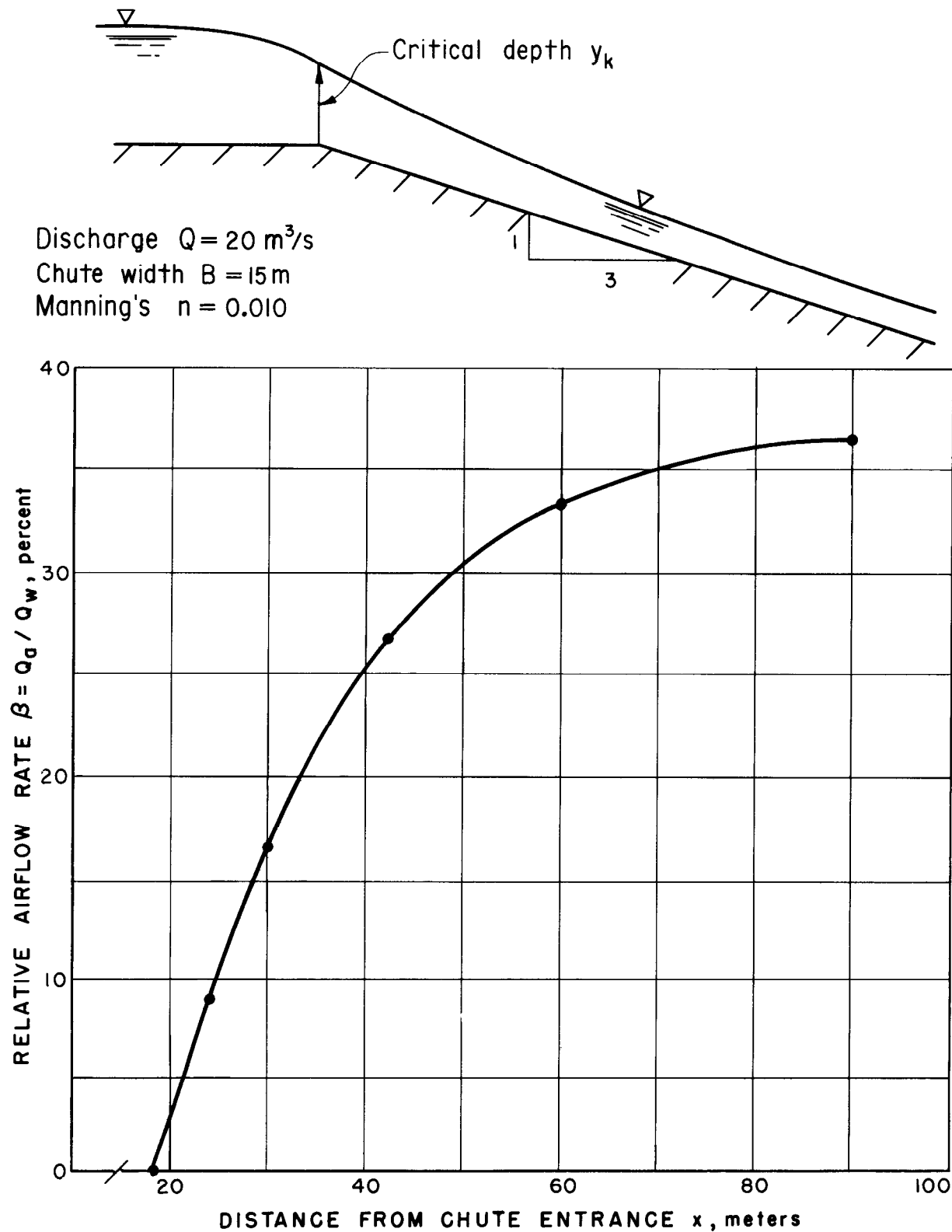


FIGURE 15.—Example of air entrainment in chutes.

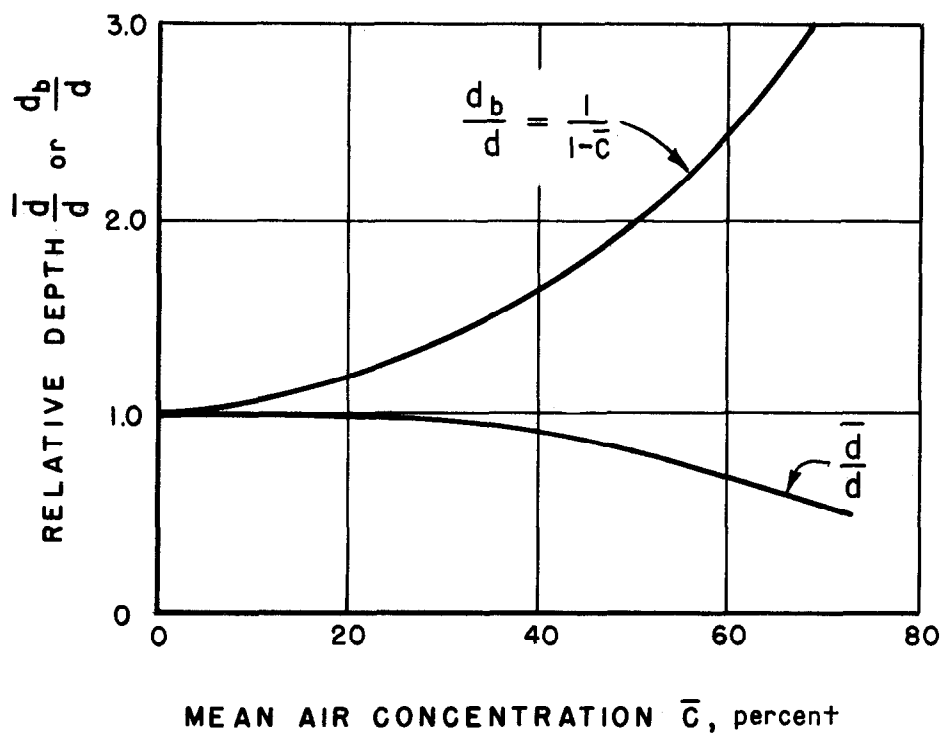
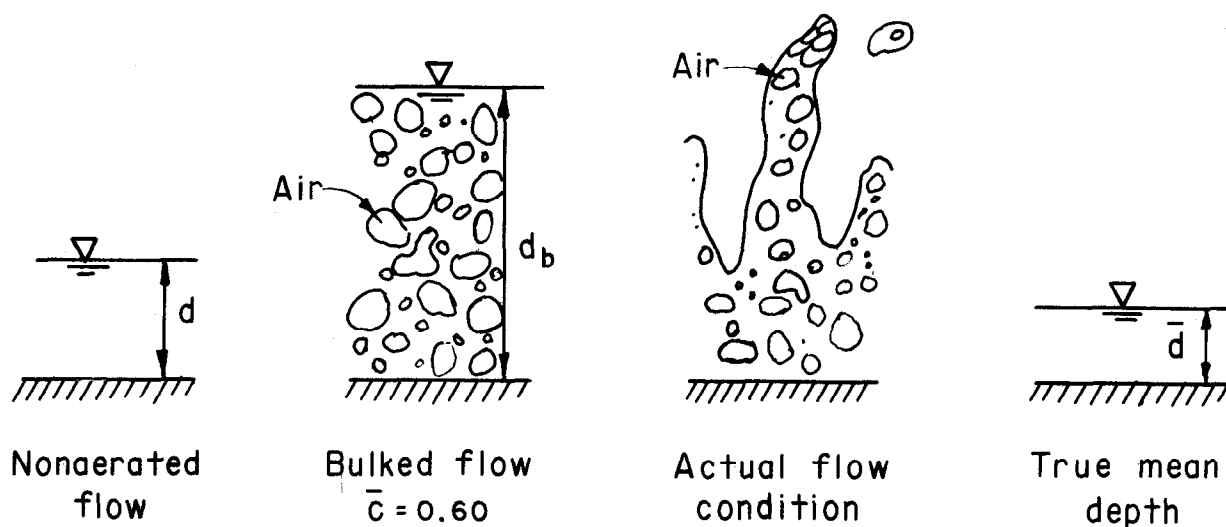


FIGURE 16.—Definitions of aerated flow depth.

For chutes having rectangular cross sections, equation 60 can be written as

$$\bar{C} = 1 - \frac{VdB}{VdbB} \quad (61)$$

where

B = width of rectangular chute

V = velocity of air-water mixture

Thomas [69] used the bulked depth concept indirectly to determine the air content on the Kittitas chute⁴. He measured the bulked depth (with some difficulty), total waterflow and the velocity of the air-water mixture. The velocity of the air-water mixture was determined by the salt velocity method. Thomas measured d_b , V , and Q . He calculated the air concentrations using equation 61 by setting

$$Q = VdB \quad (62)$$

The determination of airflow rates by this method raises two questions that need to be considered in some detail. These are:

1. Does the air content influence the flow velocity and hence, the true mean depth?
2. How accurate are the measurements of the bulked flow depth?

Straub and Anderson [66] found that the depth of the flow actually decreases as the air concentration increases above a value of 25 percent (fig. 17). In other words, as the air concentration increases, the flow velocity increases. For instance, at the 74-percent air concentration, the flow velocity is about 1.8 times the

nonaerated flow velocity. Therefore, the Standard Step Method and Manning's equation can be used to estimate the true depth up to air concentrations of about 25 percent. For higher concentrations the values must be adjusted by figure 16.

The bulked flow depth virtually is impossible to measure accurately because the surface is highly turbulent (note frontispiece). Thomas [69] noted the following:

"The choppy water surface and the large amount of spray rendered it difficult to determine where the point of the gage should be to give a reading that would be indicative of the actual depth of flow. The surface conditions also made it difficult to observe the point of the gage. The depth of flow was considered to be at the base of the loosely flying spray and drops of water. The top of the main portion of the flow included numerous small waves or rollers. The vibration of the point gage was relied upon more than visual observation to insure that the point was at relatively the same position in the flow for successive readings."

The practical difficulties of determining accurate measurements indicate a need to reexamine the actual flow conditions (fig. 16). A careful consideration of actual flow conditions, such as the frontispiece and the preceeding note, reveals that the entire concept of a bulked flow depth is a poor representation of reality. Thus, other means of describing the location of the water surface should be considered.

Water surface fluctuations that occur in open channels can be described by several methods. Longuet-Higgins [50], in studies of ocean waves, based his analysis on a probability distribution of wave heights. He defined a wave height as the difference in elevation between a crest (maximum) and its succeeding trough (minimum). Relatively good correlations were

⁴The Kittitas chute is the common name given to describe the Main Canal - Sta. 1146+30 (feet) Wasteway in the Kittitas Division, Yakima Project - Washington. The care with which the tests were conceived and executed have made them a valuable reference source—even up to the present time.

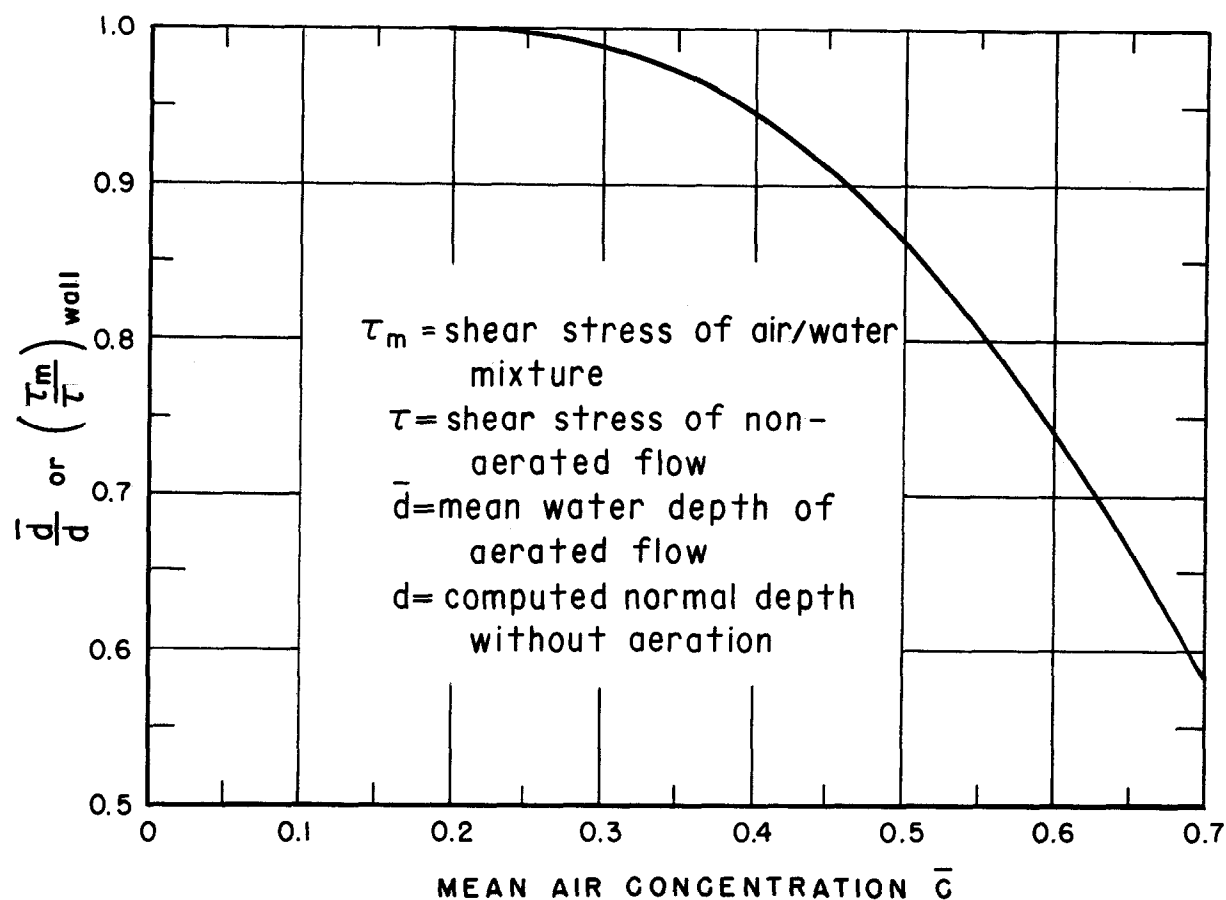


FIGURE 17.—Relation of aerated to nonaerated flow depth.

obtained between the data and a Rayleigh probability density function. This function can be written as:

$$P_h = \eta \exp(-\eta^2/2) \quad (63)$$

where

η = normalized wave height = M_o/s

M_o = wave height amplitude, (half crest to trough distance)

s = root-mean-square value of the wave height amplitudes

P_h = probability that the wave height is equal to the given height

Cartwright and Longuet-Higgins [13] used another description of the fluctuating water

surface. They based their analysis on the maximum difference on elevation between a wave crest and the mean level of the water surface for a given wave period. These differences can be normalized by dividing them by the root-mean-square value of the water surface fluctuation about the mean water surface elevation. Since a crest can occur at an elevation below the mean water surface, the dimensionless crest elevations can have negative values. The specific shape of the distribution depends upon the relative width of the frequency spectrum E . This parameter defines a series of probability distributions that range from a Rayleigh to a Gaussian distribution (fig. 18). The value of the parameter E for ocean waves is about 0.6

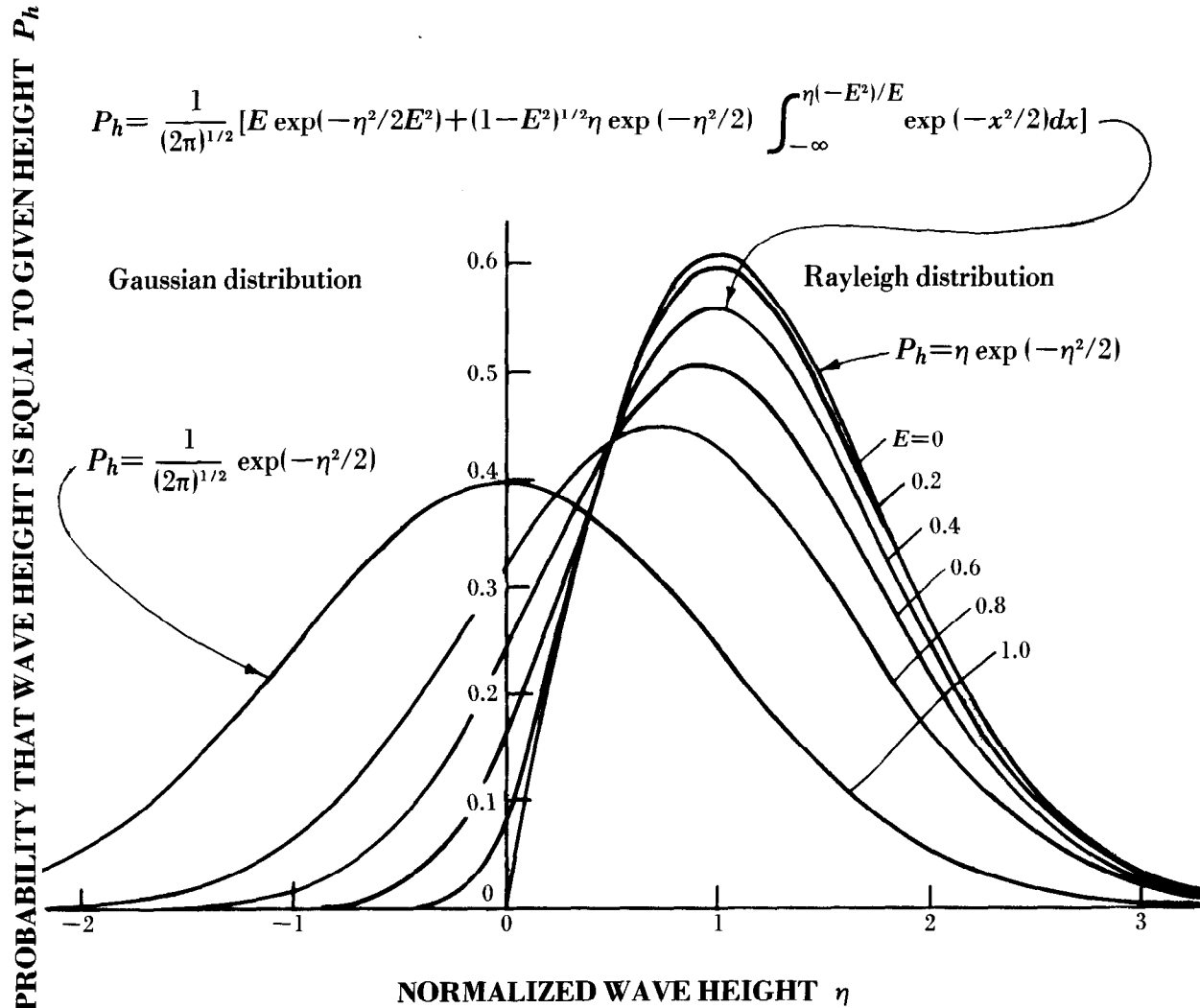


FIGURE 18.—Probability density distribution for different values of the width of the energy spectrum.

A third method of describing the water surface fluctuations is not based upon a definition of wave heights. Instead, the difference between the instantaneous water surface and the mean value of the water surface is used. This probabilistic description of the water surface is probably the most useful in hydraulic structures since designers require a knowledge of the mean flow depth and a measure of how frequently the water surface exceeds some specified elevation above the mean depth.

Unfortunately, very little research has been concerned with a probabilistic description of the water surface in open channel flow. Preliminary investigations in the laboratory indicate that the distribution of the water surface in fully developed, rough, open-channel flow is nearly Gaussian. If the distribution is Gaussian, a plot of the cumulative probability distribution versus flow depth will be a straight line on arithmetic probability paper (fig. 19). A wave depth probe of the type described by

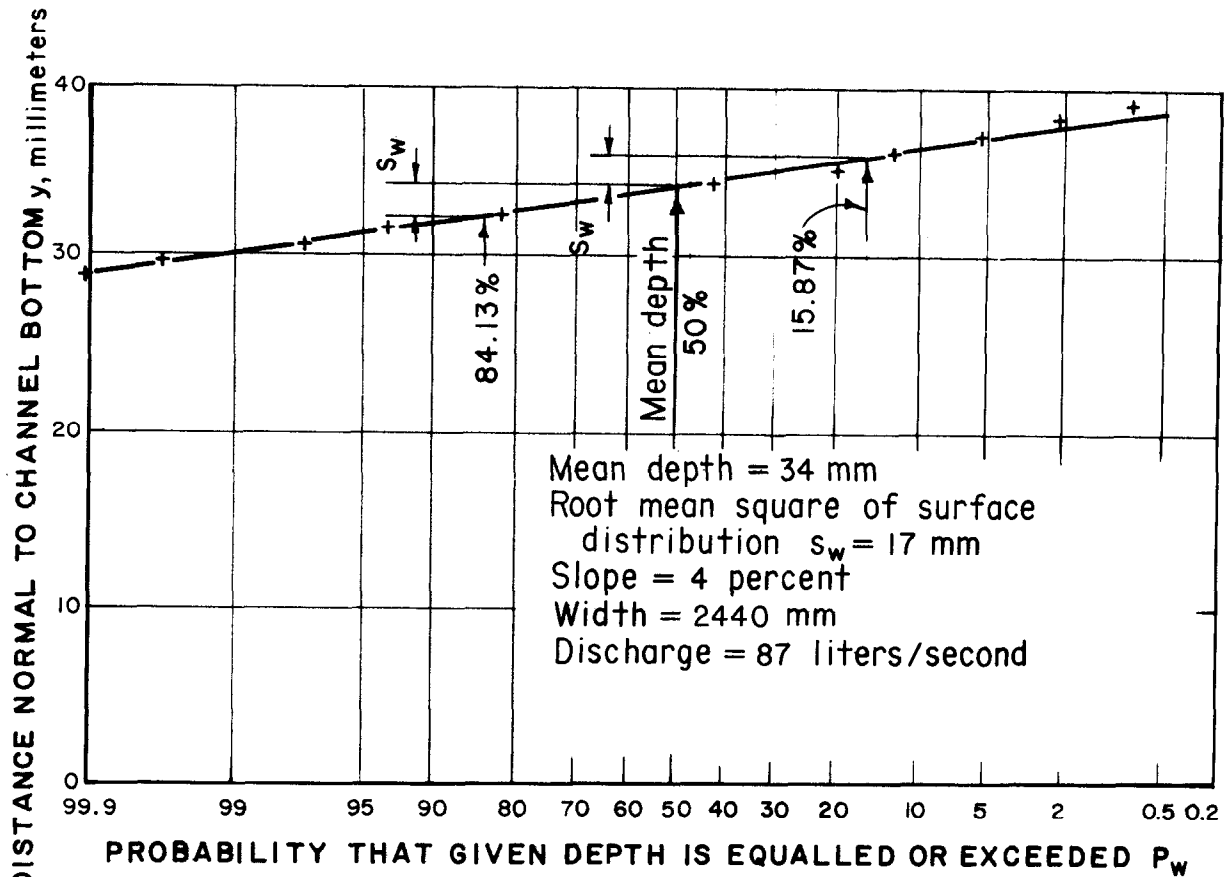


FIGURE 19.—Probability description of water surface in a chute.

Killen [41] or the circuitry given in appendix I can be used to measure the cumulative probability directly. The root-mean-square value of the water surface fluctuation can be read from the plot. The root-mean-square value is the difference between the depth having an 84.13-percent probability and the mean depth (50% probability). Alternatively, the mean depth and the 15.87-percent probable depth can be used.

Effect of Air Entrained Flow on Stilling Basin Performance

The effect of air entrained flow on the performance of stilling basins has been considered for many years. Gumensky [25] concluded that for all practical purposes the conjugate depth of the

hydraulic jump could be determined from nonaerated flow equations. Rajaratnam [57] followed with some investigations that indicated a significant effect might be produced by the air entrainment. However, later studies by Herbrand [33] showed that the coefficients used in Rajaratnam's equations produced too large an effect on the result and that they were not necessary. Therefore, in rectangular channels the conjugate depth y_c can be calculated with sufficient accuracy from

$$y_c = 0.5y_1 (\sqrt{8F^2 + 1} - 1) \quad (64)$$

where the depths and Froude numbers are calculated with the appropriate bulked flow depths (fig. 16).

Closed Conduit Flow

CLASSIFICATION OF FLOW

The conventional term for the concurrent flow of air and water is *two-phase* flow. Here, *phase* refers to one of the states of matter (gas, liquid, or solid). Technically the term two-phase flow should be reserved to describe the motion of a substance which is present in two of its phases, such as a flow of ice and water. The word *multicomponent* is a better description of flows which do not consist of the same chemical substance, such as air and water. If both components move in the same direction, the flow is termed *concurrent flow*. If the components move in opposite directions, the flow is *counter-current*.

Closed conduit flow can be classified according to the type of pattern that develops. The flow patterns which develop depend upon the airflow rate relative to the waterflow rate and the slope of the conduit. For example, the flow

patterns in horizontal conduits have been defined by Baker [7], (fig. 20). The correlation can be applied to other gases and liquids by substituting appropriate quantities into the following parameters:

G_g = mass velocity of gas, $\text{kg}/(\text{m}^2 \cdot \text{s})$

G_l = mass velocity of liquid, $\text{kg}/(\text{m}^2 \cdot \text{s})$

$\lambda = [(\rho_g/\rho_a)(\rho_l/\rho_w)]^{1/2}$

μ = dynamic viscosity, $\text{Pa} \cdot \text{s}$

ρ_g = gas density, kg/m^3

ρ_a = air density (at 101.3 kPa and 20 °C) = $1.20 \text{ kg}/\text{m}^3$

ρ_l = liquid density, kg/m^3

ρ_w = water (at 101.3 kPa and 20 °C) = $988 \text{ kg}/\text{m}^3$

σ = interfacial surface tension, N/m

σ_{aw} = air-water surface tension (at 101.3 kPa and 20 °C) = $0.0728 \text{ N}/\text{m}$

$\psi = (\rho_w/\rho_l)[\mu(\rho_w/\rho_l)^2]^{1/3}$, $\text{Pa}^{1/3} \cdot \text{s}^{1/3}$

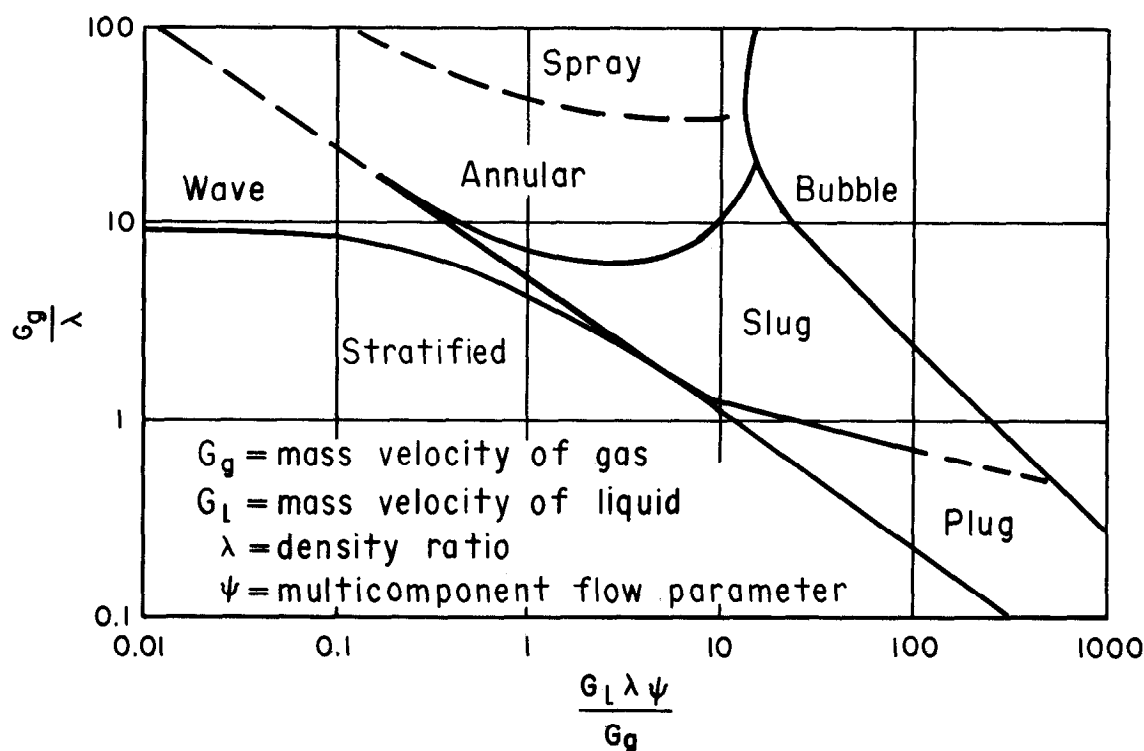


FIGURE 20.—Flow patterns in horizontal pipes, Baker [7].

These various flow patterns were described by Alves [1] according to the physical appearance of the flow as follows (fig. 21):

- **Bubble flow.**—The air forms in bubbles at the upper surface of the pipe. The bubble and water velocities are about equal. If the bubbles are dispersed through the water, the flow is called “froth flow.”
- **Plug flow.**—For increased airflow rates the air bubbles coalesce with plugs of air and water alternately flowing along the top of the pipe.
- **Stratified flow.**—A distinct horizontal interface separates the air and waterflows.
- **Wave flow.**—As the airflow rate is increased, surface waves appear on the stratified flow interface.
- **Slug flow.**—Wave amplitudes are large enough to seal the conduit. The wave

forms a frothy slug where it touches the roof of the conduit. This slug travels with a higher velocity than the average liquid velocity.

- **Annular flow.**—For greater airflow rates the water flows as a film on the wall of the pipe, while the air flows in a high-speed core down the axis of the pipe.
- **Spray flow.**—For very great airflow rates the annular film is stripped from the pipe walls and is carried in the air as entrained droplets.

A similar set of flow pattern descriptions exist for vertical flows. They are:

- **Bubble flow.**—The air is distributed in the water as spherical or spherical cap bubbles which are small with respect to the conduit diameter.

- **Slug flow.**—As the air flow increases, alternate slugs⁵ of air and water move up the pipe. The transition from bubble flow to slug flow is shown on figure 22. This transition occurs when the bubble diameter is about one-half the conduit diameter.

If the vertical conduit is rectangular instead of cylindrical, the appropriate relation for slug flow is given by Wallis [73] as

$$\frac{V_s}{V_t} = \left(0.325 + 0.184 \frac{D_s}{D_b} \right) \left(\frac{D_e}{D_s} \right)^{-1/2} \quad (65)$$

where

D_s = larger dimension of a rectangular conduit

D_b = smaller dimension of a rectangular conduit

D_e = bubble diameter

V_s = terminal velocity of air bubbles in slug flow

V_t = terminal velocity of air bubbles in still water

With respect to the flow quantities, Martin [52] found that the transition from bubbly to slug flow occurs at a void fraction somewhere between 19 and 23 percent.

The void fraction θ is the average volumetric concentration in a length of pipe (assuming uniform flow) and expressed as

$$\theta = \frac{\omega_w}{AL} \quad (66)$$

⁵It is not clear whether the term slug refers to a slug of air or a slug of water. The air bubble could be called a slug due to its bullet or slug shaped form. The water could be called a slug due to its similarity in form to the terrestrial gastropod in horizontal flows or due to its impact properties in vertical flow. The author prefers the reference to slugs of air.

where

ω_w = volume of water

A = cross sectional area of conduit

L = length of conduit over which the volume ω_w is determined

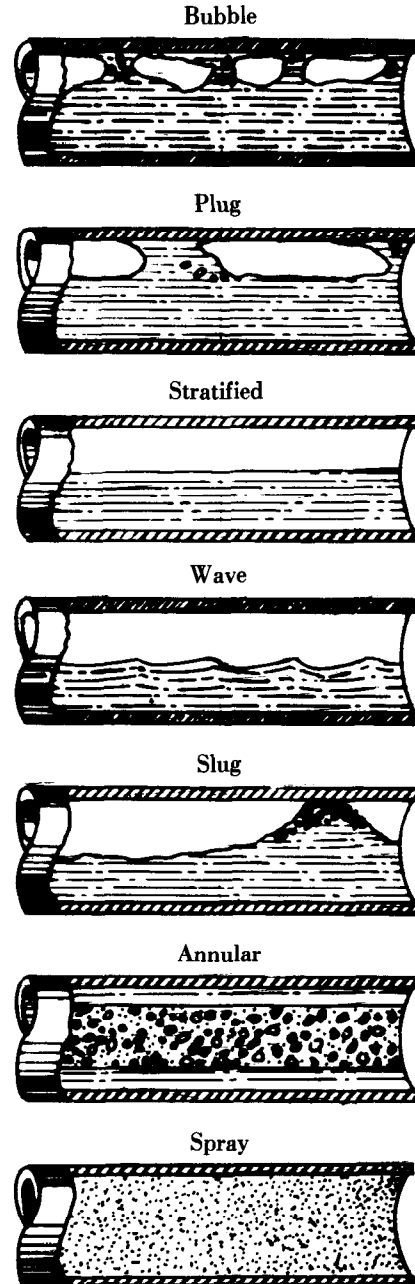


FIGURE 21.—Flow pattern sketches, Alves [1].

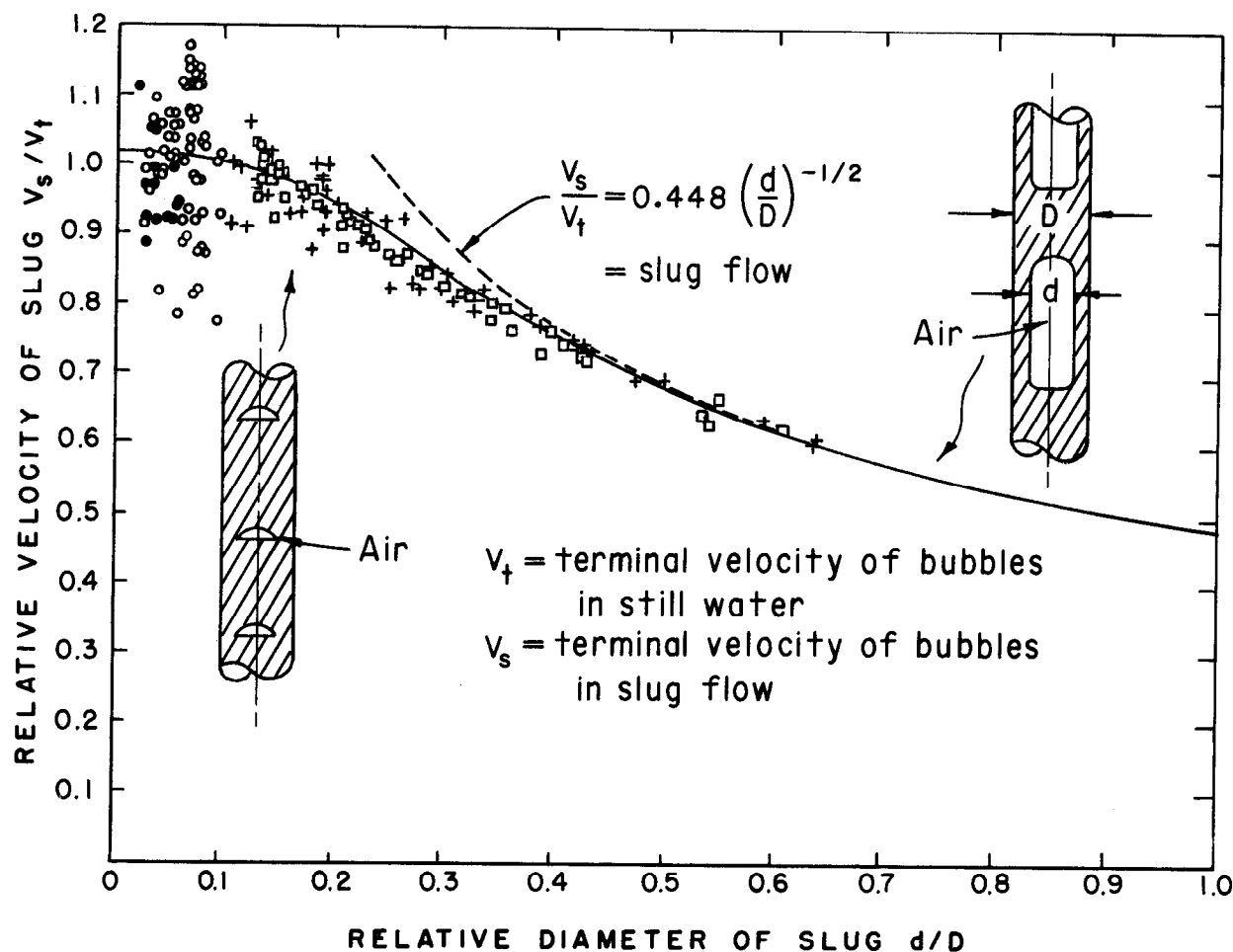


FIGURE 22.—Effect of conduit diameter on terminal velocity of a bubble, Collins [16].

- **Froth flow.**—As the airflow increases, the slugs break up into a turbulent disordered pattern of air and water.

The annular and spray flow patterns are identical in both vertical and horizontal pipes.

In hydraulic structures, the conduits may also be placed on a slope. The additional complexities in the flow patterns caused by slope will be discussed later.

From a designer's viewpoint, air-water flows in closed conduits can be classified into four general categories. Each category may contain only one or a combination of the flow patterns enumerated previously. These categories are:

1. Flow in partially filled conduits,

2. Flow having a hydraulic jump that fills the conduit,
3. Flow from control devices, and
4. Falling water surface.

Each category listed above is considered in detail in the following subsections.

In addition to the four categories of flow, two others are considered separately. These are:

- Flow in pipelines and siphons
- Flow in vertical shafts

The pipelines and siphons require special consideration because of their length. Vertical shafts present special problems because of the various types of flow which can exist in the shaft.

FLOW IN PARTIALLY FILLED CONDUITS

Model Predictions

Flow in a partially filled conduit can be thought of as open-channel flow in a closed conduit. The air flows through the passage which is formed above the water surface.

The total volume flow of air, which enters at the upstream end of the air passage, equals the sum of the air that is insufflated into the flow and that which flows above the water surface as a result of the air-water shear forces. The quantity of air insufflated into the flow can be estimated from equation 59. The quantity of air that flows above the water surface is a function of the waterflow properties and the pressure drop in the air vent. This can be expressed as

$$Q_a = f(L, V, g, p, \gamma_e, \rho_w) \quad (67)$$

where

- A = cross sectional area of water prism
- g = gravitational constant (acceleration)
- L = conduit length
- p = pressure intensity
- Q_a = total airflow rate
- T = top width of flow passage
- V = mean water velocity
- γ_e = effective depth = A/T
- ρ_w = water density

Applying dimensional analysis to equation 67 with γ_e , V , and ρ_w as the repeating variables gives

$$\frac{Q_a}{Q_w} = f\left(\frac{L}{\gamma_e}, \frac{1}{F^2}, \frac{p/\gamma}{V^2/2g}\right) \quad (68)$$

where

- F = Froude number
- Q_w = waterflow rate
- γ = specific force of water

The interrelation between these parameters can be found for a specific geometry through the use of model studies.

There are many literature references that indicate model predictions often underestimate in the quantity of air which actually flows in prototype structures. However, very careful model tests in which all air- and waterflow passages were modeled in their entirety have shown good agreement between model and prototype measurements.

For instance, Sikora [65] showed that the air-flow rates could be accurately predicted from model studies. His tests were with three geometrically similar models having scales of 1:1, 1:2, and 1:4 (fig. 23). The pressure values on the figure refer to the difference between atmospheric pressure and the air pressure at the upstream end of the waterflow passage.

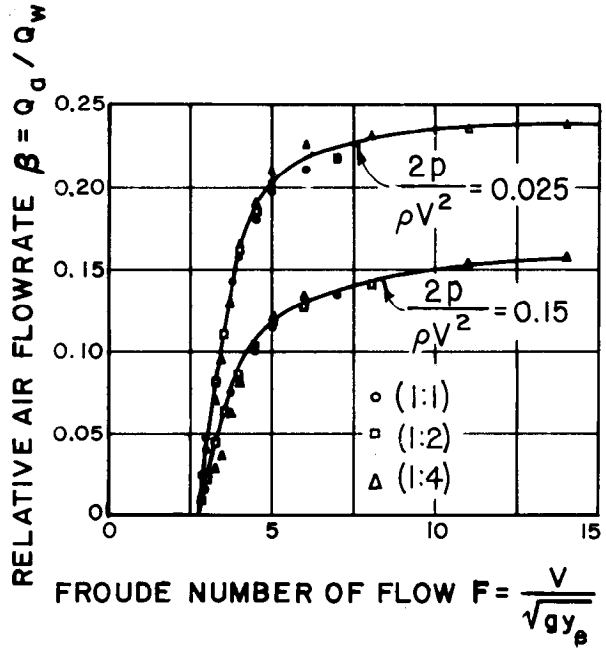


FIGURE 23.—Influence of air pressure in conduit in air-flow rate, Sikora [65].

Harshbarger, Vigander, and Hecker [32] conducted 1:20 scale model and prototype tests of a gated tunnel discharge. Free-surface flow

existed in the tunnel for all discharges. A scale effect was not detectable in their investigations.

These studies clearly indicate that for estimating airflow rates using models, it is necessary to accurately reproduce the entire airflow passage above the water surface. In those cases where air enters the water conduit through a vent, two options are available for measuring the airflow rates. The options depend upon whether or not the air vent has been designed.

Air vent not designed.—If the air vent design has not been determined, it is necessary to measure the airflow rate while controlling the air pressure at the upstream end of the water conduit. These tests must be performed for a series of flow depths and flow rates in the water conduit.

The upstream air pressures can be controlled by incorporating an air pump into the airflow measuring device. To be applicable for all possible designs, the pressure should be varied over the maximum possible range. The lowest end of the range corresponds with the condition of no airflow through the vent. The upper end of the range is achieved when the upstream air pressure is equal to the atmospheric pressure.

A good example of this procedure is the work by Sikora [65] who developed a set of curves for the airflow in the horizontal leg of morning-glory spillway (fig. 24).

Once the family of curves for the airflow rates has been experimentally determined it is possible to investigate the effect of adding various size air vents to the structure. This is done by first developing an expression for the air vent characteristics in terms of the dimensionless parameters on figure 24.

For air velocities less than 100 m/s and values of $fL/4H \geq 4$, the volume flowrate Q_a through a vent can be expressed as

$$Q_a = A_v \left\{ 2g \frac{(Q_w/Q_a)[(p_{atm}/\gamma) - (p_1/\gamma) + \Delta z(Q_a/Q_w)]}{\sum K_s + fL/4H} \right\}^{1/2} \quad (69)$$

where

A_v = cross sectional area of vent

f = Darcy-Weisbach friction factor

g = gravitational constant (acceleration)

H = hydraulic radius of prototype air vent

K_e = entrance loss

K_s = singular (form) loss in vent, the greatest of which is the entrance loss

$K_e = 0.5$

L = vent length

p_1 = pressure at vent exit

p_{atm} = atmospheric pressure

Δz = difference between vent intake and vent exit elevations

γ = specific force of water

Q_a = air density

Q_w = water density

Volume flowrate of water can be expressed as

$$Q_w = A \left[2g \left(\frac{V^2}{2g} \right) \right]^{1/2} \quad (70)$$

where

A = cross sectional area of water prism

V = mean waterflow velocity in conduit

Using these two expressions, the dimensionless airflow rate β can be expressed as

$$\beta = \frac{Q_a}{Q_w} = \frac{A_v}{A} \left\{ \frac{Q_w/Q_a}{\sum K_s + fL/4H} \left[\frac{(p_{atm}/\gamma) - (p_1/\gamma)}{V^2/2g} \right] \right\}^{1/2} \quad (71)$$

when $\Delta z \frac{Q_a}{Q_w}$ is negligible.

The first ratio inside the brackets is a function of the fluid properties, the singular losses, and the flow geometry. The second ratio is in the form of a pressure factor or Euler number. By using this equation, the characteristics of a given vent can be plotted on the dimensionless airflow curves (fig. 24). The intersection points

A = cross sectional area of water prism

A_d = cross sectional area of conduit

d_e = deflector height

F = Froude number = $\frac{V}{\sqrt{gy_e}}$

ρ = air density

g = gravitational constant

p = pressure at end of air vent

Δp = pressure drop across vent

Q_a = volume flowrate of air

Q_w = volume flowrate of water

V = mean flow velocity

y_e = effective depth

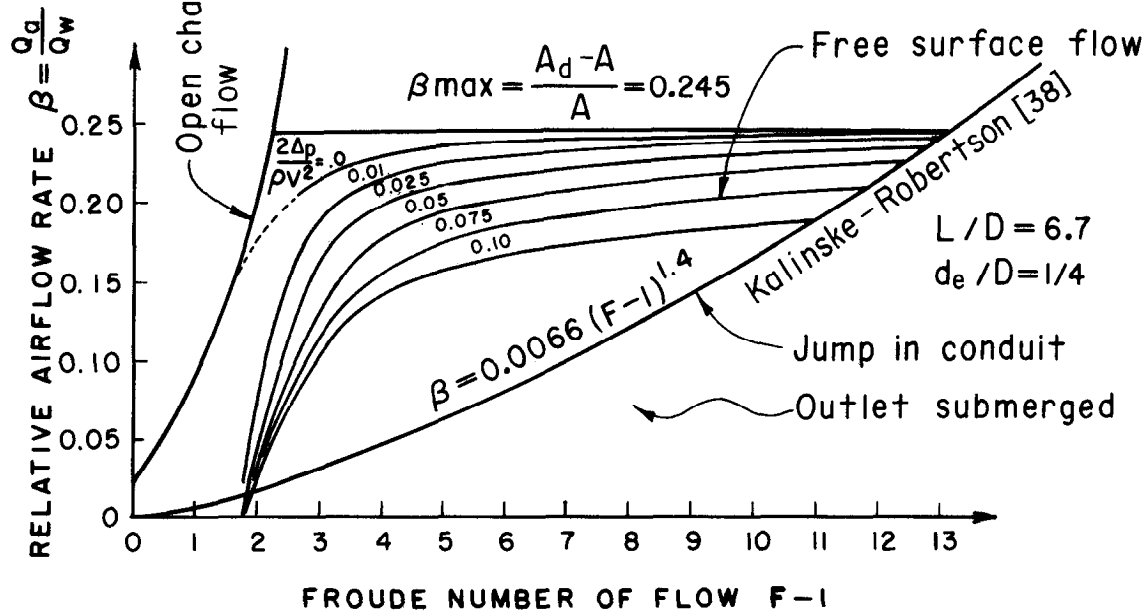
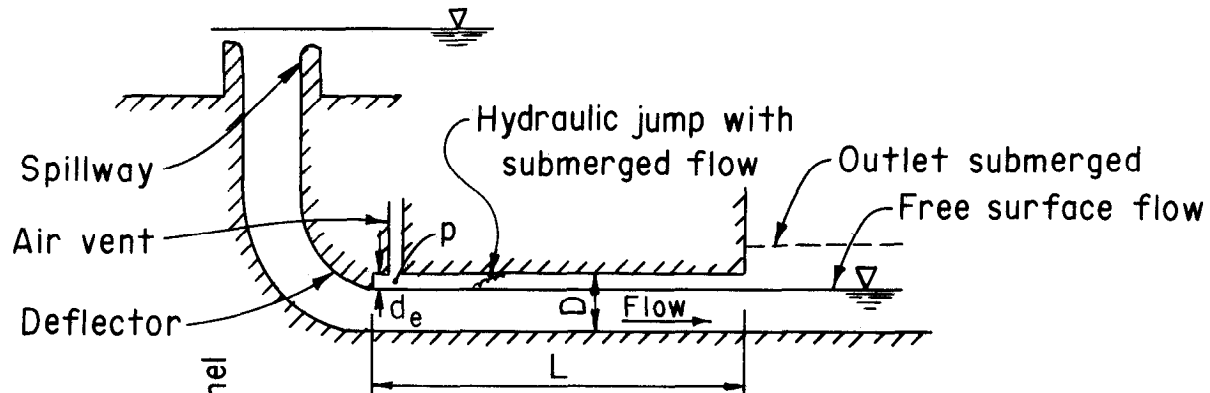


FIGURE 24.—Model tests on a spillway, Sikora [65].

of the two sets of curves gives the pressures and airflow rates for a given set of air vent parameters. If the resulting values are not satisfactory, another set of vent characteristics is chosen and the process repeated.

Air vent designed.—For some studies the design of the air vent is available. In these cases it is necessary to calculate the total loss for the vent and to simulate this loss in the model air vent. The loss for the prototype and the model must include both frictional and form losses. Normally, the air vent velocities are kept low enough so that incompressible loss coefficients are valid. The model air vent is simulated correctly when the loss coefficients in the model and prototype vents are made equal. If devices such as nozzles or orifices are installed into the model air vent for flow measurement purposes, the loss across them must be included in computing the total model air vent loss coefficient. In the case of an orifice, its loss coefficient often constitutes the entire loss for the model air vent. It is possible to express the required orifice size as

$$A_o = \frac{A_v}{C_o L_r^2 \left(1 + \sum K_s + fL/4H\right)^{1/2}} \quad (72)$$

where

A_o = orifice area

A_v = prototype air vent area

C_o = orifice discharge coefficient

f = Darcy-Weisbach factor for prototype air vent

H = hydraulic radius of prototype air vent

K_s = singular losses (including entrance, bends, and changes in area)

L = length of prototype air vent

L_r = prototype to model scale ratio

If the orifice is placed on the end of the model air vent pipe, its discharge coefficient is obtained from figure 25.

Analytic Estimates

In many instances, model tests for predicting the airflow rates have not been performed. For these cases, the airflow rates often can be estimated closely enough by an approximate method. For this estimation three rather gross assumptions must be made, namely:

1. The amount of air flowing through the vent is a function of only the air insufflated into the flow and the air that is induced to flow by the moving water boundary,
2. The amount of air insufflated into the flow can be predicted by open channel flow equations, and
3. The air motion above the water surface is determined solely by the boundary layer δ thickness at the most downstream conduit location.

These assumptions neglect the fact that air actually can enter from the downstream end of the conduit. Schlichting [63] showed that with Couette-Poiseuille⁶ flow in the laminar region, a flow reversal occurs when

$$P_o = \frac{h_a^2}{2\mu V_o} \left(\frac{dp}{dx} \right) \leq -1 \quad (73)$$

⁶The dimensionless parameter P_o is known as the Poiseuille number. Its primary use is in the laminar fluid friction field. For example, in a round circular pipe, the Poiseuille number is equal to 32. In this case the pipe diameter is substituted for the height of the airflow passage in equation 73. Couette flow exists between two parallel walls when one wall is moving and the other is stationary. The motion is due solely to the shear field created by the relative movement of the two walls. Couette flow has no pressure gradient in the direction of flow. Couette-Poiseuille flow describes a Couette type flow having a longitudinal pressure gradient. Turbulent Couette-Poiseuille flow should describe the air motion above a moving water surface in a closed conduit.

A_d = conduit area

A_o = orifice area

H_m = head across orifice

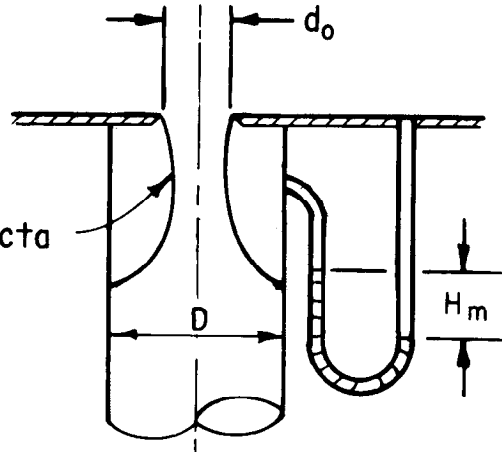
$$H_m = h_m (\rho_m / \rho_a)$$

Q = volume flowrate of air

ρ_a = density of air

ρ_m = density of manometer fluid

Vena contracta



$$\frac{A_o}{A_d} = \frac{d_o^2}{D^2}$$

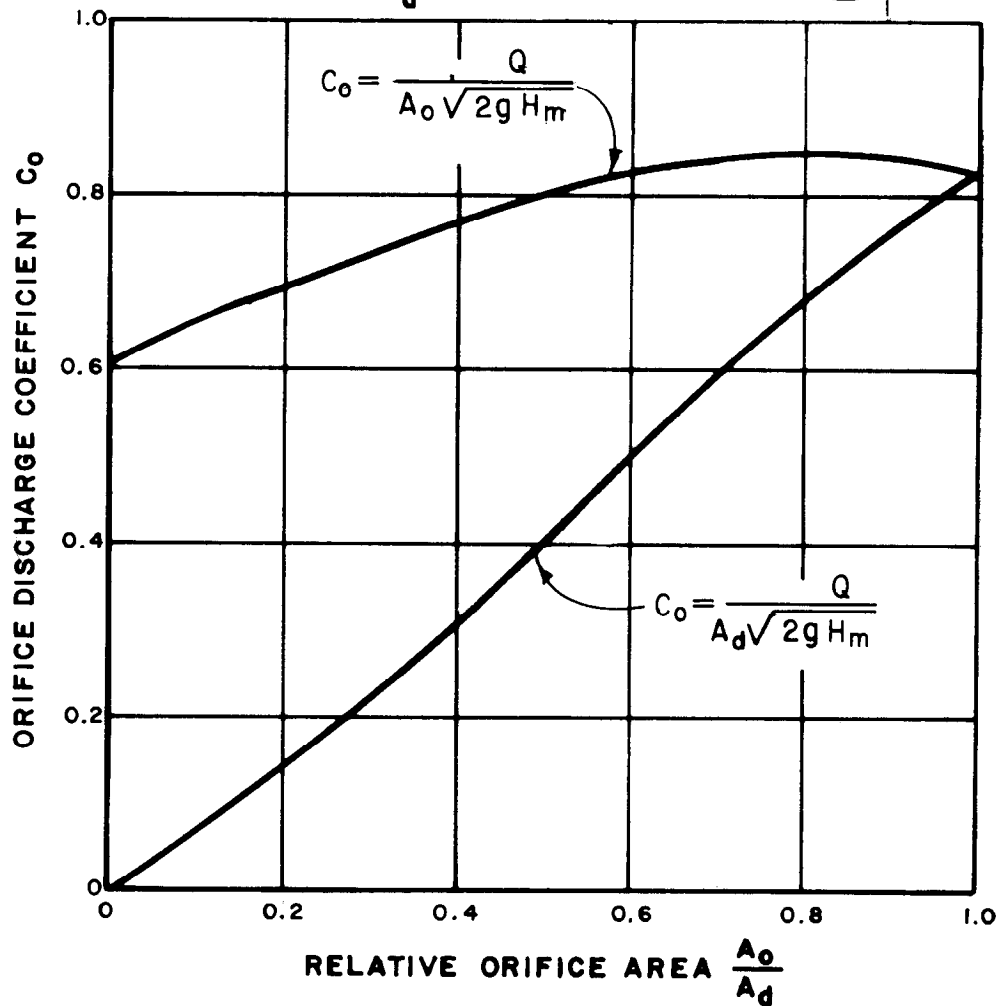


FIGURE 25.—Discharge coefficients for orifice at end of pipe.

where

h_a = height of airflow passage
 dp/dx = pressure gradient in the air
 V_o = maximum water surface velocity
 μ = dynamic viscosity of air

Leutheusser and Chu [48] have investigated Couette flow in the turbulent region. Insufficient tests have been made to determine the magnitude of the dimensionless parameter P_o for the turbulent Couette-Poiseuille flow. However, some laboratory tests indicate that with turbulence, reverse flow begins when

$$P_o \approx -1000 \quad (74)$$

The amount of air flowing above the water surface can be visualized by considering a boundary layer which increases in thickness from a value of zero at a gate, to a maximum value at the end of the conduit (fig. 26). The growth of a turbulent boundary layer that is induced by a moving rough boundary has not been studied. As a first approximation it is assumed that

$$\delta = 0.01x \quad (75)$$

where

δ = boundary layer thickness
 x = distance from gate

The velocity distribution within the boundary layer is assumed to obey a power law of the order:

$$u = V_o \left(\frac{y_a}{\delta} \right)^{1/n_v} \quad (76)$$

where

n_v = velocity distribution power law coefficient

u = local air velocity

V_o = maximum water surface velocity

y_a = distance from the water surface

δ = boundary layer thickness

The value of the coefficient n_v varies between 10 for flow over smooth surfaces to 5.4 for flow over rough surfaces when the Reynolds number is about 10^6 . Normally n_v is assumed to be equal to 7. This approach is similar to that used by Campbell and Guyton [12] except they assumed the boundary layer always coincided with the roof of the conduit.

The boundary layer entrains the maximum amount of air at the extreme downstream location in the conduit. To maintain continuity, flow at upstream locations consists of boundary layer flow plus some mean flow (fig. 26). The air velocity at the water surface must be equal to the water velocity. Therefore, at the upstream locations, the air velocity above the water surface may have a larger magnitude than that at the water surface. Careful laboratory experiments by Ghetti [24] of the Vaiont Dam (Italy) gated outlets show that the maximum air velocity near the water surface at the vent can be as much as four times the water velocity.

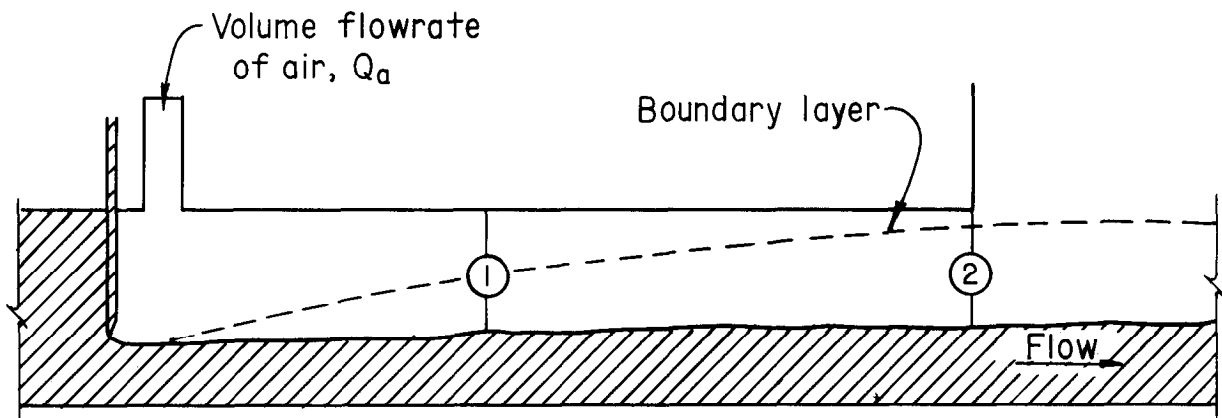
For some flow conditions the boundary layer will reach the roof of the conduit. When this happens the roof will begin to retard the flow. If the water surface and the roof of the conduit had equal roughness values, the maximum flow rate would be given by turbulent plane Couette flow. For this case the maximum airflow rate Q_m is

$$Q_m = \frac{A_a V_o}{2} \quad (77)$$

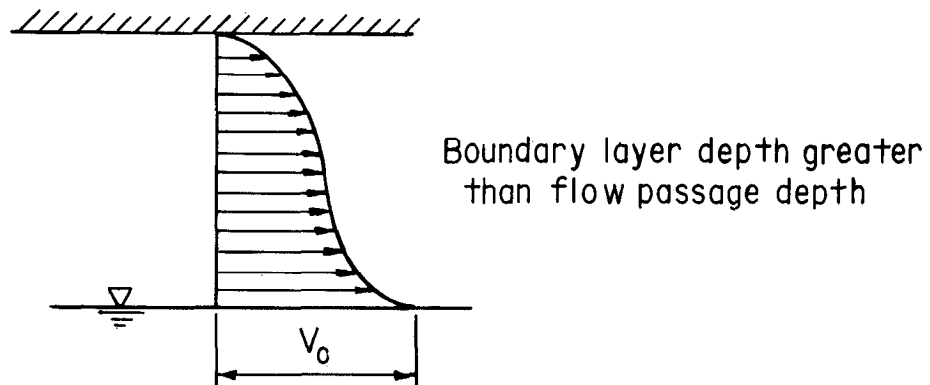
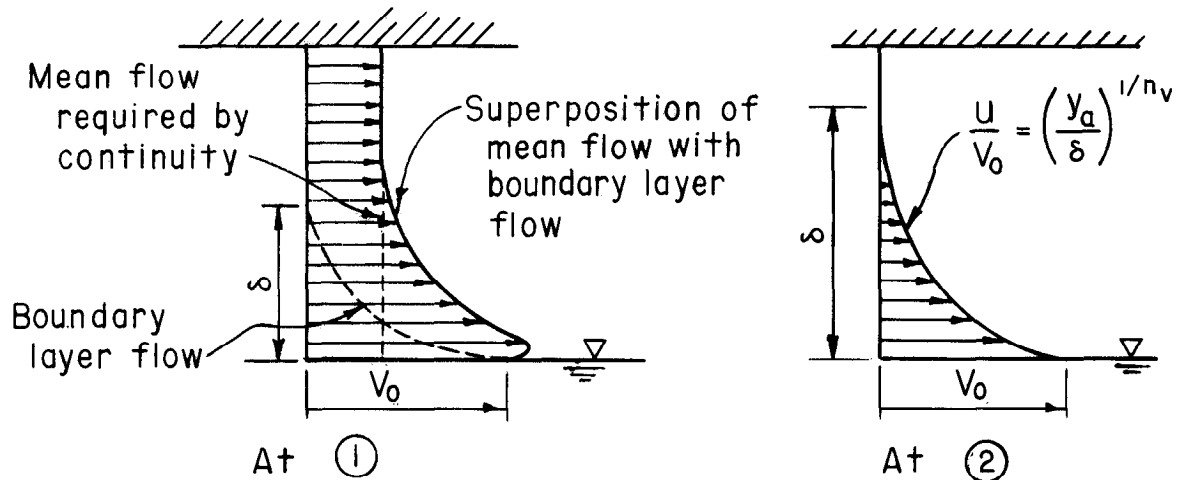
where

A_a = cross sectional area of airflow passage (rectangular)

V_o = maximum water surface velocity



A. Profile sketch



B. Velocity distribution

FIGURE 26.—Airflow above water surface.

Actually the roughness of the water surface is greater than that of the conduit roof. This increased roughness will produce higher air velocities near the water surface which result in airflow rates greater than those given by equation 77. Sikora [65] reasoned that the mean air velocity could not exceed the mean water velocity. This leads to the expression for the maximum possible airflow rate in a closed conduit, which is

$$\left(\frac{Q_a}{Q_w}\right)_{max} = \frac{A_d}{A} - 1 \quad (78)$$

where

A_d = cross sectional area of conduit
 A = maximum cross sectional area of water prism

Application of equation 78 without regard to the boundary layer thickness will result in excessively large values of the airflow rates. However, for design purposes, this approach may be satisfactory since the resulting air vent will be oversized.

FLOW HAVING A HYDRAULIC JUMP THAT FILLS THE CONDUIT

Kalinske and Robertson [38] studied the special case of two-layer flow in which a hydraulic jump fills the conduit. From dimensional analysis and model studies, they determined that the amount of air entrained by the jump is given by

$$\frac{Q_a}{Q_w} = 0.0066 (F - 1)^{1.4} \quad (79)$$

where F = Froude number upstream of the hydraulic jump.

In a circular pipe the Froude number can be calculated conveniently from the flow depth y using

$$F = \frac{V}{(gy_e)^{1/2}} \quad (80)$$

where

A = cross sectional area of water prism
 D = conduit diameter
 T = top width of flow
 passage = $2[y(D - y)]^{1/2}$
 g = gravitational constant (acceleration)
 V = mean flow velocity
 y_e = effective depth = A/T
 y = flow depth

Equation 79 is good only if all air entrained is passed downstream. Prototype tests—for which a hydraulic jump formed in the conduit and in which the conduit velocities were large enough to convey all the entrained air out of the conduit—confirm the experimentally derived curve (fig. 27).

If the conduit is horizontal or sloping upward in the direction of flow then all the entrained air will move with the flow. However, if the conduit slopes downward in the direction of flow air bubbles can either move upstream or downstream relative to the pipe wall.

The direction of movement taken by the bubbles can be examined by considering the relative magnitudes of the buoyant and drag forces upon a stationary bubble in the flow (fig. 28). For example, the bubble will move perpendicular to the pipe axis only when the upstream component of the buoyant force vector equals the drag force component. This can be written as

$$(Q_w - Q_g) \frac{\pi D_e^3}{6} (g S_o) = C_b \frac{\pi D_e^2}{4} \left(\frac{Q_w V^2}{2} \right) \quad (81)$$

where

C_b = drag coefficient on bubble
 D_e = equivalent bubble diameter
 S_o = pipe slope = $\sin \alpha$

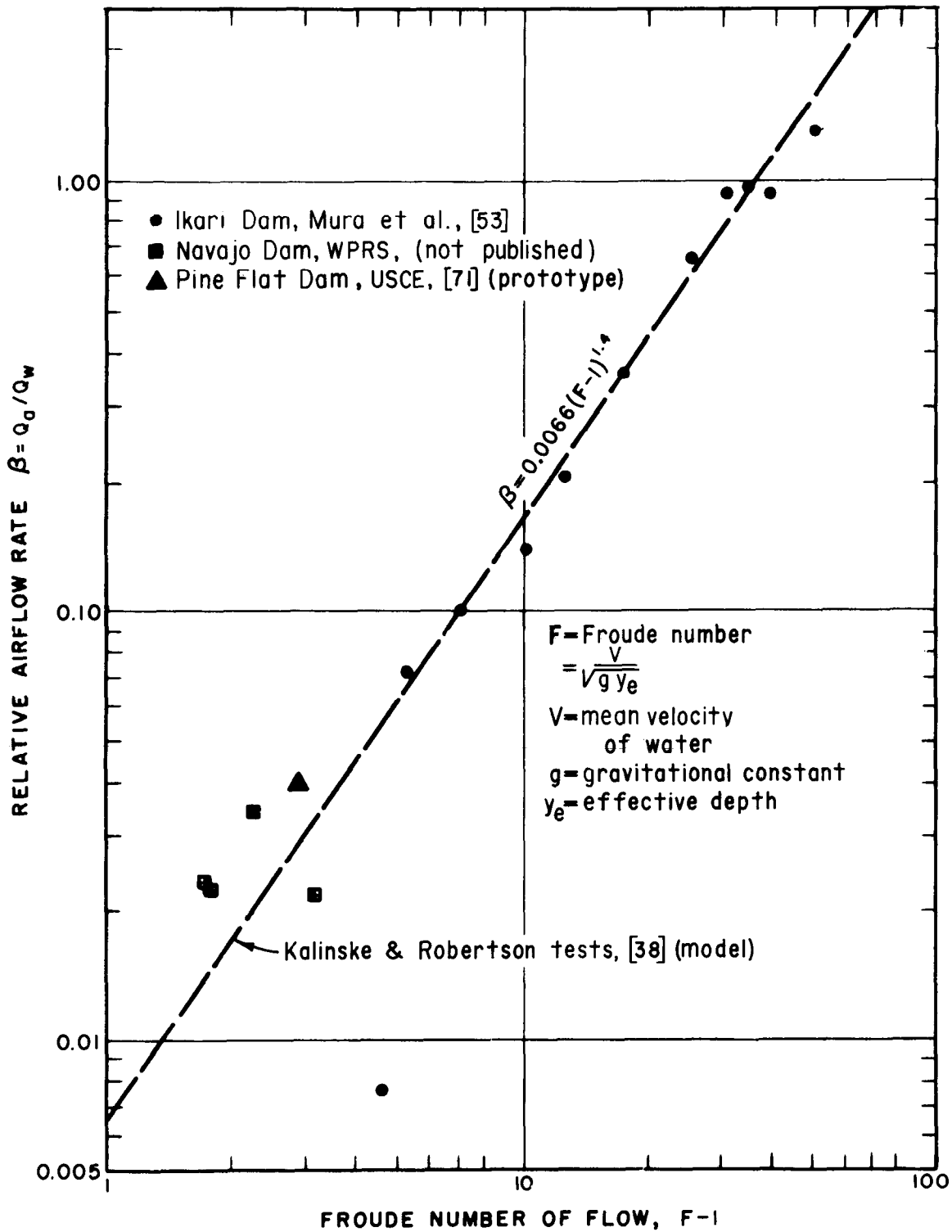


FIGURE 27.—Air entrainment with hydraulic jump closing conduit.

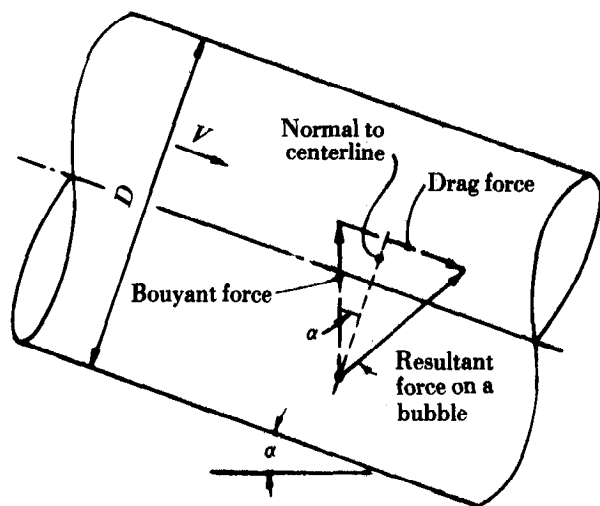


FIGURE 28.—Forces on a stationary bubble.

Rearranging terms and dividing by the conduit diameter gives

$$\frac{V^2}{gD} = \frac{4}{3} [1 - (\rho_g/\rho_w)] \frac{D_e}{D} \left(\frac{S_o}{C_b} \right) \quad (82)$$

or

$$\frac{Q_c^2}{gD^5} = \frac{\pi^2}{12} [1 - (\rho_g/\rho_w)] \frac{D_e}{D} \left(\frac{S_o}{C_b} \right) \quad (83)$$

where

Q_c = critical discharge needed to carry bubbles with the flow

D = conduit diameter

This relation shows that the critical discharge for bubble motion is a function of the effective bubble diameter D_e , the densities, ρ , the drag coefficient C_d of the bubble, and the pipe slope S_o . Unfortunately, the drag coefficient and effective bubble diameter can not be predicted for flow in a pipe. Therefore, the techniques of dimensional analysis must be used to determine the significant parameters for correlations.

As was shown under Design Parameters—*Mean air concentration*, the effective bubble

diameter is a function of the interfacial surface tension and the friction slope. In terms of dimensionless parameters, the critical discharge required to move the bubbles can be expressed as

$$\frac{Q_c^2}{gD^5} = f \left(\frac{\gamma D^2}{\sigma}, S_f, S_o, C_b \right) \quad (84)$$

The parameter $\frac{\gamma D^2}{\sigma}$ is designated frequently as the Eötvös number E .

Kalinske and Bliss [37] found relatively good correlations for the initiation of bubble movement by using only the pipe slope S_o and the Eötvös number. Data by Colgate [15] also fits their curves relatively well (fig. 29).

Additional studies are required to define the bubble motion curve (fig. 29) for slopes greater than 45 degrees. Martin [52] showed that a stationary air pocket forms when the dimensionless discharge Q_w^2/gD^5 is equal to 0.30 for vertically downward flow. Therefore, the increasing trend of the curve in figure 29 probably does not continue past the 45-degree slope.

As the bubbles travel downstream in sloping conduits, they tend to rise to the top of the conduit and form large pockets of air. Runge and Wallis [61] discovered that the rise velocity of these pockets is greater in sloping conduits than it is in vertical conduits (fig. 30). For a specific range of discharge, a flow condition can exist whereby bubbles will move downstream and form into pockets that move against the flow in an upstream direction.

Sailer [62] investigated prototype cases in which large air pockets moved against the flow with sufficient violence to completely destroy reinforced concrete platforms. The reverse flow region has been delineated on figure 29 using the data of Colgate [15] and the slug-flow curve of figure 30. The five structures pointed out by Sailer as having experienced blowbacks are indicated by crosses on figure 29. It is noted that

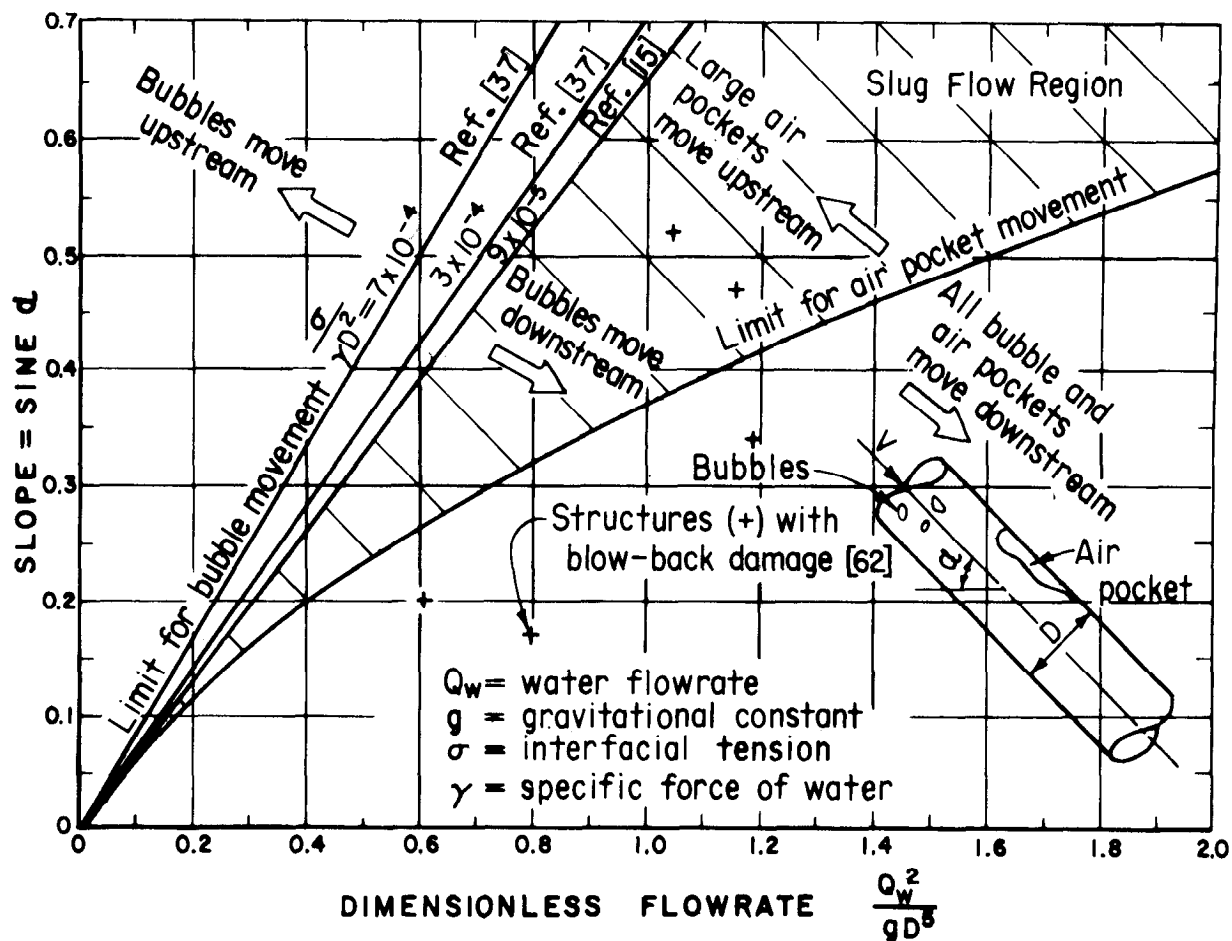


FIGURE 29.—Bubble motion in closed conduits flowing full.

two of these structures lie within the blowback zone at design discharge. The other three must pass through the blowback zone in coming up to the design discharge. For pipe slopes less than 0.1, the width of the blowback zone is so small that problems normally are not experienced.

FLows FROM CONTROL DEVICES

Flows from control devices refer to cases in which the primary cause of the air demand is due to the waterflow conditions at a control device. Two types of flow control devices that will be considered are gates and valves. These

devices also induce air movement in open channel flows. However, in unconfined flows the water movement does not cause low pressures which must be relieved by air vents.

A distinction is made in the field of hydraulic machinery between valves and gates even though both serve as flow control in a closed conduit. A valve is a device in which the controlling element is located within the flow (fig. 31). A gate is a device in which the controlling element is out of the flow when it is not controlling and which moves transverse to the flow when controlling (fig. 31). The jets from gates are different than those from valves; therefore, the two cases are considered separately.

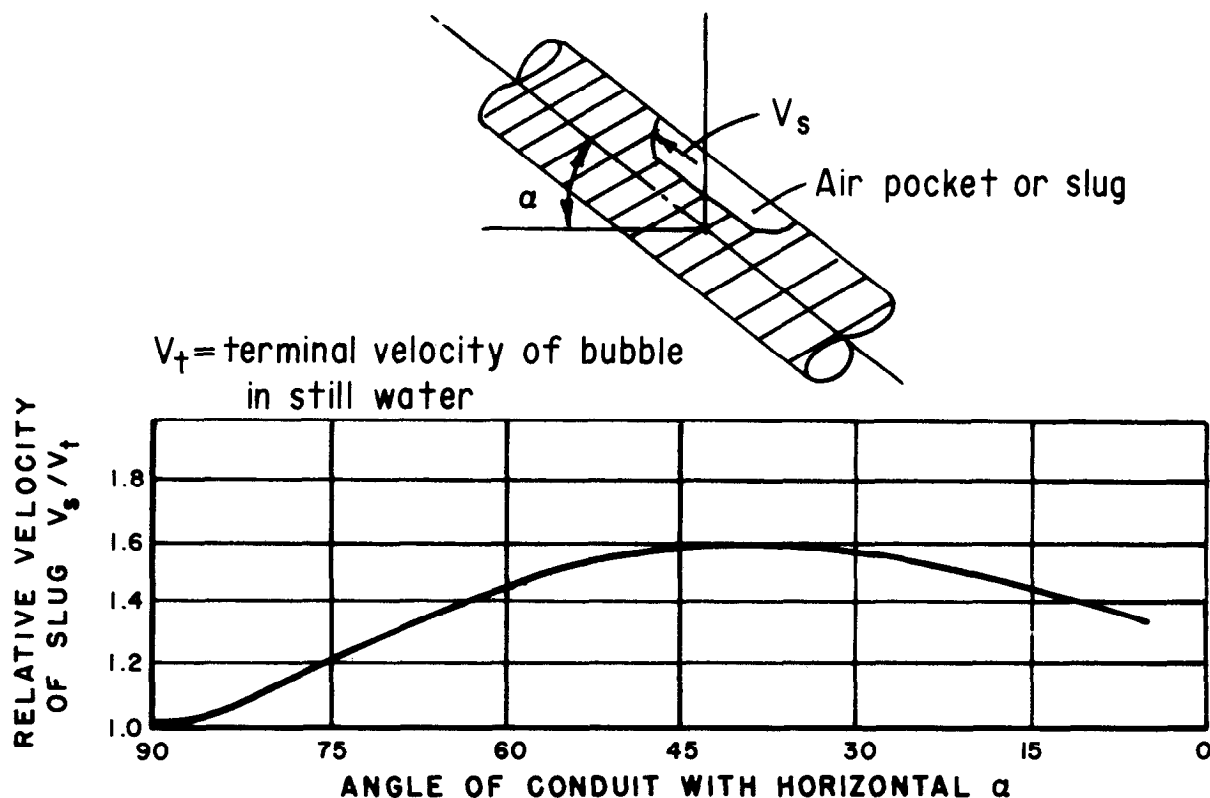


FIGURE 30.—Slug flow in inclined pipes, Runge and Wallis [61].

Flows From Valves

Around the beginning of the 20th century, many outlet valves were placed on or near the upstream faces of the dams. Nearly all were severely damaged by cavitation erosion. Since a satisfactory method could not be found to reduce or eliminate the damage at all gate positions, the operating ranges of these valves were severely restricted. Because of this limitation, the location of the throttling valves was shifted to the downstream side of the dam. Present practice is to avoid placement of throttling valves within the conduit. Nevertheless, from time to time it is necessary to place the valves within the conduits. This is especially true when the downstream conduit is a tunnel—when spray could cause icing problems—and when a flow control station is placed in a pipeline.

If stratified or wave flow exists downstream of the valve, air is induced to move by a relatively low water velocity acting over a large surface area. However, if the flow from the valve impinges on the downstream conduit walls, the airflow is induced by high velocity waterjet acting over a relatively small surface area. In this case, the significant airflow parameters are the:

- Kinetic energy of the waterflow,
- Gate opening, and
- Air pressure at some characteristic location.

Parameters such as length of conduit downstream of the valve and the Froude numbers of the downstream flows are obviously of lesser importance.

SERVICE CLASSIFICATION

THROTTLING VALVES

SCHEMATIC DIAGRAM					
	FLOW DIRECTION				
NAME	FIXED-CONE VALVE	HOLLOW-JET VALVE	NEEDLE VALVE	TUBE VALVE	SLEEVE VALVE
Maximum head (approximate)	300 m	300 m	300* m	90 m	75* m
Discharge coefficient (a)	0.85	0.70	0.45 To 0.60	0.50 To 0.55	0.80
Submerged operation	Yes (1)	No (1)	No	Yes	Yes (1)
Throttling limitations	None	Avoid very small discharge	None	None	None
Spray	Very heavy (2)	Moderate	Small	Moderate (1)	None
Leakage	None	None	None	None	None
Nominal size range, diameter (b)	200- to 2740-mm	760- to 2740-mm	250 to 2440-mm	910- to 2440-mm	310- to 610-mm*
Availability	Commercial standard (3)	Special design	Special design	Special design	Special design
Maintenance required	Paint	Paint	Paint (1)	Paint	Paint
COMMENTS AND NOTES:	(1) Air-venting required. (2) Spray rating will change to moderate if a downstream hood is added. (3) Valves are not "stock" items but standard commercial designs are available.				
(a) Coefficients are approximate and may vary somewhat with specific designs.					
(b) Size ranges shown are representative, and are not limiting.					

SERVICE CLASSIFICATION

THROTTLING GATES

SCHEMATIC DIAGRAM					
	FLOW DIRECTION				
NAME	UNBONNETED SLIDE GATE	BONNETED SLIDE GATES		JET-FLOW GATE	TOP-SEAL RADIAL GATE
		"HIGH PRESSURE" TYPE	STREAMLINED TYPE		
Maximum head (approximate)	25 m	60 m	150* m	150* m	60-75 m
Discharge coefficient (a)	0.6 To 0.8	0.95	0.97	0.80 To 0.84	0.95
Submerged operation	No	No	Yes (1)	Yes (1)	No
Throttling limitations	Avoid very small discharge	Avoid very small discharge	Avoid very small discharge	None	None
Spray	Minimum	Minimum	Minimum	Small	Minimum
Leakage	Small	Small	Small	None	Small to moderate
Nominal size range (b)	3660-wide & 3660-mm high	1830-wide & 2740-mm high	3050- to 6100-mm high	250- to 3050-mm dia.	4570-wide & 9140-mm high
Availability	Commercial standard (1)	Special design	Special design	Special design	Special design
Maintenance required	Paint	Paint	Paint (2)	Paint	Paint-seals (1)
COMMENTS AND NOTES:	(1) Gates are readily available from several commercial sources. They are not an "off-the-shelf" item, however.				
(a) Coefficients are approximate and may vary somewhat with specific designs.					
(b) Size ranges shown are representative, and are not limiting					

FIGURE 31.—Valve and gate data, Kohler [44].

Colgate [14] made model studies of airflows in valves having a fixed-cone.⁷ His results were given in terms of gate opening and discharge. Transforming these values into the appropriate dimensionless parameters results in good correlations for all conditions that were tested (fig. 32). In this case, the kinetic energy of the flow is proportional to the total upstream head. Thus

$$\frac{Q_a}{Q_w} = f \left(G, \frac{\Delta p/\gamma}{H_t} \right) \quad (85)$$

where

G = gate opening in percent

H_t = total potential and kinetic energy (upstream)

$\Delta p/\gamma$ = differential between atmospheric pressure and air pressure at end of vent

γ = specific force of water

Once curves like those presented in figure 32 are developed, it is possible to determine the airflow rates through any air vent that is connected to the structure by using equation [71]. To perform the determination, equation 71 is plotted on figure 31. The intersections of the two sets of curves give the airflow rates for any particular vent.

Flows From Gates

At small gate openings, a considerable amount of spray is produced by flow which impinges in gate slots. This spray induces considerably more air movement than that produced by stratified or wave flow. In a sense, the effect of spray in producing air movement is similar to that of flow from valves. However, with spray the jet does not impinge on the walls

of the downstream conduit; therefore, a seal does not form.

The significant parameters for flow with spray are the same as those for flow from valves; i.e.,

- Gate opening,
- A reference air pressure, and
- The total upstream energy.

Model studies can be used to obtain estimates of the airflow rates which can be expected when spray is present.

As the gate opening increases, the amount of spray decreases. Typically, spray is not significant for openings greater than 10 or 20 percent. The exact percentage depends upon the design of the gate. For the larger openings, the airflow rate is controlled by the two-layer flow relations. That is, the significant parameters are:

- Length of conduit,
- Froude number of the flow, and
- Air pressure at some reference location.

For jet-flow gates a point is reached—as the gate opening increases above some value—where the flow impinges on the downstream conduit. Typically this occurs at a 50- to 60-percent opening. With impinging flow, the airflow rate is correlated with the parameters used for flow from fixed-cone valves. For this type of flow, the length to diameter ratio of the conduit is significant only if the downstream conduit length is less than the distance to the impingement point or if the adverse pressure gradient is large.

FALLING WATER SURFACE

A falling water surface in a closed conduit induces airflow in the conduit. This flow is analogous to that induced by a piston in a cylinder; the water corresponds to the piston. A typical example of this type of flow occurs during an emergency closure of the intake gate to a penstock (fig. 33). As the gate closes, water flowing into the penstock from the reservoir is

⁷The fixed-cone valve is also called a Howell-Bunger valve after its inventors.

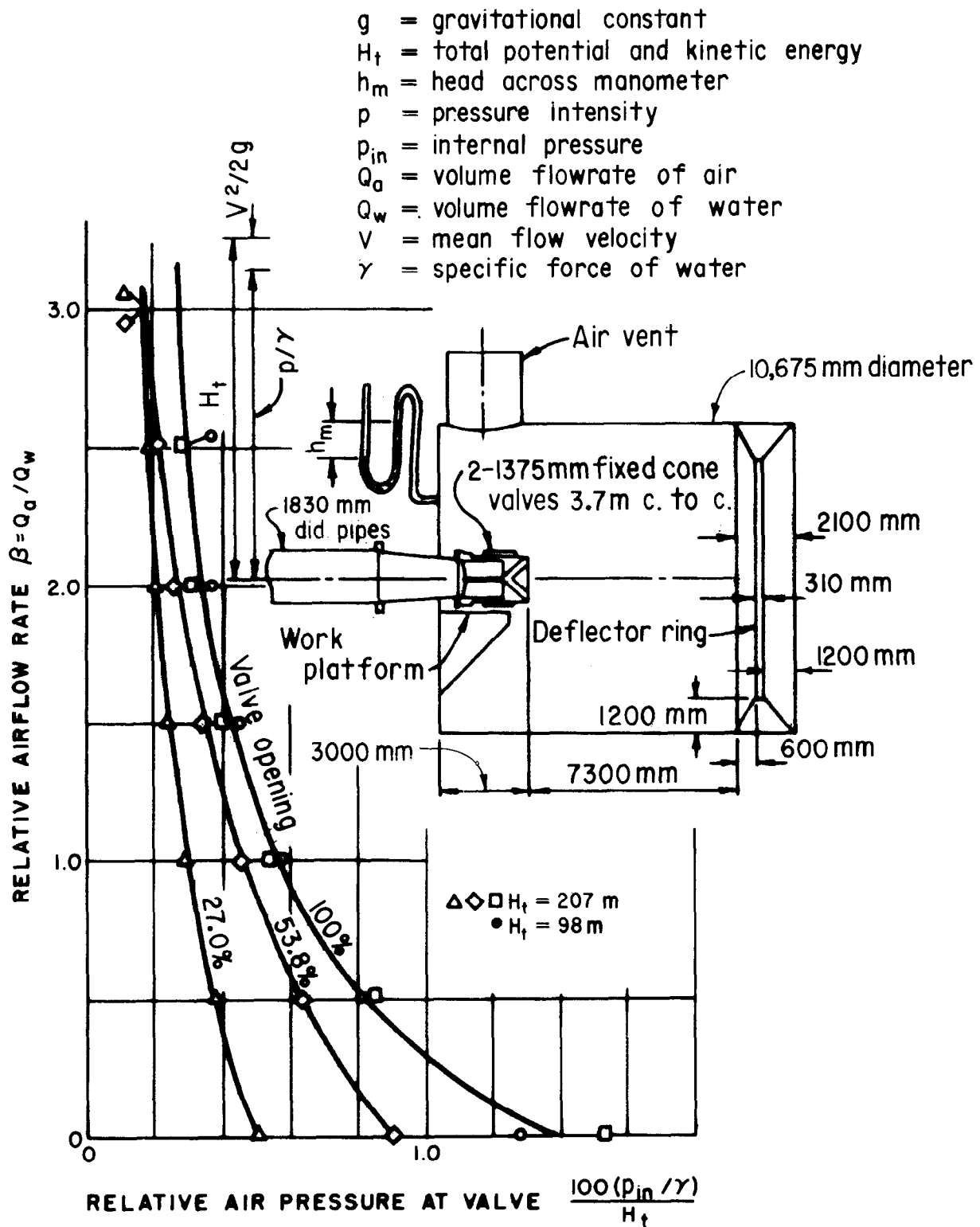


FIGURE 32.—Airflow rate for two 1375-mm fixed-cone (Howell-Bunger) valves.

gradually stopped. However, water in the penstock continues to flow through the turbine in the powerplant. Eventually the gate becomes fully closed. For water to continue flowing from the penstock, air must be allowed to enter the system through a vent located just downstream from the intake gate.

The airflow and waterflow relations—through the penstock and gate chamber—can be simulated analytically by the appropriate mathematical model, Falvey [22]. This model, based upon momentum and continuity equations, yields the airflow rates, etc., as a function of time.

With relatively long penstocks; i.e., length to diameter ratios exceeding 30, the maximum airflow rate occurs slightly after the emergency gate closes completely. The magnitude of the airflow rate is equal approximately to the penstock discharge prior to the start of the gate closure. These observations provide “rules of thumb” which can be used for the design of the air vent structures on dams. The computer program presented in appendix III should be run if a time history of the air-water flow relation is required or if shorter penstocks are being analyzed. This program is a generalized version of the original program and includes typical turbine characteristics.

Good correlations have been found between the computer model calculations and prototype measurements (fig. 34).

AIR VENT DESIGN CRITERIA FOR CLOSED CONDUITS

Purpose

The design of air vents for closed conduits requires careful consideration. The preliminary step is to decide the purpose that the vent is to perform. For instance, air vents can permit air to enter a structure to prevent collapse or to prevent the formation of low pressures within the flowing water which could lead to cavitation

and its possible attendant damage. Conversely, air vents can permit air to escape from a structure. In this case the purpose is to bleed air from a conduit prior to operation.

Location

The next step is to locate the vent properly. General rules cannot be delineated for all cases other than the vent usually is placed where the pressure in the conduit is the lowest. For instance, in gates the appropriate location is immediately downstream of the gate (fig. 31B). For valves the air vent is upstream from the point where the water jet impinges on the conduit walls (fig. 32). In some cases the location must be determined by intuition or carefully conducted model studies.

Maximum Airflow Rate

After the vent is located, the maximum airflow rate through the vent must be estimated. This estimate should be based upon a consideration of the various types of flow which are possible in the water conduit. The previous sections have presented in detail some methods of estimating the maximum airflow rates for specific types of closed conduit flows.

Structural Considerations

The pressure drop across the air vent causes a reduced pressure in the penstock and gate structure. Each part of the structure which is subjected to reduced pressure should be analyzed to determine if it will withstand the imposed loads.

Physiological Effects

The effects of noise produced by high air velocities as well as the structural integrity must

AIR-WATER FLOW IN HYDRAULIC STRUCTURES

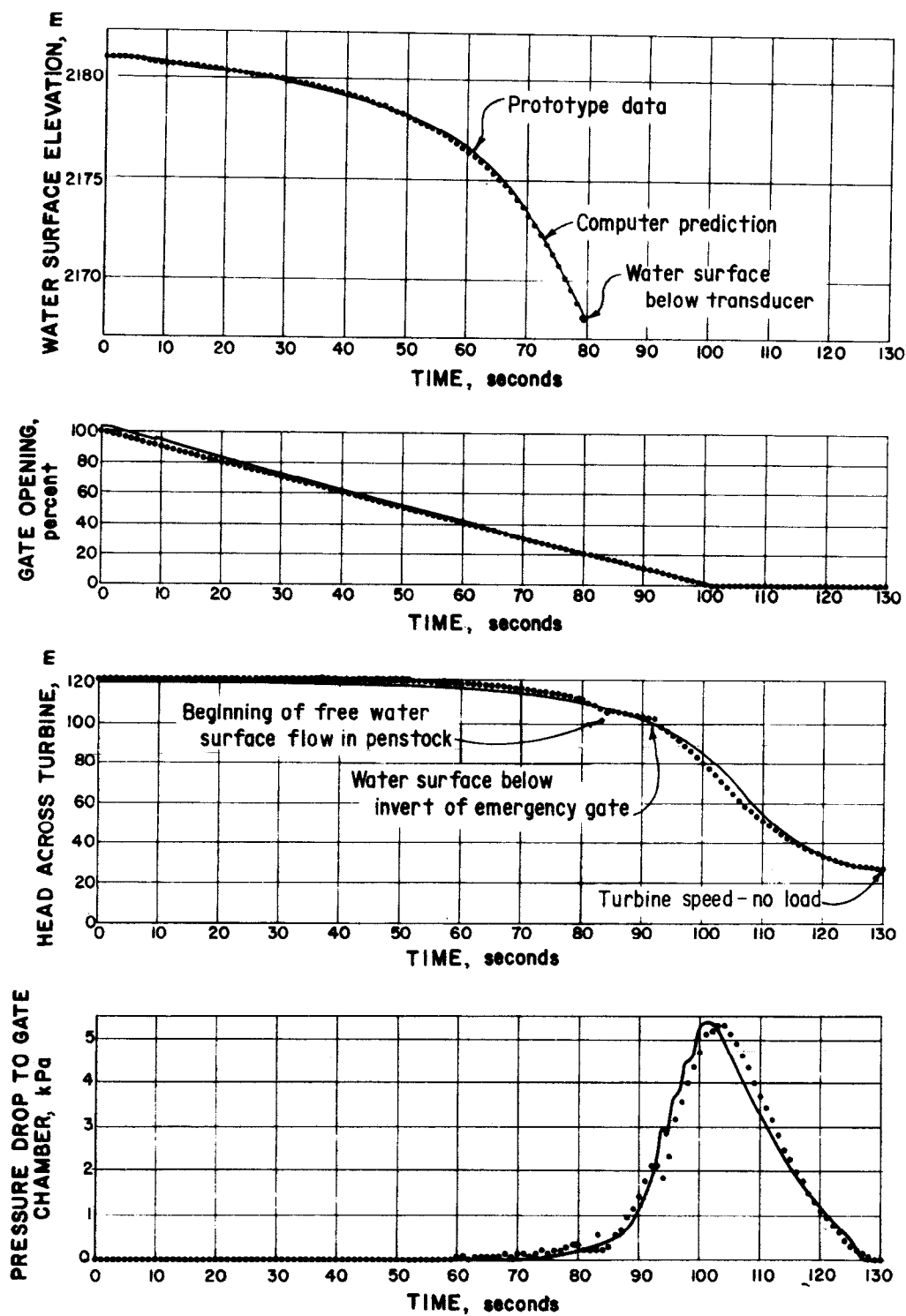


FIGURE 34.—Comparison of field data with computer prediction.

be considered in the design of air vents. The limiting air velocity—with respect to noise—in a vent has been established (by the Water and Power Resources Service) to be about 30 m/s. Above this velocity an objectionable whistling sound occurs. The intensity of the sound and not its mere presence is the governing factor. For instance, ear protection is required for exposure times greater than eight hours and pressure levels above 85 dB (decibels) Beranek and Miller [9].⁸ For pressure levels above 135 dB, ear protection is required for any exposure time.

Field measurements 5 meters from an air vent having an 80-m/s velocity produced sound level intensities of 105 dB. With this sound intensity, ear protection is required for exposure times exceeding 7 minutes. Since sound level intensities increase by the 6th to 8th power of velocity Davies and Williams [19], a 200-m/s air velocity would have produced a sound level intensity between 128 and 136 dB which is damaging to the ears for any exposure time. Based upon this limited result, a 90-m/s flow velocity appears to be a good value to use as a design criterion for air vents that operate for a short duration. If the air will flow through the vent for extended periods, the upper limit on the air velocity should be restricted to the 30-m/s value.

⁸*Construction Safety Standards*, Water and Power Resources Services, pp. 27-28, rev. 1979. The standard states * * *. Protection against the effects of noise exposure shall be provided when the sound levels exceed those shown below when measured on the A-scale of a standard Type II sound level meter at a slow response.

<i>Duration per day,</i> <i>hours</i>	<i>Sound level, dBA,</i> <i>slow response</i>
8	90
6	92
4	95
3	97
2	100
1.5	102
1	105
0.5	110
0.25 or less	115

Safety of Personnel

Another design consideration concerns the safety of personnel in the vicinity of the vent when it is operating. Generally, personnel barriers should be placed around vents at locations where the air velocities exceed 15 m/s. This will prevent personnel and loose objects from being swept either through the air vent or held on the air vent louvers.

Freeze Protection

In areas where the vents operate in cold weather for prolonged periods, the vents should be protected from freezing. Icing occurs when supercooled air passes through the louvers and screens at the vent intake. In some cases ice buildup was sufficient to completely block the flow area (fig. 35). Icing protection includes using heating elements on the louvers, rerouting the vent to place the intake in a warm portion of the structure, or redesign of the intake to eliminate ice buildup areas.

Cavitation Damage

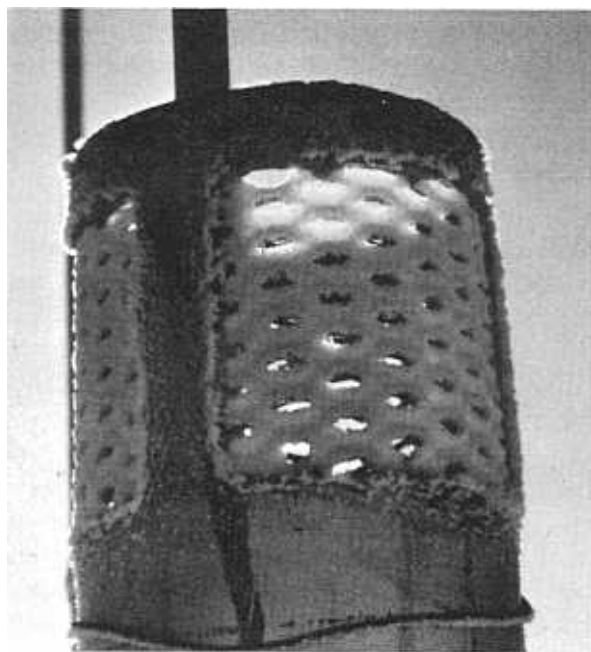
The pressure downstream of gates discharging into conduits should be prevented from becoming too low. If the pressure does drop excessively, cavitation damage may result during prolonged periods of operation. Unfortunately, general guidelines concerning minimum acceptable pressures cannot be given. Each gate or valve design has its own particular characteristics. Some designs are more susceptible to cavitation damage than others. Research studies are needed to define minimum pressure values for the different classes of gates and valves.

Water Column Separation

If the pressure in the water column reaches vapor pressure of the water a possibility exists



A.—View of the vent pipe installed to provide air for a square slide gate in an outlet works. Initial installation had a cap which required removal after frost plugged the screen. P801-D-79278



B.—Closeup view of the screen for a vent pipe after removal of the cap. P801-D-79277

FIGURE 35.—Air vent, Shadow Mountain Dam, Colorado-Big Thompson Project, Colorado.

that the column will separate. Depending upon the geometry of the conduit, the separation can occur at either one location or at several locations. If water column separation is indicated, special waterhammer computations should be performed to determine the overpressures when the water columns rejoin.

AIR VENT DESIGN CRITERIA FOR PIPELINES

Introduction

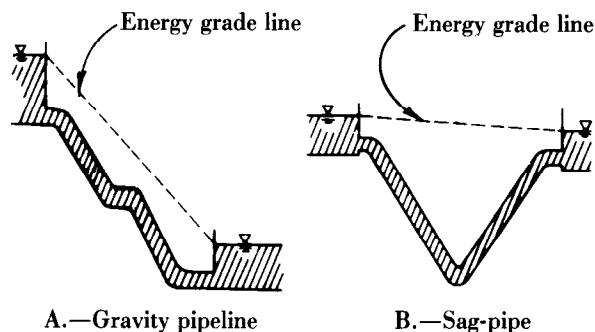
Flow in long pipelines presents a separate class of considerations from those already discussed. One of the reasons for the new set of considerations is the fact that the pipeline profile normally follows the ground surface topography very closely. This causes intermediate high locations which provide an opportunity for the collection of air pockets. To assure trouble-free pipeline operation, details of alignment, location, and sizing of vent structures must be considered.

There are essentially four main categories of pipelines. They are:

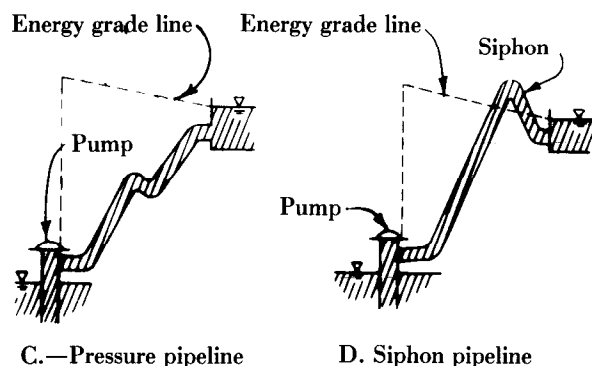
1. Gravity pipelines in which the water flows from a higher elevation to a lower one through the effect of gravity (fig. 36A).
2. Sagpipes (inverted siphons)⁹ in which the flow from one canal to another is passed under a road or across a valley (fig. 36B).
3. Pump lifts in which the water flows from a low elevation to a higher one through pump action (fig. 36C).
4. Siphons in which some portion of the pipe is designed to operate at subatmospheric pressures (fig. 36D). This type of structure is used frequently to prevent water from the upper reservoir from passing back through the pump if a loss of electrical power occurs.

⁹See footnote 1.

Gravity systems, figures 36A and B, normally have different alinement problems than pumping systems (fig. 36C and D); therefore, the two are considered separately.



GRAVITY SYSTEMS



PUMPING SYSTEMS

FIGURE 36.—Pipeline configurations.

Gravity Systems

A vertical section through a typical gravity system is shown on figure 37. The same type of layout also applies to sag pipes if the open vent structures are replaced by canal sections. Two types of summit configurations are depicted. In one case the intermediate summit is above the downstream vent structure. This forms a pool upstream of the summit at the no-flow condition. In the other case, the intermediate summit

is below the downstream vent structure. Therefore, it is submerged by the pool which forms at the no-flow condition.

To prevent difficulties during startup operations, certain criteria should be followed regarding both the vertical and horizontal alinement at the upstream vent structure and at intermediate summits whose elevations lie above the downstream open vent structure.

Vertical alinement criteria.—The pipe invert should be placed on a uniform slope between the vent or summit and the adjacent downstream pool. If this cannot be achieved then the pipe should be placed on continually steeper slopes so that during filling the flow continues to accelerate to the pool level. If the flow were allowed to decelerate, the water depth in a circular pipe could gradually increase until the pipe was about 82 percent full. At this depth the flow could become unstable, alternating between full conduit flow and the 82-percent depth.

At less than design discharge, the flow downstream of nonsubmerged summits passes from free-surface to closed-conduit flow. An air-entraining hydraulic jump always forms when the flow makes this transition. The entrained air can form large air pockets under certain circumstances which move against the direction of flow. This condition is commonly referred to as blowback (refer to previous section—Flow Having a Hydraulic Jump That Fills the Conduit).

If the alinement cannot be planned to avoid either operating in or passing through the blowback region delineated in figure 29, then the pipe diameter should be altered to avoid the region.

Some attempts have been made to collect the large air bubbles which form on the crown of the pipe and lead them away from the pipeline (fig. 38). In the example, the flow conditions never entered the blowback flow region. Therefore, the complicated air collection

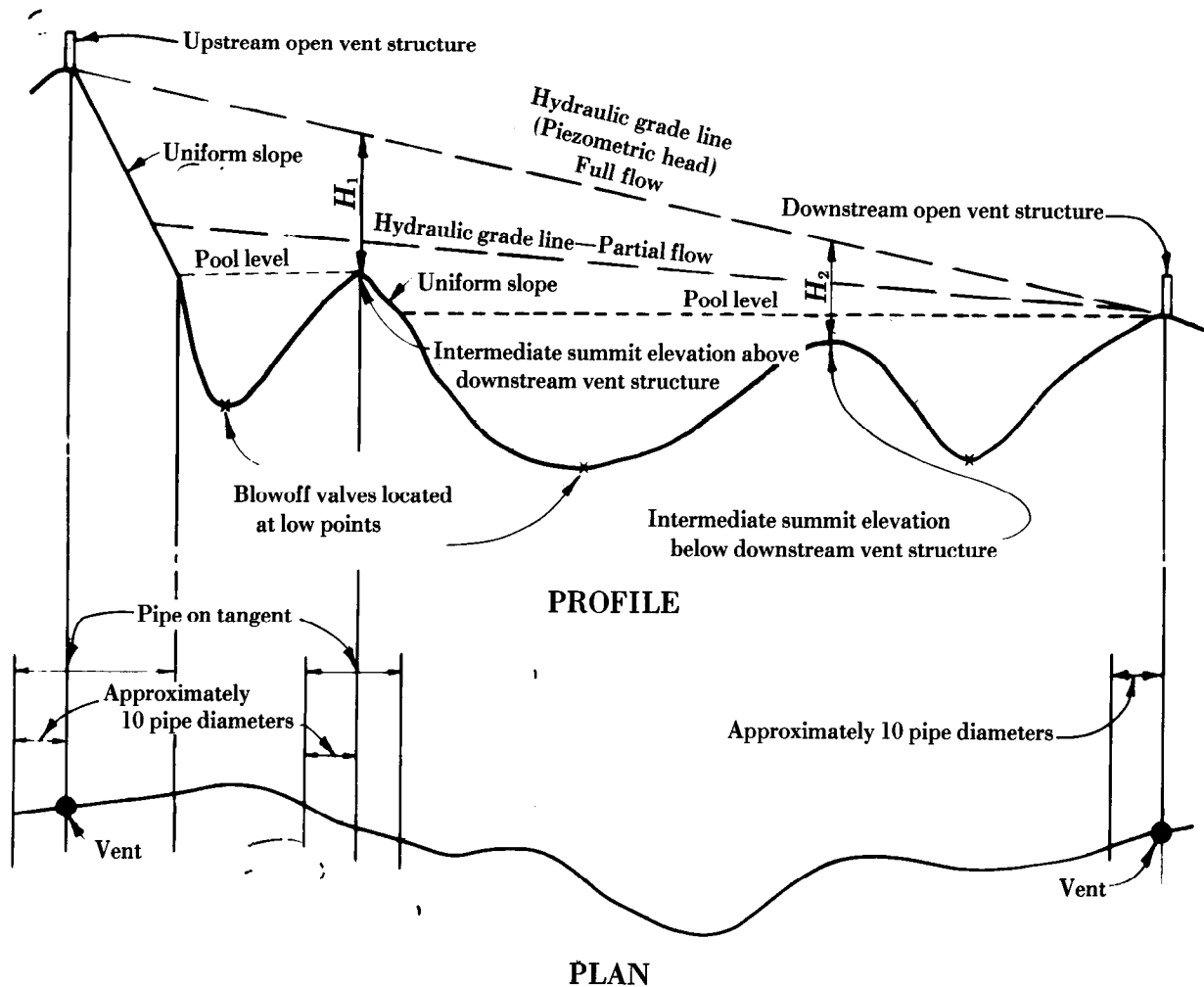


FIGURE 37.—Plan and profile of a gravity pipeline.

system was not needed. If flow had entered the blowback region, this structure probably would not have worked. Colgate [15] found that an unsteady flow condition develops when large air bubbles are bled from a pipeline with too small a vent. To minimize the unsteady flow it is necessary for the vent diameter to equal the pipeline diameter. The design of antiblowback structures like the type shown on figure 38 should not be attempted without hydraulic model studies.

Horizontal alinement criteria.—At the open vent structures and at the intermediate summits

higher than the downstream vent, the pipe should not contain bends for 10 pipe diameters upstream of the location. In addition bends should be avoided in the section between the vent on the summit and the adjacent downstream pool. These criteria prevent transverse waves from being formed on the free water surface which can exist downstream of the vent or summit at partial flows. These transverse waves could roll over with enough amplitude to intermittently seal the pipeline.

Vent location.—The type of air release structure to be used at a summit is determined by the

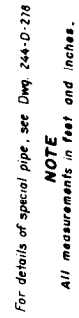


FIGURE 38.—*Vent structure*. 244-D-799

distance from the pipe invert to the hydraulic grade line at the summit. For summits higher than the downstream vent, an open vent is desirable. The maximum allowable vent height is determined from topographic, aesthetic, and economic considerations. Normally, open vents at intermediate summits are not feasible if the distance to the hydraulic grade line H_1 exceeds 6 to 10 meters.

For summits lower than the downstream vent, the type of air release structure is more difficult to determine. If the distance to the hydraulic grade line H_2 is less than about 6 meters, an open vent should be used. However, if the distance exceeds 6 meters an air valve installation should be used (fig. 39). Since mechanical air valves tend to chatter and spit water if their operating pressures are too low, the top of the air valve should be set at least 3 meters below the pool level.

To provide desirable operating characteristics at all discharges, vents also are required at locations other than at the intermediate summits. If the water velocities are of sufficient magnitude to carry air bubbles with the flow, then vents are needed downstream of changes from negative to positive pipe slopes. Without the vents the air slugs, which collect on the crown of the pipe, will attain very high velocities in areas with large positive slopes. These slugs can damage the vent structures at intermediate locations, at downstream connecting canals, and can cause slamming of air valves. These vents should be located less than 30 meters downstream from the negative to positive pipe slope change. If the distance from the intersection of the pool with the negative slope and the proposed vent exceeds $20D$, where D is the conduit diameter, then the vent should be placed at the greater of the two distances (fig. 40). The criterion for the vent type is the same as for vents placed at intermediate summits below the downstream vent structure. If the distance between the upstream and downstream vent structures is very great,



FIGURE 39.—Typical irrigation system air valve installation. P801-D-79279

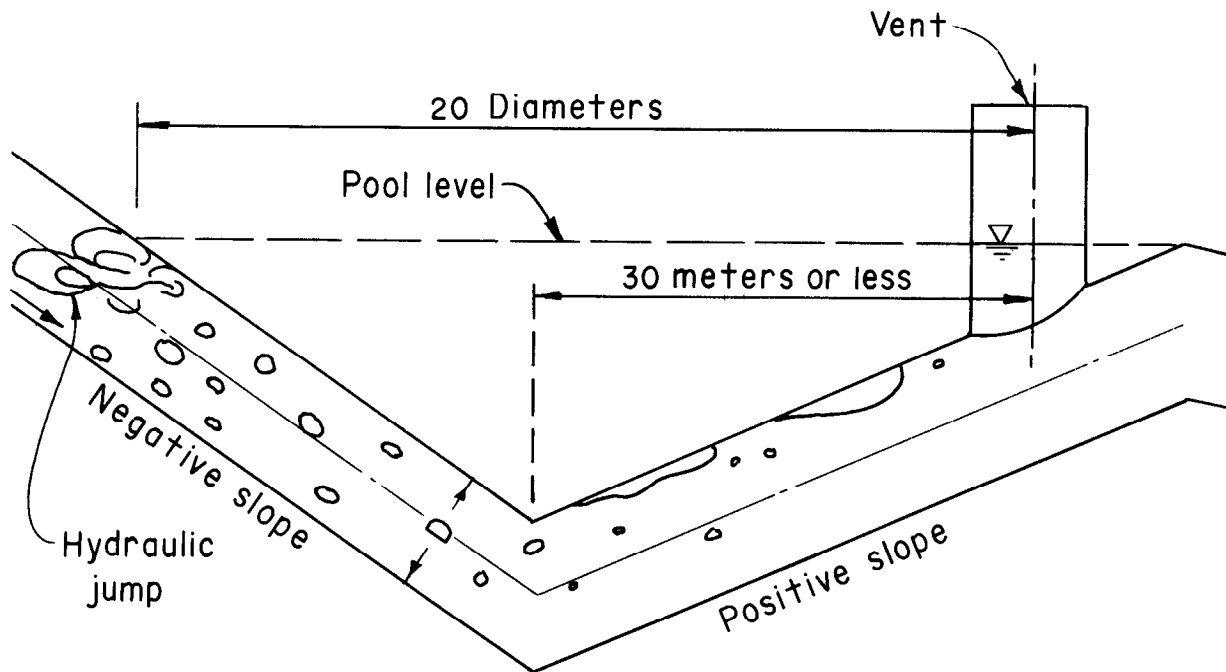


FIGURE 40.—Vent location at changes in pipe slope.

Lescovich [47] recommends that air valves be placed every 500 to 1000 meters along descending, horizontal, or ascending stretches that have no intermediate summits.

Pumping Systems

All intermediate summits are potential locations for the collection of air pockets. If these pockets begin to develop, the hydraulic gradient downstream of the summit will equal approximately the pipe slope in the area where the air pocket has formed. For a pipe slope greater than the full-flow hydraulic gradient, the air pocket will require a greater head differential to produce a given discharge. Conversely, for a constant head differential, the presence of the air pocket will result in decreased discharges. The limiting condition is a complete blockage of flow. In pumping systems this blockage is known as *air binding* [58]. With air binding

the shutoff head of the pump will have been reached (fig. 41). One obvious solution to the problem of air collection at summits is to provide air release valves or vent structures at these locations. Another solution is to align the pipeline so that all intermediate summits are eliminated.

Vent Structure Design Considerations

Vent structures have three primary purposes:

1. Evacuation of air during filling,
2. Removal of air during operation, and
3. Prevent pipe collapse during draining.

Each is considered in detail. The size of the vent and the piping connecting the vent to the pipeline is determined by the purpose for which the vent is installed.

Evacuation of air during filling.—The filling rate of pipelines usually is set at 5 to 15 percent

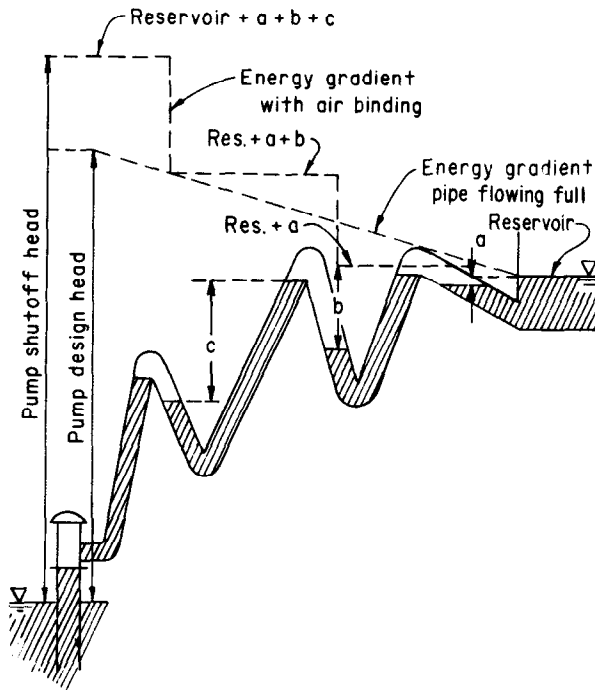


FIGURE 41.—Air binding in a pipeline.

of the design discharge. The actual rate is governed by the maximum waterhammer pressures that the pipeline and valves can withstand. These pressures are generated when the water column in the penstock reaches the air release valve. Based on waterhammer considerations the filling rate of pipelines can be computed from

$$Q_a = \frac{g A_p \Delta h_w}{c} \quad (86)$$

where

- Q_a = penstock filling rate equals airflow rate through vent
- A_p = cross sectional area of penstock
- c = celerity of waterhammer wave in penstock
- g = gravitational constant (acceleration)
- h_w = allowable head rise in penstock due to waterhammer pressures

Lescovich [47] indicated that large orifice air valves should be used to permit air escape during filling (fig. 42). In this case a large orifice refers to diameters greater than 25 millimeters. This type of air valve is designed to remain closed after the pipeline is filled. Thus, they cannot be used to release small amounts of air that accumulate during operation. These valves will open immediately when the pipeline pressure drops below atmospheric. This allows air to reenter the pipeline and prevents a vacuum from forming.

Normally, air velocities discharging from an air valve should not exceed 30 m/s. The primary reason for limiting the velocity is to prevent the air valve from being blown shut. Some air valves are designed to eliminate this problem.

With the 30-m/s velocity limitation, the air can be considered to be incompressible. The equation for the airflow rate is

$$Q_a = A_o C_o \left(\frac{2 \Delta p}{\rho_a} \right)^{1/2} \quad (87)$$

where

- A_o = orifice area, m^2
- C_o = orifice coefficient ≈ 0.6
- Δp = pressure differential across the orifice, kPa
- ρ_a = air density (at 20 °C and a pressure of 101.3 kPa, $\rho_a = 1.204 \text{ kg/m}^3$)

From this equation, performance curves for large-orifice air valves can be derived (fig. 43).

If the desired capacity cannot be achieved with a single air valve, the valves can be placed in clusters—up to four valves—on a single vent pipe from the pipeline.

Removal of air during operation.—Two types of structures are used to remove air during operation. These are an open-vent structure and small-orifice air valves. In either case the connection to the pipeline must be large enough

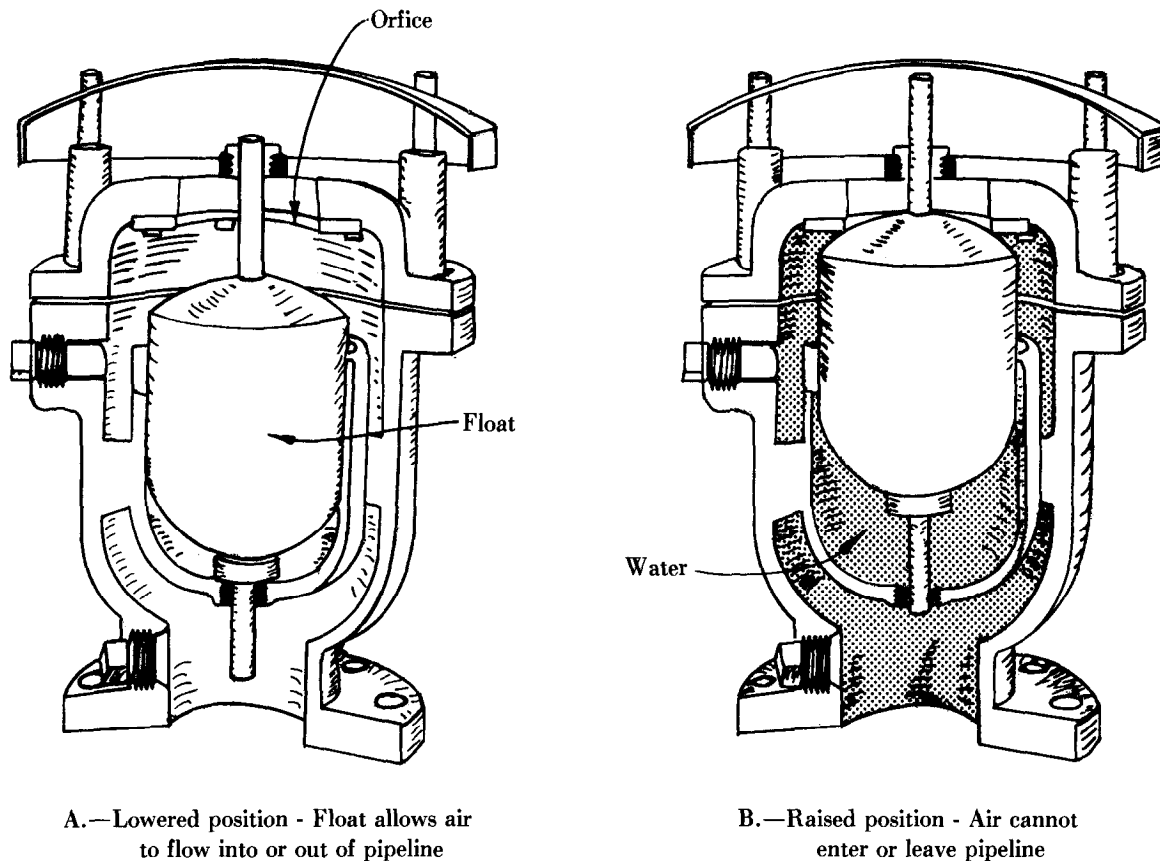


FIGURE 42.—Large-orifice air valve.

to collect the slugs and bubbles of air which are traveling on the crown of the pipeline.

Colgate [15] investigated the sizing criteria for open-vent structures. He found that if the collection port was too small, portions of large air slugs would pass by the vent. To trap all the air it was necessary for the diameter of the collection port to be equal to the pipe diameter. Additional tests were made to investigate the size of the vent structure itself. It was found that if the air vent diameter was less than the pipeline diameter, an unsteady flow was established in the vent as large air bubbles exited from the vent. This unsteady flow pumped air back into the pipeline. To minimize pumping it was necessary to make the vent diameter equal to the pipeline diameter.

Colgate [15] concluded that the collection and evacuation of air from a pipeline can be best accomplished by a vertical air vent which is connected directly to the pipeline. The diameter of the vent should be at least equal to the diameter of the pipeline. From access considerations, the minimum vent diameter usually is set at about 1 meter. Removal of air is promoted if the pipe slope immediately downstream of the vent is made steep enough to cause the air bubbles to return upstream. Figure 29 can be used to determine the required slope for a given discharge.

For the case in which the hydraulic grade line is too far above the pipeline to economically install an open vent, air valves are used to remove the air. Investigations concerning the design of

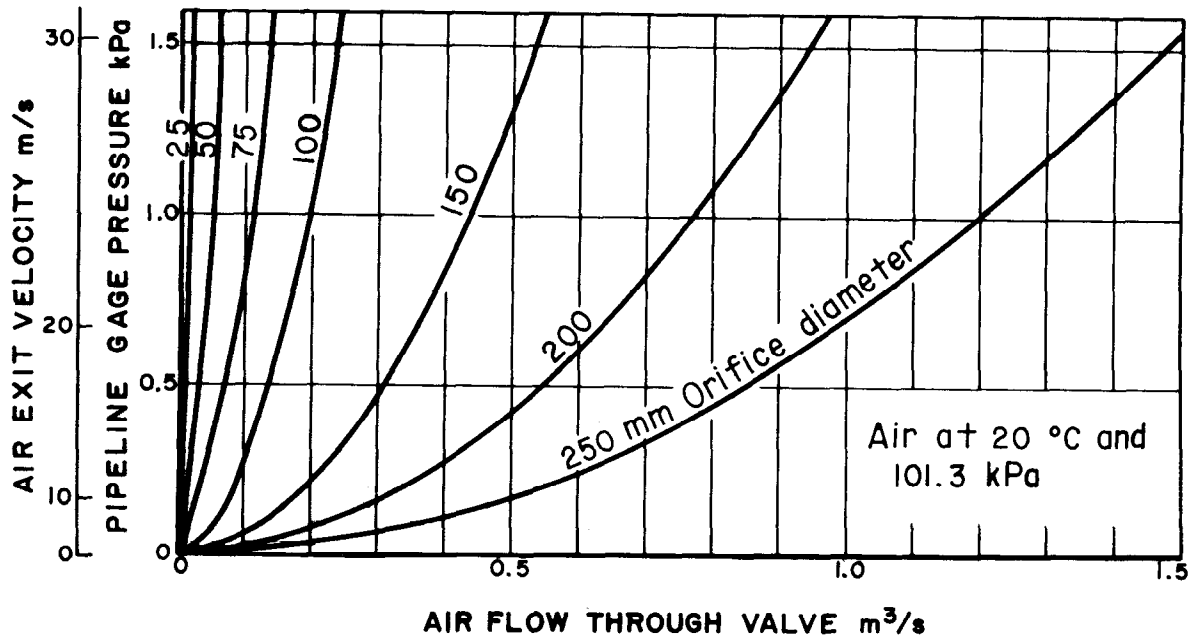


FIGURE 43.—Performance curves for large-orifice air release valves.

a collector have not been performed. Based upon the design of open vents it can be assumed that the diameter of the collector should be at least equal to that of the pipeline. The height of the collector also should be one pipeline diameter. In many cases, manholes in the pipeline can serve as collectors.

To release air from pipelines under high pressures, small-diameter orifice installations are used (fig. 44). The small orifice assures that the opening force of the float is not exceeded by the closing force whose magnitude is equal to the internal gage pipe pressures times the orifice area. The volume flow of air relation through an orifice with a back pressure is given by

$$Q_a = 460 A_o [(p_{in}/p_{atm})^{0.2857} - 1]^{1/2} \quad (88)$$

for

$$\frac{p_{atm}}{p_{in}} > 0.53$$

and

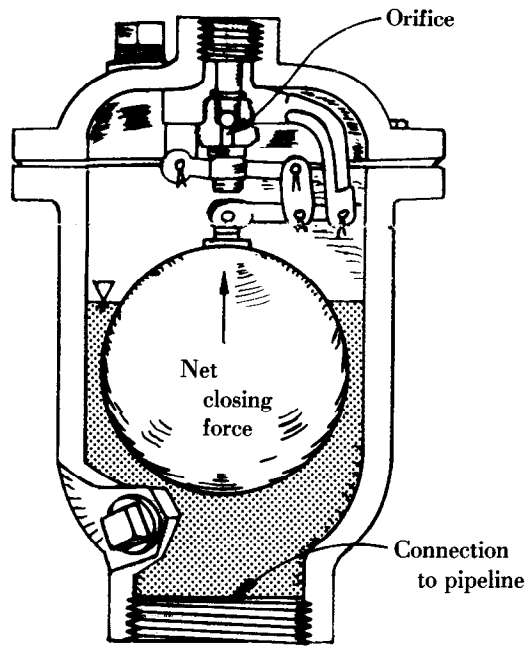
$$Q_a = 11.8 A_o [p_{in}(p_{in}/p_{atm})^{0.7143}]^{1/2} \quad (89)$$

for

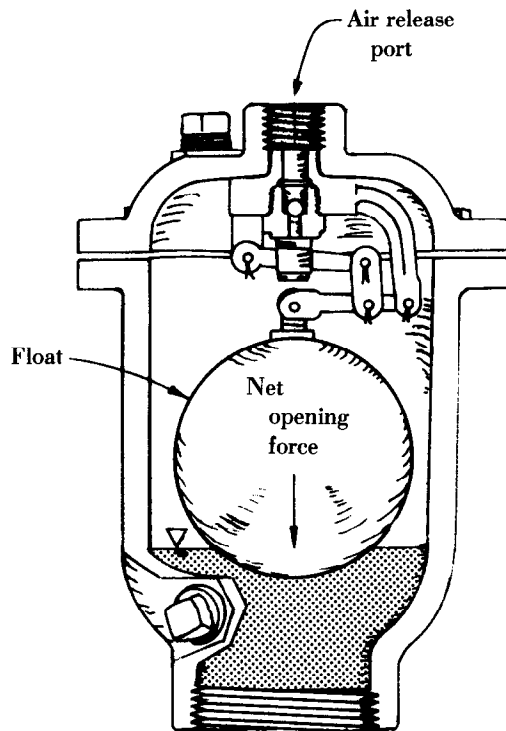
$$\frac{p_{atm}}{p_{in}} \leq 0.53$$

These equations are presented as performance curves (fig. 45).

To prevent the air valves from freezing, frequently they are placed in concrete structures located below the frost line (fig. 46). In this case it is necessary to provide adequate ventilation into or out of the structure. The required ventilation area is based upon a 2.5-m/s maximum air velocity through the gross area of a fixed louver vent. If wire mesh screen is used, the maximum air velocity is 6.6 m/s through the gross area of the screen.



A. High water level



B. Low water level

FIGURE 44.—Typical small-orifice air release valve.

Prevent pipe collapse during draining.—

The venting criteria discussed thus far are based upon the need to remove air from the pipeline. In several instances above-ground steel pipelines have collapsed because vacuum formed during rapid draining operations or because of breaks in the pipeline. Parmakian [56] developed criteria for the size and location of air valves to be placed in steel pipelines to protect them against collapse.

On steel pipes, the collapse pressure can be estimated from (Parmakian [56])

$$p_c = 3.5 \times 10^8 \left(\frac{t}{D} \right)^3 \quad (90)$$

$$= p_{atm} - (p_{in})_{abs} = -(p_{in})_{gage}$$

where

D = conduit diameter, mm

p_{atm} = atmospheric pressure, kPa

p_c = collapse pressure, kPa

p_{in} = internal absolute or gage pressure, kPa

t = pipewall thickness, mm

With stiffener rings, the appropriate equation is

$$p_c = \frac{5.1 \times 10^8 (t/D)^{2.5}}{(L_s/D)} \quad (91)$$

where L_s = distance between stiffener rings.

These two equations are presented graphically in figure 47.

Applying a safety factor N to the internal collapse pressure p_c gives the allowable internal pressure p_a as

$$p_a = p_{atm} - \frac{p_c}{N} \quad (92)$$

If the ratio of the internal to atmospheric pressure is greater than 0.53 then the volume

flow of air into the pipeline through an orifice is given by

$$Q_a = C_d A_o \left(\frac{p_{in}}{p_{atm}} \right)^{\frac{1}{\kappa}} \left\{ \frac{2 p_{in}}{2 \rho_{atm}} \left(\frac{\kappa}{\kappa+1} \right) \left[1 - \left(\frac{p_{in}}{p_{atm}} \right)^{\frac{\kappa-1}{\kappa}} \right]^{\frac{1}{2}} \right\} \quad (93)$$

If the ratio is equal to or less than 0.53 then the airflow rate into the pipeline through an orifice is given by

$$Q_a = C_d A_o \left(\frac{2}{\kappa+1} \right)^{\frac{1}{\kappa-1}} \left[\frac{2 p_{atm}}{\rho_{atm}} \left(\frac{\kappa}{1+\kappa} \right) \right]^{1/2} \quad (94)$$

Using

$$C_d = 0.6$$

$$p_{atm} = 101.3 \text{ kPa}$$

$$\kappa = 1.4$$

$$\rho_{atm} = 1.20 \text{ kg/m}^3$$

in equations 93 and 94 results in

$$Q_a = 460 A_o \left(\frac{p_{in}}{p_{atm}} \right)^{0.715} \left[1 - \left(\frac{p_{in}}{p_{atm}} \right)^{0.286} \right]^{1/2} \quad (95)$$

for

$$\frac{p_{in}}{p_{atm}} > 0.53$$

and

$$Q_a = 119 A_o \quad (96)$$

for

$$\frac{p_{in}}{p_{atm}} \leq 0.53$$

where

$$A_o = \text{orifice area, m}^2$$

$$Q_a = \text{airflow area, m}^3/\text{s}$$

These equations are presented as performance curves for various size vacuum relief valves (fig. 48).

Parmakian presented an alternate method of determining the required air vent size in terms of a dimensionless ratio. The ratio is in the form of an Euler number and is given by

$$\left(\frac{\Delta V^2}{C_o^2 p_{atm} v_{atm}} \right)^{1/4} = \frac{1}{C_o^{1/2} E_u^{1/4}} \quad (97)$$

where

$$C_o = \text{orifice discharge coefficient}$$

$$E_u = \text{Euler number} = p_{atm} / \rho_a V^2$$

$$p_{atm} = \text{atmospheric pressure}$$

$$\Delta V = \text{change in water velocity approaching and leaving air vent}$$

$$\rho_a = \text{density of air at standard atmospheric pressure}$$

$$v_{atm} = \text{specific volume of air at atmospheric pressure}$$

The pressure and specific volume of the atmosphere are both functions of elevation (fig. 49). This alternate method results in the required air vent orifice diameter as a function of the pipeline diameter (fig. 50).

Normally, air valves are placed at the crests in the pipeline profile and at locations where the pipeline begins a steep downward slope.

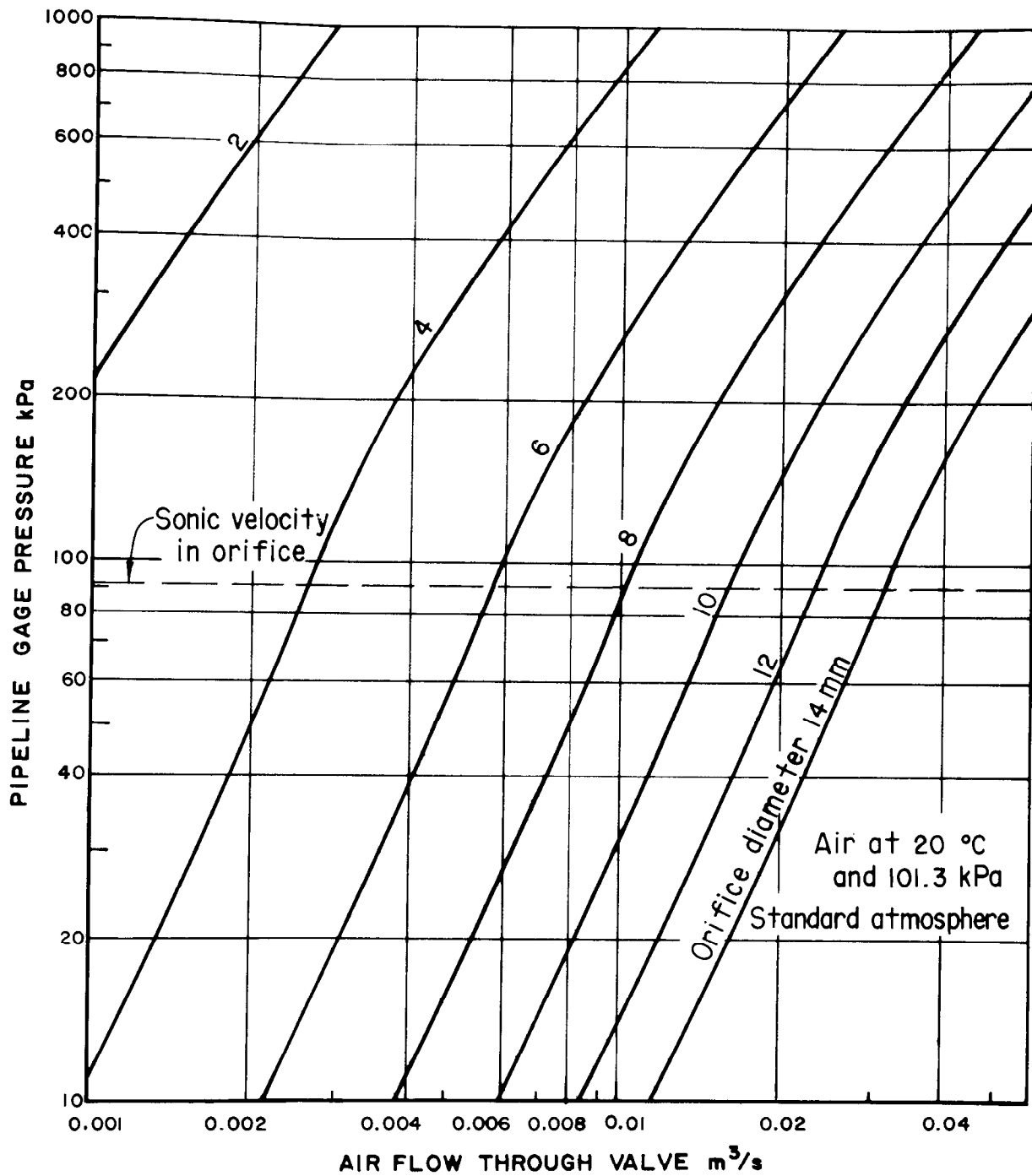


FIGURE 45.—Performance curves for small-orifice air release valves.

AIR-WATER FLOW IN HYDRAULIC STRUCTURES

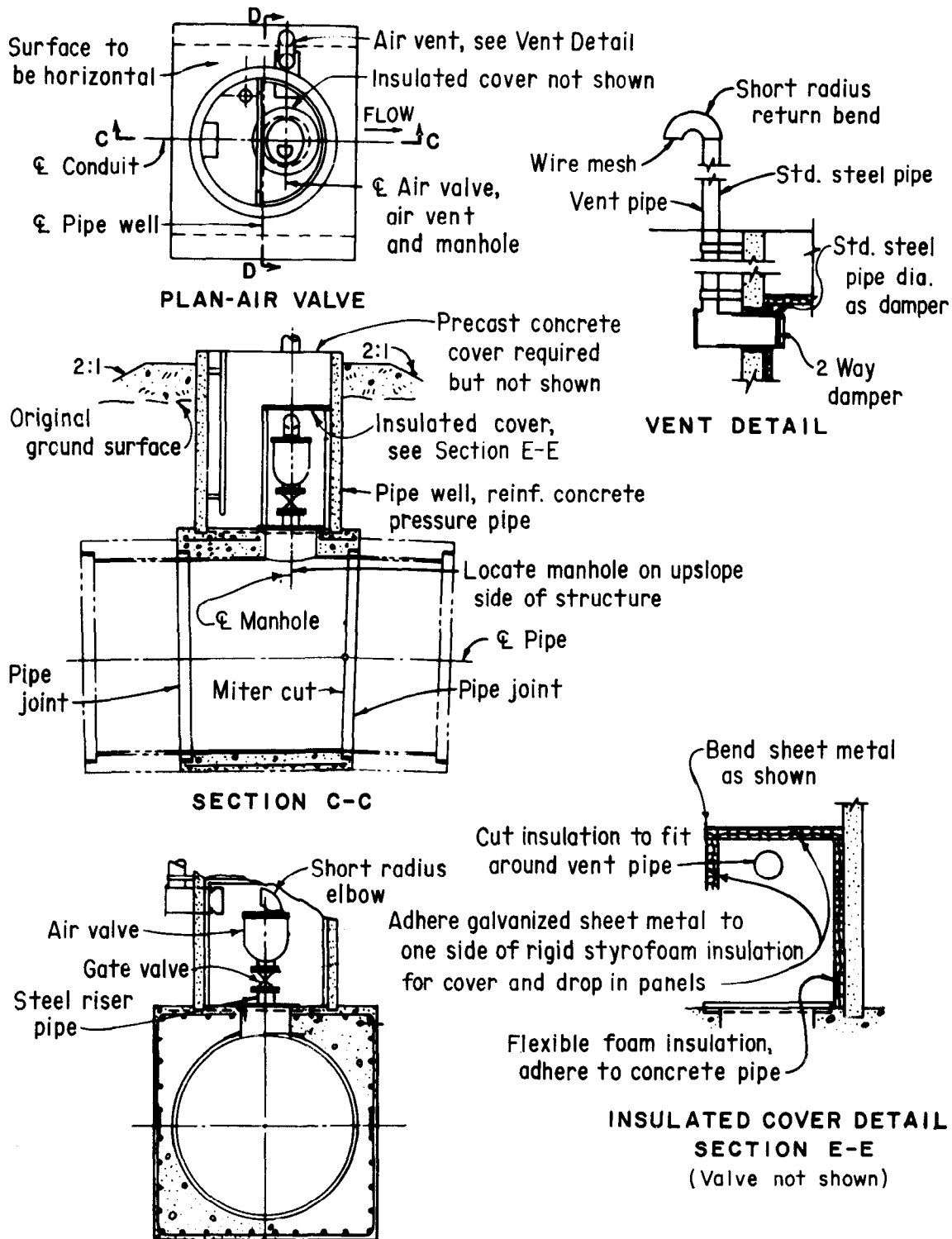


FIGURE 46.—Typical frost protection installation.

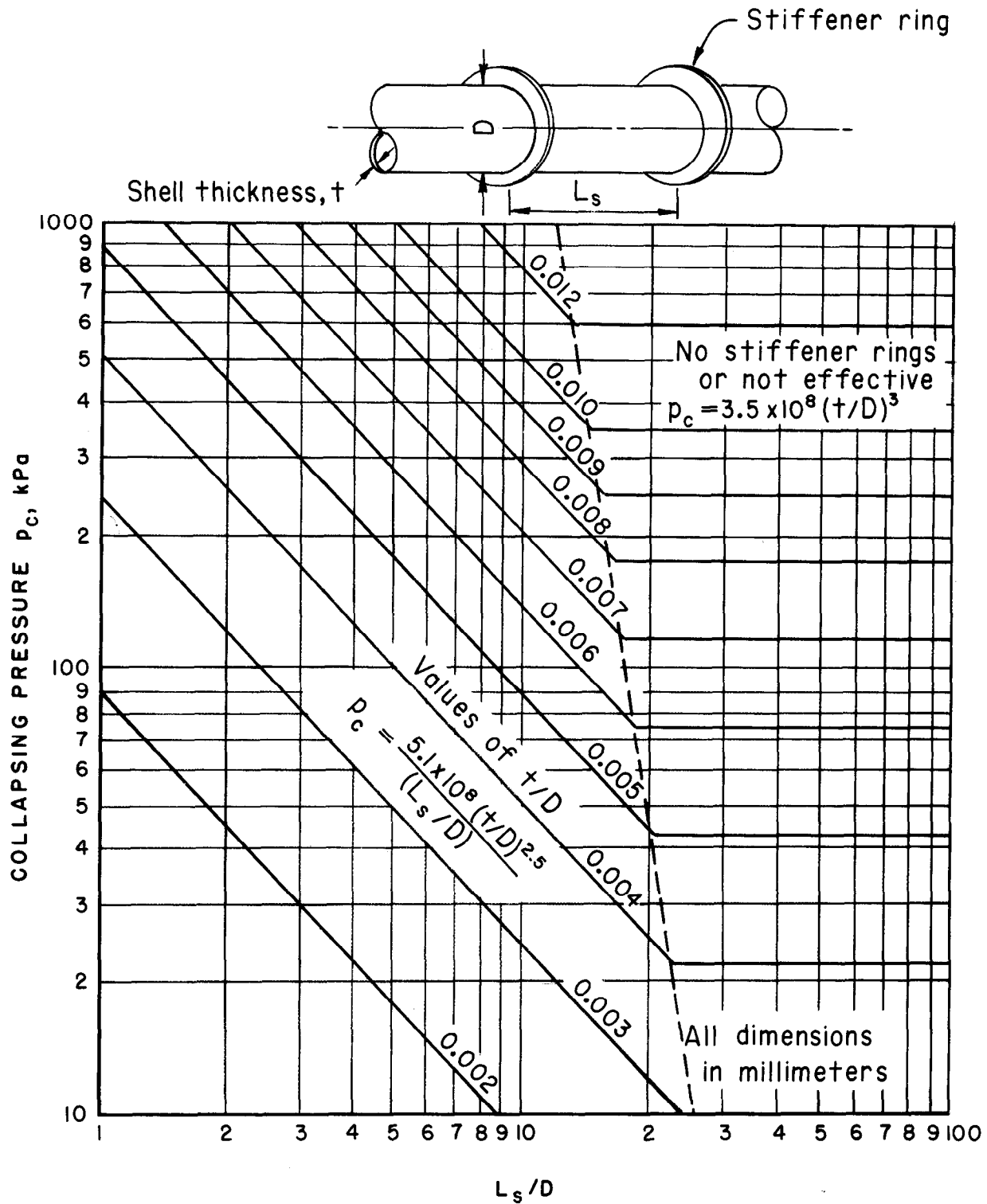


FIGURE 47.—Collapsing pressure of a steel pipe with stiffener rings.

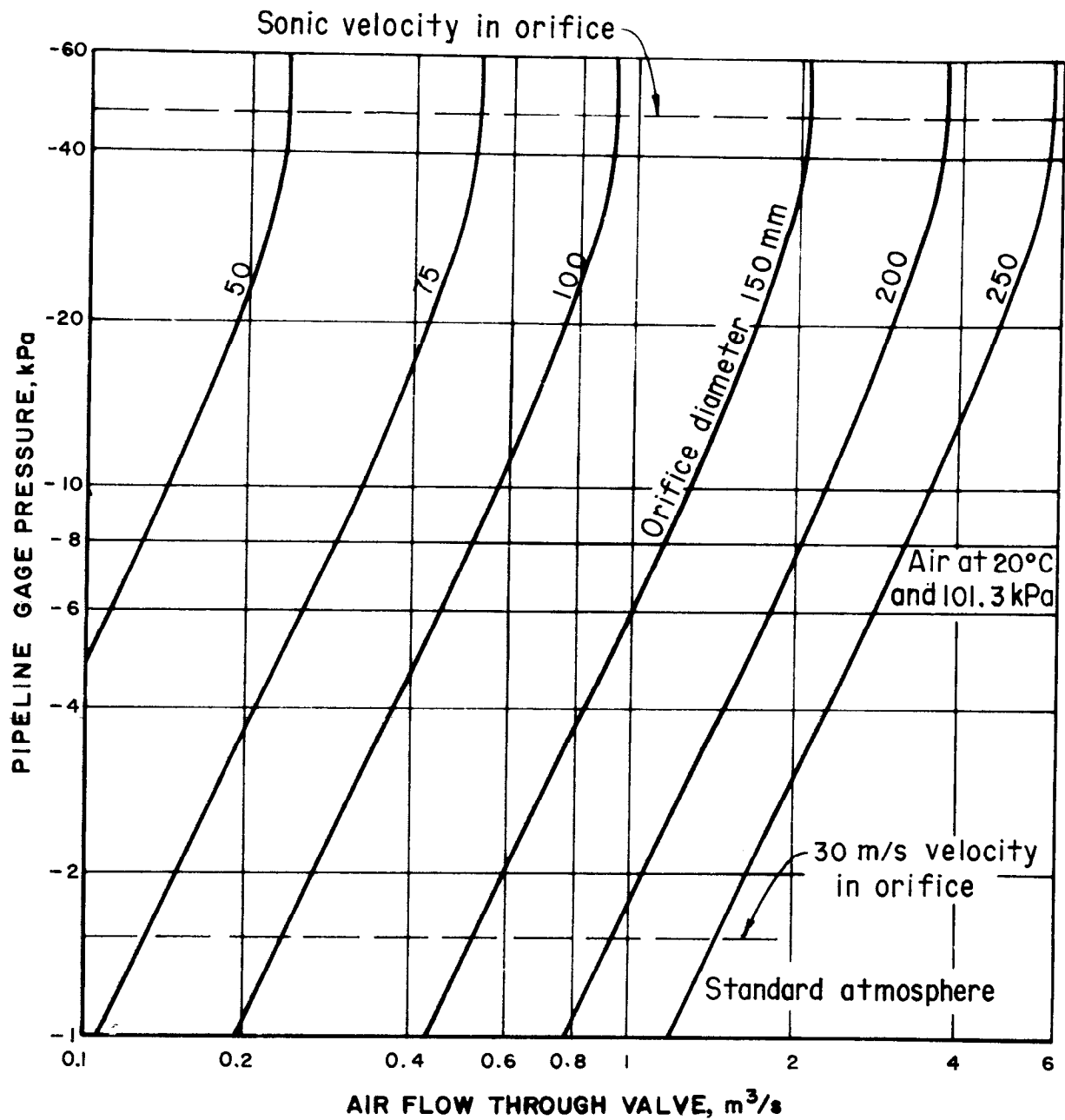


FIGURE 48.—Performance curves for large-orifice vacuum relief valves.

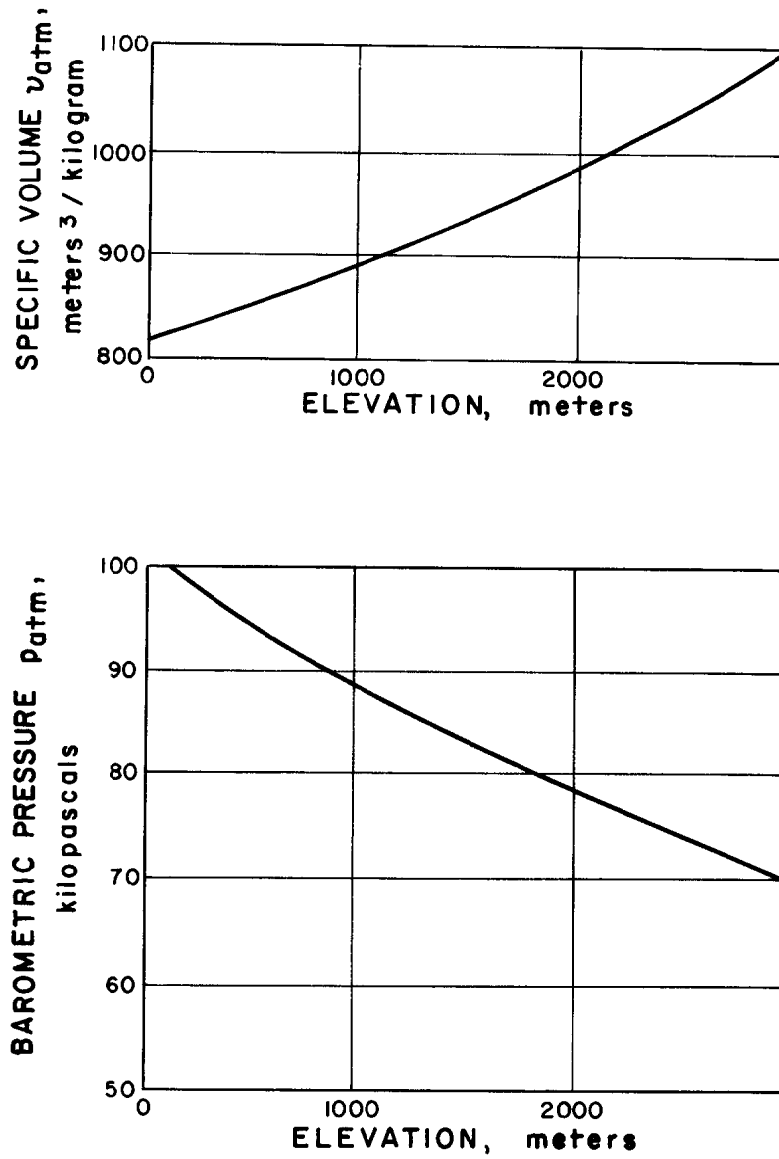


FIGURE 49.—Specific volume and barometric pressure of air as a function of elevation.

AIR-WATER FLOW IN HYDRAULIC STRUCTURES

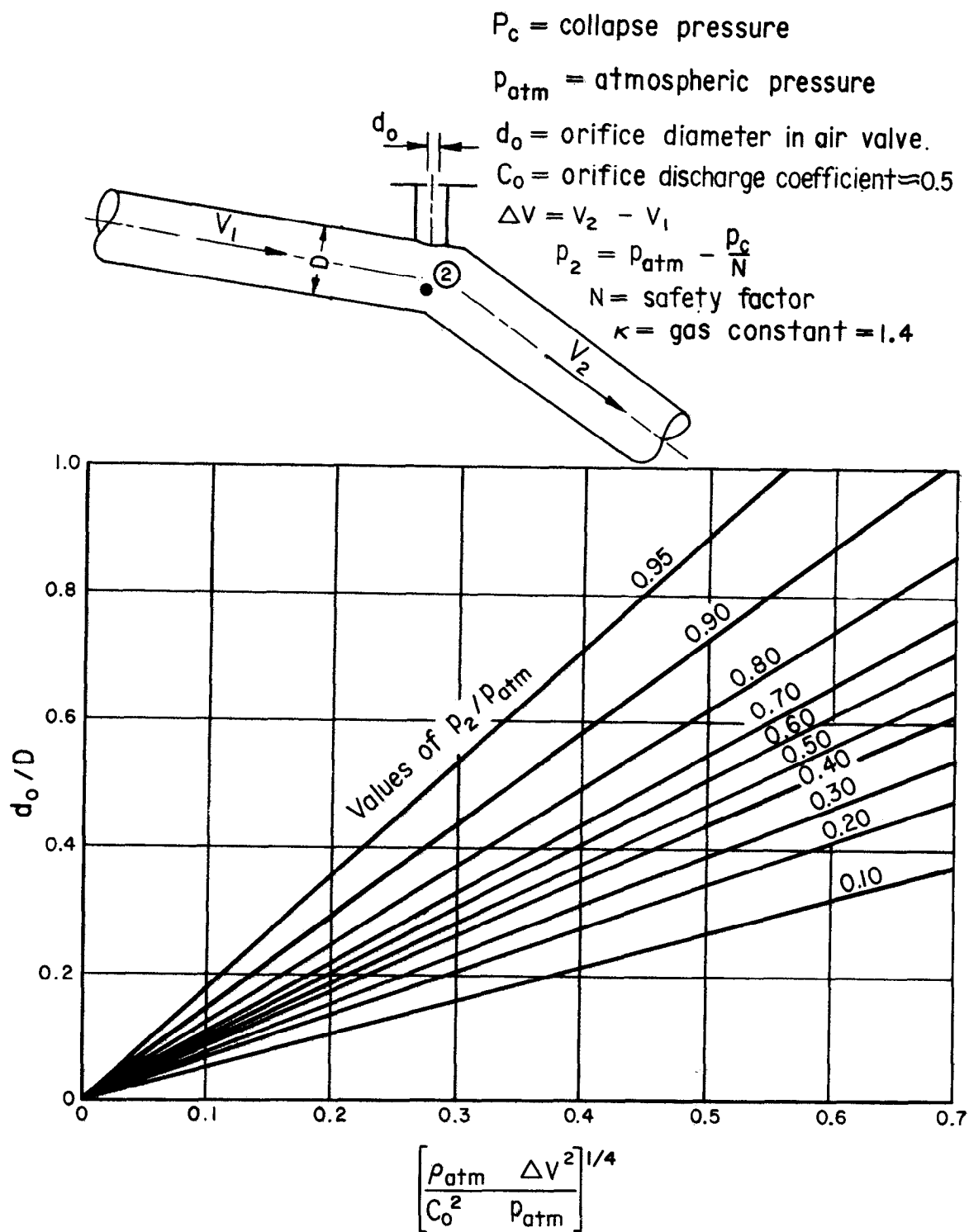


FIGURE 50.—Required air relief orifice diameter to prevent collapse of steel pipelines.

FLOWS IN VERTICAL SHAFTS

Classification of Airflows

Three types of hydraulic structures that use a vertical shaft to convey water from one elevation to another are:

- Spillways
- Intakes
- Drop shafts

The air entrainment properties of these structures are important since at certain flowrates explosive air blowbacks are possible (fig. 51). Often extensive studies are necessary to design vent structures to remove the air which is entrained in the vertical shaft Anderson [3] and Babb [6].

The amount of air entrained in the shaft is strongly dependent upon the type of flow into the shaft and upon the water level in the shaft. The inlet flow can vary from radial to tangential with flow entering around the circumference of the shaft. Typical types of inlet structures (fig. 52) are:

- Circular weirs
- Vortex inlets
- Radius elbows

The effect of water surface (reservoir) elevation at the entrance to a shaft can be examined by considering the discharge characteristics of a vertical shaft spillway (fig. 53). For low water surface levels the discharge is proportional to the three-halves power of the total head on the crest. The flow in the shaft clings to the walls in



FIGURE 51.—Observed air blowback in morning glory spillway at Owyhee Dam, Oregon. P801-D-79280

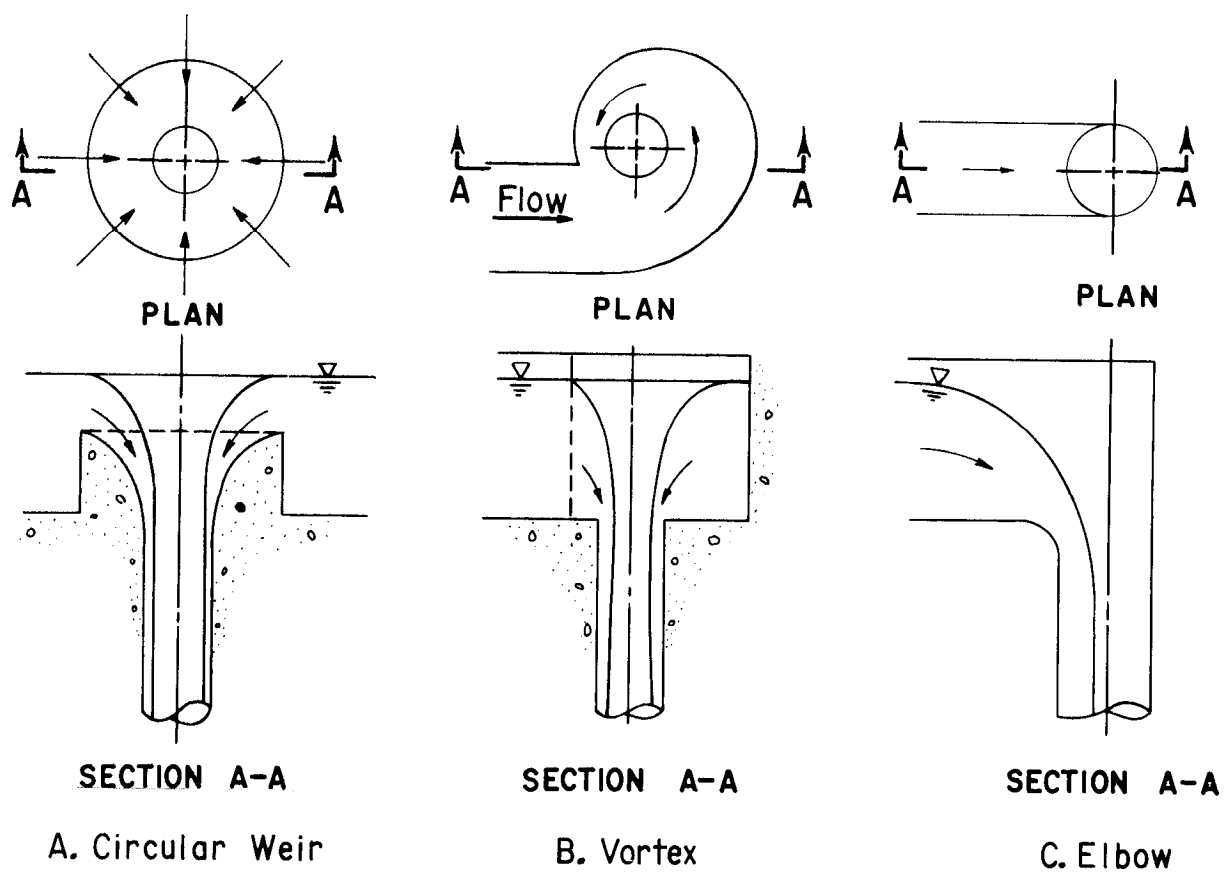


FIGURE 52.—Typical types of vertical shaft inlet structures.

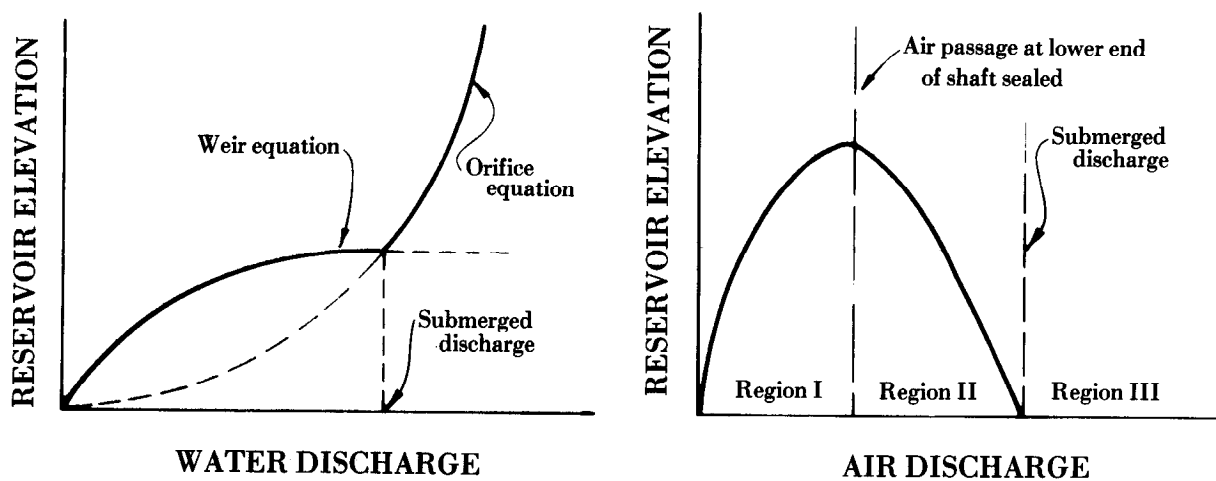


FIGURE 53.—Vertical shaft spillway discharge characteristics.

a relatively thin sheet. The volume flow rate of air is determined primarily by the shear action of the air-water interface and by entrainment into the mass of the water. This type of flow has been designated as region I on figure 53. As the water discharge increases with increasing reservoir elevation, a point is reached when the sheet of water is sufficiently thick to completely fill the upper end of the conduit. This water discharge separates region I from region II type flows.

Region II type flows are characterized by an annular hydraulic jump. Further increases in reservoir elevation merely cause the location of the jump to move upward in the vertical shaft. When the jump reaches a point near the top of the shaft, the flow is said to become submerged.

For reservoir elevations in excess of that required to produce the submerged water flow, all inflow of air to the shaft ceases. The discharge for this flow range is proportional to the one-half power of total energy over the crest.

If the bottom of the shaft is always submerged, then a region I type flow will not develop. Instead, the air motion will be described by a region II type flow up to the point when the vertical shaft is submerged.

The airflow rates discussed above should not be confused with those that are present in the portions of the structure downstream of the vertical shaft. The methods discussed in this chapter—Flow in Partially Filled Conduits—should be used to analyze the flow of air in the horizontal sections of vertical shaft spillways and similar structures. Mussalli and Carstens [55] studied surging problems that develop as the horizontal conduit seals [fig. 21 (5)]. However, they did not develop any air entrainment criteria for the vertical shaft.

Region I Airflow Rates

The airflow rate down the vertical shaft can be calculated by assuming:

- a. The water flow on the shaft walls is similar to open channel flow, and
- b. The lower end of the shaft is open to the atmosphere.

If the inlet is not designed to keep the water flow attached to the wall, the airflow rate cannot be calculated.

Several methods are available to estimate the airflow rate when the water forms in a sheet on the walls. For instance, the air insufflated into the flow can be estimated from equation 59 using open channel flow relations. The amount of air flowing on the core of the pipe can be determined from

$$Q_a = V_o A_c \quad (98)$$

where

A_c = cross sectional of air in core

V_o = maximum water velocity in vertical shaft

Hack [27] recommends that the total airflow be determined from

$$Q_a = 0.35 + 16.1 \bar{C}^{2.88} \quad (99)$$

where \bar{C} = mean air concentration

The mean air concentration is estimated from

$$\bar{C} = \{1 + [4(1 - e^{k_r(F_o^{4/3} - F^{4/3}))}]^{-1}\}^{-1} \quad (100)$$

where

D = conduit diameter

F = Froude number at end of shaft

F_o = Froude number at point where boundary layer intersects water surface

$k_r = 1.8 r_s + 0.0108$

k_s = equivalent sand grain roughness

r_s = relative roughness = k_s/D

The point where the boundary layer intersects the water surface is found through the application of equations 27 through 30.

Region II Airflow Rates

Various investigators have studied the entrainment of air by an annular jet.

Haindl [29] found that the air entrainment obeys a law very similar to that found by Kalinske and Robertson [38] for a hydraulic jump in a conduit. The relation is

$$\beta = \frac{Q_a}{Q_w} = 0.02 (F - 1)^{0.86} \quad (101)$$

where F = Froude number

$$F = \frac{Q_w}{R_j D [1 - (R_j/D)] (g R_j)^{1/2}} \quad (102)$$

D = outside jet diameter (conduit diameter)

g = gravitational constant (acceleration)

Q_a = volume flowrate of air

Q_w = volume flowrate of water

R_j = thickness of annular jet

Kleinschroth [43] found a correlation for flows in vertical shafts having a vortex inlet. The relation is

$$\beta = 0.022 \frac{h_f^{3/5}}{D} \quad (103)$$

where

h_f = distance from the inlet to the water level in the vertical shaft

D = shaft diameter

Reverse Airflow in a Vertical Shaft

All the preceding relations assume that the waterflow rates are sufficient to remove all the entrained air from the system. Martin [51] showed that slug flow begins when the dimensionless airflow β exceeds 0.223. It was shown earlier that these slugs move up the shaft for

$$\frac{Q^2}{g D^5} < 0.3 \quad (104)$$

Therefore, for dimensionless water flow ratios less than 0.3, the airflow quantities given by equations 101 and 103 are too large. In addition, it is possible that blowback will occur in the shaft.

Submergence

The water depth which causes a vertical shaft to flow submerged has been determined only for the case of radial inflow. Jain, Raju, and Garde [36] determined that the submergence at which airflow down the shaft ceases is given by

$$\frac{S}{D} = 0.47 F^{1/2} \quad (105)$$

where

D = shaft diameter

$F = V/(gD)^{1/2}$

g = gravitational constant (acceleration)

S = submergence depth

V = mean water velocity in shaft flowing full

For a vortex inlet or for approach flow having some circulation, the required submergence would be greater than that given by equation 105.

Free Falling Water Jets

Free falling water jets have important aeration effects in the case of unconfined flow discharging from gates and valves. Three main areas of concern are:

1. Jet characteristics,
2. Airflow around the jet, and
3. Air entraining characteristics as a falling jet enters a pool of water.

Each of these subtopics will be considered in detail.

Jet Characteristics

Dodu [20] and Rouse et. al., [60] have shown that the jet characteristics are a function of the conduit geometry and flow dynamics upstream from the point where the jet begins. For instance, a laminar jet exiting from a carefully shaped orifice connected to a large tank of quiescent water can have such a smooth surface that the jet appears to be made of glass. If the

water surface in the tank is disturbed, however, waves will form on the surface of the jet. For turbulent flow, the jet always disintegrates somewhere along its length if it is allowed to travel far enough. However, the distance to the point at which the breakup occurs is controlled by the turbulent intensity within the jet. By changing the flow geometry upstream of the jet, its turbulent intensity is varied.

It should be emphasize that the breakup of the jet is caused primarily by turbulence internal to the jet and only secondarily by the action of the air into which the jet discharges [60]. Tests by Schuster [64] in which a jet discharged into a vacuum show exactly the same jet texture and breakup characteristics as observed by Dodu [20] of a jet discharging into air. From this, one can conclude that physical models should accurately predict the spread and energy content of prototype jets if the turbulent intensity in the model is similar to that in the prototype.

When comparing model and prototype jets near their origin, the prototype jet apparently is surrounded by much more spray than the model (fig. 54A). This difference is due partially to the time scale relations between the two jets. The prototype represents, in essence, a high-speed photograph of the model. The many small drops in the model (fig. 54A) appear as a frothy spray when photographed at a much faster camera speed.

The effect of the air on the jet becomes significant only after the jet atomizes into individual drops.

In the region far from the origin of the jets, their trajectory is affected by air resistance and a large portion of the stream falls vertically downward as spray (fig. 54B).

Hinze [35] studied the breakup of individual falling drops. His results have been replotted in the form of Weber and Reynolds number relations (fig. 55). Here the Weber number is defined as

$$W^2 = \frac{U_d^2 D_d}{\sigma / \rho_f} \quad (106)$$

where

D_d = diameter of water drop

U_d = velocity of water drop relative to air velocity

ρ_f = water (drop) density

σ = interfacial surface tension

The Reynolds number is defined as

$$R = \frac{U_d D_d}{\nu} \quad (107)$$

where ν = kinematic viscosity of the drop

From figure 55 and fall velocity equation for a rigid sphere, it is possible to estimate the maximum stable drop diameter as about 0.4 mm.

The fall velocity of spheres can be determined from a form of the Stokes equation (eq. 1). The relationship is

$$V = \left\{ \frac{4}{3} [(\rho_w / \rho_a) - 1] \frac{g D_d}{C_s} \right\}^{1/2} \quad (108)$$

where C_s drag coefficient of a sphere

The drag coefficients of spheres can be found in fluid mechanics texts [59].

The maximum stable drop diameter usually is not observed in nature because the larger free falling drops have some survival time associated with them. As small drops atomize they pass from a spherical shape to a torus with an attached hollow bag-shaped film. As this bag bursts, the entire torus breaks up. A certain time is required for this process to take place. Komabayasi et al., [45] found that drops of 7- and 5-millimeter diameters took 10 and 200 seconds, respectively, to break up. Thus, a 7-mm-diameter-drop would have to fall more than 85 meters at a terminal velocity of 8.5 m/s to breakup into smaller drops. A distance of more than 1300 meters would be required for the 5-m-diameter drop to breakup at a terminal fall velocity of 6.7 m/s.

Airflow Around the Jet

The airflow around a jet depends primarily upon the velocity of the jet and roughness of the jet. Dodu [20] found that the velocity distribution in the air around the jet was approximately logarithmic up until the point where the jet breaks up. The velocity distribution should follow a law expressed by

$$\frac{U_j - u}{u_*} = f\left(\frac{y_a - r}{\delta}\right) \quad (109)$$

where

- r = water jet radius
- U_j = water jet velocity
- u = air velocity at a point located y_a
distance from the jet centerline
- y_a = distance from water surface
- δ = boundary layer thickness
- u_* = shear velocity = $(\tau_j/\rho_a)^{1/2}$
- ρ_a = air density
- τ_j = shear stress at water jet

The functional relation should be very similar to that for flow over a flat plate as studied by Bormann [11] (fig. 56).

Unfortunately, data are not presently available that will allow the computation of the shear velocity and boundary layer thickness in the air surrounding a jet for a given jet geometry and flow rate.

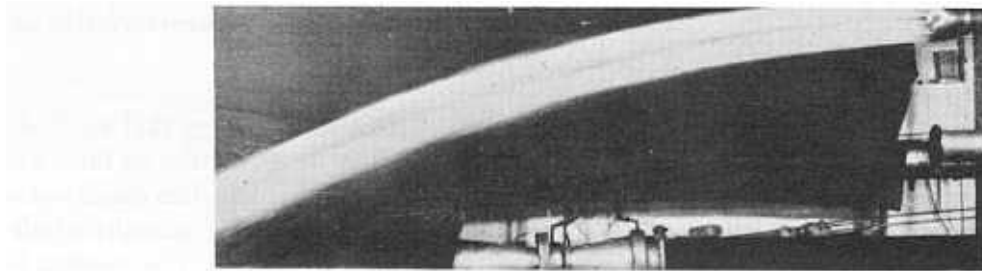
Air Entraining Characteristics as a Falling Jet Enters a Pool

Ervine and Elsayy [21] studied the air entrained by a rectangular jet falling into an open pool. They developed an empirical relation that predicts the relative quantity of air taken into the water by the jet. The relation is

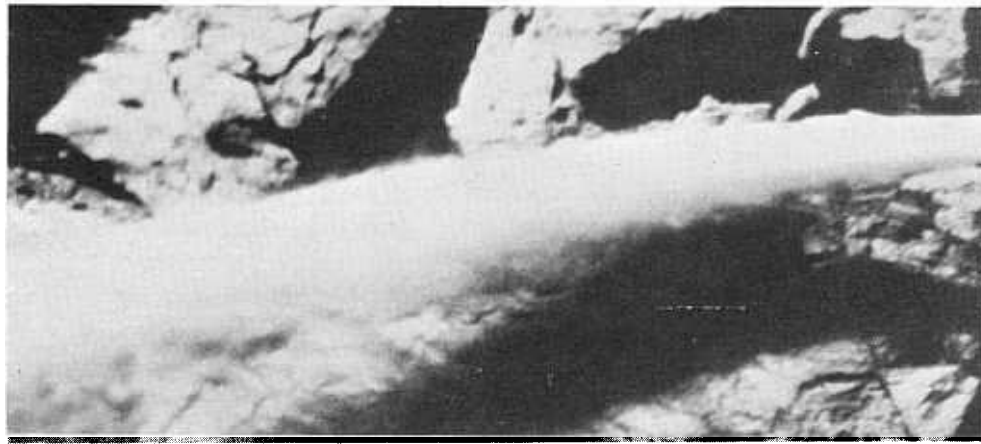
$$\beta = \frac{Q_a}{Q_w} = 0.26 \frac{b_n}{p_n} \left(\frac{H_f}{d_n} \right)^{0.446} \left(1 - \frac{V_m}{V_i} \right) \quad (110)$$

where

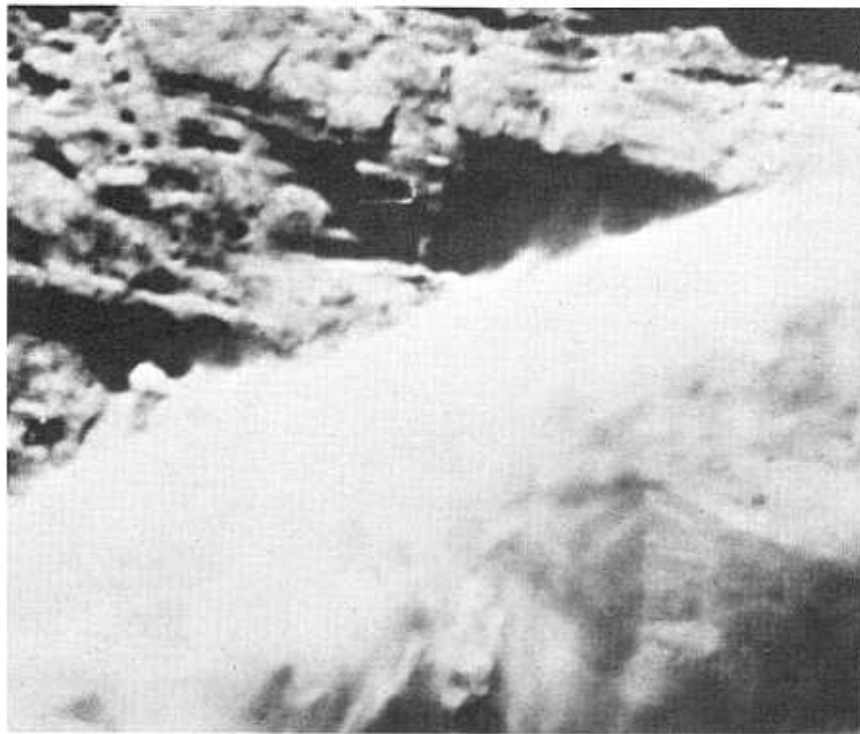
- b_n = nappe width
- d_n = nappe thickness
- H_f = fall height of a waterjet
- p_n = nappe perimeter
- Q_a = volume flow of air
- Q_w = volume flow of water
- V_i = nappe velocity at impact
- V_m = minimum velocity required to entrain
air = 1.1 m/s

Model

Valve fully open.

Prototype

A.-Jet characteristics near the valve.

Prototype

B.-Jet characteristics far from the valve.

FIGURE 54.—Breakup of a water jet from a hollow-jet valve. P801-D-79281

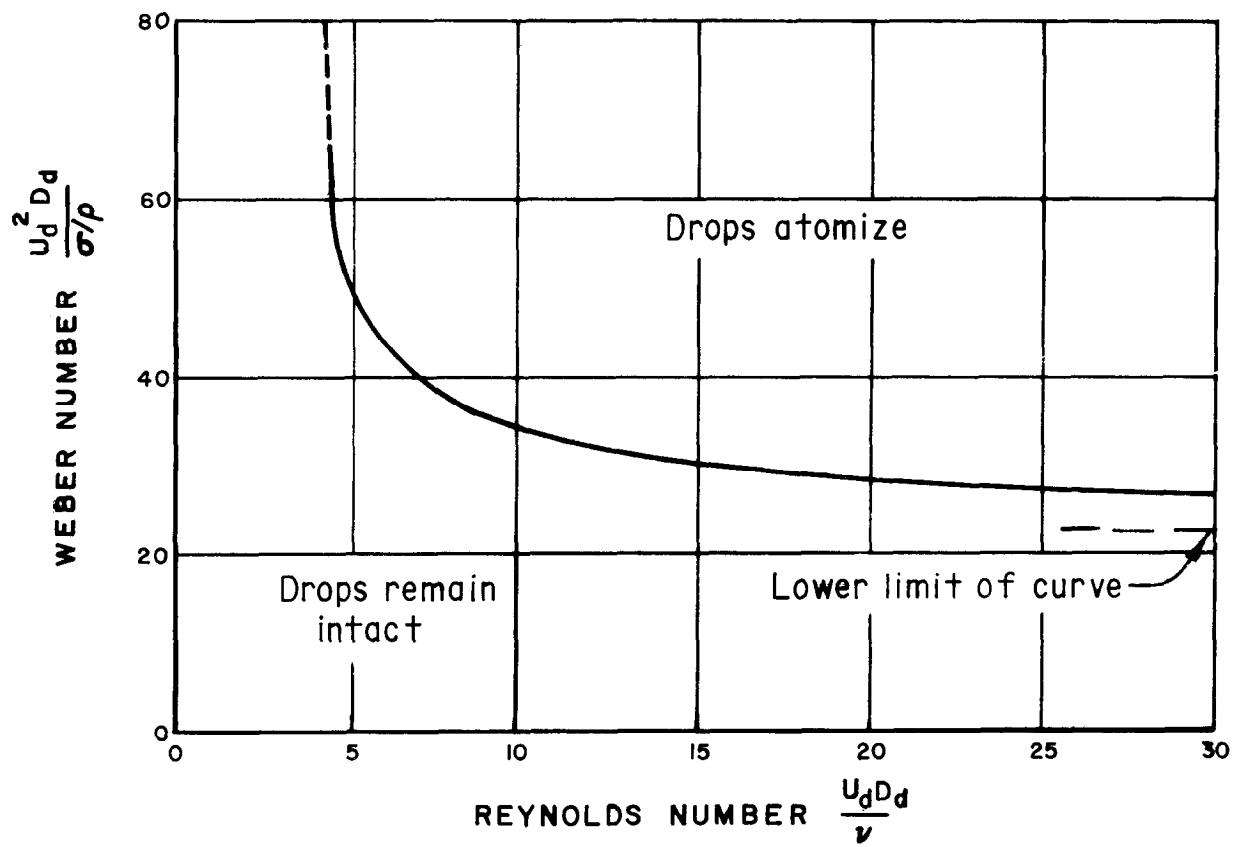


FIGURE 55.—*Water drop breakup.*

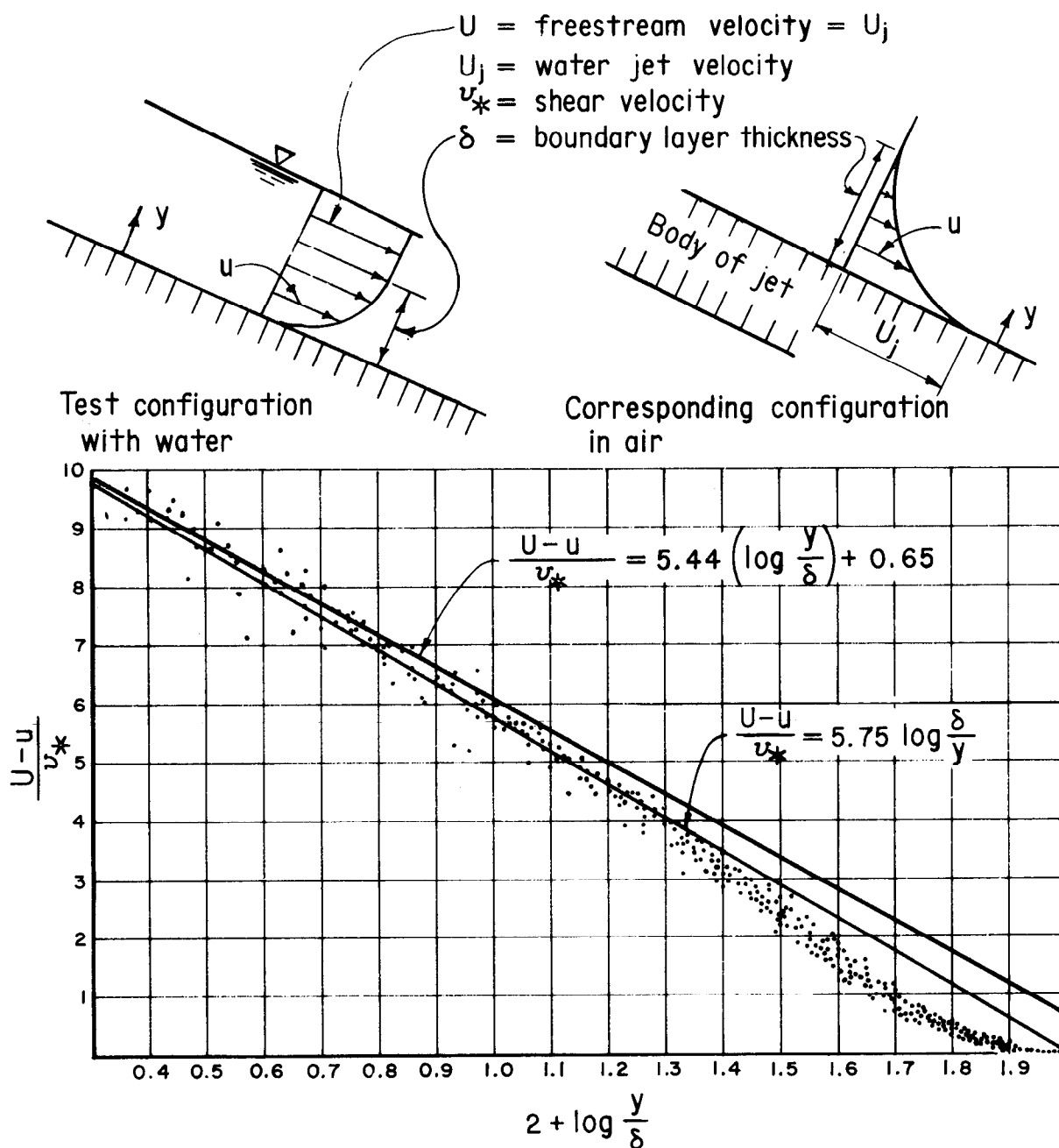


FIGURE 56.—Velocity distribution for flow over a flat plate, Bormann [11].

Bibliography

- [1] Alves, G. E., "Chemical Engineering Progress," vol. 50, pp. 449-456, 1954.
- [2] Anderson, A. G., "The Distribution of Air in Self Aerated Flow in a Smooth Open Channel," University of Minnesota, St. Anthony Falls Hydraulic Laboratory Project, Report No. 48, 1955.
- [3] Anderson, S. H., "Model Studies of Storm-Sewer Drop Shafts," St. Anthony Falls Hydraulic Laboratory, University of Minnesota, Technical Paper No. 35, Series B, 1961.
- [4] Annemuller, H., "Luftaufnahme Durch Fliessendes Wasser," Theodor-Rehvoek Flussbaulaboratorium Universitat Fridericiana Karlsruhe, Heft 146, 22 p., (Air Entrainment in Flowing Water) 1958.
- [5] ASCE Task Committee on Air Entrainment in Open Channels, "Aerated Flow in Open Channels," Proc., Am. Soc. Civ. Eng., J. Hyd. Div., vol. 87, No. HY3, pp. 73-86, May 1961.
- [6] Babb, A. F., Schneider, J. P., Thompson, K., "Air Flow in Combined Intake and Shaft Spillways," Proc., Am. Soc. Civ. Eng., J. Hyd. Div., vol. 99, No. HY7, pp. 1097-1108, July 1973.
- [7] Baker, O., Oil Gas J., vol. 53, No. 12, pp. 185-190, 192, 195, July 26, 1954.
- [8] Bauer, W. J., "Turbulent Boundary Layer on Steep Slopes," Trans., Am. Soc. Civ. Eng., vol. 119, pp. 1212-1234, 1954.
- [9] Beranek, L. L., Miller, L. N., "The Anatomy of Noise," Machine Design, vol. 39, No. 21, September 1967.
- [10] Beta, G., Jovanovic, S., Bukmirovic, V., "Nomographs for Hydraulic Calculation," Part 1, Trans., Jaroslav Cerni Institute for Development of Water Resources, Belgrade, Yugoslavia, vol. X, No. 28, Transl. from Serbo-Croat, OTS 63-11451/3, p. 163, 1963.

- [11] Bormann, K., "Der Abfluss in Schussrinnen Unter Berücksichtigung der Luftaufnahme, Versuchsanstalt für Wasserbau der Technischen Hochschule München, Bericht Nr 13, (Discharge in Chutes Considering Air Entrainment) 1968.
- [12] Campbell, F. B., Guyton, B., "Air Demand in Gated Outlet Works," International Association for Hydraulic Research, American Society of Civil Engineers Joint Conference, Minneapolis Minnesota, pp. 529-533, 1953.
- [13] Cartwright, D. E., Longuet-Higgins, M. S., "The Statistical Distribution of the Maxima of a Random Function," Proc. Royal Society of London, Series A., Mathematical and Physical Sciences, vol. 127, pp. 212-232, November 1956.
- [14] Colgate, D., "Hydraulic Model Studies of the River Outlet Works at Oroville Dam, Hydraulic Laboratory Report HYD-508, Bureau of Reclamation, Denver, Colorado, fig. 19, 10 p., October 1963.
- [15] Colgate, D., "Hydraulic Model Studies of the Flow Characteristics and Air Entrainment in the Check Towers of the Main Aqueduct, Canadian River Project, Texas," Hydraulic Laboratory Report HYD-555, Bureau of Reclamation, Denver, Colorado, 12 p., 1966
- [16] Collins, R., "The Effect of a Containing Cylindrical Boundary on the Velocity of a Large Gas Bubble in a Liquid," J. Fluid Mech, vol. 28, part 1, pp. 97-112, 1967.
- [17] Comolet, R., "Sur le mouvement d'une bulle de gaz dans un liquide," La Houille Blanche, No. 1, pp. 31-42. (On the Movement of a Gas Bubble in a Liquid) 1979.
- [18] Davies, R. M., Taylor, G. I., Proc. Roy. Soc. (London), vol. 200, ser. A, pp. 375-390, 1950.
- [19] Davies, H. G., Williams, J.E.F., "Aerodynamic Sound Generation in a Pipe," J. Fluid Mech., vol. 32, part 4, pp. 765-778, 1968.
- [20] Dodu, J., "Etude de la couche limite d'air autour d'un jet d'eau a grande vitesse, Seventh Congress of the International Association of Hydraulic Research, Lisbon, Portugal, (Study of the Boundary Layer Around a High Water Jet) 1957.
- [21] Ervine, D. A., Elsayy, E. M., "Effect of a Falling Nappe on River Aeration," 16th Congress of the International Association for Hydraulic Research, Brazil, vol. 3, pp. 390-397, 1975.
- [22] Falvey, H. T., "Air Vent Computations, Morrow Point Dam," Hydraulic Laboratory Report HYD-584, Bureau of Reclamation, Denver, Colorado, 39 p, 1968.
- [23] Gardner, M., "Reflections on the Packing of Spheres,"-Mathematical Games,-Sci. Am., vol. 202, No. 5, pp. 174-187, May 1960.
- [24] Ghetti, A., "Elementi per lo studio idraulico degli organi di scarico profondo da serbatoi desunti da ricerche sperimentali," studi e ricerche N. 211, Istituto di idraulica e costruzioni idrauliche, Dell'universita di padova, Italy, 1959. (Data for Hydraulic Studies of Deeply Submerged Discharges at Reservoirs, Derived from Experimental Research).
- [25] Gumensky, D. B., "Air Entrained in Fast Water Affects Design of Training Walls and Stilling Basin," Civ. Eng. vol. 889, pp. 35-37 and 93, 1949.
- [26] Haberman, W. L., Morton, R. K., "David Taylor Model Basin" Report 802, 1953.

- [27] Hack, H. "Luftteinzug in Fallschächten mit Ringformiger Stromung durch Turbulente Diffusion," Versuchsanstalt für Wasserbau, Technischen Universität München, Bericht Nr. 36, Germany, (Air Inflow in Vertical Shafts with Circular Flow Through Turbulent Diffusion) 1977.
- [28] Haindl, K., "Zone Lengths of Air Emulsion in Water Downstream of the Ring Jump in Pipes," 13th Congress of the International Association for Hydraulic Research, August 31-September 5, vol. 2, pp. 9-19, Kyoto, Japan, 1969.
- [29] Haindl, K., "Transfer of Air by the Ring Jump of Water," 14th Congress of the International Association for Hydraulic Research, France, vol. 1, pp. 365-372, 1971.
- [30] Halbronn, G., Discussion to "Turbulent Boundary Layer or Steep Slopes," by W. J. Bauer, Trans., Am. Soc. Civ. Eng., vol. 119, pp. 1234-1242, 1954.
- [31] Halbronn, G., Durand R., Cohen de Lara, G., "Air Entrainment in Steeply Sloping Flumes," International Association for Hydraulic Research - American Society of Civil Engineers, Joint Conference, Minneapolis, Minnesota, pp. 455-466, 1953.
- [32] Harshbarger, E. D., Vigander, S., Hecker, G. E., "Air Entrainment in High Head Gated Conduits", Discussion of paper by H. R. Sharma, Proc., Am. Soc. Civ. Eng., vol. 93, No. HY12, pp. 1486-1489, December 1977.
- [33] Herbrand, K., "Der Wechselsprung unter dem Einfluss der Luftbeimischung," Die Wasserwirtschaft, Heft 9, pp. 254-260, (The Hydraulic Jump under the Influence of Air Mixtures) 1969.
- [34] Hickox, G. H., "Air Entrainment on Spillway Faces," Civ. Eng., vol. 9, pp. 89-96, 1939.
- [35] Hinze, J. O., "Fundamentals of the Hydrodynamic Mechanism of Splitting in Dispersion Processes," Am. Inst. Chem. Eng. J., vol. 1, No. 3, pp. 289-295, September 1955.
- [36] Jain, A. K., Raju, K.G.R., Garde, R. J., "Air Entrainment in Radial Flow Toward Intakes," Proc. Am. Soc. Civ. Eng., J. Hyd. Div., vol. 104, No. HY9, pp. 1323-1329, September 1978.
- [37] Kalinske, A. A., Bliss, P. H., "Removal of Air from Pipe Lines by Flowing Water," Civ. Eng., vol. 13, No. 10, pp. 480-482, 1943.
- [38] Kalinske, A. A., Robertson, J. M., "Closed Conduit Flow," Trans., Am. Soc. Civ. Eng., vol. 108, pp. 1435-1516, 1943.
- [39] Keller, R. J., Lai, K. K., Wood, I. R., "Developing Region in Self Aerating Flows," Proc., Am. Soc. Civ. Eng., J. Hyd. Div., vol. 100, No. HY4, pp. 553-568, April 1974.
- [40] Keller, R. J., Rastogi, A. K., "Prediction of Flow Development on Spillways," Proc., Am. Soc. Civ. Eng., J. Hyd. Div., vol. 101, No. HY9, pp. 1171-1184, September 1975.
- [41] Killen, J., "The Surface Characteristics of Self Aerated Flow in Steep Channels," Minn. Univ., thesis, University Microfilms, Inc., Ann Arbor, Mich., 69-6824, 138 pp. 1968.
- [42] Killen, J. M., Anderson, A. G., "A Study of the Air-Water Interface in Air Entrained Flow in Open Channels," 13th Congress of the International Association for Hydraulic Research, Japan, vol. 2, pp. 339-347, 1969.
- [43] Kleinschroth, A., "Stromungsvorgänge im Wirbelfallschacht," Institut für Hydraulik und Gewässerkunde, Technische Universität München, Mitteilungen Heft Nr. 8, Germany, (Flow

- Conditions in a Vortex Vertical Shaft) 1972.
- [44] Kohler, W. H., "Selection of Outlet Works Gates and Valves," preprint 1057, Annual Meet., Am. Soc. Civ. Eng. Chicago, Illinois, October 1969.
 - [45] Kombayasi, M., Gonda, T., Isono, K., "Lifetime of Water Drops Before Breaking and Size Distribution of Fragment Droplets," Meteorol. Soc. Japan, vol. 42, pp. 330-340, 1964.
 - [46] Lane, E. W., "Entrainment on Spillway Faces," Civ. Eng. vol. 9, pp. 89-96, 1939.
 - [47] Lescovich, J. E., "Locating and Sizing Air-Release Valves," J. Am. Water Works Assoc., vol. 64, No. 7. pp. 457-461, July 1972.
 - [48] Leutheusser, H. J., Chu, V. H., "Experiments on Plane Couette Flow," Proc., Am. Soc. Civ. Eng., J. Hyd. Div., vol. 97, No. HY9, pp. 1169-1283, September 1971.
 - [49] Levi, E., "Macroturbulence Produced by Vortex Breakdown in High Velocity Flows," 12th Congress of the International Association for Hydraulic Research, vol. 2, pp. 54-60, September 1967.
 - [50] Longuet-Higgins, M. S., "On the Statistical Distribution of the Heights of Sea Waves," J. Mar. Res., vol. XI, No. 3, pp. 245-266, 1952.
 - [51] Martin, C. S., "Characteristics of an Air-Water Mixture in a Vertical Shaft," Proc. Hyd. Div. Specialty Conference, Am. Soc. Civ. Eng., Bozeman, Mont., August 15-17, pp. 323-334, 1973.
 - [52] Martin, C. S., "Vertically Downward Two-Phase Slug Flow," J. Fluids Eng., Trans. Am. Soc. Mech. Eng., vol. 98, series I, No. 4, pp. 715-722, December 1976.
 - [53] Mura, Y., Ijuin, S., Nakagawa, H., "Air Demand in Conduits Partly Filled with Flowing Water," Eighth International Association of Hydraulic Research Congress, vol. II, Montreal Canada, 1959.
 - [54] Michels, V., Lovely, M., "Some Prototype Observations of Air Entrained Flow, International Association for Hydraulic Research - American Society of Civil Engineers, Joint Conference, Minneapolis, Minnesota, p. 403, 1953.
 - [55] Mussalli, Y. G., Carstens, M. R., "A Study of Flow Conditions in Shaft Spillways," School of Civil Engineering, Georgia Institute of Technology, Atlanta, Georgia, Report WRC-0669, 1969.
 - [56] Parmakian, J., "Air-inlet Valves for Steel Pipelines," Trans. Am. Soc. Civ. Eng., vol. 115, pp. 438-444, 1950.
 - [57] Rajaratnam, N., "Hydraulic Jumps," Advances in Hydrosience, vol. 4, Ven Te Chow, ed., 1967.
 - [58] Richards, R. T., "Air Binding in Water Pipelines," J. Am. Water Works Assoc., pp. 719-730, June 1962.
 - [59] Rouse, H., ed., Engineering Hydraulics, John Wiley & Sons, 1949.
 - [60] Rouse, H., Howe, J. W., and Metzler, D. E., "Experimental Investigation of Fire Monitors and Nozzles," Proc. Am. Soc. Civ. Eng., vol. 77, pp. 1147-1175, October 1951.
 - [61] Runge, D. E., and Wallis, G. B., Atomic Energy Commission Report NYO-3114-8 (EURAE - 1416) 1965.
 - [62] Sailer, R. E., "Air Entrainment in Siphon Barrels," Civ. Eng., vol. 25, No. 5, pp. 268-271, 1955.
 - [63] Schlichting, H., Boundary Layer Theory, McGraw-Hill, 1968.
 - [64] Schuster, J. C., "Hydraulic Model Studies of the Eucumbene-Tumut Tunnel Junction Shaft," Hydraulics Laboratory Report HYD-392, Bureau of Reclamation, Denver, Colorado, August 1954.
 - [65] Sikora, A., "Zavdusnenie Sachtovych Priepadov," Vyskumny Ustav

- Vodohospodarsky, Bratislava, Prace a studie 37, p. 112, (Air Entrainment in Shaft Spillways, Czechoslovakia), 1965.
- [66] Straub, L. G., Anderson, A. G., "Self Aerated Flow in Open Channels," Trans., Am. Soc. Civ. Eng., vol. 125, pp. 456-486, 1960.
- [67] Straub, L. G., Lamb, O. P., "Experimental Studies of Air Entrainment in Open Channel Flow, International Association for Hydraulic Research, American Society of Civil Engineers, Joint Conference, Minneapolis, Minnesota , pp. 425-437, 1953.
- [68] Streeter, V., Handbook of Fluid Dynamics, McGraw-Hill, 1961.
- [69] Thomas, C. W., "Progress Report on Studies of the Flow of Water in Open Channels with High Gradients," Hydraulic Laboratory Report No. HYD-35, Bureau of Reclamation, Denver, Colorado, 30 p, 1938.
- [70] Thorsky, G. N., Tilp, P. J., Haggman, P. C., Slug Flow in Steep Chutes, Report No. CB-2, Bureau of Reclamation, Denver, Colorado, 91 pp., February 1967.
- [71] "Vibration, Pressure and Air Demand Tests in Flood-Control Sluice, Pine Flat Dam," U.S. Army Engineer Waterways Experiment Station, Misc. Pap. No. 2-75, February 1954.
- [72] Viparelli, M., "The Flow in a Flume with 1:1 Slope," International Association for Hydraulic Research, American Society of Civil Engineers, Joint Conference, Minneapolis, Minnesota, pp. 415-423, 1953.
- [73] Wallis, G. B., One-dimensional Two-phase Flow, McGraw-Hill, 1969.
- [74] Wisner, P., "Air Demand and Pulsatory Pressures in Bottom Outlets," High Velocity Flow Symposium, Bangalore, India, 1967.

Appendix

I - Probability Depth Probe

II - Mean Air Concentration, Free Surface Flow, Computer Program

III - Air Demand, Falling Water Surface, Computer Program

Appendix I - Probability Depth Probe

A water surface probe was developed by Killen [41] at the St. Anthony Falls Hydraulic laboratory (University of Minnesota) which permits a direct determination of the probability that the water surface is greater than or equal to a given elevation. The original probe circuitry has been modernized to function with operational amplifiers (fig. I-1).

Experiments showed that a probe consisting of two parallel wires separated by a short distance exhibited a temperature drift when the probe was removed from the water. By connecting one wire to a metal point gage and the other to an electrode in the body of water, the drift was eliminated (fig. I-2).

The electronics, battery, and controls are conveniently mounted in a utility box (fig. I-3).

The following steps are necessary to put the unit in operation:

- Zero integrating voltmeter with zero control on box (within about 5 millivolts acceptable)
- Set gain control on box for 10 volts when probe is shorted (in water). Note reading on digital voltmeter.
- Repeat steps one and two (if necessary repeat twice).
- Take reading. Voltage read should indicate percentage of the probe shorted (i.e., in water).

Appendix II - Mean Air Concentration, Free Surface Flow, Computer Program

A detailed description of the computer program input is given in the program listing. The program was written to read the input data from a file called **HSPWY**.

An example of the input format and its output is presented at the end of the computer listing.

AIR-WATER FLOW IN HYDRAULIC STRUCTURES

PROGRAM HFWS

```

1      PROGRAM HFWS(HSPWY=/80,OUTPUT,TAPE2=HSPWY,TAPE3=OUTPUT)
      COMMON A,B,HR,W,SS,R,IS,PI,ELINV,SB,ELC,R1,T,G,JIC
      DIMENSION TITL(10)

5      C
      C      THIS PROGRAM COMPUTES THE AMOUNT OF AIR INSUFFLATED INTO OPEN
      C      CHANNEL FLOW.  THE CHANNEL CAN HAVE A TRAPEZOIDAL, CIRCULAR, OR
      C      A TRANSITIONAL CROSS SECTION.  THE PROGRAM IS GOOD FOR RESERVOIR,
      C      DRAWDOWN,AND BACKWATER CURVES.  IF A HYDRAULIC JUMP FORMS IN
      C      THE CIRCULAR OR TRANSITION SECTIONS, THE AIR CONTENT OF THE
10     C      WATER IS COMPUTED WITH EQUATIONS GIVEN BY KALINSKI AND
      C      ROBERTSON. A KINETIC ENERGY CORRECTION FACTOR OF 1.1 IS APPLIED
      C      TO EVERY STATION .
      C
      C
15     C      THE PROGRAM ALSO CHECKS FOR THE FORMATION OF DAMAGING
      C      CAVITATION.  IF A POTENTIAL FOR DAMAGE EXISTS, THE
      C      PROGRAM INDICATES THE SITE AND THE HEIGHT OF THE
      C      OFFSET.  IT IS ASSUMED THAT THE OFFSETS ARE INTO THE
      C      FLOW.
      C
20     C
      C      THE REQUIRED INPUT IS ;
      C      1) DISCHARGE,INITIAL DEPTH, RUGOSITY, DIRECTION OF
      C      COMPUTATION, METRIC, INITIAL BOTTOM SLOPE (DISTANCE VERTICAL
25     C      TO DISTANCE HORIZONTAL).
      C
      C      TYPICAL RUGOSITIES
      C      -----
      C      CONCRETE 0.3-3.0 MM
30     C      STEEL    0.05  MM
      C      TUBING   0.0015 MM
      C
      C      DIRECTION OF COMPUTATION
      C      -----
35     C      UPSTREAM    0
      C      DOWNSTREAM  1
      C
      C      DIMENSIONAL UNITS
      C      -----
40     C      METRIC      0
      C      ENGLISH     1
      C
      C      2) THE TITLE, CENTERED IN A FIELD OF 60 CHARACTERS
45     C
      C
      C      3) THE NUMBER OF STATIONS
      C
50     C      4) THREE DESCRIPTION CARDS ARE REQUIRED FOR EACH STATION.
      C      THESE CONSIST OF THE FOLLOWING;
      C
      C      CARD 1
      C      -----
55     C      SHAPE OF CROSS SECTION
      C      I=0-RECTANGULAR OR TRAPEZOIDAL
      C      I=1-CIRCULAR
      C      I=2-TRANSITION
      C
60     C      SLOPE OF CROSS SECTION AT TRANSITION
      C      IS=1-SECTION VERTICAL
      C      IS=2-SECTION NORMAL TO FLOOR
      C
      C

```

APPENDIX II

99

PROGRAM HFWS

```

65      C      CARD 2. IS ONE OF THE FOLLOWING;
      C      -----
      C
      C      A) RECTANGULAR OR TRAPEZOIDAL
      C      STATION, INVERT ELEVATION, BOTTOM WIDTH,
70      C      CHANNEL SIDE SLOPE (DISTANCE HORIZONTAL TO UNITY
      C      VERTICAL).
      C
      C
      C      B) CIRCULAR SECTION
      C      STATION, INVERT ELEVATION, RADIUS OF
75      C      CIRCULAR SECTION.
      C
      C
      C      C) TRANSITION SECTION
      C      THE TRANSITION SECTION IS ESSENTIALLY A SQUARE
      C      WITH CIRCULAR FILLETS IN THE FOUR CORNERS AND
      C      A CENTER SUPPORT WALL. THE DATA TO DESCRIBE THIS
      C      SECTION INCLUDES;
80      C
      C      THE STATION, INVERT ELEVATION,
      C      WIDTH OF SECTION, RADIUS OF UPPER FILLETS,
      C      (IF NOT CLOSED CONDUIT FLOW, SET EQUAL TO ZERO),
      C      ELEVATION OF CENTERLINE OF UPPER RADIUS POINT,
      C      (IF NOT CLOSED CONDUIT FLOW, SET EQUAL TO ZERO),
90      C      RADIUS OF LOWER FILLETS, THICKNESS OF SUPPORT
      C      WALL.
      C
      C
      C      CARD 3
      C      -----
95      C
      C      THE TRANSITION LOSS FACTOR, THE BEND LOSS
      C      FACTOR, THE BEND RADIUS, THE BEND ANGLE.
      C
      C      THE HEAD LOSS DUE TO TRANSITIONS IS EQUAL TO THE
100     C      THE TRANSITION LOSS FACTOR TIMES THE DIFFERENCE
      C      IN UPSTREAM AND DOWNSTREAM VELOCITY HEADS.
      C
      C      THE HEAD LOSS DUE TO VERTICAL BENDS IS EQUAL TO THE BEND
      C      LOSS FACTOR TIMES ONE HALF THE SUM OF THE UPSTREAM
105     C      AND DOWNSTREAM KINETIC ENERGIES.
      C
      C      THE BEND ANGLE IS EQUAL TO THE INCLUDED ANGLE OF
      C      OF THE VERTICAL CURVE, IN RADIANS, BETWEEN STATIONS.
      C      IF THE VERTICAL RADIUS OF CURVATURE VARIES FROM
110     C      ONE STATION TO ANOTHER, ADJUST THE BEND ANGLE
      C      SO THAT THE RUN BETWEEN THE STATIONS IS EQUAL
      C      TO THE BEND ANGLE*ABS(BEND RADIUS)
      C
      C      IF THE INVERT MOVES AWAY FROM THE FLOW, THE SIGN OF THE
115     C      VERTICAL RADIUS OF CURVATURE IS NEGATIVE. IF THE SECTION
      C      BETWEEN STATIONS IS STRAIGHT, SET THE VERTICAL RADIUS OF
      C      CURVATURE EQUAL TO 0.
      C
      C      =====
120     C
      C      THE INPUT IS READ WITH A FREE FORMAT. THIS MEANS THAT
      C      THE DATA FOR EACH CARD MUST BE ON A SINGLE LINE AND
      C      SEPARATED BY ONE OR MORE BLANKS, OR BY A COMMA OR A
      C      SLASH, EITHER OF WHICH MAY BE PRECEDED OR FOLLOWED BY
125     C      ANY NUMBER OF BLANKS. BLANKS ARE NOT ALLOWED AS
      C      SUBSTITUTES FOR ZERO. A DECIMAL POINT
      C      OMITTED FROM A REAL CONSTANT IS ASSUMED TO OCCUR TO
      C      THE RIGHT OF THE RIGHTMOST DIGIT OF THE MANTISSA.
      C      EXTRANEIOUS DATA ON A CARD WILL BE READ ON

```

AIR-WATER FLOW IN HYDRAULIC STRUCTURES

PROGRAM HFWS

```

130      C      SUBSEQUENT READ COMMANDS. THIS WILL RESULT IN
      C      *ERROR DATA INPUT*DIAGNOSTICS.
      C
      C
      C      THE INITIAL DEPTH MUST BE AT LEAST 0.5 PERCENT LARGER
135      C      OR SMALLER THAN THE CRITICAL DEPTH TO INITIATE THE
      C      COMPUTATIONS.
      C
      C      THE AIR CONTENT IS COMPUTED FROM
      C
140      C      C= 0.05*F-SQRT(SINE(ALPHA))*W/(61*F)
      C
      C      WHERE F= V/SQRT(G*Y(EFF))
      C      W= V/SQRT(SIGMA/RHO*HR)
      C      HR= HYDRAULIC RADIUS
      C      SIGMA= INTERFACIAL TENSION
145      C      RHO= DENSITY OF WATER
      C      G= ACCELERATION OF GRAVITY
      C      Y(EFF)= EFFECTIVE DEPTH
      C      = AREA/TOP WIDTH OF WATER PRISM
150      C      THE AIR RATIO IS DEFINED AS BETA= Q(AIR)/Q(WATER)= C/(1-C)
      C
      C      IF A HYDRAULIC JUMP FORMS IN THE CONDUIT,
      C
      C      BETA= 0.0066*(F-1.)**1.4
155      C
      C
      C      =====
160      C      INITIALIZATION OF DATA
      C
      C      1 S= -0.1
      C      V= 0.0
      C      HV= 0.
165      C      ELINV= 0.
      C      STA= 0.
      C      EGL= 0.
      C      F= 0.
      C      TOTAL= 0.0
      C      BETA= 0.0
170      C      PI= 3.1415926
      C      JIC= 0
      C      K= 0
      C      NL= 1
175      C      DIA= 0.
      C      DT= 0.
      C
      C      INPUT OF FLOW DATA
      C
180      C      READ (2,*) Q,DN,RUG,NCURV,MET,SB
      C      IF(MET.EQ.0)RUG=RUG/1000.
      C      IF(EOF(2))2,3
      C      2 CALL EXIT
      C      3 G= 9.807
185      C      IF(MET.EQ.1)G= 32.2
      C      VIS= 1.4E-05
      C      IF(MET.EQ.0)VIS= 1.3E-06
      C      DNO= DN
      C      READ(2,4)(TITL(I),I=1,10)
190      C      4 FORMAT(10A6)
      C      READ (2,*) NS
      C
      C      LOOP WHICH INCREMENTS THE STATIONS
      C

```

APPENDIX II

101

PROGRAM HFWS

```

195      CHECK= EGL
      DO 68 NT=1,NS
          SAVE=STA
          STORE=S
          STORE1=ELINV
200      EGL= CHECK
          HIDE1=HV
          IF(NT.NE.2)GO TO 14

C
C      COMPUTATION OF HYDRAULIC PROPERTIES OF FIRST STATION
205      IF(BENDR.EQ.0.) GO TO 5

C
C      HYDROSTATIC DEPTH WITH BEND
      D= DN/SQRT(1.0+SB*SB)+2.0*HV*DN/BENDR
210      GO TO 6

C
C      HYDROSTATIC DEPTH WITHOUT BEND
      5 D= DN/SQRT(1.0+SB*SB)
      6 TOTAL= ELINV+D+HV
215

C
C      WRITE STATEMENTS FOR TITLES
C
      WRITE(3,7)(TITL(I),I=1,10)
      7 FORMAT(1H1,28X,10A6/28X,20H-----
220      40H----- //)
      IF(MET.EQ.1)WRITE(3,8)Q,DN,RUG,CN
      8 FORMAT(19X,3HQ =,F7.1,4H CFS,3X,15HINITIAL DEPTH =,F6.2,
      + 3H FT,3X,10HRUGOSITY =, F8.6,3H FT,3X,3HN =,F6.4//)
      IF(MET.EQ.1)WRITE (3,9)
225      9 FORMAT(66X,6HENERGY,33X,5HDEPTH/
      + 47H STATION INVERT ELEV SLOPE DEPTH VEL
      + 42HOCITY PIEZ GRADE LINE Q AIR/Q WATER,
      + 27H PROFILE NORMAL CRITICAL /
      + 4X,2HFT,9X,2HFT,20X,2HFT,6X,6HFT/SEC,6X,2HFT,9X,2HFT,
230      + 32X,2HFT,7X,2HFT/)
      IF(MET.EQ.0)RUG= RUG*1000.
      IF(MET.EQ.0)WRITE(3,10)Q,DN,RUG,CN
      IF(MET.EQ.0)RUG= RUG/1000.
      10 FORMAT(19X,3HQ =,F9.3,4H CMS,3X,15HINITIAL DEPTH =,F6.3,
235      + 2H M,3X,10HRUGOSITY =,F8.4,3H MM,3X,3HN =,F6.4//)
      IF(MET.EQ.0)WRITE (3,11)
      11 FORMAT(66X,6HENERGY,33X,5HDEPTH/
      + 47H STATION INVERT ELEV SLOPE DEPTH VEL
      + 42HOCITY PIEZ GRADE LINE Q AIR/Q WATER,
240      + 27H PROFILE NORMAL CRITICAL /
      + 3X,2H M,10X,2H M,19X,2H M,6X,6H M/SEC,6X,2H M,9X,2H M,
      + 33X,1HM,8X,1HM/)
      WRITE (3,12) STA,ELINV,SB,DN,V,D,TOTAL,BETA,AN,M,YN,YC
      12 FORMAT (1X,F7.2,F12.3,F10.4,F10.3,F11.3,F9.3,3X,F10.3,F12.3
245      + ,9X,A1,I1,1X,F9.3,F9.3/)
      IF(SIG.GT.SIG1.AND.SIG.GT.SIGR)GO TO 14
      IF(SIG1.GT.SIGR.AND.SIG1.GT.SIG)GO TO 13
      WRITE(3,64)
      GO TO 14
250      13 IF(MET.EQ.1)WRITE(3,66)HO,NSL
      IF(MET.EQ.0)WRITE(3,67)HO,NSL
      14 ILOOP= (NL-1)/21-K
      IF(ILOOP.NE.1)GO TO 15
      K= K+1
255      WRITE(3,7)(TITL(I),I=1,10)
      IF(MET.EQ.1)WRITE(3,9)
      IF(MET.EQ.0)WRITE(3,11)
      15 READ (2,*) I,IS
      IF(EOF(2))71,16

```

AIR-WATER FLOW IN HYDRAULIC STRUCTURES

PROGRAM HFWS

```

260      16  IF (I-1) 17,18,19
      C
      C      RECTANGULAR OR TRAPEZOIDAL CHANNELS
      17  READ (2,*) STA,ELINV,W,SS
      READ (2,*) TLF,BLF,BENDR,BENDA
265      CALL TRAP(DN)
      GO TO 22
      C
      C      CIRCULAR CONDUITS
      18  READ (2,*) STA,ELINV,R
270      READ (2,*) TLF,BLF,BENDR,BENDA
      DIA= 1.99999*R
      CALL CIRC(DIA)
      GO TO 22
      C
      C      CIRCULAR TO RECTANGULAR TRANSITIONS
      19  READ (2,*) STA,ELINV,W,R,ELC,R1,T
      READ (2,*) TLF,BLF,BENDR,BENDA
      IF(ELC.LT.ELINV)GO TO 20
      SB= (ELINV-STORE1)/ABS(SAVE-STA)
280      IF(NCURV.EQ.1)SB= -SB
      WMIN= (W-T)/2.
      IF(R.GE.WMIN.AND.IS.EQ.1)DT= 0.99999*(ELC-ELINV+SQRT(
      + R*(W-T)-0.25*(W-T)*(W-T)))
      IF(R.GE.WMIN.AND.IS.EQ.2)DT= 0.99999*((ELC-ELINV)*SQRT(SB*SB
285      + 1.))+SQRT(R*(W-T)-0.25*(W-T)*(W-T)))
      IF(R.LT.WMIN.AND.IS.EQ.1)DT= 0.99999*((ELC-ELINV)+R)
      IF(R.LT.WMIN.AND.IS.EQ.2)DT= 0.99999*((ELC-ELINV)*SQRT(SB*SB
      + 1.))+R)
      GO TO 21
290      20  DT= DN
      21  CALL TRANS(DT)
      C
      C      USING EQ 4-13 FROM OPEN CHANNEL FLOW BY HENDERSON,
      C      MACMILLAN, 1970. THIS IS THE COLEBROOK EQUATION.
295      C
      22  REY= 4.*HR*(Q/A)/VIS
      FRICO= 0.
      DO 23 N=1,20
      FRICT= -2.*ALOG10(RUG/(12.*HR)+2.5*FRICO/REY)
300      IF(ABS(1.-FRICO/FRICT).LE.0.01)GO TO 24
      FRICO= FRICT
      23  CONTINUE
      24  IF(MET.EQ.0)CN=(HR**0.166667)/(SQRT(8.*G)*FRICT)
      IF(MET.EQ.1)CN=(HR**0.166667)*1.49/(SQRT(8.*G)*FRICT)
305      C
      C      COMPUTATION OF BOTTOM SLOPE
      C
      IF(NT.EQ.1)GO TO 25
      SB= (ELINV-STORE1)/ABS(SAVE-STA)
310      IF(NCURV.EQ.1)SB= -SB
      C
      C      CHECK FOR MAXIMUM DISCHARGE IN CLOSED CONDUITS
      C
      25  IF(I.EQ.0)GO TO 26
      QMAX= A*SQRT(ABS(SB))*HR**0.66667/CN
      IF(MET.EQ.1)QMAX= 1.49*QMAX
315      C
      C      COMPUTATION OF CRITICAL DEPTH BY NEWTONS METHOD
      C
      26  DY= DN/2.
      YC= DN
      DO 31 NN=1,25
      IF(I-1)27,28,29
320      27  CALL TRAP(YC)

```


APPENDIX II

103

PROGRAM HFWS

```

325          DBDY= 2.*SS
              GO TO 30
          28  CALL CIRC(YC)
              DBDY= (DIA-2.*YC)/SQRT(YC*DIA-YC*YC)
              GO TO 30
330          29  CALL TRANS(YC)
              DBDY= 0.
          30  VC= Q/A
              HVC= VC*VC/(2.*G)
              HVCK= A/(2.*B)
335          DHVC= HVC-HVCK
              IF (ABS(DHVC/HVCK).LE.0.001)GO TO 32
              DFDY= DBDY*HVCK/B-0.5*(1.+2.*B*HVC/A)
              YCO= YC
              YC= YC-DHVC/DFDY
340          IF (YC.LE.0.)YC=ABS(YC)
              IF (I.EQ.1.AND.YC.GT.DIA)YC= (YCO+DIA)/2.
              IF (I.EQ.2.AND.YC.GT.DT)YC= (YCO+DT)/2.
          31  CONTINUE
C
345  C      COMPUTATION OF NORMAL DEPTH BY NEWTONS METHOD
C
          32  IF (I.EQ.0.AND.SB.GE.0.)GO TO 33
              IF (SB.GT.0..AND.QMAX.GT.Q)GO TO 33
              YN= 1000.
350          IF (SB.LT.0.)YN= -1000.
              GO TO 41
          33  DY= -DN/2.
              YN= ABS(DN)
              DO 40 NN=1,25
355          IF (I-1)34,35,36
          34  CALL TRAP(YN)
              GO TO 37
          35  CALL CIRC(YN)
              GO TO 37
360          36  CALL TRANS(YN)
C
C      USING EQ 4-13 FROM OPEN CHANNEL FLOW BY HENDERSON,
C      MACMILLAN, 1970. THIS IS THE COLEBROOK EQUATION.
C
365          37  REY= 4.*HR*(Q/A)/VIS
              FRICO= 0.
              DO 38 N=1,20
                  FRICT= -2.*ALOG10(RUG/(12.*HR)+2.5*FRICO/REY)
                  IF (ABS(1.-FRICO/FRICT).LE.0.01)GO TO 39
                  FRICO= FRICT
370          38  CONTINUE
          39  IF (MET.EQ.0)CN=(HR**0.166667)/(SQRT(8.*G)*FRICT)
              IF (MET.EQ.1)CN=(HR**0.166667)*1.49/(SQRT(8.*G)*FRICT)
              QM= A*SQRT(SB)*HR**0.66667/CN
375          IF (MET.EQ.1)QM=1.49*QM
              DHDY= HR/YN-2.*HR/(B+2.*YN)
              FUN= Q-QM
              IF (ABS(FUN/Q).LE.0.001)GO TO 41
              DFDY= -B*QM/A-2.*QM*DHDY/(3.*HR)
380          YNO= YN
              YN= YN-FUN/DFDY
              IF (YN.LE.0.)YN=ABS(DY)
              IF (I.EQ.1.AND.YN.GT.DIA)YN= (DIA+YNO)/2.
              IF (I.EQ.2.AND.YN.GT.DT)YN= (DT+YNO)/2.
385          40  CONTINUE
C
C      DETERMINATION OF PROFILE TYPE
C
          41  IF (YN.LT.YC)GO TO 42

```

AIR-WATER FLOW IN HYDRAULIC STRUCTURES

PROGRAM HFWS

```

390          IF(YN.EQ.YC)GO TO 43
             IF(SB.EQ.0.)GO TO 44
             IF(SB.LT.0.)GO TO 45
C
C          MILD SLOPE
395          AN= 1HM
             IF(DN.GE.YN)M=1
             IF(DN.LT.YN.AND.DN.GT.YC)M=2
             IF(DN.LE.YC)M=3
400          GO TO 46
C
C          STEEP SLOPE
C
C          42  AN=1HS
405          IF(DN.GE.YC)M=1
             IF(DN.GT.YN.AND.DN.LT.YC)M=2
             IF(DN.LE.YN)M=3
             GO TO 46
C
C          CRITICAL SLOPE
C
C          43  AN= 1HC
410          IF(DN.GE.YN)M=1
             IF(DN.LT.YN)M=3
415          GO TO 46
C
C          HORIZONTAL
C
C          44  AN= 1HH
420          IF(DN.GE.YC)M=2
             IF(DN.LT.YC)M=3
             GO TO 46
C
C          ADVERSE
C
C          45  AN= 1HA
425          IF(DN.GE.YC)M=2
             IF(DN.LT.YC)M=3
C
C          COMPUTATIONAL LOOP TO DETERMINE WATER DEPTH
C
C          46  DO 60 J=1,100
435          C
C          COMPUTATION OF HYDRAULIC PROPERTIES
C
C          IF (I-1) 47,48,49
C
C          HYDRAULIC PROPERTIES FOR RECTANGULAR SECTION
440          C
C          47  CALL TRAP(DN)
             FRUD= F
C
C          NOTE THE FROUDE NUMBER IS NOT CORRECTED FOR SLOPE
C          AND ENERGY CORRECTION FACTOR
445          F=(Q/A)/(SQRT(G*A/B))
             IF(NT.EQ.1)GO TO 50
             CKFRUD= (FRUD-1.)/(F-1.)
450          GO TO 50
C
C          HYDRAULIC PROPERTIES FOR CIRCULAR SECTION
C
C          48  CALL CIRC(DN)

```

APPENDIX II

105

PROGRAM HFWS

```

455      IF(JIC.EQ.1)GO TO 69
          FRUD= F
          F=(Q/A)/(SQRT(G*A/B))
          IF(NT.EQ.1)GO TO 50
          CKFRUD= (FRUD-1.)/(F-1.)
460      GO TO 50
          C
          C
          C      HYDRAULIC PROPERTIES IN TRANSITION
          49      CALL TRANS(DN)
465      IF(JIC.EQ.1)GO TO 69
          FRUD= F
          F=(Q/A)/(SQRT(G*A/B))
          IF(NT.EQ.1)GO TO 50
          CKFRUD= (FRUD-1.)/(F-1.)
470      C
          C
          C      COMPUTATION OF DEPTH BY STANDARD STEP METHOD
          50      V=Q/A
          HV= 1.1*V*V/(2.*G)
475      C
          C
          C      COMPUTATION OF MANNINGS N VALUE FROM THE RUGOSITY
          C      USING EQ 4-13 FROM OPEN CHANNEL FLOW BY HENDERSON,
          C      MACMILLAN, 1970. THIS IS THE COLEBROOK EQUATION.
480      REY= 4.*HR*(Q/A)/VIS
          FRICO= 0.
          DO 51 N=1,20
              FRICT= -2.*ALOG10(RUG/(12.*HR)+2.5*FRICO/REY)
              IF(ABS(1.-FRICO/FRICT).LE.0.01)GO TO 52
485      FRICO= FRICT
          51      CONTINUE
          52      IF(MET.EQ.0)CN=(HR**0.166667)/(SQRT(8.*G)*FRICT)
          IF(MET.EQ.1)CN=(HR**0.166667)*1.49/(SQRT(8.*G)*FRICT)
          C
          C
          C      1.1 IS THE KINETIC ENERGY CORRECTION FACTOR
          HT= TLF*ABS(HV-HIDE1)
          HB=BLF*(HV+HIDE1)/2.0
          S=(CN*CN*V*V)/(HR**1.3333)
495      D= DN/SQRT(1.0+SB*SB)
          IF(MET.EQ.1)S=S/2.208
          C
          C
          C      NT= 1 IS THE CONDITION FOR THE FIRST STATION
          500      IF(NT.EQ.1)DYDX= (SB-S)/(1.-F*F)
          IF(NT.EQ.1)CHECK= ELINV+HV+DN/SQRT(1.+SB*SB)
          IF(NT.EQ.1)GO TO 63
          AVGS=(STORE+S)/2.0
          IF(BENDR.NE.0.)GO TO 53
505      C
          C
          C      COMPUTATION OF HEAD LOSS WITHOUT BENDS
          RUN= SQRT((STA-SAVE)*(STA-SAVE)+(STORE1-ELINV)*(STORE1-ELINV)
          +
          )
          HF=RUN*AVGS
          SUM=HF+HT+HB
          GO TO 54
          C
          C
          C      COMPUTATION OF HEAD LOSS WITH BENDS
515      C
          53      RUN= BENDA*ABS(BENDR)
          HF= RUN*AVGS
          SUM= HF+HT+HB
          D= DN / SQRT(1.0+SB*SB)+2.0*HV*DN / BENDR

```

AIR-WATER FLOW IN HYDRAULIC STRUCTURES

PROGRAM HFWS

```

520      C
      C      COMPUTATION OF ENERGY GRADE LINE
      C
      54      TOTAL=ELINV+D+HV
      CHECK= EGL+SUM
525      IF(NCURV.EQ.1)CHECK= EGL-SUM
      C
      C      DETERMINATION OF FLOW DEPTH USING NEWTONS METHOD
      C
      EGLCK= TOTAL-CHECK
530      DTDY= 1./SQRT(1.+SB*SB)-2.*HV*B/A
      DCDY= 2.*(HF+HB+HT)*B/A+4.*HF*B*B/
      (3.*HR*(B+2.*DN)*(B+2.*DN))
      IF(NCURV.EQ.1)DCDY= -DCDY
      DEDY= DTDY+DCDY
535      DINC= EGLCK/DEDY
      C
      C      CHECK TO ENSURE THAT NEWTONS METHOD DOES NOT CAUSE A
      C      JUMP ACROSS NORMAL DEPTH IF COMPUTATIONS ARE PROCEEDING
      C      TOWARD THE NORMAL DEPTH.
540      C
      IF(AN.EQ.1HM.AND.NCURV.EQ.0)GO TO 55
      IF(AN.EQ.1HS.AND.NCURV.EQ.1)GO TO 56
      GO TO 58
      55      IF(M.EQ.3)GO TO 58
545      IF(ABS(DINC).GT.ABS(DN-YN))GO TO 57
      GO TO 58
      56      IF(M.EQ.1)GO TO 58
      IF(ABS(DINC).GT.ABS(DN-YN))GO TO 57
      GO TO 58
550      57      DINC= ABS(DN-YN)*DINC/(ABS(DINC)*2.)
      C
      58      DN= DN-DINC
      IF(DN.LE.0.)DN= (DN+DINC)/2.
      C
555      C
      C      CHECK ON THE ACCURACY OF COMPUTATIONS
      C
      PCTEL= 100.*((TOTAL-CHECK)/(ABS(STORE1-ELINV)+D+HV))
      IF(CKFRUD.LT.0.0)GO TO 73
      IF(ABS(PCTEL).LT.0.01)GO TO 59
560      GO TO 60
      C
      C      COMPUTATION OF AIR CONTENT WITH OPEN CHANNEL FLOW
      C
      59      IF(SB.LE.0.)C=0.
565      IF(SB.LE.0.)GO TO 61
      ALPHA= ATAN(SB)
      W= 100.*V/SQRT(0.74/HR)
      IF(MET.EQ.1)W= V/SQRT(0.00257/HR)
      C= 0.05*F-SQRT(SIN(ALPHA))*W/(63.*F)
570      IF(C.LT.0.)C= 0.
      IF(C.GE.0.74)C= 0.74
      BETA= C/(1.-C)
      GO TO 61
      60      CONTINUE
575      61      IF(J.GE.100)GO TO 73
      C
      C      WRITE OUTPUT
      C
      WRITE (3,12) STA,ELINV,SB,DN,V,D,CHECK,BETA,AN,M,YN,YC
580      NL= NL+1
      C
      C      CHECK ON SPACING OF STATIONS
      C      (THIS KEEPS ERROR IN DEPTH TO LESS THAN 1-PERCENT)
      C

```

APPENDIX II

107

PROGRAM HFWS

```

585      DYDX= (SB-S)/(1.-F*F)
          IF(DYDX.LE.1.E-10)GO TO 63
          ERRY= 100.*0.5*(RUN/DNO)*(RUN/DNO)*ABS((SB-STORE)/(
+      (1.-FRUDO*FRUDO)*(1.-FRUDO*FRUDO))*(10./3.*STORE-3.*(SB-STORE)*
+      FRUDO*FRUDO/(1.-FRUDO*FRUDO)))
590      IF(ERRY.LT.1.0)GO TO 63
          DX= RUN/2.
          WRITE(3,62)ERRY,DX
62      FORMAT(15X,22HERROR IN DEPTH EXCEEDS ,F4.0,9H PERCENT, ,
+      4X,42HPLEASE ADD INTERMEDIATE STATIONS WITH DX = ,F6.0)
595      NL= NL+1
C
C      CHECK ON CAVITATION FORMATION
C
63      DNO= DN
600      FRUDO= F
          PABS= 33.9*(1.-ELINV/145400.))**5.255-0.39
          IF(MET.EQ.0)PABS=10.33*(1.-ELINV/44303)**5.255-0.13
          SIG= 2.*G*(PABS+D)/(V*V)
          SIG1= 0.061*(V*DN/VIS)**0.196
605      SIGR= 32.*G*CN*CN/HR**0.33333
          IF(MET.EQ.1)SIGR= SIGR/2.208
          IF(SIG.GT.SIG1.AND.SIG.GT.SIGR)GO TO 68
C      CAVITATION OF BOUNDARY ROUGHNESS
C
610      IF(SIG1.GT.SIGR.AND.SIG1.GT.SIG)GO TO 65
          WRITE(3,64)
64      FORMAT(25X,38HSURFACE SUFFICIENTLY ROUGH TO CAVITATE /)
          NL= NL+1
          GO TO 68
615      C
C      ASSUME BOUNDARY LAYER THICKNESS = FLOW DEPTH
C      CIRCULAR ARC ASSUMPTION
65      HO= 10800.*DN*(SIG**2.91)*(VIS/(V*DN))**0.776
C
620      C
C      CHECK THAN KEEP OFFSETS GREATER TO OR EQUAL
C      TO THE RUGOSITY.
          IF(RUG.GE.HO)HO= RUG
C
C      COMPUTATION OF REQUIRED CHAMFER
625      ALPHA= 18.762*SIG
          NSL= INT(1./TAND(ALPHA))+1
          IF(MET.EQ.1)HO= 12.*HO
          IF(NT.EQ.1)GO TO 68
          IF(MET.EQ.1)WRITE(3,66)HO,NSL
630      66      FORMAT(16X,41HCAVITATION WILL OCCUR FOR OFFSETS GREATER,
+      5H THAN,F6.2,4H IN, ,3X,
+      4H1 TO,I3,18H CHAMFERS REQUIRED/)
          IF(MET.EQ.0)WRITE(3,67)HO,NSL
635      67      FORMAT(18X,41HCAVITATION WILL OCCUR FOR OFFSETS GREATER,
+      5H THAN,F7.3,4H M, ,3X,
+      4H1 TO,I3,18H CHAMFERS REQUIRED/)
          NL= NL+1
68      CONTINUE
C
640      C
C      NORMAL TERMINATION OF PROGRAM
          GO TO 1
C
C      ABNORMAL TERMINATION OF PROGRAM
645      C
C      COMPUTATION OF AIR CONTENT WITH A HYDRAULIC JUMP
C
69      IF(F.GT.0.)BETA= 0.0066*(F-1.))**1.4

```

AIR-WATER FLOW IN HYDRAULIC STRUCTURES

PROGRAM HFWS

```

650         IF(F.LE.0.)BETA=0.
           WRITE (3,70) STA,BETA
70  FORMAT (1X,F10.3,10X,29H HYDRAULIC JUMP FILLS CONDUIT,
+         4X,6HBETA= ,F5.2)
           GO TO 76
655  C
           C      INSUFFICIENT DATA
           C
71  WRITE (3,72) STA
72  FORMAT(40X,35HINSUFFICIENT DATA. LAST STATION WAS ,F8.0)
660  GO TO 76
           C
           C      IMPOSSIBLE FLOW CONDITION SPECIFIED
           C
73  WRITE(3,74)
665  74  FORMAT(1H0,43X,30HENERGY BALANCE WAS NOT REACHED/
+         38X,41HSEVERAL CONDITIONS CAN CAUSE THIS PROBLEM//
+         38X,40HCURVILINEAR FLOW MAY HAVE CAUSED PROBLEM/33X
+         ,50HOR YOU MAY HAVE SPECIFIED AN IMPOSSIBLE CONDITION.//
+         33X,
670  +         50HPLEASE REVIEW YOUR NORMAL DEPTH AND CRITICAL DEPTH /
+         36X,41HCOMPUTATIONS AS WELL AS THE PROFILE TYPE. //
+         28X,40HALSO, CHECK INPUT DATA FILE FOR MISSING
+         21HOR INCORRECT ENTRIES. //)
           FTEST= Q*Q*B/(G*A*A*A)
675  WRITE(3,75)STA,DN,AVGS,FTEST,YC,YN
75  FORMAT(20X,5HSTA =,F7.2,9H DEPTH =,F8.4,20H AVG SLOPE OF EGL =,
+         ,F8.5,13H FROUDE NO =,F6.2/47X,16HCRITICAL DEPTH =,F8.3/
+         47X,14HNORMAL DEPTH =,F8.3)
76  CONTINUE
680  END

```

SUBROUTINE TRAP

```

1  SUBROUTINE TRAP(DN)
           C
           C      HYDRAULIC PROPERTIES OF TRAPEZOIDAL SECTIONS
           C
5  COMMON A,B,HR,W,SS,R,IS,PI,ELINV,SB,ELC,R1,T,G,JIC
           A=W*DN+SS*DN*DN
           B= W+2.*SS*DN
           HR= A/(W+2.0*SQRT(DN*DN+((SS*DN)*(SS*DN))))
           RETURN
10  END

```

SUBROUTINE CIRC

```

1  SUBROUTINE CIRC(DN)
           C
           C      HYDRAULIC PROPERTIES OF CIRCULAR SECTIONS
           C
5  COMMON A,B,HR,W,SS,R,IS,PI,ELINV,SB,ELC,R1,T,G,JIC
           IF (DN-R) 1,2,3
           C
           C      LESS THAN HALF FULL
           C

```

APPENDIX II

109

SUBROUTINE CIRC

```

10          1 ROOT= SQRT(R*R-(R-DN)*(R-DN))
            TERM=ROOT/(R-DN)
            ANGLE= ATAN(TERM)
            A=((R*R)*ANGLE)-((R-DN)*ROOT)
            HR=A/(R*2.0*ANGLE)
15          B= 2.*ROOT
            RETURN

            C
            C      EXACTLY HALF FULL
            C

20          2 A=(PI*R*R)/2.0
            B= 2.*R
            HR=R/2.0
            RETURN

            C
            C      GREATER THAN HALF FULL
            C

30          3 IF(DN.GT.2.*R)GO TO 5
            IF(DN.EQ.2.*R)GO TO 4
            ROOT= SQRT(R*R-(DN-R)*(DN-R))
            TERM=ROOT/(DN-R)
            ANGLE= ATAN(TERM)
            A=(PI*R*R)-((R*R*ANGLE)-((DN-R)*ROOT))
            B= 2.*ROOT
            HR=A/((2.0*PI*R)-(R*2.0*ANGLE))
35          RETURN

            C
            C      EXACTLY FULL
            C

40          4 A= PI*R*R
            B= 0.
            HR= R/2.
            RETURN

            C
            C      FLOW FILLS CONDUIT
            C

45          5 JIC= 1
            RETURN
            END

```

SUBROUTINE TRANS

```

1          SUBROUTINE TRANS(DN)

            C
            C      HYDRAULIC PROPERTIES OF CIRCULAR TO RECTANGULAR
            C      SECTIONS WITH AND WITHOUT DIVIDER WALLS
            C

5          COMMON A,B,HR,W,SS,R,IS,PI,ELINV,SB,ELC,RL,T,G,JIC
            SEC= (1.-PI/4.)
            IF(ELC.LE.ELINV)GO TO 3
            DELV= ELC-ELINV
10         IF(IS.EQ.1)GO TO 1

            C
            C      SECTION NORMAL TO FLOOR
            C

            DELV= (ELC-ELINV)*SQRT(SB*SB+1.)
15         DIFF1= DN-DELV
            GO TO 2

            C
            C      SECTION VERTICAL
            C

```

AIR-WATER FLOW IN HYDRAULIC STRUCTURES

SUBROUTINE TRANS

```

20      1 DN= DN*SQRT(SB*SB+1.)
      DIFF1=DN-DELV
      2 IF (DIFF1.GT.0.)GO TO 7
C
C      EQUAL TO OR LESS THAN THE DEPTH OF THE RECTANGULAR SECTION
25      3 IF(DN.LT.R1)GO TO 5
      A= DN*(W-T)-2.*SEC*R1*R1
      B= W-T
      IF(T.GT.0.)GO TO 4
30      HR= A/(W+2.*DN-4.*SEC*R1)
      RETURN
C
C      WITH DIVIDER WALL
35      4 HR= A/(W-T+4.*DN-4.*SEC*R1)
      RETURN
C
C      EQUAL TO OR LESS THAN DEPTH OF RADIUS IN THE BOTTOM CORNER OF
C      TRANSITION
40      5 ROOT= SQRT(2.*DN*R1-DN*DN)
      TERM=ROOT/(R1-DN)
      ANGLE= ATAN(TERM)
      A= R1*R1*ANGLE-ROOT*(R1-DN)+(W-2.*R1-T)*DN
45      B= W-T-2.*R1+2.*SQRT(R1*R1-(R1-DN)*(R1-DN))
      IF(T.GT.0.)GO TO 6
      HR=A/(W-2.0*R1+2.0*R1*ANGLE)
      RETURN
C
C      WITH DIVIDER WALL
50      6 HR=A/(W-2.0*R1+2.0*R1*ANGLE-T+2.0*DN)
      RETURN
C
C      GREATER THAN THE DEPTH OF THE RECTANGULAR SECTION
55      7 IF(R-DIFF1) 12,9,8
      8 ROOT= SQRT(R*R-DIFF1*DIFF1)
      ARG2= DIFF1/ROOT
60      PH1= ATAN (ARG2)
      TW= W-2.0*R
      IF(TW.GE.T)GO TO 10
C
C      CHECK WITH UPPER RADIUS GREATER THAN HALF WIDTH OF SECTION
65      OR WITH RADIUS POINT INSIDE CENTER PIER
C
      DEPTH= SQRT(R*(W-T)-0.25*(W-T)*(W-T))
      IF(DIFF1.GT.DEPH)GO TO 12
      GO TO 10
70      C
C      FLOW DEPTH EQUAL CONDUIT DEPTH
C
75      9 PH1= PI/2.
      ROOT= 0.
C
C      COMPUTATION OF AREA AND TOP WIDTH OF WATER SURFACE
10     A= DN*(W-T)-DIFF1*(W-TW)-2.*SEC*R1*R1+R*R*PH1 +
      +ROOT*DIFF1
      B= TW+2.*ROOT
80     IF(T.EQ.0.)GO TO 11
      HR= A/(W-4.*SEC*R1-T+2.*(DN-DIFF1)+2.*DN +
      +2.0*R*PH1)
      RETURN
11     HR= A/(W-4.*SEC*R1+2.*(DN-DIFF1)+2.*R*PH1)

```


APPENDIX II

111

SUBROUTINE TRANS

```

85      RETURN
      C
      C      FLOW FILLS CONDUIT
      C
      12 JIC= 1
90      A= DN*(W-T)-DEPTH*(W-TW)-2.*SEC*R1*R1+R*R*PHI1+ROOT*DEPTH
      B=0.
      IF(T.EQ.0.)GO TO 13
      HR= A/(W-4.*SEC*R1-T+2.*(DN-DEPTH)+2.*DN+2.*R*PHI1)
      RETURN
95      13 HR= A/(W-4.*SEC*R1+2.*(DN-DEPTH)+2.*R*PHI1)
      RETURN
      END

```

EXAMPLE - WATER SURFACE PROFILE

Q = 20.000 CMS INITIAL DEPTH = .563 M RUGOSITY = 1.7000 MM N = .0142

STATION M	INVERT ELEV M	SLOPE	DEPTH M	VELOCITY M/SEC	PIEZ M	ENERGY GRADE LINE M	Q AIR/Q WATER	PROFILE	DEPTH	
									NORMAL M	CRITICAL M
0.00	100.000	.3333	.563	2.368	.534	100.849	0.000	S2	.126	.566
.72	99.760	.3333	.369	3.618	.350	100.844	0.000	S2	.126	.566
1.39	99.538	.3338	.316	4.215	.300	100.834	0.000	S2	.126	.566
2.62	99.127	.3333	.264	5.042	.251	100.804	0.000	S2	.126	.566
5.13	98.289	.3333	.213	6.254	.202	100.684	0.000	S2	.126	.566
11.59	96.136	.3332	.164	8.132	.156	100.000	0.000	S2	.126	.566
18.03	93.989	.3333	.146	9.147	.138	98.819	0.000	S2	.126	.566
24.22	91.927	.3333	.138	9.695	.130	97.329	0.000	S2	.126	.566
37.45	87.515	.3334	.130	10.228	.124	93.507	.033	S2	.126	.566
60.69	79.771	.3333	.128	10.420	.121	85.982	.056	S2	.126	.566
75.67	74.778	.3333	.128	10.417	.121	80.985	.055	S2	.126	.566

DATA FILE - HSPWY

```

20.,0.563,0.01,1,0,0.33333      0,1
11                                11.593,96.136,15.,0.
0,1                                0.,0.,0.,0.
0.,100.,15.,0.                    0,1
0.,0.,0.,0.                        18.034,93.989,15.,0.
0,1                                0.,0.,0.,0.
0.720,99.76,15.,0.                0,1
0.,0.,0.,0.                        24.22,91.927,15.,0.
0,1                                0.,0.,0.,0.
1.385,99.538,15.,0.                0,1
0.,0.,0.,0.                        37.454,87.515,15.,0.
0,1                                0.,0.,0.,0.
2.618,99.127,15.,0.                0,1
0.,0.,0.,0.                        60.687,79.771,15.,0.
0,1                                0.,0.,0.,0.
5.132,98.289,15.,0.                0,1
0.,0.,0.,0.                        75.667,74.778,15.,0.
                                0.,0.,0.,0.

```


Appendix III - Air Demand, Falling Water Surface, Computer Program

INTRODUCTION

The original version of the falling water surface computer program¹ contained simplifications that could have led to significant errors in the flow simulation. The present program was modified to represent more realistically the flow conditions at the gate and to include a better representation of the hydraulic turbine characteristics. The complicated prototype geometry is input into the program through the use of a few parameters which approximate the actual geometry.

JUNCTION ENERGY EQUATIONS

The original study¹ assumed that the relation between the flow from the reservoir and gate chamber could be described by the junction flow equations for a pipe tee. A more realistic flow description—considering the varying area

created by the closing gate—would be the formation of a submerged hydraulic jump downstream from the gate (fig. III-1).

Writing the momentum equation in the horizontal direction on the prism of water between points V and P gives:

$$\frac{p_V}{\gamma} = \frac{2A_G}{(A_P + A_G)} \left[\left(\frac{p_P}{\gamma} \right) \frac{(A_G + A_P)}{2A_G} \right] + \frac{2A_P}{A_G} \frac{V_P^2}{2g} - \frac{2}{C_c G_P} \frac{A_P^2}{A_G^2} \frac{V_V^2}{2g} \quad (1)$$

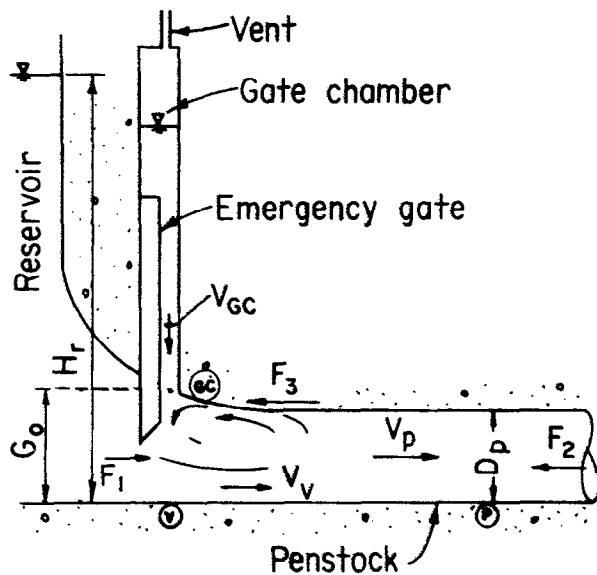
where

$$V_V = \frac{Q_R}{G_P A_G C_c} \text{ and } V_P = \frac{Q_P}{A_P}, \text{ figure III-1}$$

The contraction coefficient C_c is related to the discharge coefficient C_d through [59]

$$C_c = \frac{(C_d/G_P)^2 (G/H_r)}{2} + \frac{(C_d/G_P)^4 (G/H_r)^2 + 4(C_d/G_P)^2}{2} \quad (2)$$

¹H. T. Falvey, *Air Vent Computations, Morrow Point Dam*, Hydraulic Laboratory Report HYD-584, Bureau of Reclamation, Denver, Colorado, 39 p., 1968.



A_p = penstock area
 A_G = total area of gate opening
 C_c = contraction coefficient
 C_d = discharge coefficient
 D_p = penstock diameter
 D_3 = Discharge diameter of runner
 F_1 = upstream force
 F_2 = penstock force
 F_3 = force of walls on jump
 G = partial gate opening

G_o = full gate opening
 $G_P = (G/G_o)$ = percent gate opening
 g = gravitational constant (acceleration)
 H_r = reservoir head on gate
 K_t = turbine loss coefficient
 p_{GC} = pressure at lower end of gate chamber
 p_P = penstock pressure
 p_V = pressure at vena contracta
 Q = discharge
 Q_P = penstock discharge
 Q_R = reservoir discharge
 Q_{11} = specific discharge through a turbine
 V_{GC} = velocity in gate chamber
 V_P = penstock velocity
 V_V = velocity at vena contracta
 W = gate width
 γ = specific force of water
 $\pi = 3.14159...$

The forces F are defined as

$$\begin{aligned}
 F_1 &= \gamma(p_V/\gamma - G_o/2) A_G \\
 F_2 &= \gamma(p_V/\gamma - D_P/2) A_P \\
 F_3 &= \frac{\gamma}{2} [(p_V/\gamma + p_P/\gamma)(A_G - A_P) + (D_P A_P - G_o A_G)]
 \end{aligned}$$

The velocities V are defined as

$$\begin{aligned}
 V_V &= Q_R / (C_c G_o W) = Q_R / (C_c G_P A_G) \\
 V_P &= Q_P / A_P
 \end{aligned}$$

FIGURE III-1.—Definition sketch at penstock intake.

The discharge coefficient in equation 2 is based on the area of the fully open gate.

If the kinetic energy in the submerged hydraulic jump is assumed small, the pressure at the lower end of the gate chamber is given by

$$\frac{p_{GC}}{\gamma} = \frac{p_V}{\gamma} - D_P \quad (3)$$

When all water has drained from the gate chamber, but the gate is still submerged, the pressure at point P is given by

$$\begin{aligned}
 \frac{p_P}{\gamma} &= \frac{Q_R^2}{g G C_c^2 A_G A_P} \\
 &+ \frac{2}{\pi} \left(\frac{p_V}{\gamma} \right)^2 \frac{1}{D_P} - \frac{2 V_P^2}{2g} + \frac{D_P}{2}
 \end{aligned} \quad (4)$$

The pressure at point V , which is also the water depth at that point, is determined from the air volume in the penstock and assuming a 1:7 slope for the free water surface of the hydraulic jump.

If the hydraulic jump is not submerged, the pressure at V is given by

$$\frac{p_V}{\gamma} = C_c A_G G \quad (5)$$

TURBINE CHARACTERISTICS

The head loss coefficient across the turbine was arbitrarily assumed constant in the original study.² The validity of the assumption is investigated in the following paragraphs.

The energy loss across the turbine is given by

$$h_d = K_t \frac{V_P^2}{2g} \quad (6)$$

The loss coefficient K_t can be written

$$K_t = \frac{2gh_d}{V_P^2} \quad (7a)$$

or

$$K_t = \frac{\pi^2 g}{8} \left(\frac{D_P}{D_3} \right)^4 \left(\frac{D_3^2 \sqrt{h_d}}{Q} \right)^2 \quad (7b)$$

where D_3 is a characteristic dimension of the turbine runner.

The quantity $\frac{Q}{D_3^2 \sqrt{h_d}}$ is a basic parameter used in describing the turbine characteristics. The quantity is known as the specific discharge and usually is written Q_{11} . The subscripts signify the discharge from a one-meter-diameter runner having a one-meter head across the turbine runner. Thus, the loss coefficient also can be written:

$$K_t = \frac{\pi^2 g}{8} \left(\frac{D_P}{D_3} \right)^4 \left(\frac{1}{Q_{11}} \right)^2 \quad (8)$$

The discharge through a turbine is dependent upon the head across the unit, runner speed, and wicket gate opening. The runner speed and head across the unit are described by

a dimensionless parameter known as ϕ (phi) defined by

$$\phi = \frac{\pi D_3 n}{60 \sqrt{2gh_d}} \quad (9)$$

where n is the rotational speed in revolutions per minute.

Typical turbine characteristic curves for a runner having a specific speed³ of about 230 show that the specific discharge is not significantly affected by changes in the rotational speed (fig. III-2). The maximum change in specific discharge between the maximum efficiency and the runaway condition at a constant gate opening amounts to about 3 percent. The corresponding change in the loss coefficient is about 6 percent.

Loss coefficient curves can be prepared for any turbine runner. These curves will be a function of the wicket gates opening and the ϕ value (fig. III-3).

If the generator unit remains connected to the electrical system during a closure of the emergency gate, the turbine will operate at a constant speed. The condition with the turbine at synchronous speed but with no flow is called *motoring*.⁴ During motoring the turbine will develop a head in the penstock. The magnitude of this head must be input into the computer program. For reaction turbines the magnitude

³The specific speed of a turbine is given by

$$n_s = \frac{n(P_d)^{1/2}}{(h_d)^{5/4}}$$

where

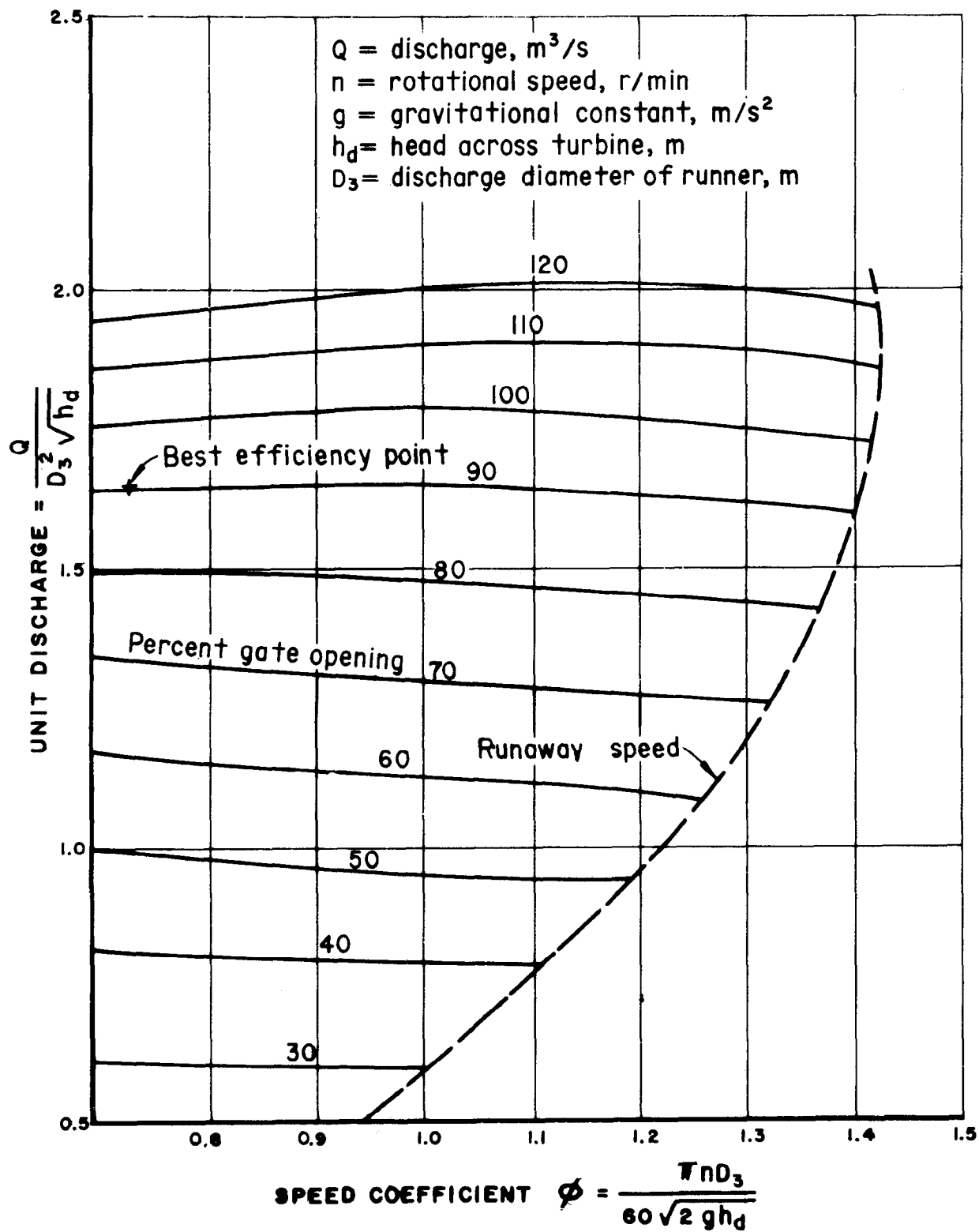
h_d = turbine head, m

n = rotational speed, r/min

P_d = turbine power output, kW

⁴Power requirements for motoring can be minimized by depressing the water surface in the draft tube. This is used for either power factor adjustment or for spinning reserve. During an emergency, depression of the water surface in the draft tube cannot be assumed to occur.

²Ibid.

FIGURE III-2.—Typical turbine characteristics of runner specific speed 230 in $m\text{-kW}$ units.

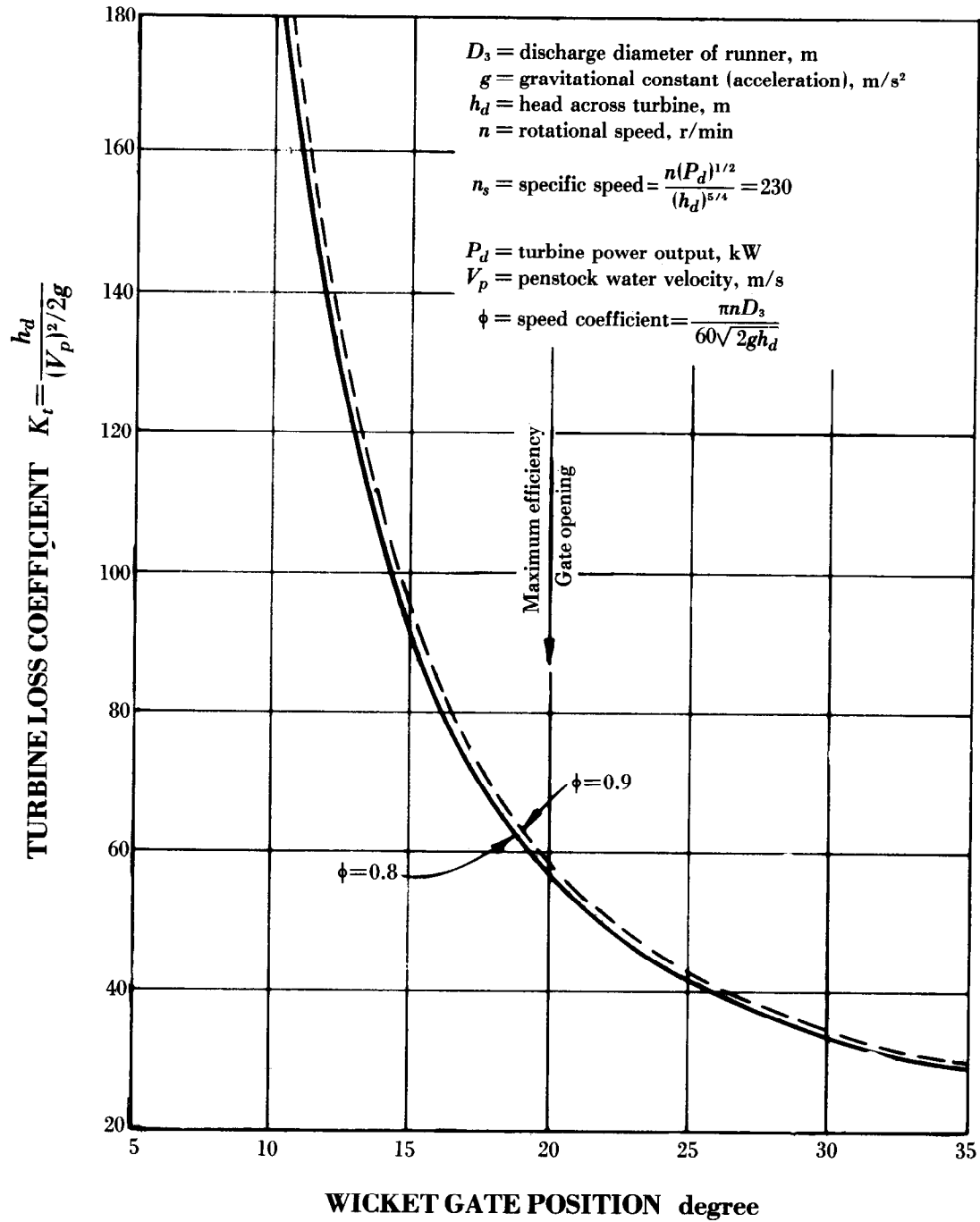


FIGURE III-3.—Turbine loss coefficient.

of the motoring head is about 20-to 25-percent of the turbine net head.

GEOMETRY

The two most significant geometric effects which must be calculated for free surface flow in the penstock are the air volume in the penstock and the water surface area as a function of water surface elevation.

The actual variation of the air volume in the penstock is a complicated function due to the

circular section of the penstock and vertical bends. The air volume must be computed as a function of elevation for enough points to define the prototype curve. Two straight lines are fitted through the prototype values (fig. III-4). The coefficients of these two straight lines are input into the program.

A similar procedure is used for the water surface area as a function of elevation. However, the prototype curve is fitted with a sine wave and a vertical line instead of two straight lines (fig. III-5).

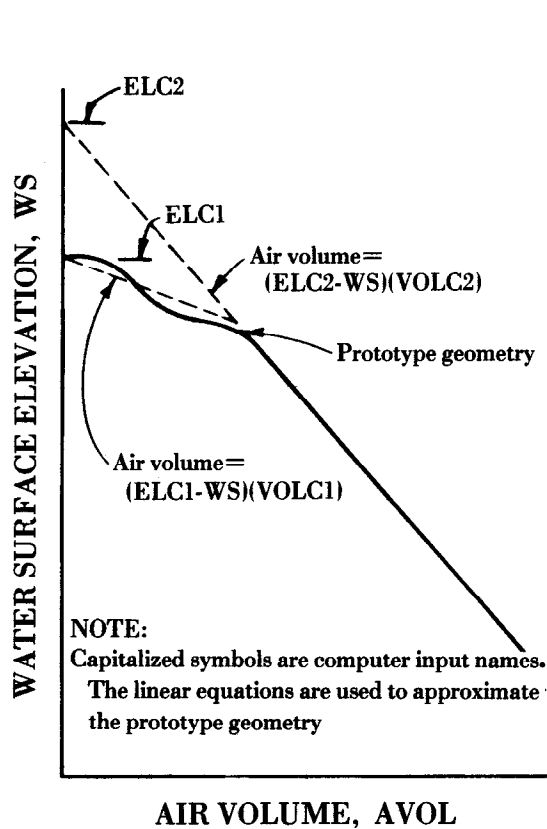


FIGURE III-4.—Air volume in penstock.

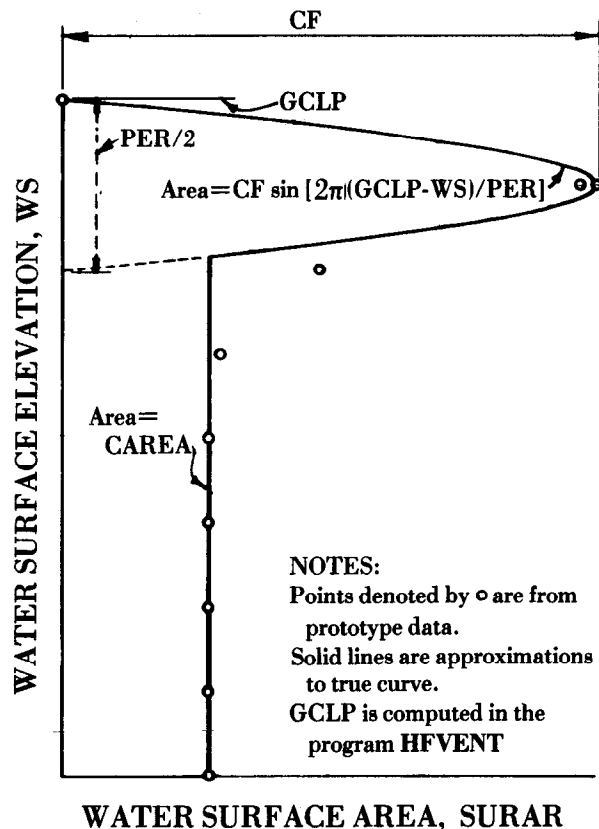


FIGURE III-5.—Water surface area.

APPENDIX III

119

PROGRAM HFVENT

```

1      PROGRAM HFVENT(INPUT=65,OUTPUT=65,TAPE3=OUTPUT)
      C      COMPUTATION OF AIR FLOW INTO GATE CHAMBER DURING AN EMERGENCY
      C      CLOSURE OF GATES FOR THE PENSTOCK INTAKE STRUCTURE
      C
5      REAL MACHA,MACHGA,NVENTS
      COMMON CD,CKV,ABSPGC,PATM,PGC,WSREF,HCOL,WS,QR,QP,GRAV,PTOHD,
+PP,P3(50),J,PL,FP,TLOSS,AU,AD,AREAP,AG,EK,GCR,PGO,JFIRST,WTFLA(50)
+MACHA(50),MACHGA(50),AVOL,PIN,CVEL,T(50),JCK,GCLP,RES,ZP,DP,TW,
+UGCLGC,GCLL,HYDDIA,VOLC1,ELC1,VOLC2,ELC2,CF,PER,CAREA,HMOTOR,
10     +NVENTS,TGC,ENRTAP(50),SO,VOLR,CKX,PR,FSAV,FSAV1,DELX,DELY
+ACURAC,ABSTEM,GASCTE,VAPOR,AGCCTE,SLOSS,METRIC,PENLEN
      DIMENSION QGA(50),AR(50),AP(50),AS(50),AGC(50),
+VIN(50),VOUT(50),PA(50),PGA(50),CA(50),ERTAGC(50),
+RHOAG(50),SPVOL(50),DX(50),DY(50),
15     +CKB(50),X(50),Y(50),VP(50),VGC(50),DPL(50),DVC(50),JCT(50)
      WRITE(3,1)
1     FORMAT(1H1,/)
      C
      C      INPUT DATA
20     C      =====
      C
      C      COMPUTATION CONTROLS
      C      -----
25     C
      C      SYSTEM OF UNITS
      C      METRIC, SET METRIC = 1
      C      ENGLISH, SET METRIC = 0
      C      METRIC= 1
30     C
      C      INITIAL TIME
      C      T(1)= 0.
      C
      C      TIME INTERVAL BETWEEN CALCULATIONS (SEC)
35     C      DELT= 1.
      C
      C      MAXIMUM TIME WHICH IS TO BE CALCULATED (SEC)
      C      TMAX= 40.
      C
40     C      THE TITLE AND AIR VENT DESCRIPTION ARE INPUT IN THE
      C      FORMAT STATEMENTS. THEY CAN CONTAIN UP TO 60 CHARACTERS
      C      EACH. BOTH DESCRIPTIONS MUST BE CENTERED IN THE FIELD.
      C      2 FORMAT(6X,60H
      C      MORROW POINT DAM
      C      +
45     C      3 FORMAT(6X,60H
      C      ONE 840MM BY 915MM AIR VENT
      C      +
      C
      C      WATER FLOW QUANTITIES
50     C      -----
      C
      C      TURBINE LOSS COEFFICIENT
      C      TLOSS= 111.2
      C
55     C      TYPE OF TURBINE OPERATION DURING CLOSURE
      C      (IF UNIT RUNS AT CONSTANT SPEED, SET NSPEED = 1.
      C      IF THE CIRCUIT BREAKERS ARE OPEN SO THAT
      C      THE SPEED CAN VARY, SET NSPEED = 0. BOTH
      C      OF THESE TYPES OF OPERATION ASSUME A BLOCKED
60     C      GATE OPERATION.)
      C      NSPEED = 1
      C
      C      HEAD DEVELOPED BY TURBINE DURING MOTORING
      C      (SPEED NO LOAD)
65     C      HMOTOR= 27.5
      C

```

AIR-WATER FLOW IN HYDRAULIC STRUCTURES

PROGRAM HFVENT

```

C      GATE CLOSING RATE (PERCENT/SEC)
C      GCR= 0.9901
70      C
C      DARCY-WIESBACH FRICTION FACTOR IN PENSTOCK
C      FP= 0.009
C
C      SINGULAR LOSS BETWEEN UPPER AND LOWER GATE CHAMBER
C      EK= 0.3
75      C
C      AIR FLOW QUANTITIES
C      -----
C
C      TEMPERATURE
80      C      TEMP= 4.5
C
C      ATMOSPHERIC PRESSURE (PSI OR KPA)
C      PATM= 77.6
C
85      C      INCOMPRESSIBLE FRICTION FACTOR FOR THE AIR FLOW IN
C      THE DUCT (FL/D)
C      FRIC= 0.93
C
C      COMPRESSIBLE DISCHARGE COEFFICIENT OF AIR
90      C      AT DUCT INLET
C      CINC= 0.5
C
C      GEOMETRY
C      -----
95      C
C      RESERVOIR WATER LEVEL
C      RES= 2181.64
C
C      TAIL WATER LEVEL
100     C      TW= 2059.23
C
C      ELEVATION UPPER GATE CHAMBER TO LOWER GATE CHAMBER
C      UGCLGC= 2168.04
C
105     C      ELEVATION INVERT AT GATE
C      ZP= 2155.93
C
C      ELEVATION OF TOP OF GATE CHAMBER
C      TGC= 2183.89
110     C
C      AREA UPPER GATE CHAMBER
C      AU= 13.80
C
C      AREA LOWER GATE CHAMBER
115     C      AD= 4.33
C
C      AREA GATE
C      AG= 20.64
C
120     C      CROSS-SECTIONAL AREA OF EACH AIR VENT
C      AVENT= 0.766
C
C      NUMBER OF VENTS
C      NVENTS= 1.
125     C
C      CONSTANTS WHICH DESCRIBE THE VOLUME OF THE
C      -----
C      PENSTOCK AS A FUNCTION OF THE WATER SURFACE
C      SEE THE DOCUMENTATION FOR THE DEFINITION OF
130     C      THESE CONSTANTS
C      VOLC1= 46.16
C      VOLC2= 13.3

```

APPENDIX III

121

PROGRAM HFVENT

```

      ELC1= 2155.93
      ELC2= 2170.21
135      C
      C      PENSTOCK LENGTH
      PL= 143.56
      C
      C      PENSTOCK LENGTH AS A FUNCTION OF WATER SURFACE PARAMETER
140      C      PENLEN= 2016.48
      C
      C      PENSTOCK DIAMETER
      DP= 4.12
      C
145      C      HEIGHT OF GATE
      SO= 5.01
      C
      C      HYDRAULIC DIAMETER OF LOWER GATE CHAMBER
      HYDDIA= 1.41
150      C
      C      CONSTANTS WHICH DESCRIBE THE FREE WATER SURFACE AREA
      C      -----
      C      IN THE PENSTOCK.  SEE THE DOCUMENTATION FOR THE
      C      DEFINITION OF THESE CONSTANTS
155      CF= 48.83
      PER= 8.23
      CAREA= 13.5
      C
      C      END OF INPUT DATA
160      C      =====
      C
      C      COMPUTED CONSTANTS
      C
      PI= 3.14159
165      K= INT((TMAX-T(1))/(40.*DELT))+1
      GRAV= 32.2
      GASCTE= 53.3
      PTOHD= 2.30769
      VAPOR= PTOHD*0.0256*10.**(.0162*TEMP)
170      AGCCTE= 144.
      ACURAC= .01
      PGCINC= 0.01
      ABSTEM= TEMP+459.67
      RHOA= AGCCTE*PATM/(GASCTE*ABSTEM)
175      CD= 0.9303
      IF(METRIC.EQ.0)GO TO 4
      GASCTE= 287.
      PTOHD= 0.000102
      VAPOR= PTOHD*.582*10.**(.0292*TEMP+3.)
180      AGCCTE= 1000.
      PATM= PATM*AGCCTE
      ACURAC= 0.003
      PGCINC= 50.
      GRAV= 9.807
185      ABSTEM= TEMP+273.15
      RHOA= PATM/(GASCTE*ABSTEM)
      4 ABSPGC = PATM
      AREAP= PI*DP*DP/4.
      HEAD= RES-TW
190      PGD= 1.
      BH= SO/(RES-ZP)
      CC= (CD*CD*BH+SQRT(CD**4*BH**2+4.*CD**2))/2.
      CONST= TLOSS-1.+FP*PL/DP+(AREAP/(AG*CD))**2-4.*ARC**2*AREAP/(
      +(AG+AREAP)*CC*PGD*AG)+4.*AREAP/(AG+AREAP)
195      QR= AREAP*SQRT(2.*GRAV*HEAD/CONST)
      VHP= (QR/AREAP)**2./(2.*GRAV)
      VHR= VHP
      PR= RES-ZP-VHR*(AREAP/AG/CD)**2

```

AIR-WATER FLOW IN HYDRAULIC STRUCTURES

PROGRAM HFVENT

```

200      WS= ZP+PR
      PP= PR+2.*AG/(AG+AREAP)*(2./CC*VHR*(AREAP/AG)**2-2.*VHP*AREAP/AG)
      WSREF = WS
      HCOL= WSREF-UGCLGC
      GCLP= ZP+DP
      GCLL= UGCLGC- GCLP
205      QP = QR
      QGC = 0.
      AVOLRE= (TGC-WS)*AU
      WTAIR = RHOA * AVOLRE
      AVOL= AVOLRE
210      PIN = PATM
      PGC = PTOHD*PATM
      CONST = PATM / RHOA**1.4
      CKA= 0.
      JFIRST= 1
215      DELTIM= 0.
      JCK= 1
      NT= 1
      IF(NSPEED.EQ.0)HMOTOR= 0.
      SLOSS= 1.-HMOTOR/(TLOSS*VHP)
220      PVAPOR= VAPOR-PGC
      C
      C
      C
      C
      C      SIGNIFICANCE OF JFIRST
225      C      1 - FIRST TIME THRU MAIN LOOP
      C      2 - SECOND TIME THRU MAIN LOOP,
      C      WATER SURFACE IN UPPER GATE CHAMBER
      C      3 - LAST TIME INCREMENT IN UPPER GATE CHAMBER
      C      4 - FIRST TIME INCREMENT IN LOWER GATE CHAMBER
230      C      5 - WATER SURFACE IN LOWER GATE CHAMBER
      C      6 - LAST TIME INCREMENT IN LOWER GATE CHAMBER
      C      7 - FIRST TIME INCREMENT IN PENSTOCK
      C      8 - WATER SURFACE IN PENSTOCK
235      C      9 - WATER ELEVATION LESS THAN TAIL WATER SURFACE
      C      ELEVATION
      C      10 - VAPOR PRESSURE FORMED AT GATE
      C      11 - SONIC VELOCITY IN AIR VENT
      C
      C
      C      =====
240      C
      C      *** COMPUTATIONS IN MAIN LOOP ***
      C      DO 48 NTIM=1,K
      C      IF(NTIM.GE.2)NT= 2
      C      IF(NTIM.LE.1)GO TO 5
245      C
      C      DATA INITIALIZATION FOR SUBSEQUENT PASSES THRU MAIN LOOP
      C      T(1)= T(41)
      C      QGA(1)= QGA(41)
      C      AR(1)= AR(41)
250      C      AP(1)= AP(41)
      C      VP(1)= VP(41)
      C      VGC(1)= VGC(41)
      C      X(1)= X(41)
      C      Y(1)= Y(41)
255      C      AS(1)= AS(41)
      C      AGC(1)= AGC(41)
      C      VIN(1)= VIN(41)
      C      VOUT(1)= VOUT(41)
      C      PGA(1)= PGA(41)
260      C      CA(1)= CA(41)
      C      ENRTAP(1)= ENRTAP(41)
      C      ERTAGC(1)= ERTAGC(41)
      C      DPL(1)= DPL(41)
      C      DVC(1)= DVC(41)

```

APPENDIX III

123

PROGRAM HFVENT

```

265      PA(1)= PA(41)
          MACHA(1)= MACHA(41)
          MACHGA(1)= MACHGA(41)
          RHOAG(1)= RHOAG(41)
          SPVOL(1)= SPVOL(41)
270      WTFLA(1)= WTFLA(41)
          CKB(1)= CKB(41)
          P3(1)= P3(41)
          JCT(1)= JCT(41)

C
C
275      C      COMPUTATIONAL LOOP FOR 40 TIME INCREMENTS
C
5      DO 25 M=NT,41
          J= M
          JN= J-1
280      IF (NTIM.EQ.2.AND.J.LE.3)GO TO 6
          GO TO 7
6      JM2= J+38
          IF (J.GE.3)JM2= J-2
          JM1= J+39
285      IF (J.GE.2)JM1= J-1

C
C
C      TRIAL DETERMINATION OF WATER SURFACE
C
7      IF (JFIRST.EQ.1) GO TO 19
          IF (JFIRST.GE.6) GO TO 10
          IF (JFIRST.GE.3)GO TO 8
          IF (J.LE.4)GO TO 17
          WSTEST= AS(J-2)-(5.*VGC(JN)+VGC(J-2)+DELT*FUNCT2(Y(JN),
+          VP(JN),VGC(JN)))*DELT/3.
295      GO TO 9
8      IF (JFIRST.EQ.3) WSTEST= AS(JN)-(DELT-DELTIM)*VGC(JN)*AU/AD
          IF (JFIRST.EQ.3)GO TO 9
          WSTEST= AS(JN)-DELT*(VGC(JN)+DELT*FUNCT2(Y(JN),VP(JN),
+          VGC(JN))/2.)
300      IF (JFIRST.EQ.4)WSTEST= AS(JN)-(DELT+DELTIM)*VGC(JN)
          IF (WSTEST.LE.GCLP)GO TO 10
          IF (WSTEST.LE.UGCLGC)GO TO 14
          GO TO 17

C
C
305      C      WATER SURFACE IN PENSTOCK
C
10     IF (JFIRST.EQ.6)GO TO 11
          IF (JFIRST.EQ.7)GO TO 12
          IF (JFIRST.EQ.8)GO TO 13
310      C      LAST INCREMENT BEFORE PENSTOCK FLOW
          VOLGC= (AS(JN)-GCLP)
          IF (J.GE.3)JM2= J-2
          TOUT= T(JN)+VOLGC*2./(VGC(JN)+VGC(JM2))
          IF (JFIRST.EQ.4) TOUT= T(JN)+VOLGC*2.*AU/(AD*(VGC(JN)+VGC(JM2))
315      +      )
          IF (TOUT.GE.(T(JN)+DELT))TOUT= T(JN)+VOLGC/VGC(JN)
          VEL2= VGC(JN)+FUNCT2(Y(JN),VP(JN),VGC(JN))*
          +      (TOUT-T(JN))
          IF (JFIRST.EQ.4)DELT= DELT+DELTIM
          DELTIM= VOLGC*2./(VEL2+VGC(JN))
          IF (DELTIM.GT.DELT)GO TO 17
          IF (DELTIM.LE.0.)DELTIM= TOUT-T(JN)
          JFIRST= 6
          CALL DE2(X,Y,VP,VGC,T,DELTIM,JN)
325      AS(J)= UGCLGC-Y(J)
          IF (AS(J).LT.GCLP)AS(J)=GCLP
          WS= AS(J)
          X(J)= 0.
          CALL AMACH(CINC,FRICT,AVENT,DELTIM,PGCINC,WTAIR,CONST,
330      +      CKA)

```

AIR-WATER FLOW IN HYDRAULIC STRUCTURES

PROGRAM HFVENT

```

      C      TIME INCREMENT AS WATER ENTERS PENSTOCK
      GO TO 20
      11      DELT= DELT-DELTIM
      JFIRST= 7
335      GO TO 13
      12      DELT= DELT+DELTIM
      JFIRST= 8
      13      CALL DE1(X,VP,DELT)
      AS(J)= WS
340      GO TO 18

      C
      C      WATER SURFACE IN LOWER GATE CHAMBER
      C
      14      IF(JFIRST.EQ.3)GO TO 15
      IF(JFIRST.EQ.4)GO TO 16
      IF(JFIRST.EQ.5)GO TO 17
      C      LAST INCREMENT IN UPPER GATE CHAMBER
      VOLGC= (AS(JN)-UGCLGC)
      TOUT= T(JN)+VOLGC/VGC(JN)
350      VEL2= VGC(JN)+FUNCT2(Y(JN),VP(JN),VGC(JN))*
      +      (TOUT-T(JN))
      DELTIM= VOLGC*2./ (VEL2+VGC(JN))
      JFIRST= 3
      CALL DE2(X,Y,VP,VGC,T,DELTIM,JN)
355      AS(J)= WSREF-Y(J)
      WS= AS(J)
      CALL AMACH(CINC,FRICT,AVENT,DELTIM,PGCINC,WTAIR,CONST,
      +      CKA)
      GO TO 20
360      C      TIME INCREMENT AS WATER ENTERS LOWER GATE CHAMBER
      15      DELT= DELT-DELTIM
      JFIRST= 4
      WSREF= UGCLGC
      JCK=2
365      GO TO 17
      16      DELT= (DELT+DELTIM)
      JFIRST= 5

      C
      C      WATER SURFACE IN UPPER OR LOWER GATE CHAMBER
      C
370      17      CALL DE2(X,Y,VP,VGC,T,DELT,JN)
      AS(J)= WSREF-Y(J)
      WS= AS(J)

      C
      C      DETERMINATION OF AIR FLOW RATE IN VENT
      C
375      18      CALL AMACH(CINC,FRICT,AVENT,DELT,PGCINC,WTAIR,CONST,
      +      CKA)
      IF(JFIRST.GE.7)P3(J)= PTOHD*(ABSPGC-PATM)
380      GO TO 20

      C
      C      ASSIMILATION OF RESULTS FOR FIRST TIME THRU
      C
385      19      QGA(1)= QGC
      AR(1)= QR
      AP(1)= QP
      VP(1)= AP(1)/AREAP
      VGC(1)= 0.
      X(1)= 0.
390      Y(1)= 0.
      DX(1)= 0.
      DY(1)= 0.
      AS(1)= WS
      AS(2)= WS
395      AGC(1)=ABSPGC
      IF(METRIC.EQ.1)AGC(1)= AGC(1)/AGCCTE

```

APPENDIX III

125

PROGRAM HFVENT

```

VIN(1)= 0.
VOUT(1)= 0.
ENRTAP(1)= FUNCT1(VP(1),VGC(1),T(1))
400 ERTAGC(1)= FUNCT2(Y(1),VP(1),VGC(1))
DVC(1)= P3(1)+DP
PGA(1)= PGO
CA(1)= CD
PA(1)= PP
405 MACHA(1)= 0.
MACHGA(1)= 0.
RHOAG(1)= RHOA
SPVOL(1)= 1./RHOA
WTFLA(1)= 0.
410 CKB(1)= 0.
JCT(1)= JCK
VOLR= 0.
JFIRST= 2
DPL(1)= TLOSS*SLOSS*(AP(1)/(.785*DP*DP))*2./(2.*GRAV)+HMOTOR
415 GO TO 25

C
C
C
20 ASSIMILATION OF RESULTS FOR REMAINING TIME INCREMENTS
420 CALL Q(QGC,VP,VGC)
QGA(J)= QGC
PCHECK= ABS(P3(J)-PVAPOR)
IF(PCHECK.LE.0.0001)JFIRST=10
IF(JFIRST.EQ.10)GO TO 26
IF(JFIRST.EQ.11)GO TO 26
425 IF(W.S.LE.TW.OR.QP.LT.0.)JFIRST= 9
IF(JFIRST.EQ.9)GO TO 26
AR(J)= QR
AP(J)= QP
AGC(J)=ABSPGC
430 IF(METRIC.EQ.1)AGC(J)= AGC(J)/AGCCTE
IF(JFIRST.GE.7) GO TO 21
ENRTAP(J)= FUNCT1(VP(J),VGC(J),T(J))
ERTAGC(J)= FUNCT2(Y(J),VP(J),VGC(J))
IF(JFIRST.GE.4)ERTAGC(J)= ERTAGC(J)*(GCLP-WS)/GRAV
435 GO TO 22
21 ENRTAP(J)= FUNCT3(X(J),VP(J),T(J))
ERTAGC(J)= 0.
22 WTAIR= WTAIR+(WTFLA(JN)+WTFLA(J))*DELT/2.
IF(JFIRST.EQ.3.OR.JFIRST.EQ.6)WTAIR= WTAIR+(WTFLA(JN)
440 +WTFLA(J))*(DELTIM-DELT)/2.
RHOAG(J)= WTAIR/AVOL
SPVOL(J)= 1./RHOAG(J)
VOLR= VOLR+(QR+AR(JN))*DELT/2.
IF(JCK.LT.4)VOLR= 0.
445 DPL(J)= TLOSS*SLOSS*(AP(J)/(.785*DP*DP))*2./(2.*GRAV)+HMOTOR
DVC(J)= PR
PGA(J)= PGO
PA(J)= PP
CA(J)= CD
450 JCT(J)= JCK
DX(J)= DELX
DY(J)= DELY
VOUT(J)= MACHGA(J)*SQRT(GRAV*SPVOL(J)*1.4*AGC(J)*AGCCTE)
IF(METRIC.EQ.1)VOUT(J)= VOUT(J)/SQRT(GRAV)
455 IF(PIN.GE.PATM)GO TO 23
VIN(J)= CVEL*SQRT(7.*GASCTE*GRAV*ABSTEM*
+ (1.-(PIN/PATM))*(2./7.))
IF(METRIC.EQ.1)VIN(J)= VIN(J)/SQRT(GRAV)
IF(MACHA(J).LT.0.)VIN(J)= (-1.)*VIN(J)
460 GO TO 24
23 VIN(J)= VOUT(J)
24 CKB(J)= CKA

```

AIR-WATER FLOW IN HYDRAULIC STRUCTURES

PROGRAM HFVENT

```

25  CONTINUE
C
465  C      *** WRITE STATEMENTS FOR OUTPUT OF RESULTS ***
C
26  J= JN+1
    IF(JFIRST.EQ.10) J=J-1
    IF(JFIRST.EQ.11) J=J-1
470  IF(JFIRST.EQ.9) J=J-1
    IF(METRIC.EQ.1) PATM= PATM/AGCCTE
C
C      FLOW QUANTITIES
C
475  IF(METRIC.EQ.1) GO TO 38
    WRITE(3,27)
    WRITE(3,2)
    WRITE(3,28) PATM,RHOA
    WRITE(3,3)
480  27  FORMAT (1H1,8X,
+          48H COMPUTATION OF AIR FLOW INTO THE GATE CHAMBER D
+          8HURING AN / 16X,
+          40H EMERGENCY GATE CLOSURE IN THE PENSTOCK- / 27X,
+          18H INTAKE STRUCTURE )
485  28  FORMAT(/ 8X,21H ATMOSPHERIC PRESSURE ,14X,
+          23H SPECIFIC MASS OF AIR / 13X
+          ,F6.2, 5H PSI ,
+          ,23X,F6.4,11H LB/CU.FT. //)
    WRITE(3,29) (T(N),PGA(N),CA(N),AR(N),QGA(N),AP(N),N=1,J)
490  29  FORMAT(28X,15HFLOW QUANTITIES //
+          8X,
+          34H TIME      GATE      COEFF      Q
+          20H          Q      Q / , 16X,
+          49H OPENING  DISCH.    RESERVOIR  GATE    PENSTOCK /
495  +          48X,8HCHAMBER /
+          8X,46H(SEC)      (0/0)              (CFS)      (CFS)
+          9H      (CFS) /
+          (5X,F8.1,2X,F8.1,1X,F8.2,4X,F8.1,1X,F8.1,3X,F8.1))
    IF(JFIRST.EQ.10) WRITE(3,30) T(J+1)
500  30  FORMAT(4X,F8.1,5X,38H VAPOR PRESSURE FORMED IN GATE CHAMBER )
    IF(JFIRST.EQ.11) WRITE(3,31) T(J+1)
505  31  FORMAT(4X,F8.1,9X,23H SONIC VELOCITY IN VENT)
C
C      WATER PRESSURES
C
510  WRITE(3,27)
    WRITE(3,2)
    WRITE(3,28) PATM,RHOA
    WRITE(3,3)
    WRITE(3,32) (T(N),AS(N),DPL(N),P3(N),DVC(N),PA(N),N=1,J)
515  32  FORMAT(28X,15HWATER PRESSURES //
+          8X,
+          45H TIME      WS      HEAD      END GATE      VENA
+          12H      PENSTOCK /
+          16X,40H ELEV      ACROSS      CHAMBER      CONTRACTA /
+          29X,4HUNIT /
+          8X,46H(SEC)      (FT)      (FT)      (FT)      (FT)
+          9H      (FT) /
+          (5X,F8.1,3X,F8.2,2X,F8.2,2X,F8.2,2X,F8.2,2X,F8.2))
520  IF(JFIRST.EQ.10) WRITE(3,33) T(J+1)
    33  FORMAT(7X,F8.1,5X,38H VAPOR PRESSURE FORMED IN GATE CHAMBER )
    IF(JFIRST.EQ.11) WRITE(3,34) T(J+1)
525  34  FORMAT(7X,F8.1,9X,23H SONIC VELOCITY IN VENT )
C
C      AIR FLOW PROPERTIES
C
    WRITE(3,27)
    WRITE(3,2)

```


APPENDIX III

127

PROGRAM HFVENT

```

WRITE(3,28)PATM,RHOA
530 WRITE(3,3)
WRITE(3,35)(T(N),VIN(N),VOUT(N),WTFLA(N),RHOAG(N),AGC(N),
+ N=1,J)
IF(JFIRST.EQ.10)WRITE(3,33)T(J+1)
IF(JFIRST.EQ.11)WRITE(3,34)T(J+1)
535 35 FORMAT(24X,21H AIR FLOW PROPERTIES //
+ 8X,
+ 47H TIME INLET OUTLET AIR FLOW SPECIFIC
+ 8H GATE /
+ 16X,
540 + 48H AIR VEL AIR VEL RATE MASS CHAMBER /
+ 48X,17HOF AIR PRESSURE /
+ 8X,50H(SEC) (FT/SEC) (FT/SEC) (LBM/SEC) (LB/CU FT)
+ 7H (PSIA) /
+ (5X,F8.1,3X,F8.1,2X,F8.1,2X,F8.2,2X,F8.4,2X,F8.2))

545 C
C COMPUTATIONAL PROPERTIES
C
WRITE(3,27)
WRITE(3,2)
550 WRITE(3,28)PATM,RHOA
WRITE(3,3)
WRITE(3,36)(T(N),CKB(N),DY(N),DX(N),JCT(N),N=1,J)
36 FORMAT(24X,24HCOMPUTATIONAL PROPERTIES //
+ 14X,44HTIME ACCURACY INTEGRATION ERROR FLOW /
555 + 20X,41H GATE GATE PENSTOCK CONDITION /
+ 20X,39H CHAMBER CHAMBER (* SEE /
+ 20X,40H PRESS LEGEND) /
+ 12X,36H (SEC) (PSI) (FT) (FT) /
+ (10X,F8.1,2X,F8.3,3X,F8.4,2X,F8.4,4X,14))
560 IF(JFIRST.EQ.10)WRITE(3,33)T(J+1)
IF(JFIRST.EQ.11)WRITE(3,34)T(J+1)
IF(NTIM.EQ.K.OR.JFIRST.EQ.9)WRITE(3,37)
37 FORMAT(11H,29X,6HLEGEND//
+ 8X,49H* 1 WATER SURFACE IN UPPER GATE CHAMBER /
565 + 8X,49H 2 WATER SURFACE BELOW TOP OF GATE /
+ 8X,49H 3 WATER SURFACE JUST ENTERING PENSTOCK /
+ 8X,49H 4 HYDRAULIC JUMP FILLS PENSTOCK, GATE SUBMERGED/
+ 8X,49H 5 HYDRAULIC JUMP FILLS PENSTOCK, GATE FREE FLOW/
+ 8X,48H 6 WATER SURFACE IN PENSTOCK //)
570 IF(NTIM.EQ.K.OR.JFIRST.EQ.9)GO TO 49
GO TO 48

C
C METRIC WRITE STATEMENTS
C
575 38 WRITE(3,27)
WRITE(3,2)
WRITE(3,39)PATM,RHOA
WRITE(3,3)
WRITE(3,40)(T(N),PGA(N),CA(N),AR(N),QGA(N),AP(N),N=1,J)
580 39 FORMAT(// 8X,21H ATMOSPHERIC PRESSURE ,14X,
+ 23H SPECIFIC MASS OF AIR / 13X
+ , F6.2, 5H KPA ,
+ ,23X,F6.4,11H KG/CU.M. //)
585 40 FORMAT(28X,15HFLOW QUANTITIES //
+ 8X,
+ 34H TIME GATE COEFF Q
+ 20H Q Q / , 16X,
+ 49H OPENING DISCH. RESERVOIR GATE PENSTOCK /
+ 48X,8HCHAMBER /
590 + 8X,46H(SEC) (O/O) (CMS) (CMS)
+ 9H (CMS) /
+ (5X,F8.1,2X,F8.1,1X,F8.2,4X,F8.3,1X,F8.3,3X,F8.3))
IF(JFIRST.EQ.10)WRITE(3,41)T(J+1)
41 FORMAT(4X,F8.1,5X,38H VAPOR PRESSURE FORMED IN GATE CHAMBER )

```

AIR-WATER FLOW IN HYDRAULIC STRUCTURES

PROGRAM HFVENT

```

595      IF(JFIRST.EQ.11)WRITE(3,42)T(J+1)
      42  FORMAT(4X,F8.1,9X,23H SONIC VELOCITY IN VENT)
      C
      C      WATER PRESSURES
      C
600      WRITE(3,27)
      WRITE(3,2)
      WRITE(3,39)PATM,RHOA
      WRITE(3,3)
      WRITE(3,43)(T(N),AS(N),DPL(N),P3(N),DVC(N),PA(N),N=1,J)
605      43  FORMAT(28X,15HWATER PRESSURES //
      +      8X,
      +      53H TIME          WS          HEAD          END GATE          VENA          PENS
      +      4HTOCK /
      +      16X,40H  ELEV          ACROSS          CHAMBER          CONTRACTA /
610      +      29X,4HUNIT /
      +      8X,45H(SEC)          (M)          (M)          (M)          (M)
      +      9H          (M) /
      +      (5X,F8.1,3X,F8.2,2X,F8.2,1X,F8.2,2X,F8.2,2X,F8.2))
      IF(JFIRST.EQ.10)WRITE(3,44)T(J+1)
615      44  FORMAT(7X,F8.1,5X,38H VAPOR PRESSURE FORMED IN GATE CHAMBER )
      IF(JFIRST.EQ.11)WRITE(3,45)T(J+1)
      45  FORMAT(7X,F8.1,9X,23H SONIC VELOCITY IN VENT )
      C
      C      AIR FLOW PROPERTIES
      C
620      WRITE(3,27)
      WRITE(3,2)
      WRITE(3,39)PATM,RHOA
      WRITE(3,3)
625      WRITE(3,46)(T(N),VIN(N),VOUT(N),WFLA(N),RHOAG(N),AGC(N),
      +      N=1,J)
      IF(JFIRST.EQ.10)WRITE(3,44)T(J+1)
      IF(JFIRST.EQ.11)WRITE(3,45)T(J+1)
      46  FORMAT(24X,21H AIR FLOW PROPERTIES //
      +      8X,
      +      47H TIME          INLET          OUTLET          AIR FLOW SPECIFIC
      +      9H  GATE / , 16X,
      +      48H AIR VEL          AIR VEL          RATE          MASS          CHAMBER /
      +      48X,17HOF AIR PRESSURE /
635      +      8X,48H(SEC)          (M/SEC)          (M/SEC)          (KG/SEC) (KG/CU M)
      +      7H (KPA) /
      +      (5X,F8.1,3X,F8.1,2X,F8.1,2X,F8.3,2X,F8.4,2X,F8.2))
      C
      C      COMPUTATIONAL PROPERTIES
      C
640      WRITE(3,27)
      WRITE(3,2)
      WRITE(3,39)PATM,RHOA
      WRITE(3,3)
645      WRITE(3,47)(T(N),CKB(N),DY(N),DX(N),JCT(N),N=1,J)
      47  FORMAT(24X,24HCOMPUTATIONAL PROPERTIES //
      +      14X,44HTIME          ACCURACY          INTEGRATION ERROR          FLOW /
      +      20X,41H  GATE          GATE          PENSTOCK          CONDITION /
      +      20X,39H  CHAMBER          CHAMBER          (*LAST /
650      +      20X,40H  PRESS          PRESS          PAGE) /
      +      12X,36H (SEC)          (PA)          (M)          (M) /
      +      (10X,F8.1,1X,F8.0,4X,F8.4,2X,F8.4,4X,14))
      IF(JFIRST.EQ.10)WRITE(3,44)T(J+1)
      IF(JFIRST.EQ.11)WRITE(3,45)T(J+1)
655      IF(NTIM.EQ.K.OR.JFIRST.EQ.9)WRITE(3,37)
      IF(NTIM.EQ.K.OR.JFIRST.EQ.9)GO TO 49
      PATM= AGCCTE*PATM
      48  CONTINUE
      49  CALL EXIT
660      END

```

APPENDIX III

129

SUBROUTINE Q

```

1      SUBROUTINE Q(QGC,VP,VGC)
      C
      C      THIS PROGRAM COMPUTES THE DISCHARGE THROUGH THE EMERGENCY
      C      GATE AS A FUNCTION OF GATE OPENING, RESERVOIR ELEVATION,
5      C      DOWNSTREAM PRESSURE (FREE OR SUBMERGED), AND THE FREE
      C      FLOW DISCHARGE COEFFICIENT.
      C
      REAL MACHA,MACHGA,NVENTS
      DIMENSION VP(50),VGC(50)
10     COMMON CD,CKV,ABSPGC,PATM,PGC,WSREF,HCOL,WS,QR,QP,GRAV,PTOHD,
      +PP,P3(50),N,PL,FP,TLOSS,AU,AD,AREAP,AG,EK,GCR,PGO,JFIRST,WTFLLA(50)
      +,MACHA(50),MACHGA(50),AVOL,PIN,CVEL,T(50),JCK,GCLP,RES,ZP,DP,TW,
      +UGCLGC,GCLL,HYDDIA,VOLC1,ELC1,VOLC2,ELC2,CF,PER,CAREA,HMOTOR,
      +NVENTS,TGC,ENRTAP(50),SO,VOLR,CKX,PR,FSAV,FSAV1,DELX,DELY
15     +,ACURAC,ABSTEM,GASCTE,VAPOR,AGCCTE,SLOSS,METRIC,PENLEN
      QP= VP(N)*AREAP
      IF(JFIRST.GT.6)GO TO 1
      QGC=VGC(N)*AU
      IF(JFIRST.GT.3)QGC= VGC(N)*AD
      GO TO 2
20     1 QGC=0.
      2 QR= QP-QGC
      IF(JFIRST.GE.7)QR=AG*CD*SQRT(2.*GRAV*((RES-ZP)+PGC-PTOHD*PATM))
      IF(JCK.EQ.4)QR= AG*CD*SQRT(2.*GRAV*((RES-ZP)-PR+PGC-PTOHD*PATM))
25     IF(JFIRST.GE.7.AND.QR.GE.QP)QR= QP
      IF(QR.LE.0.)QR=0.
      RETURN
      END

```

SUBROUTINE DE2

```

1      SUBROUTINE DE2 (X,Y,VX,VY,U,DELT,N)
      C
      C      THIS PROGRAM SOLVES TWO DIFFERENTIAL EQUATIONS OF MOTION
      C      SIMULTANEOUSLY. THE TWO EQUATIONS ARE DEFINED BY FUNCT1
5      C      AND FUNCT2. THE OUTPUTS ARE DISTANCE (X AND Y) AND
      C      VELOCITY (VX AND VY).
      C
      C      FOR THE MATHEMATICS SEE ...LEVY,H.,BAGGOTT,E.A.,
      C      NUMERICAL SOLUTIONS OF DIFFERENTIAL EQUATIONS,
10     C      DOVER PUBLICATIONS, P103, 1950.
      C
      REAL MACHA,MACHGA,NVENTS
      DIMENSION X(50),Y(50),VX(50),VY(50),RKT(5),RKX(5),
      +RKY(5),RKVX(5),RKVY(5),F(5),G(5),U(50)
15     COMMON CD,CKV,ABSPGC,PATM,PGC,WSREF,HCOL,WS,QR,QP,GRAV,PTOHD,
      +PP,P3(50),L,PL,FP,TLOSS,AU,AD,AREAP,AG,EK,GCR,PGO,JFIRST,WTFLLA(50)
      +,MACHA(50),MACHGA(50),AVOL,PIN,CVEL,T(50),JCK,GCLP,RES,ZP,DP,TW,
      +UGCLGC,GCLL,HYDDIA,VOLC1,ELC1,VOLC2,ELC2,CF,PER,CAREA,HMOTOR,
      +NVENTS,TGC,ENRTAP(50),SO,VOLR,CKX,PR,FSAV,FSAV1,DELX,DELY
20     +,ACURAC,ABSTEM,GASCTE,VAPOR,AGCCTE,SLOSS,METRIC,PENLEN
      C
      C      EACH TIME INTERVAL IS DIVIDED INTO FOUR EQUAL INCREMENTS.
      C      THIS PORTION OF THE PROGRAM DETERMINES THE INITIAL VALUES
      C      OF THE INTEGRAL FOR THE FIRST FOUR VALUES. THAT IS,
25     C      TO (KNOWN)T1,T2,T3,AND T4.
      C      THESE ARE DETERMINED USING KUTTA'S SIMPSON'S RULE
      C
      C
      RKX(1)= X(N)

```

SUBROUTINE DE2

```

30      RKY(1)= Y(N)
      RKVX(1)= VX(N)
      RKVY(1)= VY(N)
      IF(JFIRST.EQ.4)RKVY(1)= RKVY(1)*AU/AD
      IF(JFIRST.EQ.4)RKY(1)= 0.
35      RKT(1)= T(N)
      H= DELT/4.
      F(1)= FUNCT1(RKVX(1),RKVY(1),RKT(1))
      G(1)= FUNCT2(RKY(1),RKVX(1),RKVY(1))
      DO 1 K=1,4
40          AK1= RKVX(K)*H
          AL1= RKVY(K)*H
          AM1= H*FUNCT1(RKVX(K),RKVY(K),RKT(K))
          AP1= H*FUNCT2(RKY(K),RKVX(K),RKVY(K))
          AK2= (RKVX(K)+AM1/2.)*H
          AL2= (RKVY(K)+AP1/2.)*H
45          B1= RKY(K)+AL1/2.
          C1= RKVX(K)+AM1/2.
          D1= RKVY(K)+AP1/2.
          E1= RKT(K)+H/2.
50          AM2= FUNCT1(C1,D1,E1)*H
          AP2= FUNCT2(B1,C1,D1)*H
          AK3= (RKVX(K)+AM2/2.)*H
          AL3= (RKVY(K)+AP2/2.)*H
          B2= RKY(K)+AL2/2.
55          C2= RKVX(K)+AM2/2.
          D2= RKVY(K)+AP2/2.
          E2= RKT(K)+H/2.
          AM3= FUNCT1(C2,D2,E2)*H
          AP3= FUNCT2(B2,C2,D2)*H
          AK4= (RKVX(K)+AM3)*H
60          AL4= (RKVY(K)+AP3)*H
          B3= RKY(K)+AL3
          C3= RKVX(K)+AM3
          D3= RKVY(K)+AP3
          E3= RKT(K)+H
65          AM4= FUNCT1(C3,D3,E3)*H
          AP4= FUNCT2(B3,C3,D3)*H
          DELTX= (AK1+2.*AK2+2.*AK3+AK4)/6.
          DELTY= (AL1+2.*AL2+2.*AL3+AL4)/6.
70          DELTVX= (AM1+2.*AM2+2.*AM3+AM4)/6.
          DELTVY= (AP1+2.*AP2+2.*AP3+AP4)/6.
          RKT(K+1)= RKT(K)+H
          RKX(K+1)= RKX(K)+DELT X
          RKY(K+1)= RKY(K)+DELT Y
75          RKVX(K+1)= RKVX(K)+DELT VX
          RKVY(K+1)= RKVY(K)+DELT VY
          IF(JFIRST.EQ.6.AND.K.EQ.4)JCK= 3
          F(K+1)= FUNCT1(RKVX(K+1),RKVY(K+1),RKT(K+1))
          G(K+1)= FUNCT2(RKY(K+1),RKVX(K+1),RKVY(K+1))
80          IF(K.EQ.2)FSAV1= G(K+1)
          IF(K.EQ.3)FSAV=G(K+1)
      1 CONTINUE
      C
      C      CORRECTION OF INITIAL VALUES
      C
85      DELXS= 0.
      DELYS= 0.
      JCK= 2
      CALL DELTD (F,DELF,DEL2F,DEL3F,DEL4F)
      CALL DELTD (G,DELG,DEL2G,DEL3G,DEL4G)
90      RKVX(2)= RKVX(1)+H*(F(1)+DELF/2.-DEL2F/12.+DEL3F/24.-DEL4F/40.)
      RKVY(2)= RKVY(1)+H*(G(1)+DELG/2.-DEL2G/12.+DEL3G/24.-DEL4G/40.)
      RKX(2)= RKX(1)+H*(RKVX(1)+RKVX(2))/2.
      RKY(2)= RKY(1)+H*(RKVY(1)+RKVY(2))/2.

```

APPENDIX III

131

SUBROUTINE DE2

```

95      DO 2 J=1,3
          F(J+1)= FUNCT1(RKVX(J+1),RKVY(J+1),RKT(J+1))
          G(J+1)= FUNCT2(RKY(J+1),RKVX(J+1),RKVY(J+1))
          RKVX(J+2)= RKVX(J)+(F(J+2)+4.*F(J+1)+F(J))*H/3.
          RKVY(J+2)= RKVY(J)+(G(J+2)+4.*G(J+1)+G(J))*H/3.
100     RKX(J+2)= RKX(J)+(RKVX(J+2)+4.*RKVX(J+1)+RKVX(J))*H/3.
          RKY(J+2)= RKY(J)+(RKVY(J+2)+4.*RKVY(J+1)+RKVY(J))*H/3.
          IF(JFIRST.EQ.6.AND.J.EQ.3)JCK= 3
          FC= FUNCT1(RKVX(J+2),RKVY(J+2),RKT(J+2))
          GC= FUNCT2(RKY(J+2),RKVX(J+2),RKVY(J+2))
105     IF(J.EQ.1)FSAV1= GC
          OLDX= RKX(J+2)
          OLDY= RKY(J+2)
          IF(J.EQ.2)FSAV= GC
          RKVX(J+2)= RKVX(J+2)+(FC-F(J+2))*H/3.
          RKVY(J+2)= RKVY(J+2)+(GC-G(J+2))*H/3.
110     RKX(J+2)= RKX(J+1)+H*(RKVX(J+2)+RKVX(J+1))/2.
          RKY(J+2)= RKY(J+1)+H*(RKVY(J+2)+RKVY(J+1))/2.
          DELX= ABS(OLDX-RKX(J+2))
          DELY= ABS(OLDY-RKY(J+2))
115     IF(DELXS.GE.DELX)DELX= DELXS
          IF(DELXS.GE.DELX)DELY= DELYS
          F(J+2)= FC
          G(J+2)= GC
          2 CONTINUE
120     C
          C      VALUES AT END OF INTEGRATION PERIOD
          C
          VX(N+1)= RKVX(5)
          VY(N+1)= RKVY(5)
125     X(N+1)= RKX(5)
          Y(N+1)= RKY(5)
          T(N+1)= T(N)+DELT
          C
          C      IF THE INTEGRATION ACCURACY IS EXCEEDED, THE
130     C      PREVIOUS VALUE OF VX AND OR VY IS USED TO
          C      EXTRAPOLATE THE NEW VALUE OF X AND OR Y.
          C
          IF(DELX.LE.0.01)GO TO 3
          VX(N+1)= VX(N)+DELT/(T(N)-T(N-1))*(VX(N)-VX(N-1))
          P3(N+1)= P3(N)+DELT/(T(N)-T(N-1))*(P3(N)-P3(N-1))
135     X(N+1)= (VX(N)+VX(N+1))*DELT/2.+X(N)
          3 IF(DELY.LE.0.01)GO TO 4
          VY(N+1)= VY(N)+DELT/(T(N)-T(N-1))*(VY(N)-VY(N-1))
          P3(N+1)= P3(N)+DELT/(T(N)-T(N-1))*(P3(N)-P3(N-1))
140     Y(N+1)= (VY(N)+VY(N+1))*DELT/2.+Y(N)
          C
          C      END OF EXTRAPOLATION
          C
          4 CKV= VY(N+1)
          CKX= X(N+1)
145     RETURN
          END

```

AIR-WATER FLOW IN HYDRAULIC STRUCTURES

SUBROUTINE DELTD

```

1      SUBROUTINE DELTD(A,B,E,D,DEL4)
      C
      C      THIS PROGRAM COMPUTES THE 4TH DIFFERENCE OF A SERIES
      C      OF FIVE EQUALLY SPACED QUANTITIES
5      C
      REAL MACHA,MACHGA,NVENTS
      COMMON CD,CKV,ABSPGC,PATM,PGC,WSREF,HCOL,WS,QR,QP,GRAV,PTOHD,
+PP,P3(50),J,PL,FP,TLOSS,AU,AD,AREAP,AG,EK,GCR,PGO,JFIRST,WTFLA(50)
10     +,MACHA(50),MACHGA(50),AVOL,PIN,CVEL,T(50),JCK,GCLP,RES,ZP,DP,TW,
+UGCLGC,GCLL,HYDDIA,VOLC1,ELC1,VOLC2,ELC2,CF,PER,CAREA,HMOTOR,
+NVENTS,TGC,ENRTAP(50),SO,VOLR,CKX,PR,FSAV,FSAV1,DELX,DELY
+ACURAC,ABSTEM,GASCTE,VAPOR,AGCCTE,SLOSS,METRIC,PENLEN
      DIMENSION A(5),DEL(4),DEL2(3),DEL3(2)
      DO 1 I=1,4
15     1 DEL(I)= A(I+1)-A(I)
      DO 2 K=1,3
      2 DEL2(K)= DEL(K+1)-DEL(K)
      DO 3 JK=1,2
      3 DEL3(JK)= DEL2(JK+1)-DEL2(JK)
20     B= DEL(1)
      E= DEL2(1)
      D= DEL3(1)
      DEL4= DEL3(2)-DEL3(1)
      RETURN
25     END

```

FUNCTION FUNCT1

```

1      FUNCTION FUNCT1(CA,DA,EA)
      C
      C      THIS PROGRAM GIVES THE VALUE OF THE SECOND ORDER
      C      DIFFERENTIAL EQUATION OF FLOW DISTANCE WITH RESPECT TO
5      C      TIME FOR THE WATER IN THE PENSTOCK.THE VALUE OF THE
      C      DIFFERENTIAL IS FUNCT1.
      C
      REAL MACHA,MACHGA,NVENTS
      COMMON CD,CKV,ABSPGC,PATM,PGC,WSREF,HCOL,WS,QR,QP,GRAV,PTOHD,
10     +PP,P3(50),J,PL,FP,TLOSS,AU,AD,AREAP,AG,EK,GCR,PGO,JFIRST,WTFLA(50)
+MACHA(50),MACHGA(50),AVOL,PIN,CVEL,T(50),JCK,GCLP,RES,ZP,DP,TW,
+UGCLGC,GCLL,HYDDIA,VOLC1,ELC1,VOLC2,ELC2,CF,PER,CAREA,HMOTOR,
+NVENTS,TGC,ENRTAP(50),SO,VOLR,CKX,PR,FSAV,FSAV1,DELX,DELY
+ACURAC,ABSTEM,GASCTE,VAPOR,AGCCTE,SLOSS,METRIC,PENLEN
15     PGO= 100.-GCR*EA
      CD= (1.049E-04)+(7.062E-03)*PGO-(5.830E-05)*PGO**2+(2.398E-06)
+*PGO**3-(3.578E-08)*PGO**4+(1.987E-10)*PGO**5
      VHP= CA**2/(2.*GRAV)
      VHR= (CA-DA*AU/AREAP)**2/(2.*GRAV)
20     IF (JFIRST.GE.4) VHR=(CA-DA*AD/AREAP)**2/(2.*GRAV)
      PR= RES-ZP-VHR*(AREAP/AG/CD)**2
      PGD= PGO/100.
      BH= PGD*SO/(RES-ZP)
      CC= (BH*(CD/PGD)**2+SQRT((CD/PGD)**4*BH**2+4.*(CD/PGD)**2))/2.
25     PT= PR-DP
      PP= PR+2.*AG/(AG+AREAP)*(2./CC/PGD*VHR*(AREAP/AG)**2-2.*VHP*AREAP
+AG)
      PVAPOR= VAPOR-PTOHD*PATM
      IF (PT.GT.PVAPOR)GO TO 1
      PT= PVAPOR
30     1 P3(J)= PT
      FUNCT1= GRAV/PL*(PP-VHP*(TLOSS*SLOSS-1.+FP*PL/DP)+ZP-TW-HMOTOR)
      RETURN
      END

```

APPENDIX III

133

FUNCTION FUNCT2

```

1      FUNCTION FUNCT2(BB,CB,DB)
      C
      C      THIS PROGRAM GIVES THE VALUE OF THE SECOND ORDER
      C      DIFFERENTIAL EQUATION OF DEPTH WITH RESPECT TO TIME
5      C      FOR THE WATER IN THE GATE CHAMBER.  THE VALUE OF THE
      C      DIFFERENTIAL IS FUNCT2.
      C
      REAL MACHA,MACHGA,NVENTS
      COMMON CD,CKV,ABSPGC,PATM,PGC,WSREF,HCOL,WS,QR,QP,GRAV,PTOHD,
10     +PP,P3(50),J,PL,FP,TLOSS,AU,AD,AREAP,AG,EK,GCR,PGO,JFIRST,WTFLA(50)
      +,MACHA(50),MACHGA(50),AVOL,PIN,CVEL,T(50),JCK,GCLP,RES,ZP,DP,TW,
      +UGCLGC,GCLL,HYDDIA,VOLC1,ELC1,VOLC2,ELC2,CF,PER,CAREA,HMOTOR,
      +NVENTS,TGC,ENRTAP(50),SO,VOLR,CKX,PR,FSAV,FSAV1,DELX,DELY
      +,ACURAC,ABSTEM,GASCTE,VAPOR,AGCCTE,SLOSS,METRIC,PENLEN
15     VHGC= DB**2/(2.*GRAV)
      VHR= (CB-DB*AU/AREAP)**2/(2.*GRAV)
      IF(JFIRST.GE.4)VHR= (CB-DB*AD/AREAP)**2/(2.*GRAV)
      PR= RES-ZP-VHR*(AREAP/AG/CD)**2
      PT= PR-DP
20     PVAPOR= VAPOR-PTOHD*PATM
      IF(PT.GT.PVAPOR)GO TO 1
      PT= PVAPOR
      1 P3(J)= PT
      IF(JFIRST.GE.4)GO TO 2
25     C
      C      WATER SURFACE IN UPPER GATE CHAMBER
      C
      FUNCT2= GRAV/(HCOL-BB+GCLL*AU/AD)*(PGC-PTOHD*PATM-PT+HCOL-BB
30     +GCLL-VHGC*((1.+FP*GCLL/HYDDIA+EK)*(AU/AD)**2-1.)/2.)
      RETURN
      C
      C      WATER SURFACE IN LOWER GATE CHAMBER
      C
      2 IF(JCK.EQ.3)GO TO 3
35     FUNCT2= GRAV*((PGC-PTOHD*PATM-PT)/(GCLL-BB)+1.0-
      +VHGC*FP/HYDDIA)
      IF(DB.LT.0.)FUNCT2= GRAV*((PGC-PTOHD*PATM-PT)/(GCLL-BB)+1.0+
      +VHGC*FP/HYDDIA)
      RETURN
40     C
      C      EXTRAPOLATION OF FUNCT2 TO ENTRANCE OF PENSTOCK
      C      (ZERO LENGTH OF WATER COLUMN)  JCK=3 SIGNIFIES NO
      C      MORE WATER IN GATE CHAMBER.
      C
45     3 FUNCT2= 2.*FSAV-FSAV1
      RETURN
      END

```

SUBROUTINE DE1

```

1      SUBROUTINE DE1(X,VX,DELT)
      C
      C      THIS PROGRAM SOLVES THE DIFFERENTIAL EQUATION OF MOTION
      C      FOR FLOW IN THE PENSTOCK WHEN THE WATER SURFACE IS IN THE
5      C      PENSTOCK.  THE OUTPUTS ARE DISTANCE(X) AND VELOCITY (VX).
      C
      REAL MACHA,MACHGA,NVENTS
      DIMENSION X(50),VX(50),RX(5),RVX(5),RT(5),RF(5)
      COMMON CD,CKV,ABSPGC,PATM,PGC,WSREF,HCOL,WS,QR,QP,GRAV,PTOHD,
10     +PP,P3(50),M,PL,FP,TLOSS,AU,AD,AREAP,AG,EK,GCR,PGO,JFIRST,WTFLA(50)

```

```

SUBROUTINE DE1

      +,MACHA(50),MACHGA(50),AVOL,PIN,CVEL,T(50),JCK,GCLP,RES,ZP,DP,TW,
      +UGCLGC,GCLL,HYDDIA,VOLC1,ELC1,VOLC2,ELC2,CF,PER,CAREA,HMOTOR,
      +NVENTS,TGC,ENRTAP(50),SO,VOLR,CKX,PR,FSAV,FSAV1,DELX,DELY
      +,ACURAC,ABSTEM,GASCTE,VAPOR,AGCCTE,SLOSS,METRIC,PENLEN

15      C
      C      DETERMINATION OF INITIAL VALUES
      C
      N= M-1
      RX(1)= X(N)
20      RVX(1)= VX(N)
      RT(1)= T(N)
      H= DELT/4.
      RF(1)= FUNCT3(RX(1),RVX(1),RT(1))
      DO 1 K=1,4
25          AK1= FUNCT3(RX(K),RVX(K),RT(K))*H
          A1= RX(K)+RVX(K)*H/2.+AK1*H/8.
          B1= RVX(K)+AK1/2.
          C1= RT(K)+H/2.
          AK2= FUNCT3(A1,B1,C1)*H
30          B2= RVX(K)+AK2/2.
          AK3= FUNCT3(A1,B2,C1)*H
          A3= RX(K)+RVX(K)*H+AK3*H/2.
          B3= RVX(K)+AK3
          C3= RT(K)+H
35          AK4= FUNCT3(A3,B3,C3)*H
          DELTX= H*(RVX(K)+(AK1+AK2+AK3)/6.)
          DELTVX= (AK1+2.*AK2+2.*AK3+AK4)/6.
          RX(K+1)= RX(K)+DELTX
          RVX(K+1)= RVX(K)+DELT VX
40          RT(K+1)= RT(K)+H
          RF(K+1)= FUNCT3(RX(K+1),RVX(K+1),RT(K+1))
1      CONTINUE
      C
      C      CORRECTION OF INITIAL VALUES
45      C
      DELY= 0.
      DELXS= 0.
      CALL DELTD(RVX,DELF,DEL2F,DEL3F,DEL4F)
      RX(2)= RX(1)+H*(RVX(1)+DELF/2.-DEL2F/12.+DEL3F/24.-DEL4F/40.)
50      CALL DELTD(RF,DELF,DEL2F,DEL3F,DEL4F)
      RVX(2)= RVX(1)+H*(RF(1)+DELF/2.-DEL2F/12.+DEL3F/24.-DEL4F/40.)
      DO 2 J=1,3
          RF(J+1)= FUNCT3(RX(J+1),RVX(J+1),RT(J+1))
          RVX(J+2)= (RF(J+2)+4.*RF(J+1)+RF(J))*H/3.+RVX(J)
55          OLDX= RX(J+2)
          RX(J+2)= (RVX(J+2)+4.*RVX(J+1)+RVX(J))*H/3.+RX(J)
          DELX= ABS(OLDX-RX(J+2))
          IF(DELXS.GE.DELX)DELX= DELXS
2      CONTINUE
60      C
      C      VALUES AT END OF INTEGRATION PERIOD
      C
      VX(N+1)= RVX(5)
      X(N+1)= RX(5)
65      CKX= X(N+1)
      CKV= VX(N+1)
      T(N+1)= T(N)+DELT
      RETURN
      END

```


FUNCTION FUNCT3

```

1      FUNCTION FUNCT3(AC,BC,DC)
      C
      C      THIS PROGRAM GIVES THE VALUE OF THE SECOND ORDER
      C      DIFFERENTIAL EQUATION OF FLOW DISTANCE WITH RESPECT
5      C      TO TIME FOR A FREE WATER SURFACE IN THE PENSTOCK.
      C
      REAL MACHA,MACHGA,NVENTS
      COMMON CD,CKV,ABSPGC,PATM,PGC,WSREF,HCOL,WS,QR,QP,GRAV,PTOHD,
      +PP,P3(50),J,PL,FP,TLOSS,AU,AD,AREAP,AG,EK,GCR,PGO,JFIRST,WTFIA(50)
10     +,MACHA(50),MACHGA(50),AVOL,PIN,CVEL,T(50),JCK,GCLP,RES,ZP,DP,TW,
      +UGCLGC,GCLL,HYDDIA,VOLC1,ELC1,VOLC2,ELC2,CF,PER,CAREA,HMOTOR,
      +NVENTS,TGC,ENRTAP(50),S0,VOLR,CKX,PR,FSAV,FSAV1,DELX,DELY
      +,ACURAC,ABSTEM,GASCTE,VAPOR,AGCCTE,SLOSS,METRIC,PENLEN
      JN= J-1
15     VHP= BC**2/(2.*GRAV)
      PGO= 100.-GCR*DC
      IF(PGO.LE.0.)GO TO 1
      CD= (1.049E-04)+(7.062E-03)*PGO-(5.830E-05)*PGO**2+(2.398E-06)
      +*PGO**3-(3.578E-08)*PGO**4+(1.987E-10)*PGO**5
20     PGD= PGO/100.
      BH= PGD*S0/(RES-ZP)
      CC= (BH*(CD/PGD)**2+SQRT((CD/PGD)**4*BH**2+4.*(CD/PGD)**2))/2.
      GO TO 2
25     1 PGO= 0.
      CD= 0.
      PGD= 0.
      CC= .611
2     HVC= S0*CC*PGD
      IF(WS.LE.ZP)GO TO 6
      AVOLCK= AC*AREAP-QR*(DC-T(JN))-VOLR
30     IF(AVOLCK.LT.0.)AVOLCK= .1E-30
      CKWS= GCLP-AVOLCK/VOLC1
      IF(JCK.EQ.6)GO TO 6
      IF(JCK.EQ.5)GO TO 3
35     C
      C      JUMP IN CONDUIT, GATE SUBMERGED
      C
      DEPT= SQRT(AVOLCK/3.5/DP)
      PR= DP-DEPT
40     QR= AG*CD*SQRT(2.*GRAV*((RES-ZP)-PR+PGC-PTOHD*PATM))
      IF(PR.LT.HVC)GO TO 3
      JCK= 4
      IF(PGD.LE.0.)GO TO 4
      PP= QR**2/(CC*PGD*AG*AREAP*GRAV)+PR*(DP-DEPT)/(2.*DP)-2.*VHP
45     +*DP/2.+PGC-PTOHD*PATM
      GO TO 5
      C
      C      JUMP IN CONDUIT, GATE NOT SUBMERGED
      C
50     3 PR= HVC
      JCK=5
      IF(PGD.LE.0.)GO TO 4
      PP= (2.*CD**2*AG*(RES-ZP+PGC-PTOHD*PATM))/(PGD*CC*AREAP)
      +*PR*CC*AG*PGD/(2.*AREAP)-2.*VHP+DP/2.+PGC-PTOHD*PATM
55     DEPT2= QR*QR/(16.1*DP*DP*CC*S0*PGD)+HVC*HVC-QP*QP/(16.1*DP*AREAP)
      IF(PP.LE.DP.AND.DEPT2.GT.0.)PP= SQRT(DEPT2)+PGC-PTOHD*PATM
      IF(DEPT2.LE.0.)GO TO 6
      GO TO 5
4     PP= PR+PGC-PTOHD*PATM
60     5 WS= ZP+PR
      IF(PP.LE.DP)WS= ZP+PP
      PL= WS-PENLEN
      IF(CKWS.LT.(ZP+PR).AND.JFIRST.EQ.8)GO TO 6
      FUNCT3= GRAV/PL*(PP-VHP*(TLOSS*SLOSS-1.+FP*PL/DP)+ZP-TW-HMOTOR)
65     RETURN
      C

```

AIR-WATER FLOW IN HYDRAULIC STRUCTURES

FUNCTION FUNCT3

```

C      WATER SURFACE BELOW GATE SEAT
C
70      6 QRTST= AG*CD*SQRT(2.*GRAV*(RES-ZP+PGC-PTOHD*PATM))
        IF(QRTST.GT.QP)QRTST= QP
        JCK= 6
        DT= (DC-T(JN))
        IF(DT.LE.0.)GO TO 7
        DQRDT= (QR-QRTST)/DT
75      WS= ZP+DP-(AC*AREAP-(2.*QRTST-DQRDT*DT)*DT/2.-VOLR)/VOLC1
        IF(WS.LE.ELC1)WS= ELC2-(AC*AREAP-(2.*QRTST-DQRDT*DT)*DT/2.-
        +VOLR)/VOLC2
        7 IF(WS.GE.GCLP)GO TO 8
        PL= WS-PENLEN
80      SURAR= CF*SIN((GCLP-WS)/PER)
        IF(SURAR.LE.CAREA)SURAR= CAREA
        8 IF(ABS(GCLP-WS).LE.DP/4.)SURAR= AREAP
        VWS= (AREAP*BC-QRTST)/SURAR
        VHWS= VWS**2/(2.*GRAV)
85      IF(PGD.GT.0.) GO TO 9
        VHVC= 0.
        GO TO 10
        9 VHVC= (QRTST/(AG*CC))**2/(2.*GRAV)
90      10 VHUS= SQRT(VHVC**2+VHWS**2)
        FUNCT3= GRAV/PL*(PGC-PTOHD*PATM+WS-TW-HMOTOR+VHUS-VHP*
        +(TLOSS*SLOSS+FP*PL/DP))
        IF(WS.LT.ELC1)FUNCT3= GRAV/PL*(PGC-PTOHD*PATM-VHP*
        +(TLOSS*SLOSS+FP*PL/DP)+VHWS+WS-TW-HMOTOR)
        PP= PTOHD*(ABSPGC-PATM)
95      IF(WS.GE.ZP)PP= WS-ZP
        PR=HVC
        RETURN
        END

```

SUBROUTINE AMACH

```

1      SUBROUTINE AMACH(CINC,FRICT,AVENT,DELT,PGCINC,WTAIR,CONST,
      +CKA)
C
C      THIS PROGRAM GIVES THE AIR FLOW RATE IN THE AIR VENT AS A
5      C      FUNCTION OF THE WATER SURFACE ELEVATION.
C
      REAL M1R,M1I,MACHIN,MACHGC
      REAL MACHA,MACHGA,NVENTS
      COMMON CD,CKV,ABSPGC,PATM,PGC,WSREF,HCOL,WS,QR,QP,GRAV,PTOHD,
10      +PP,P3(50),J,PL,FP,TLOSS,AU,AD,AREAP,AG,EK,GCR,P60,JFIRST,WTFLA(50)
      +,MACHA(50),MACHGA(50),AVOL,PIN,CVEL,T(50),JCK,GCLP,RES,ZP,DP,TW,
      +UGCLGC,GCLL,HYDDIA,VOLC1,ELC1,VOLC2,ELC2,CF,PER,CAREA,HMOTOR,
      +NVENTS,TGC,ENRTAP(50),SO,VOLR,CKX,PR,FSAV,FSAV1,DELX,DELY
      +,ACURAC,ABSTEM,GASCTE,VAPOR,AGCCTE,SLOSS,METRIC,PENLEN
15      EQ(MACH)= (1.-MACH*MACH)/(1.4*MACH*MACH)+.8571*
      +ALOG((1.2*MACH*MACH)/(1.+1.2*MACH*MACH))
      JN= J-1
      MACHIN= MACHA(JN)
      MACHGC= MACHGA(JN)
20      IF(ABS(MACHA(JN)).LE.0.0001)MACHIN=.0001
      IF(ABS(MACHGA(JN)).LE.0.0001)MACHGC=.0001
C      SETS AIR FLOW DIRECTION INTO VENT
      CKSN= 1.
      IF(CKV.LT.0.)CKSN= -1.
25      IF(CKSN.LT.0.)MACHIN= CKSN*ABS(MACHIN)
      IF(CKSN.LT.0.)MACHGC= CKSN*ABS(MACHGC)

```

APPENDIX III

137

SUBROUTINE AMACH

```

      M11= 0.50
      CKASAV= 0.001
      DM11= -0.24999
30      C
      C
      C      COMPUTATION OF AIR VOLUME IN GATE CHAMBER AND PENSTOCK
      RC= 1./((1.2)**3.5)
      OVER= 0
35      AVOL= AU*(TGC-WS)
      AVOLU= AU*(TGC-UGCLGC)
      IF(WS.LE.UGCLGC)AVOL= AVOLU+(UGCLGC-WS)*AD
      IF(WS.LE.GCLP)AVOL= AVOLU+AD*GCLL+(GCLP-WS)*VOLC1
      IF(JFIRST.EQ.6)AVOL= AVOLU+(UGCLGC-GCLP)*AD
40      IF(JCK.GE.4)AVOL= AVOLU+AD*GCLL+AREAP*CKX-VOLR-QR*DELT
      IF(WS.LE.ELC1)AVOL= AVOLU+AD*GCLL+(ELC2-WS)*VOLC2
      C
      C      COMPUTATION OF THE PRESSURE RATIO,THE COMPRESSIBLE DISCHARGE
      C      COEFFICIENT, THE REAL MACH NUMBER AT 1,AND THE AIR FLOW RATE
45      C      GIVEN THE IDEAL MACH NUMBER AT THE BEGINNING OF THE DUCT REGION
      C
      DO 14 NDO=1,30
      R= 1./((1+.2*M11**2)**3.5)
      IF((R/RC).LE.1.)GO TO 1
50      C      COMPRESSIBLE DISCHARGE,COEFFICIENT
      C= 1.-((1.-CINC)*(1.-.7*(CINC-.1)*(1./R-1.))/(1./RC-1.))
      GO TO 2
1      C= 1.-((1.-CINC)*(1.-.7*(CINC-.1)-(.27+.1*CINC)*(1.-((R/RC)**2)))
2      RADICL= 1+.8*C*C*(M11*M11+.2*M11*M11*M11*M11)
55      ROOT= SQRT(RADICL)
      C      TRUE MACH NUMBER AT AIR VENT
      M1R= SQRT((-1.+ROOT)/.4)
      IF(ABS(M1R).LE.0.00001)M1R= .1E-10*CKSN
      IF(CKSN.LT.0.)M1R= -1.*M1R
60      MACHIN= M1R
      C      ENTROPY INCREASE IN INLET REGION
      ENT= (C*M11/M1R)**7.
      IF(ABS(M11).LE.0.001)ENT=1.
      C      STAGNATION PRESSURE AT END OF INLET
65      PIN= ENT*PATM
      IF(CKSN.LT.0.)PIN= ENT*PGCTRL
      C      VELOCITY COEFFICIENT
      CVEL= (M1R/M11)**2/C
      C      MASS FLOW RATE
70      WTFLA(J)= AGCCTE/SQRT(ABSTEM*GASCTE/(1.4*GRAV))*AVENT*PATM*ENT*
      + M1R*NVENTS/((1+.2*M1R**2)**3)
      IF(CKSN.LT.0.)WTFLA(J)=AGCCTE/SQRT(ABSTEM*GASCTE/(1.4*GRAV))*
      + AVENT*PGCTRL*ENT*CKSN*((1+.2*M1R**2)**3)
      IF(METRIC.EQ.1)WTFLA(J)= WTFLA(J)/(AGCCTE*SQRT(GRAV))
75      C
      C      COMPUTATION OF MACH NO. AT OUTLET OF AIR DUCT
      C      CONSIDERING THE FRICTION LOSSES IN THE DUCT
      C
      FMAX= EQ(MACHIN)
      IF(FRICT.GT.FMAX)GO TO 5
80      MACHGC= MACHIN
      CKM= -0.01
      DM= MACHGC/2.
      IF(DM.GE.0.5)DM= (1.-MACHGC)/2.
85      EQRH= FMAX
      EQLH= EQ(MACHGC)
      C      THIS LOOP FINDS THE VALUE OF MACHGC
      DO 4 K=1,35
      EQLH= EQ(MACHGC)
      CK= EQRH-EQLH-FRICT
90      CALL NEWX(CK,CKM,MACHGC,DM)
      IF(K.EQ.1)GO TO 3

```

AIR-WATER FLOW IN HYDRAULIC STRUCTURES

```

SUBROUTINE AMACH

      T1= ABS(CK/FRICT)
      IF(T1.LE.0.002)GO TO 12
95      3   CKM= CK
      4   CONTINUE
      GO TO 12

C
C
C      COMPUTATION OF AIR FLOW RATE WITH MACH 1 AT DUCT OUTLET
100      5   MACHGC= 1.
      MACHIN = 1.
      DMIN= -0.25
      C2= -0.01
105      DO 6 N=1,30
      EQRH= EQ(MACHIN)
      C1= EQRH-FRICT
      CALL NEWX(C1,C2,MACHIN,DMIN)
      C2= C1
110      T1= ABS(C1/FRICT)
      IF(T1.LE.0.005)GO TO 7
      6   CONTINUE
      7   M1I= MACHIN
      DMIN= -0.25
115      C2= -0.01
      M1I= 1.0
      DO 10 MOON=1,30
      R= 1./(1+.2*M1I**2)**3.5
      IF((R/RC).LE.1.)GO TO 8
120      C= 1.-(1.-CINC)*(1.-.7*(CINC-.1)*(1./R-1.)/(1./RC-1.))
      GO TO 9
      8   C= 1.-(1.-CINC)*(1.-.7*(CINC-.1)-(.27+.1*CINC)*(1.-(R/RC)**2))
      9   RADICL= 1+.8*C**2*(M1I**2+.2*M1I**4)
      ROOT= SQRT(RADICL)
125      M1R= SQRT((-1.+ROOT)/.4)
      C1= MACHIN-M1R
      CALL NEWX(C1,C2,M1I,DMIN)
      T1= ABS(C1/M1R)
      IF(T1.LE.0.005)GO TO 11
130      10  CONTINUE
      11  ENT= (C*M1I/M1R)**7.
      PIN= ENT*PATM
      CVEL= (M1R/M1I)**2/C
      WTFLA(J)= AGCCTE/SQRT(ABSTEM*GASCTE/(1.4*GRAV))*AVENT*PATM*ENT*
135      + M1R*NVENTS/(1+.2*M1R**2)**3
      IF(CKSN.LT.0.)WTFLA(J)=AGCCTE/SQRT(ABSTEM*GASCTE/(1.4*GRAV))*
      + AVENT*PGCTRL**2/(1+.2*M1R**2)**3
      IF(METRIC.EQ.1)WTFLA(J)= WTFLA(J)/(AGCCTE*SQRT(GRAV))
      JFIRST= 11
140      GO TO 15

C
C
C      ADIABATIC EXPANSION OF AIR IN THE GATE CHAMBER GIVES THE GATE
      CHAMBER PRESSURE PGCTST
145      12  RHOA= (2.*WTAIR+(WTFLA(JN)+WTFLA(J))*DELT)/(2.*AVOL)
      PGCTST= CONST*RHOA**1.4
      IF(JFIRST.EQ.4.OR.JFIRST.EQ.7)PGCTST= CONST*((WTAIR+WTFLA(J)*
      + DELT)/AVOL)**1.4

C
C
C      COMPUTATION OF PRESSURE AT END OF DUCT FLOW SECTION
150
      PGCTRL= PIN*MACHIN/MACHGC*SQRT(((1+.2*MACHGC**2)/
      + (1+.2*MACHIN**2))**6)
      IF(CKSN.LT.0.)PGCTRL= PATM/ENT*MACHIN/MACHGC*SQRT(((1+.2*MACHGC
155      + **2)/(1+.2*MACHIN**2))**6)
      CKA = PGCTRL - PGCTST
      ABSPGC = (PGCTRL + PGCTST) / 2.
      PGC = PTOHD*ABSPGC

```

APPENDIX III

139

SUBROUTINE AMACH

```

160      IF (ABS(CKA).LE.PGCINC)GO TO 15
      CALL NEWX(CKA,CKASAV,M11,DM11)
      CKASAV= CKA
      IF (M11.GE.0.0.AND.CKV.GE.0.0)GO TO 13
      IF (M11.LT.0.0.AND.CKV.LT.0.0)GO TO 13
      M11= ABS(M11)*CKSN/2.
165      DM11= DM11/2.
      13 IF (ABS(M11).GE.1.238)M11= 1.238*CKSN
      14 CONTINUE
      OVER= 1
      15 MACHA(J)= M1R
      MACHGA(J)= MACHGC
      IF (CKSN.LT.0.)MACHGA(J)= M1R
      IF (CKSN.LT.0.)MACHA(J)= MACHGC
      IF (OVER.EQ.1)WRITE(3,16)WS
170      16 FORMAT(1H1,19X,35HONE OR MORE LOOPS IN AMACH EXCEEDED /
175      +      30X,4HWS = ,F9.2)
      RETURN
      END

```

SUBROUTINE NEWX

```

1      SUBROUTINE NEWX(C1,C2,X,D)
      C
      C      THIS SUBROUTINE DETERMINES THE NEXT TRIAL VALUE OF X WHICH
      C      SATISFIES A FUNCTION C= F(X). IF THE CORRECT ROOT LIES
5      C      BETWEEN THE OLD VALUE OF THE FUNCTION (C1) AND THAT VALUE
      C      JUST COMPUTED (C2), THEN THE INCREMENT IS HALVED. OTHERWISE,
      C      X IS INCREMENTED BY D. THE LOGIC OF THIS PROGRAM RESULTS
      C      IN INCREASES OF C AS X INCREASES. IF THE OPPOSITE IS TRUE
      C      THEN D MUST BE MADE NEGATIVE IN THE CALLING ROUTINE. IN
10     C      THE CALLING ROUTINE THE INITIAL VALUE OF C1 SHOULD BE EQUAL
      C      TO ZERO.
      C
      C      C1= PREVIOUS VALUE OF FUNCTION
      C      C2= VALUE OF FUNCTION JUST COMPUTED
15     C      X= INDEPENDENT VARIABLE
      C      D= INCREMENT OF X
      C
      IF (C1.GT.0.)GO TO 2
      IF (C2.LT.0.)GO TO 1
20     D= D/2.
      GO TO 3
      1 X= X+D
      RETURN
      2 IF (C2.GT.0.)GO TO 3
25     D= D/2.
      GO TO 1
      3 X= X-D
      RETURN
      END

```

AIR-WATER FLOW IN HYDRAULIC STRUCTURES

COMPUTATION OF AIR FLOW INTO THE GATE CHAMBER DURING AN
EMERGENCY GATE CLOSURE IN THE PENSTOCK-
INTAKE STRUCTURE
MORROW POINT DAM

ATMOSPHERIC PRESSURE
77.60 KPA

SPECIFIC MASS OF AIR
.9738 KG/CU.M.

ONE 840MM BY 915MM AIR VENT
FLOW QUANTITIES

TIME	GATE	COEFF	Q	Q	Q
(SEC)	OPENING	DISCH.	RESERVOIR	GATE CHAMBER	PENSTOCK
(SEC)	(O/O)		(CMS)	(CMS)	(CMS)
0.0	100.0	.93	61.845	0.000	61.845
1.0	99.0	.91	61.800	.045	61.845
2.0	98.0	.89	61.685	.160	61.845
3.0	97.0	.86	61.510	.335	61.845
4.0	96.0	.84	61.329	.515	61.844
5.0	95.0	.82	61.198	.646	61.844
6.0	94.1	.81	61.128	.715	61.843
7.0	93.1	.79	61.132	.711	61.843
8.0	92.1	.77	61.201	.642	61.843
9.0	91.1	.75	61.306	.537	61.842
10.0	90.1	.74	61.416	.426	61.842
11.0	89.1	.72	61.508	.333	61.841
12.0	88.1	.71	61.553	.288	61.840
13.0	87.1	.69	61.537	.301	61.839
14.0	86.1	.68	61.474	.362	61.836
15.0	85.1	.67	61.371	.462	61.834
16.0	84.2	.65	61.262	.568	61.831
17.0	83.2	.64	61.175	.652	61.827
18.0	82.2	.63	61.114	.710	61.824
19.0	81.2	.62	61.089	.731	61.821
20.0	80.2	.61	61.102	.715	61.817
21.0	79.2	.60	61.139	.675	61.813
22.0	78.2	.59	61.184	.625	61.809
23.0	77.2	.58	61.203	.602	61.805
24.0	76.2	.57	61.210	.590	61.800
25.0	75.2	.56	61.194	.601	61.795
26.0	74.3	.55	61.154	.635	61.790
27.0	73.3	.54	61.097	.686	61.784
28.0	72.3	.53	61.036	.741	61.777
29.0	71.3	.52	60.976	.794	61.770
30.0	70.3	.51	60.922	.841	61.763
31.0	69.3	.50	60.883	.872	61.755
32.0	68.3	.49	60.851	.897	61.747
33.0	67.3	.48	60.830	.909	61.739
34.0	66.3	.47	60.819	.911	61.730
35.0	65.3	.47	60.791	.929	61.720
36.0	64.4	.46	60.757	.953	61.710
37.0	63.4	.45	60.703	.996	61.699
38.0	62.4	.44	60.651	1.035	61.687
39.0	61.4	.43	60.595	1.079	61.674
40.0	60.4	.43	60.528	1.133	61.661

APPENDIX III

141

COMPUTATION OF AIR FLOW INTO THE GATE CHAMBER DURING AN EMERGENCY GATE CLOSURE IN THE PENSTOCK- INTAKE STRUCTURE MORROW POINT DAM

ATMOSPHERIC PRESSURE
77.60 KPA

SPECIFIC MASS OF AIR
.9738 KG/CU.M.

ONE 840MM BY 915MM AIR VENT WATER PRESSURES

TIME	WS	HEAD	END GATE	VENA	PENSTOCK
(SEC)	ELEV	ACROSS	CHAMBER	CONTRACTA	
	(M)	UNIT	(M)	(M)	(M)
0.0	2181.11	122.10	21.06	25.18	24.55
1.0	2181.11	122.10	21.03	25.15	24.55
2.0	2181.10	122.10	21.01	25.13	24.55
3.0	2181.09	122.10	20.98	25.10	24.55
4.0	2181.05	122.10	20.96	25.08	24.55
5.0	2181.01	122.10	20.93	25.05	24.55
6.0	2180.96	122.10	20.90	25.02	24.55
7.0	2180.91	122.09	20.87	24.99	24.55
8.0	2180.86	122.09	20.84	24.96	24.54
9.0	2180.82	122.09	20.80	24.92	24.54
10.0	2180.78	122.09	20.76	24.88	24.54
11.0	2180.76	122.09	20.73	24.85	24.54
12.0	2180.73	122.09	20.69	24.81	24.54
13.0	2180.71	122.08	20.65	24.77	24.53
14.0	2180.69	122.07	20.61	24.73	24.52
15.0	2180.66	122.07	20.58	24.70	24.51
16.0	2180.62	122.06	20.54	24.66	24.51
17.0	2180.58	122.05	20.50	24.62	24.50
18.0	2180.53	122.04	20.47	24.59	24.48
19.0	2180.48	122.03	20.42	24.54	24.47
20.0	2180.42	122.02	20.38	24.50	24.46
21.0	2180.37	122.00	20.33	24.45	24.45
22.0	2180.33	121.99	20.28	24.40	24.44
23.0	2180.28	121.98	20.24	24.36	24.43
24.0	2180.24	121.96	20.19	24.31	24.41
25.0	2180.19	121.95	20.14	24.26	24.40
26.0	2180.15	121.93	20.09	24.21	24.38
27.0	2180.10	121.91	20.04	24.16	24.36
28.0	2180.05	121.89	19.98	24.10	24.34
29.0	2179.99	121.87	19.93	24.05	24.32
30.0	2179.94	121.85	19.87	23.99	24.30
31.0	2179.87	121.83	19.82	23.94	24.27
32.0	2179.81	121.80	19.75	23.87	24.25
33.0	2179.74	121.78	19.69	23.81	24.22
34.0	2179.68	121.75	19.62	23.74	24.19
35.0	2179.61	121.72	19.55	23.67	24.16
36.0	2179.54	121.69	19.48	23.60	24.13
37.0	2179.47	121.65	19.41	23.53	24.10
38.0	2179.40	121.62	19.33	23.45	24.06
39.0	2179.32	121.58	19.25	23.37	24.02
40.0	2179.24	121.54	19.17	23.29	23.98

AIR-WATER FLOW IN HYDRAULIC STRUCTURES

COMPUTATION OF AIR FLOW INTO THE GATE CHAMBER DURING AN
EMERGENCY GATE CLOSURE IN THE PENSTOCK-
INTAKE STRUCTURE
MORROW POINT DAM

ATMOSPHERIC PRESSURE
77.60 KPA

SPECIFIC MASS OF AIR
.9738 KG/CU.M.

ONE 840MM BY 915MM AIR VENT
AIR FLOW PROPERTIES

TIME (SEC)	INLET AIR VEL (M/SEC)	OUTLET AIR VEL (M/SEC)	AIR FLOW RATE (KG/SEC)	SPECIFIC MASS OF AIR (KG/CU M)	GATE CHAMBER PRESSURE (KPA)
0.0	0.0	0.0	0.000	.9738	77.60
1.0	.0	.0	.000	.9734	77.58
2.0	.3	.3	.243	.9741	77.62
3.0	.3	.3	.243	.9742	77.62
4.0	.6	.7	.547	.9737	77.59
5.0	.7	.8	.608	.9739	77.60
6.0	.8	1.0	.730	.9739	77.60
7.0	.8	.9	.669	.9739	77.60
8.0	.8	.9	.669	.9740	77.61
9.0	.6	.7	.486	.9741	77.61
10.0	.5	.6	.425	.9738	77.60
11.0	.4	.4	.304	.9737	77.59
12.0	.4	.4	.304	.9739	77.60
13.0	.3	.3	.243	.9736	77.59
14.0	.5	.6	.425	.9740	77.61
15.0	.4	.5	.365	.9739	77.60
16.0	.7	.8	.608	.9735	77.58
17.0	.7	.8	.608	.9738	77.60
18.0	.8	1.0	.730	.9738	77.60
19.0	.8	.9	.669	.9737	77.59
20.0	.8	1.0	.730	.9736	77.58
21.0	.7	.8	.608	.9734	77.57
22.0	.8	1.0	.730	.9741	77.62
23.0	.5	.6	.425	.9737	77.59
24.0	.8	1.0	.730	.9737	77.59
25.0	.5	.6	.425	.9737	77.59
26.0	.9	1.1	.790	.9739	77.60
27.0	.6	.7	.486	.9738	77.60
28.0	1.1	1.2	.912	.9738	77.60
29.0	.7	.8	.608	.9741	77.61
30.0	1.1	1.3	.973	.9739	77.60
31.0	.8	1.0	.730	.9742	77.62
32.0	1.1	1.3	.973	.9740	77.61
33.0	.8	1.0	.730	.9735	77.58
34.0	1.3	1.5	1.095	.9740	77.61
35.0	.8	.9	.669	.9738	77.60
36.0	1.4	1.6	1.216	.9742	77.62
37.0	.7	.8	.608	.9736	77.59
38.0	1.6	1.8	1.338	.9734	77.57
39.0	.8	1.0	.730	.9735	77.58
40.0	1.7	2.0	1.459	.9737	77.59

APPENDIX III

143

COMPUTATION OF AIR FLOW INTO THE GATE CHAMBER DURING AN EMERGENCY GATE CLOSURE IN THE PENSTOCK- INTAKE STRUCTURE MORROW POINT DAM

ATMOSPHERIC PRESSURE
77.60 KPA

SPECIFIC MASS OF AIR
.9738 KG/CU.M.

ONE 840MM BY 915MM AIR VENT COMPUTATIONAL PROPERTIES

TIME	ACCURACY	INTEGRATION ERROR	FLOW
	GATE	GATE	CONDITION
	CHAMBER	CHAMBER	(*LAST
	PRESS		PAGE)
(SEC)	(PA)	(M)	(M)
0.0	0.	0.0000	0.0000
1.0	44.	.0000	.0000
2.0	-33.	.0000	.0000
3.0	-43.	.0000	.0000
4.0	16.	.0000	.0000
5.0	-7.	.0000	.0000
6.0	-9.	.0000	.0000
7.0	-6.	.0000	.0000
8.0	-22.	.0000	.0000
9.0	-26.	.0000	.0000
10.0	6.	.0000	.0000
11.0	11.	.0000	.0000
12.0	-4.	.0000	.0000
13.0	20.	.0000	.0000
14.0	-17.	.0000	.0000
15.0	-5.	.0000	.0000
16.0	34.	.0000	.0000
17.0	5.	.0000	.0000
18.0	-2.	.0000	.0000
19.0	11.	.0000	.0000
20.0	28.	.0000	.0000
21.0	49.	.0000	.0000
22.0	-34.	.0000	.0000
23.0	9.	.0000	.0000
24.0	11.	.0000	.0000
25.0	13.	.0000	.0000
26.0	-4.	.0000	.0000
27.0	6.	.0000	.0000
28.0	-4.	.0000	.0000
29.0	-27.	.0000	.0000
30.0	-14.	.0000	.0000
31.0	-45.	.0000	.0000
32.0	-24.	.0000	.0000
33.0	32.	.0000	.0000
34.0	-21.	.0000	.0000
35.0	7.	.0000	.0000
36.0	-46.	.0000	.0000
37.0	23.	.0000	.0000
38.0	47.	.0000	.0000
39.0	41.	.0000	.0000
40.0	5.	.0000	.0000

LEGEND

- * 1 WATER SURFACE IN UPPER GATE CHAMBER
- 2 WATER SURFACE BELOW TOP OF GATE
- 3 WATER SURFACE JUST ENTERING PENSTOCK
- 4 HYDRAULIC JUMP FILLS PENSTOCK, GATE SUBMERGED
- 5 HYDRAULIC JUMP FILLS PENSTOCK, GATE FREE FLOW
- 6 WATER SURFACE IN PENSTOCK



Printed on Recycled Paper

U.S. GOVERNMENT PRINTING OFFICE: 1993-839-572

On November 6, 1979, the Bureau of Reclamation was renamed the Water and Power Resources Service in the U.S. Department of the Interior.

SELECTED ENGINEERING MONOGRAPHS

Monograph No.	Title
2	Multiple Correlation in Forecasting Seasonal Runoff
3	Welded Steel Penstocks Design and Construction
6	Stress Analysis of Concrete Pipe
7	Friction Factors for Large Conduits Flowing Full
8	Theory and Problems of Water Percolation
13	Estimating Foundation Settlement by One-Dimensional Consolidation Tests
14	Beggs Deformeter Stress Analysis of Single-Barrel Conduits
19	Design Criteria for Concrete Arch and Gravity Dams
20	Selecting Hydraulic Reaction Turbines
25	Hydraulic Design of Stilling Basins and Energy Dissipators
26	Rapid Method of Construction Control for Embankments of Cohesive Soil
27	Moments and Reactions for Rectangular Plates
30	Stress Analysis of Hydraulic Turbine parts
31	Ground-water Movement
32	Stress Analysis of Wye Branches
34	Control of Cracking in Mass Concrete Structures
35	Effect of Snow Compaction on Runoff from Rain or Snow
36	Guide for Preliminary Design of Arch Dams
37	Hydraulic Model Studies for Morrow Point Dam
38	Potential Economic Benefits from the Use of Radioisotopes in Flow Measurements through High-Head Turbines and Pumps
39	Estimating Reversible Pump-Turbine Characteristics
40	Selecting Large Pumping Units
41	Air-Water Flow in Hydraulic Structures